CALCIUM PHOSPHATE MINERALIZATION AS A NEXUS OF GEOSPHERE – BIOSPHERE INTERACTIONS

A DISSERTATION
SUBMITTED TO THE FACULTY OF THE
UNIVERSITY OF MINNESOTA
by

CHRISTINE H. CROSBY

IN PARTIAL FULFILLMENT
OF THE REQUIREMENTS
FOR THE DEGREE OF DOCTOR OF PHILOSOPHY

Advisor:
JAKE V. BAILEY

OCTOBER, 2017

Acknowledgements

This work would not have been possible without the much appreciated support and guidance of my advisor, Jake Bailey. As expected, he has been an insightful, kind and supportive advisor who both enabled me and allowed me to follow my own research path. My heartfelt thanks, Jake – what a grand adventure it's been!

I thank my committee members for their willingness to do all of the thankless extra work required of committee members, and I am grateful and proud to be able to include your names on the title page of this dissertation.

The companionship and assistance of all the many people who have been a part of the Bailey lab during the years of my graduate studies, is gratefully acknowledged – particularly Beverly Flood who was tasked with the difficult job of trying to help me get up to speed on the details of laboratory-based microbiology.

I am particularly grateful to the taxpayers of the United States of America, unsung heroes whose tax dollars in part fund the National Science Foundation, enabling the important NSF mission of supporting fundamental research and education in science and engineering. NSF grants to Jake funded much of my graduate studies. The fruits of taxpayer-funded research are enjoyed by all of us in a world made increasingly safe through many years of meticulous research and work that the NSF – as well as a number of other research and funding bodies – have made possible.

My graduate work and life were also financially supported by the University of Minnesota through a Graduate School Fellowship, a Doctorial Dissertation Fellowship and Earth Science Department fellowships and funding. Go gophers!

I want to also acknowledge my primary undergraduate institution, Northeastern Illinois University, and the faculty and classmates I was fortunate to work with while I was there, and my parents, Ron and Lois Crosby, for instilling in me a sense of wonder and curiosity about the world. In particular, I wish to thank Elizabeth Ricci for her friendship, positive encouragement and engaging discussions, and especially my partner Kerry Martin, for her undying support and belief in me.

I thank you all, and look forward to 'paying it forward' to other non-traditional students as they reach out to follow their dreams against all odds and offer their individual talents and gifts to the world.

Dedication

This work is dedicated to all who value the excitement of learning for learning's sake.

Abstract

There is arguably no more direct example of the dynamic relationship between the geosphere and the biosphere than the element phosphorus. Originally sourced from the rocky material of Earth, phosphorus enters the biosphere as the highly charged phosphate ion that is incorporated into every cell of every organism, and eventually returns to the geosphere in sedimentary phosphate rock. Although both igneous and sedimentary phosphate rock is mined for use in fertilizers, mineable phosphate rock is not evenly distributed across the Earth which imbues this vital resource with global economic significance and makes it an important issue in international relations, with wide-ranging implications for global human population growth trends. Phosphorus-related research is conducted in a wide variety of fields, including the medical and dental sciences, environmental and agricultural sciences, wastewater treatment technology, geology and mining. Indeed, there are many angles from which to explore the function and importance of phosphorus. In this thesis, I focus on some of the aspects of the phosphorus-related interplay between the geosphere and the biosphere through both 1) the ancient rock record, through analysis and interpretation of ~2 billion year old phosphate rock carrying an imprint of the biologically influenced cycling of phosphorus and 2) the modern, through laboratory experiments designed to elucidate details of the nucleation and precipitation of solid calcium-phosphate minerals in proximity with biological material. My work in the rock record carries significance for our understanding of the co-evolution of a relatively young, only recently oxygenated Earth and coeval life as it evolved to adapt to this changing environment. In addressing challenges inherent in determining *bona fide* biogenicity of putative microfossils, this work is also relevant to the field of micropaleontology. Finally, I offer a newly developed apparatus and protocol for use in the experimental examination of mineral precipitation over time and in the context of polymeric matrices such as those implicated in both biologically directed mineralization and biologically influenced precipitation of calcium-phosphate minerals and their precursors.

Table of Contents

List of Tables

List of Figures

Chapter 1

—

Thesis introduction

General introduction

The geosphere and the biosphere[*] are increasingly recognized as interconnected, and the field of geobiology is now a maturing scientific discipline. Many avenues are pursued in our search for an understanding of the intricacies of the dynamic interplay between these two spheres, and my work has focused on phosphorus as a link between the geosphere and biosphere, including in the context of micropaleontology.

To help place this research in context – of both the history and development of scientific thought and a complex framework of interrelated systems – I include introductory sections of background information, beginning with a very brief discussion of the arc of scientific (empirical) exploration toward today's increased interdisciplinarity, and some of the relatively recent discoveries upon which the field of geobiology rests. Following that is a brief history and description of the field of geobiology and a short discussion of Earth's changing redox regime – the slow incessant widening of which is largely attributed to the impact of life on the geosphere.

Because my work focuses on phosphorus as a nexus between the geosphere and biosphere, I also include a discussion of the importance and global cycle of the element phosphorus and a quick overview of the breadth of fields involved in phosphorus research. Chapter two gives a review of the relationship between microbes and the formation of marine phosphate rock.

From this broad background I then report on my investigation of the influence of microbes on the formation of a ~2 billion-year old phosphorus-rich stromatolitic phosphate rock formation and its implications for the co-evolution of Earth and life (Jhamarkotra, chapter 3). Next I address the challenge of distinguishing bona fide phosphatic microfossils from abiotically created features that may resemble fossils (biogenicity and pseudofossils, chapter 4). Finally, I report on my development of a protocol and apparatus for microscopic observation of mineral

---

[*] *Perhaps more accurately 'metabolism' or 'life' but see background section 'Geobiology.' The scientific definition of life is elusive, and beyond the scope of this dissertation, but see Appendix A, "What is life?" for a brief discussion.*

precipitation over time, that is amenable to unadulterated harvesting for subsequent analysis (apparatus, chapter 5).

Throughout this thesis, the issues of biogenicity, energy gradients, the cycling of elements between the geosphere & biosphere and the co-evolution of life and the Earth, are intertwined.

They are central to this research – fundamental, foundational concepts at the center of expanding fields of scientific enquiry.

Thesis objectives & strategy

This dissertation describes my exploration of the element phosphorus (P) as a link between the geosphere and the biosphere, an exploration approached from two perspectives: The phosphate rock record and experimental precipitation of calcium phosphate minerals (aka apatites). The goal of this work was to explore the influence of microbes on the precipitation of apatite through the following projects:

From the rock record:

1) Examination of microfossils in the 2 billion-year old (Ga) phosphatic Jhamarkotra Formation

Through mineral precipitation experiments:

2) Abiotic reproduction of apatitic morphologies and surface textures resembling features observed in microfossils
3) Development of an apparatus for microscopic observation of precipitation over time

In chapter three I describe paleontological research that incorporates a variety of analyses to ascertain the nature of features observed in ~2 Ga phosphatic rock. The interpretation of the findings bears on our understanding of the Earth's geosphere and biosphere during the Precambrian.

From there, I move on to examine the veracity of putative biogenicity of fossil microbes through experiments designed to test the biogenicity of morphological features (chapter 4), after which I describe, in chapter five, the development and potential of a new apparatus suited to microscopic observation of mineral precipitation over time. In my concluding chapter, I present a quick discussion of the impact of human activity on the global P cycle.

Background

Segmentation of scientific disciplines and trans- and interdisciplinarity

The necessity of survival draws a sharp distinction between the need for empirical knowledge and a search for meaning. Survival being paramount, the questions that arise out of curiosity – such as "when and how did life evolve on Earth?" and the even more basic question "what is life?" – have historically been the province of the non-empirical, or 'idealistic' fields of philosophy, mythology and theology, while empirical knowledge is recognized as the 'more practical' province of science. Yet questions such as these, which are some of humanity's most enduring and enigmatic questions, are increasingly being investigated through rigorous scientific inquiry.

Aristotle, ca. 350 BC, is considered by many to be the father of [western*] science – most notably because his experiential and empirical approach to understanding the Natural World largely established observation and quantification as the fundamental language of scientific exploration. Through new analytical methodologies and ever-increasing analytical resolution, quantified empiricism has produced much new knowledge and has led, and continues to lead, to new and expanded questions, as well as enabling the duplication and testing of hypotheses, so that now the canonical Scientific Method rests firmly on empirical experimentation and analysis.

Yet until relatively recently, scientific explorations were broad, both practically and conceptually, and practitioners were as often considered Naturalists as Scientists (Chalmers, 1936). The relatively modern concept of the physical sciences (chemistry, physics, mathematics, biology and geology) as distinct disciplines grew gradually, initially spurred by the advent of discipline-specific scientific journals ca. 1780 and a resulting refinement and inevitable divergence in the languages and the scientific questions of different disciplines. Over time, these differences effectively distanced the disciplines and led to an academic paradigm in which

---

* *This thesis does not address the contributions of early non-European scientists and philosophers of the East (Africa, India, China, etc.) Extensive exploration into a variety of scientific disciplines and questions was carried out in these cultures, but the early sharing of scientific knowledge between 'east' and 'west' was effectively interrupted by an apparent lull in communication during what is now colloquially called the 'Dark Ages.' The later rise of the European 'Scientific Revolution,' during which the questioning of scientific concepts flourished, led to the explorations and advancing thoughts among European scientists that resulted in an explosive redirecting of scientific endeavors. The subsequent 'Age of Enlightenment' thus built on the foundation of this European exploration.*

"disciplinary boundaries meant that … if one decided to … work in another domain, one had to accept that a change over to another discipline would be necessary." (Smelser and Baltes, 2001).

These basic fields of science, having largely achieved maturity, have now given rise to a 'new generation' of fields that investigate scientific questions specifically at the intersections of fields – interdisciplinary fields that bring to bear the knowledge and approaches of once distinct disciplines.

Despite the potential for confusion between the refined languages of different disciplines (as for instance, acknowledged and addressed by Sleep and Bird (Sleep and Bird, 2008)) we are increasingly aware that many natural phenomenon cannot be fully understood through the lens of a single discipline (Rafols et al., 2010) and as a result, the advantages of interdisciplinary scientific approaches are increasingly recognized and valued. Questions such as "when and how did life evolve on Earth" and "what is life?" which don't fit neatly into one discipline, are now explored as legitimate scientific questions.

In part, this may result from our taking up again age-old questions and examining them from the perspective of increasingly sensitive yet disparate empirical scientific fields, and most certainly is also a result of increased technological capacity. Many scientific fields are flowering in the wake of increased knowledge and technology: astrobiology, geobiology, physiology, genomics – all of which are rooted in various phenomenological observations. Like Aristotle before us, we develop knowledge by observation and contemplation of phenomena. We notice things, measure them, quantify their characteristics, and compare them in order to arrive at a sense of what those things are and how they relate to each other.

The field of geomicrobiology is one in which disciplines previously considered as unrelated are now recognized as intimately linked.

Background : Geobiology

With the exception of paleontology, the realms of geology and biology have generally been taught as quite separate from each other.

Not only are they still generally taught in separated courses in separated disciplines, each discipline has distinguished itself from the other in the way it describes its domain. Geology is the realm of the abiotic, solid material of the Earth, and biology is the realm of living organisms — two fields, still largely taught as fundamentally distinct and separate.

Yet their interrelationship is beginning to be recognized. A simple example is the evolving textbook definition a mineral. One of the long-standing defining characteristics of a mineral is an

abiotic origin: "… a mineral … has been formed as a result of geological processes. … Biogenic substances are chemical compounds produced entirely by biological processes without a geological component and are not regarded as minerals." (Nickel, 1995). More recently, introductory textbooks are tending to shift the focus from that of geological production to a qualification that a mineral be inorganic: "A naturally occurring, *inorganic* crystalline material with a unique chemical composition" (emphasis added) (Tarbuck and Lutgens, 2003) and some are now expanding the definition of minerals to imply the possibility of an organic origin, as "A naturally occurring, solid crystalline substance, *usually inorganic*, with a specific chemical composition." (emphasis added) (Jordan and Grotzinger, 2008).

Today, there is growing recognition among the scientific community of the role of biological processes in the production of (bio)minerals. Most commonly, biominerals form under conditions that have been altered by organisms (pH, ion activity, etc.) and have become conducive to mineral formation (Dunham-Cheatham et al., 2011). Less commonly, a mineral forms under the direction of biological processes, as when diatoms form their siliceous shells, or coccolithophores and foraminifers their calcium carbonate shells – or vertebrates such as us, our calcium-phosphate mineralized bones and teeth.

The conceptual foundation of geobiology has fairly deep roots in Eastern Europe, almost a century before its debut in the West. The Russian microbiologist Sergei Winogradsky's groundbreaking elucidation of chemolithotrophy in 1887 – the ability of microbes to gain energy from chemical reactions involving inorganic electron donors – provided a mechanism for the active involvement of living organisms in the alteration of the geosphere at the elemental level. As noted by Martin Dworkin in his biographical paper on Winogradsky, "While it was Louis Pasteur who introduced the notion of microorganisms as agents of chemical change, *it was Winogradsky who directed that view to the soil* " (emphasis added) bridging the realms of biology and geology (Dworkin, 2012).

Winogradsky's recognition of chemolithotrophy set the stage for the field of geomicrobiology by supplying a functional link between the abiotic world of the geosphere and the metabolic functions of the biosphere (Dworkin, 2012). Around the same time (ca. 1885), the Austrian geologist Eduard Suess published his textbook *Antlitz der Erde* ("Face of the Earth") in which he coined the [German] term "biosphere." Exploring this concept, Vladimir Vernadsky, in his 1926 work *The Biosphere*, defined the biosphere "as a region of transformers that convert cosmic

radiations into active energy in electrical, chemical, mechanical, thermal and other forms." (Vernadsky, 1998).

In the West, the 1961 Woodring Conference on Major Biologic Innovations and the Geological Record was a marker in the nascent field of geobiology, and one in which micropaleontology joined the field (Cloud and Abelson, 1961; Cloud, 1976). In the conference proceedings, paleontologist Preston Cloud described the field he termed 'biogeology': "[…the field of biogeology] bears on our understanding of life processes in crustal evolution – biological, paleontological, sedimentological, and chemical, including biochemical, geochemical, and cosmochemical" effectively shifting the focus of the term from that of a region, to a variety of processes.

As noted above, Vernadksy's concept of the biosphere was rooted in photosynthesis (more specifically, 'conversion of cosmic radiations') and, despite the potential of chemolithotrophy, the belief that the energy of sunlight (photons) fuels all of life remained largely unquestioned. And yet, although it is believed to represent only ≤ 1% of primary production, chemolithotrophy is an agent of carbon fixation and the transfer of elements, particularly the metallic elements, between the geosphere and the biosphere.

With the 1977 discovery of an active biosphere at deep-sea vents where sunlight is not available to support life, the field of biology suddenly expanded to include a new, non-solar paradigm. (Corliss et al., 1979; Jannasch and Wirsen, 1979; Jørgensen and Boetius, 2007; Sievert and Vetriani, 2012). This unexpected discovery threw a spotlight on the role of chemolithotrophy and the interplay between the geosphere and the biosphere. Today geobiologists recognize that microbes tend to evolve to take advantage of any energy gradient that is available and accessible to them (Lane, 2006) and geobiology research since then has flourished.

The advent and growth of genetics technology has given us a window into the variety of metabolic pathways and mechanisms by which microbes cycle inorganic elements (Newman and Banfield, 2002) and an expanded ability to detect and interpret stable isotopes has provided evidence of life on Earth as early as 3.5 Ga. (Canfield et al., 2000; Farquhar et al., 2000; Canfield, 2006) by providing us an additional tool for the detection and characterization of elusive biosignatures.

And so, once seen as distinct, the geosphere and the biosphere are increasingly recognized as intimately connected, parts of a larger system within which they affect and are affected by each

other. Whether or not an encompassing Gaia Hypothesis[*] (Lovelock, 1972) suitably describes the Earth system, it is clear that at least at the local level – and particularly at the local level – the relationship between the geo- and biosphere involves a dynamic interplay of chemistry and physics, toward a thermodynamic equilibrium seeking to resolve environmental energy gradients while accessing the resultant flow of energy. Or, as succinctly put by Falkowski (2006) "metabolic pathways evolved to form an interdependent, planetary 'electron market' where reductants and oxidants are traded across the globe." (p1) (Falkowski, 2006). Such trading is accomplished through redox reactions.

Background : Redox review

In 1926, Albert Jan Kluyver and Hendrick Jean Louise Donker published "Die Einheit in der Biochemie" (Unity in Biochemistry) in which they describe hydrogen transfer as the basis of metabolic reactions (Kluyver and Donker, 1926).

And indeed, life is driven by the capture and controlled utilization of electron energy, driven by flow along a redox gradient, either present in the environment or initiated by the energy of photons. Where there exists a gradient (defined here simply as a difference in adjacent concentrations of some property) there exists a drive toward equilibrium. In the case of electrons that property is electronegativity, the ability of an atom[†] to attract electrons toward itself and away from others in oxidation-reduction (redox) reactions. In such a system, the magnitude of the gradient is the redox potential of that system, with the more reduced substance the one with the lowest (most negative, or electron-rich) charge.

An electron (aka redox) gradient occurs where atoms near enough to affect each other have different electronegativities. However, a flow toward equilibrium, or the transfer of an electron from one molecule toward another, is often impeded by the amount of energy required to initiate the flow – the amount of energy required to pull the electron away from the contributing atom – which is the reaction's activation energy requirement.

---

[*] *Gaia Hypothesis: The belief that the geosphere and living organisms are involved in an ongoing feedback dynamic by which conditions conducive to life [on Earth] are maintained. From the seminal work in which James Lovelock proposed the term 'Gaia' for his hypothesis: "life at an early stage of its evolution acquired the capacity to control the global environment to suit its needs and … this capacity has persisted and is still in active use."*

[†] *…or functional group, the part of a molecule that carries the most charge and is therefore most reactive.*

Redox reactions are not the exclusive domain of life – inorganic redox reactions, such as the common example of rusting (the oxidation of Fe(II) by O_2) also occur. The Fe(II) ion is soluble under non-oxygenated conditions, where there is no O_2 to oxidize it, but once oxygen is available, oxidation proceeds quickly. Despite how commonly we encounter this example, many inorganic redox reactions are inhibited by the activation energy requirement [were this not the case, (closed) systems would spontaneously proceed toward equilibrium, reducing the redox potential to eventually result in an inert system.]

This inhibition is overcome by the addition of heat energy in the familiar case of fire, in which a 'burning' material is rapidly oxidized by oxygen. In many cases, however, activation energy requirements significantly inhibit inorganic redox reactions, holding them in check, thus maintaining the redox gradient. The ability of organisms to tap such a redox gradient is gained by biological synthesis of catalytic enzymes that reduce the amount of activation energy required to initiate the transfer of the electron(s) into the cellular metabolic pathways that support life.

On Earth today, oxygen is the most prevalent strong oxidant available. Oxygen's ubiquity in Earth's atmosphere (as O_2), combined with its high electronegativity, is what drives the metabolic processes that sustain animal life on Earth – including ours. But free oxygen was rare on early Earth, although water was not.

Discussion : Oxygen and the evolution of the Earth and early life

Early Earth, including its atmosphere and oceans, was generally reduced and anoxic. Today, Earth's atmosphere has ~21% O_2 content (by volume). Where did this oxygen come from?

Identification of filamentous microfossils in stromatolites of the ~3.465 Ga Apex chert (Schopf and Packer, 1987) suggested a mechanism for the rise of molecular oxygen through microbial oxygenic photosynthesis, and today the rise of atmospheric oxygen is attributed primarily to the emergence and rise of cyanobacteria, microbes able to utilize the energy of light (photons) to strip electrons from liquid water and divert them to drive biochemical redox reactions – in the process releasing unutilized ('waste') molecular oxygen, as shown in equation 1, below.

Water-splitting & concomitant generation of molecular oxygen:

$$2H_2O + h\nu = 4H^+ + 4e^- + O_2 \qquad 1$$

Based on fossil evidence of stromatolites microbial mats and isotope records, it is generally believed that marine oxygenic photosynthesis was in play by ~3.5 Ga (Schidlowski et al., 1983; Schopf and Packer, 1987; De Gregorio and Sharp, 2006) though the details of the development of marine oxygenic photosynthesis, as well as the details of the oxygenation of Earth's atmosphere are still debated. However, it is generally believed (though not undisputed) that by ~2.2 Ga, Earth's atmosphere contained ≥10% present levels of oxygen, likely a consequence of near-shore stromatolite-forming oxygenic phototrophs that may have increased pO_2 locally i.e. (Holland, 1999; Nisbet et al., 2007; Petsch, 2010), and recent work suggests that the oxygenation of Earth's atmosphere may have been underway as early as 3 Ga (Crowe et al., 2013), hundreds of millions of years before the 'Great Oxidation Event' of ~2.3 Ga.

With the microbial release of oxygen, first niche (small-scale local) and then global redox potential would have expanded, enabling life to increase in both diversity and size and heralding a ~thousand-fold expansion of the number of metabolic reactions, as aerobes evolved to utilize the strong electronegativity of O_2[*] (Falkowski, 2006).

Not only was the evolution of life impacted by the rise of oxygen, so too was the evolution of Earth's mineralogy itself, as free O_2 induced the formation of oxides and other minerals that require oxygenated conditions for their stability – expanding the number of minerals on Earth an order of magnitude, from ~ 400 to > 4500 (Hazen and Ferry, 2010). In addition, the motility of organisms plays a part in the relocation of a variety of elements, affecting their flux rates and pool sizes. Figure 18 shows the generally accepted geologic history of the oxygenation of Earth's atmosphere and the general nature of Earth's evolving ocean chemistry.

But how did we learn that organisms are involved in the release of this powerful oxidant?

Background : Discovery of oxygen & photosynthesis

In the late 1700s the French chemist Antoine Lavoisier experimentally isolated and named the element oxygen, but it was the English theologian and chemist Joseph Priestley who

[*] *Quoting Falkowski, 2006: "O_2 is predicted to be either directly involved in, or indirectly associated with, more than 10^3 metabolic reactions not found in anaerobes. Hence, the evolution of O_2 not only created redox energy couples that would allow complex animal life to evolve in the Ediacarian and Cambrian periods (approximately 630 to 490 million years ago), but also precipitated an evolutionary explosion of unpredictable, alternative, as well as novel pathways …"*

discovered the effects of photosynthesis in plants when he established in 1771 that plants produced a gas able to sustain [animal] life. By the end of the decade, this effect had been expanded into an understanding of oxygenic photosynthesis by Jan Ingenhousz (Canfield, 2014) (equation 3, below).

In 1931, Keita Shibata published a theory of photosynthesis that involved the photo-dissociation of water, in which the photon energy of light drives the oxidation of water and splits water molecules into constituent protons, electrons and molecular oxygen (equation 2, below).

Shortly thereafter, in the early 1930s, Cornelius B. van Niel published the then revolutionary concept that anoxygenic photoautotrophy (reduction of CO_2) (equation 4, below) was possible, and, furthermore, performed by (some) bacteria (Gest and Blankenship, 2004).

Despite the clearly recognized fact that microbes predate plants, some recent introductory Earth Science textbooks still attribute Earth's oxygenation solely to the photosynthesis of green plants (Tarbuck and Lutgens, 2003) while some are beginning to attribute photosynthesis to "green plants, algae, and certain types of bacteria" (Jordan and Grotzinger, 2008).

Water-splitting & concomitant generation of molecular oxygen:

$$2H_2O + h\nu = 4H^+ + 4e^- + O_2 \quad (2)$$

Oxygenic photosynthesis:

$$CO_2 + H_2O + h\nu = CH_2O + O_2 \quad (3)$$

Anoxygenic photosynthesis:

$$CO_2 + 2H_2A + h\nu = CH_2O + H_2O + 2A \quad (4)$$

Where H_2A is an electron donor but need not be H_2O

Background : P interest, broadly & specifically

Biogeochemistry and the impact of microbes on the evolution of Earth's atmosphere has now been recognized and studied for decades (Gest and Blankenship, 2004), but recent advances in research have highlighted the extent of the role of microbes in the cycling of numerous elements of Earth.

There is arguably no more direct example of the relationship between the geosphere and the biosphere than the phosphorus cycle. Phosphorus (P) cycles between the geosphere, where it

occurs as a variety of P-containing minerals – most commonly calcium phosphate minerals within the apatite group – and the biosphere as an element necessary to life and found in every cell of every organism, incorporated into a variety of biomolecules including those which carry cellular genetic information (DNA, RNA), phospholipid membranes, and the adenosine phosphates (ATP, ADP and AMP) which serve as a form of energy currency within cells. This ubiquity makes P well suited as a lens through which to investigate a number of fields (Westheimer, 1987), and phosphorus-related research is conducted in fields as varied as health-related disciplines such as dentistry (teeth/calculus) nephrology (kidney stones) orthopedics (bone repair/replacement) and cardiology (arteriosclerosis); and waste water treatment (P removal) environmental sciences (lake eutrophication) and geology (mining/remediation), oceanography and microbiology. Of these, the environmental sciences and waste water treatment research have been most active in exploring the impact of microbes on environmental phosphate cycling. Nonetheless, much of the microbe-mineral research has not focused on phosphorus. For instance, significant environmental research on microbe-mineral interactions includes work on acid mine drainage with a focus on iron microbes (Banfield et al., 2000; Newman and Banfield, 2002; Dold, 2014; Williams et al., 2016) and much marine microbe-mineral research has been done not on apatite, but rather on calcite. (Berner, 1965; Visscher and Sciences, 2000; Dupraz et al., 2009).

Discussion : Nature & significance of P & phosphate bonds

Unlike some elemental cycles, P is largely limited to the solid and aqueous phases. Despite the importance of phosphorus to life, it is only the 11th most abundant element of Earth's crust, ~ 0.1% by mass (Paytan and McLaughlin, 2007). Gaseous phosphine (PH_3) has been detected in natural environments (ng/m^3 levels in the atmosphere at 'locations around the world') but is not favored to be produced abiotically (Roels and Verstraete, 2001). Hence it is thought to be produced biologically, though not for energy conservation as the reduction of phosphate to phosphine is endergonic when adjusted for natural conditions by Nernst.*

Elemental phosphorus has the electron configuration [Ne] $3s^2$ $3p^3$ and forms the $P^{(V)}$ (P^{5+}) cation. As such, it is three electrons shy of the most stable atomic (full octet) configuration.

* *But as noted by Roels and Verstraete (2001), nitrogen fixation, a process vital to life, is an extremely costly process and yet happens, so we may yet discover biotic reduction of phosphate to phosphine, though this is controversial.*

Hence, instead of existing in its elemental form, phosphorus is readily oxidized as the three outer shell electrons of the P^{5+} cation are attracted by, and shifted toward, available oxidants. On Earth, since oxygen is a (generally) ubiquitous and strong oxidant, phosphorus is almost always found in its oxidized form, the phosphate ion, PO_4^{3-} (Essington, 2004). Where phosphorus is referred to as reactive, it is most commonly the phosphate ion that is meant, and it is this tetrahedral phosphate ion that enters into the bonds so critical to life. The strongly negative, trivalent charge of the phosphate ion renders it an active anion that behaves as a unit that readily binds with other ions. In ATP, for instance, when anhydride bonds joining the three phosphate ions are broken, both phosphate ions and energy are released in an exergonic reaction. The free energy associated with this exergonic hydrolysis is biologically coupled to various endergonic metabolic reactions, and the phosphate is recycled.

Because P is required for life, phosphate-rich rocks are mined for use in agricultural fertilizers. Increasing fertilizer demand is foreshadowing a depletion of P-containing reserves, while at the same time, field runoff of P-containing fertilizers too often results in bodies of water in which the rapid recycling of P into biomass ultimately results in oxygen depletion and eutrophication. The drawdown and potential dearth of mineable phosphate (Cordell et al., 2009) has implications for life, giving our understanding of the P cycle heightened significance, and provides another link between the geosphere and biosphere, this one freighted with the implications of our increasing use of global phosphate reserves.

Geologically, apatite group minerals form under both igneous and sedimentary conditions. Apatite group minerals are found in diluted concentrations in many marine sediments, but is most commonly found concentrated in phosphorites, masses of apatite-rich sedimentary rock, which contributes ~80% of the mined phosphate rock (Van Kauwenbergh, 2010). Of phosphorites forming today, most are found in association with distinctive microbial mats of sulfide-oxidizing bacteria (SOxB) found in marine upwelling zones. This proximity of SOxB to modern phosphorites, as well as the ability of some microbes to take up and store phosphate and later expel it in pulses (Schulz and Schulz, 2005; Brock and Schulz-Vogt, 2011) and experimental evidence of the flow of phosphate through microbial biomass into precipitated apatite (Goldhammer et al., 2010) all strongly suggest that the precipitation of sedimentary apatite may be microbially mediated.

The next chapter provides an overview of the role of microbes in the formation of modern and ancient phosphorites.

Chapter 2

—

Microbes and the formation of phosphate rock

The role of microbes in the formation of modern and ancient phosphatic mineral deposits

Chris H. Crosby and Jake V. Bailey

Department of Earth Sciences, University of Minnesota-Twin Cities, Minneapolis, MN 55455

Published in 'Frontiers of Microbiology' 05 July 2012 doi: 10.3389/fmicr.2012.00241

The formation of marine phosphatic mineral deposits remains incompletely understood, despite decades of research. The involvement of bacteria in this process has long been suspected, and both modern and ancient associations between bacteria and phosphorites have been recorded. Only recently has a specific bacterial metabolic process associated with the formation of phosphorites been discovered. Recent studies demonstrate that polyphosphate utilization by sulfide-oxidizing bacteria results in the rapid precipitation of apatite – providing at least a partial mechanism to explain the close spatial correlation between accumulations of sulfide-oxidizing bacteria and modern phosphorites. Possible fossilized bacteria are known from ancient phosphatic mineral deposits. Potentially, the fossilized cells represent the remains of bacteria that induced the formation of those phosphorites. However, robust criteria for the recognition of these bacteria have yet to be identified.

The Phosphorous Cycle and Phosphatic Mineral Deposits

Phosphorus (P) is one of the few elements that all life requires. Phosphorus is a constituent of the molecules of genetic information, energy currency, and many membranes of living organisms (Sterner and Elser, 2002). In addition, polymers of P (polyphosphates, aka PolyP) serve in a wide variety of active cellular functions (Achbergerova and Nahalka, 2011). As a limiting nutrient for primary productivity, phosphorus is rapidly recycled in the environment, limiting its accumulation in sediments (e.g., (Benitez-Nelson, 2000). While most organic matter and its

associated phosphorus is transformed into an inorganic state and recycled in the water column, some organic phosphorus reaches the sediments as particulate organic matter such as phytodetritus and fish debris (Suess, 1981). Additionally, phosphate commonly adsorbs to iron oxyhydroxides, including on the surfaces of clay particles and colloids, that are eventually deposited in the sediment (Krom and Berner, 1980; Crosby et al., 1984). As they become buried in sediment, iron minerals encounter a zone in which bacterial dissimilatory iron reduction commonly results in the dissolution of iron oxides and the concomitant release of HPO_4^{2-} (Ruttenberg and Berner, 1993). The ubiquitous degradation of organic compounds and dissolution of Fe-oxides in the sediments thus limits the sedimentary accumulation of P. However, under still not fully constrained conditions, the complex interaction of biological concentration, mineral precipitation, and sedimentary reworking results in the concentration of phosphorus in the form of phosphorite rock deposits (Cook, 1976; Sheldon, 1981; Glenn et al., 1994; Krajewski et al., 1994; Föllmi, 1996; Schulz and Schulz, 2005; Dornbos, 2010; Filippelli, 2011).

Phosphorites are relatively rare marine sedimentary units containing significant amounts of P resulting from the concentration of the mineral apatite $Ca_5(PO_4)_3(F,Cl,OH)$, or its more complex form carbonate fluorapatite (CFA) (Nathan, 1984). Phosphorites contain 6% to 18% P_2O_5, distinguishing them from most sedimentary rock and marine sediments, which generally have less than 0.3 wt % P_2O_5 (Van Cappellen and Berner, 1988; Jarvis et al., 1994). Phosphate rock, in a range of morphologies including phosphorite mud, laminae, crusts, pellets, nodules, skeletal fragments, and cements has been recognized in geologic rock strata since the late 1700s (Glenn et al., 1994; Föllmi, 1996; Rakovan, 2002). The discovery of a way to extract phosphate from phosphorites led to a heightened interest in the use of phosphate as a fertilizer, where it now accounts for approximately 85% of the world's phosphate consumption. Phosphorites have now been identified in ancient sedimentary rock strata on every continent, but it wasn't until the British "Challenger" expedition of 1873-1876 that geologically recent phosphorites were recovered from modern marine sediments of the Agulhas Bank area off South Africa (Murray and Renard, 1891). Since then, extensive phosphorites have been found to be forming under the low-latitude upwelling zones on the western shelves and continental margins of North and South America, Africa and India, as well as off the east coast of Australia, extending the age of known phosphorite formations from the Proterozoic to the present (Baturin et al., 1972; Parker and Andseisser, 1972; Veeh et al., 1973; Burnett et al., 1980; Sheldon, 1981). But what processes and mechanism(s) are responsible for the formation of these enigmatic geological deposits?

The formation of phosphorites in modern sediments

Understanding the processes that lead to the deposition of phosphatic minerals is necessary for understanding the distribution and occurrence of this important non-renewable resource and its place within the broader phosphorous cycle. The process of phosphogenesis begins with the precipitation of CFA or its metastable precursors within the top few centimeters of marine sediment. It is generally thought that disseminated CFA is then concentrated through a variety of sedimentological processes such as reworking. Concentrated CFA can undergo additional diagenetic transformations such as the precipitation of additional authigenic apatite or carbonate precipitation, perhaps accompanied by multiple cycles of sedimentary reworking (e.g. Baturin cycles and variations thereof). The details of this process are beyond the scope of this review, but see Filippelli (2011) for a recent review.

The majority of modern and ancient phosphorites are associated with sediments beneath coastal upwelling zones and these are the subject of active research and the following discussion. Briefly, in upwelling zones, nutrient-rich waters stimulate primary productivity in the photic zone that results in a downward flux of phytodetritus, much of which can accumulate in the sediments due to the high organic flux, high biological oxygen demand, and short sinking transit time on the shallow continental shelf. Some combination of biochemical and geochemical mechanisms then act to release P and inhibit its recycling back into the water column. Pore water conditions that are supersaturated and kinetically favorable for the precipitation of apatite then result in mineral precipitation that proceeds through the initial formation of amorphous apatite precursors or other metastable precursors that eventually transform into CFA (Nancollas et al., 1979; Gunnars et al., 2004; Omelon and Grynpas, 2008).

Various mechanisms and pathways have been proposed to produce conditions favoring the precipitation of apatite precursors. One model invoking direct microbial involvement, with both experimental and in situ evidence to support it, involves polyphosphate utilization by sulfide-oxidizing bacteria (Schulz and Schulz, 2005). In shelf sediments beneath eutrophic marine waters, such as the subtropical eastern boundary current regions, high rates of aerobic remineralization in the water column followed by bacterial dissimilatory sulfate reduction in the sediments lead to oxygen depletion and production of copious hydrogen sulfide in the sediments (Jørgensen, 1982). These conditions stimulate the growth of chemolithotrophic sulfide-oxidizing bacteria that oxidize the sulfide using oxygen or nitrate as terminal electron acceptor (Jørgensen, 1977; Robertson and Kuenen, 2006; Lavik et al., 2009). Gammaproteobacteria that oxidize sulfide in these settings include among others, the conspicuous vacuolated sulfur bacteria,

Beggiatoa sp., *Thioploca*, and *Thiomargarita* sp. (Jørgensen and Gallardo, 1999; Schulz et al., 2000; Schulz and Schulz, 2005; Salman et al., 2011). Schulz and Schulz (2005) noted not just a regional correlation between the habitats of these sulfide-oxidizing bacteria, but also an intimate spatial association in the sediments between mats of *Thiomargarita namibiensis* and enrichment in pore water phosphate and apatite. Schulz and Schulz (2005) also proposed a mechanism to explain this correlation by demonstrating that *Thiomargarita* take up and store polyphosphate intracellularly. Through subsequent polyphosphate hydrolysis, they release enough phosphate as a pulse within a few centimeters of the sediment-water interface to account for the enriched pore water P and precipitation of hydroxyapatite observed in *Thiomargarita*-inhabited sediments. This mechanism was later revised by Brock and Schulz-Vogt (2011) with laboratory investigations of *Beggiatoa* that suggest exposure to sulfidic conditions initiates the utilization of stored polyphosphate in *Beggiatoa* and perhaps also in its close relative, *Thiomargarita*. Recently, Goldhammer et al., (2010) have documented the microbial uptake of ^{33}P-labelled phosphate that rapidly passes from intracellular polyphosphate and into precipitated apatite, strengthening the evidence of active microbial processing of P culminating in apatite precipitation. The isotope labeling experiments of Goldhammer et al. (2010) demonstrate that phosphate sequestration in apatite occurs at a rate of 69-78 nmol cm^{-2} day^{-1} under anoxic conditions, exceeding phosphate release from organic matter remineralization (9 to 36 nmol cm^{-2} day^{-1}). The rate of phosphate released by *Thiomargarita* in the laboratory was calculated to be sufficient to explain the mineral and pore water phosphate enrichment observed in phosphogenic sediments off of Namibia (Schulz and Schulz, 2005). Thus, polyphosphate accumulating sulfide-oxidizing bacteria, experiencing alternating aerobic – anaerobic regimes, appear to be influential in the focusing of pore water phosphate where apatite precursors are actively forming.

Other microbial processes might also be important for phosphate enrichment in certain shallow marine sediments. Work by Arning et al. (2008, 2009) attributes the build-up of pore water P to release from organics by sulfate-reducing bacteria, perhaps funneling P to polyphosphate-utilizing vacuolated sulfur bacteria. Investigations by Lucas & Prevot (1985) and Hirschler (1990) present evidence of P accumulation by enzymatic breakdown of P-rich molecules like DNA, by alkaline phosphatase. It should be mentioned that polyphosphate utilization is by no means unique to the sulfide-oxidizing bacteria, and considerable attention is given to the role of polyphosphate accumulating bacteria in wastewater (Mino et al., 1987; Ohtake et al., 1998; Crocetti et al., 2000). Bacteria not know to accumulate substantial polyphosphate, such as the common heterotrophic alphaproteobacterium, *Caulobacter crescentus,*

when cultured in the presence of high calcium concentration, precipitated minor amounts of carbonate hydroxyapatite (Benzerara et al., 2004), hence the processes that result in apatite precipitation in phosphogenic settings may be more complex than simple uptake and pulsed release of phosphate. Indeed, concentrations of phosphate in eutrophic lacustrine waters can become elevated (Penn et al., 2000), and yet the documented formation of calcium phosphate minerals in lake sediments is uncommon (Swirydczuk et al., 1981). Factors such as pH, redox potential (Eh), and the presence of other ions, as well as the existence of a suitable nucleation site and sufficient energy to activate precipitation, all have an effect on the rate and degree of precipitation. Microbial activity may influence these factors, particularly in fluids associated with microbial mats or heavily colonized sediments. For example, sulfide oxidation using oxygen as a terminal electron acceptor can produce acid:

$H_2S + 2O_2 \rightarrow 2H^+ + SO_4^{2-}$ manuscript equation (1)

While sulfide oxidation with nitrate as the terminal electron acceptor consumes protons, whether it proceeds via denitrification:

$5HS^- + 8NO_3^- + 3H^+ \rightarrow 5SO_4^{2-} + 4N_2 + 4H_2O$ manuscript equation (2)

or dissimilatory nitrate-reducing ammonification:

$HS^- + NO_3^- + H^+ + H_2O \rightarrow SO_4^{2-} + NH_4^+$ manuscript equation (3)

In addition to the effects of active microbial metabolisms, the chemistry of the cell ultrastructure can influence mineral precipitation. For example, charged cell walls and/or extracellular polymeric substances may bind ions, provide nucleation sites, and lower the activation energy required for precipitation (Ferris, 1989).

While considerable evidence supports the conclusion that polyphosphate utilization by sulfide-oxidizing bacteria contributes to apatite formation, this may not be the only microbial process involved in phosphogenesis. Though less commonly, phosphorite formation is known to occur in non-upwelling regimes (e.g., Ruttenberg and Berner, 1993) where the mechanisms for its deposition may differ markedly from those just described. For example, under anoxic conditions, dissimilatory iron reduction can dissolve iron-bearing minerals, releasing and concentrating adsorbed P in the pore water. Soluble reduced iron diffuses into bottom waters, precipitates, adsorbs more P, and sinks again, establishing an “iron-redox pump” whereby pore water P may be concentrated without direct concentration by microorganisms.

Microbes and ancient phosphorites

While microbes are thought to play a role in the apatite precipitation that leads to modern phosphorite formation, their role in ancient phosphogenesis is less clear. However, for many geological phenomena the present is the key to the past, and a number of microfossils and geochemical indicators suggest that microorganisms played an important role in the formation of ancient phosphatic deposits.

Phosphorites are known throughout much of the rock record, beginning with relatively minor phosphorites in the Paleoproterozoic (Papineau, 2010). Widespread volumetrically-substantial phosphorites first occur during the Neoproterozoic-Cambrian transition, and afterward the occurrence of phosphorites is episodic and their abundances fluctuate substantially, with the Permian, Eocene, Miocene, and the Recent as intervals marked by substantial phosphorite formation (Cook, 1976; Cook and McElhinny, 1979; Cook and Shergold, 1986; Notholt and Sheldon, 1986; Riggs and Sheldon, 1990; Cook et al., 1990). Perhaps the most prominent phosphogenic episode in Earth's history occurred during the Neoproterozoic and continued across the Cambrian-Precambrian boundary ~600-550 Ma (Cook and Shergold, 1984). These phosphorites are associated with times of low latitude glaciation, the spread of oxygen into benthic settings, the rifting of continents, sea level rise, and excursions of stable isotopes of sulfur and carbon (McFadden et al., 2008; Li et al., 2010; Planavsky et al., 2010). Many late Proterozoic and Cambrian phosphorites include episodes of black organic shales and pyritized materials, indicating at least locally sulfidic or stratified sulfidic conditions which may have supported extensive communities of sulfide-oxidizing bacteria (Cook and Shergold, 1984).

The proliferation of phosphorites across the Precambrian-Cambrian transition also occurs during an interval that records the origin and evolution of early metazoan life (Canfield et al., 2007). The ~600 Ma Doushantuo phosphorites of South China contain microfossils currently under study and variously interpreted as metazoan diapause-stage embryos, sulfide-oxidizing bacteria, and protists (Xiao et al., 1998; Bailey et al., 2007; Yin et al., 2007; Cunningham et al., 2011; Huldtgren et al., 2011). Following the Neoproterozoic-Cambrian phosphorite proliferation, phosphorite occurrences are episodic. Extensive phosphorites are known from the Permian, such as the Phosphoria Formation of the Western United States (Emigh, 1958; Cook, 1970), the Cretaceous to Eocene including the South Tethyan Phosphogenic Province (Pufahl et al., 2003), and the Miocene, including the Monterey Formation (Garrison et al., 1990) among others. The episodic timing of phosphorite deposition throughout geologic time may represent an interplay between the evolution of the geochemistry of marine waters, establishment of gradients

between sulfidic and oxygenated waters, and the evolution of microbes able to exploit those geochemical conditions and gradients. Alternatively, or additionally, geologic intervals rich in phosphatic mineral deposits may simply represent relatively rare confluences of biological, sedimentological, tectonic, and ocean geochemical conditions resulting in massive phosphorite deposits (Filippelli, 2011).

But what evidence is there that microbial activity influenced the deposition of ancient phosphorites? Possible apatite-bound bacterial microfossils in phosphorites were first described by Cayeux in 1936 and have since been found in phosphorite outcrops of many geologic ages (Cayeux, 1936; Riggs, 1979; Soudry and Champetier, 1983; Williams and Reimers, 1983; Garrison and Kastner, 1990; Baturin et al., 2000; Soudry, 2000). Several workers have suggested that these possible bacterial fossils represent microbes capable of mediating phosphorite formation (O'Brian and Veeh, 1980; Williams and Reimers, 1983; Lamboy, 1990; Bailey et al., 2007). For example, the apparent remains of microbial mats within phosphate-rich laminations deposited below the photic zone in the Miocene Monterey Formation lead investigators to suggest that sulfide-oxidizing bacteria had been involved in phosphogenesis (Williams and Reimers, 1983; Williams, 1984; Reimers et al., 1990). However, the rather nondescript bacterial filaments put forward by Williams and Reimers (1983) include few morphological or geochemical features that could support their interpretation as the remains of sulfide-oxidizing bacteria. In addition to microfossils, phosphatic stromatolites provide possible evidence of the microbial-mediation of phosphorite mineral precipitation (Banerjee, 1971; Krajewski et al., 2000). However, at present none of these microfossils or sedimentary structures contain strong diagnostic indicators that the phosphatized cells represent sulfide-oxidizing bacteria, or that the organisms preserved were involved in the phosphatization process. The identification of sulfide-oxidizing bacteria associated with the ancient phosphorite record has the potential to uncover the history of bacterial interactions with the marine phosphorous cycle, but diagnostic features that can be preserved in the ancient rock record will be required in order to conclusively identify them.

Concluding remarks and unanswered questions

It seems that we are in the midst of a revolution in our understanding of the origins of phosphatic mineral deposits. Knowledge gained in fields as varied as wastewater treatment, geochemistry, and paleontology have all strengthened the argument for the role of microbes in the precipitation of apatite and the formation of phosphorite rock. A compelling mechanism for the concentration of phosphate in pore waters where apatite is actively precipitating has been

discovered in the form of polyphosphate utilization by vacuolated sulfide-oxidizing bacteria. Many gaps remain in our understanding of the complete story. The processes and substrates involved in the transition from pore waters enriched in phosphate to the precipitation of apatite precursors remain poorly constrained. Eventual cultivation of vacuolated sulfide-oxidizing bacteria may allow for the experimental recreation of microbially-mediated apatite precipitation in the lab. The rapid advancement of genomic and metagenomic approaches may bring us closer to understanding the genes involved in polyphosphate utilization, or help us understand community interactions in sediments where phosphogenesis is occurring.

Fossilized microbes have been identified in ancient phosphorites, and potentially some microfossils from ancient settings record the presence of sulfide-oxidizing bacteria. However, morphological criteria can frequently be insufficient for the identification of specific bacterial ecotypes. Future discovery and confirmation of evidence for microbially-mediated phosphogenesis in the ancient rock record would be aided by the identification of diagnostic chemical signatures of microbes, such as lipid biomarkers, or signatures of the microbially-mediated phosphatization process itself – perhaps a distinctive isotopic signature in phosphate-associated geochemical species. Additional investigation into the role of changing geological and oceanographic conditions in the production and preservation of ancient phosphorites, as well as sedimentary basin analysis, may reveal potentially relevant paleophysiographic features such as cratonic placement and orientation, or detailed isotopic characterization of phosphatic lithologies.

Phosphorite formation requires interactions among many aspects of the geosphere and biosphere, and a comprehensive understanding of the processes involved will require a multi-disciplinary approach applied to both modern phosphogenic environments and their ancient analogues. The results could have important ramifications for the exploration and sustainable management of this mineral resource so intimately connected to the global phosphorous cycle and to modern agriculture.

Acknowledgments

We thank Dan Jones and three anonymous reviewers for comments that helped improve this mini-review. JVB and CHC are supported by NSF CAREER grant EAR-1057119.

Conflict of Interest Statement

The authors declare no commercial or financial relationships that could be construed as a potential conflict of interest.

Figures

Figure 01 | **The phosphorous cycle**

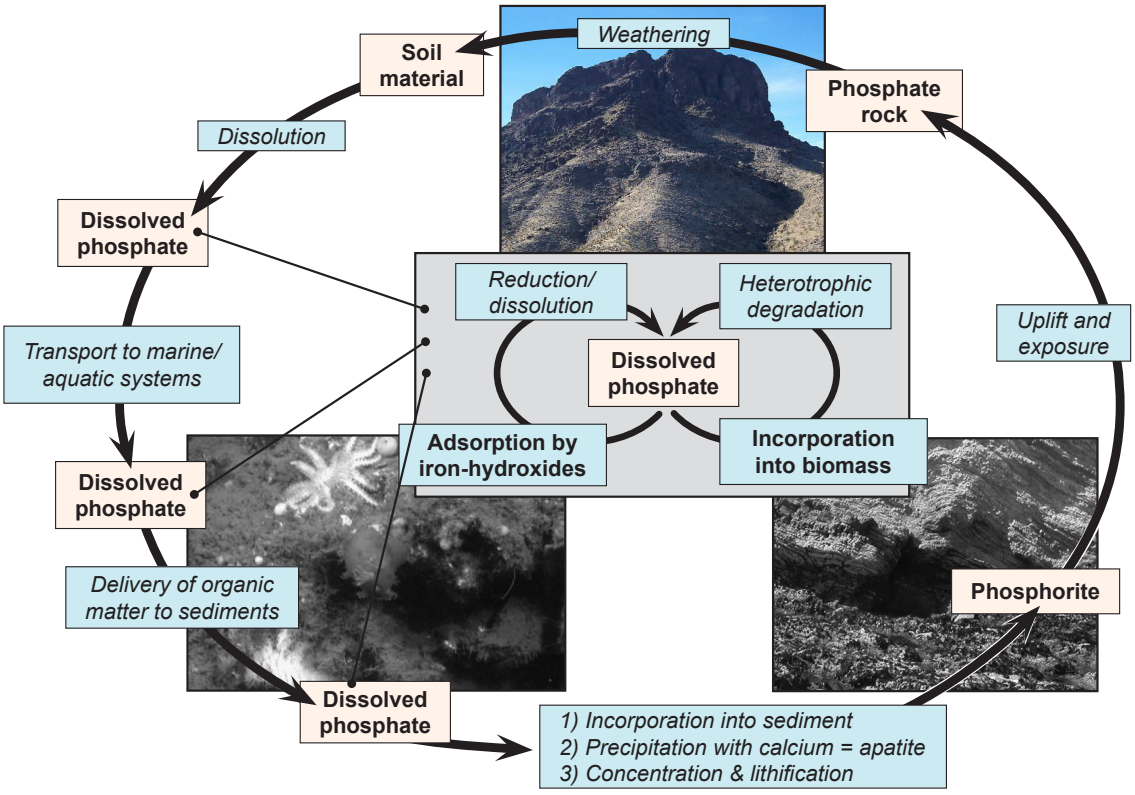

The phosphorus cycle, showing the complexity of phosphorus cycling and relative inaccessibility of phosphorus once it has been lithified. The inset reflects a cycle through which phosphorus can cycle repeatedly wherever the biosphere can access it.

Figure 02 | **Phosphorites, phosphate rock and fossils**

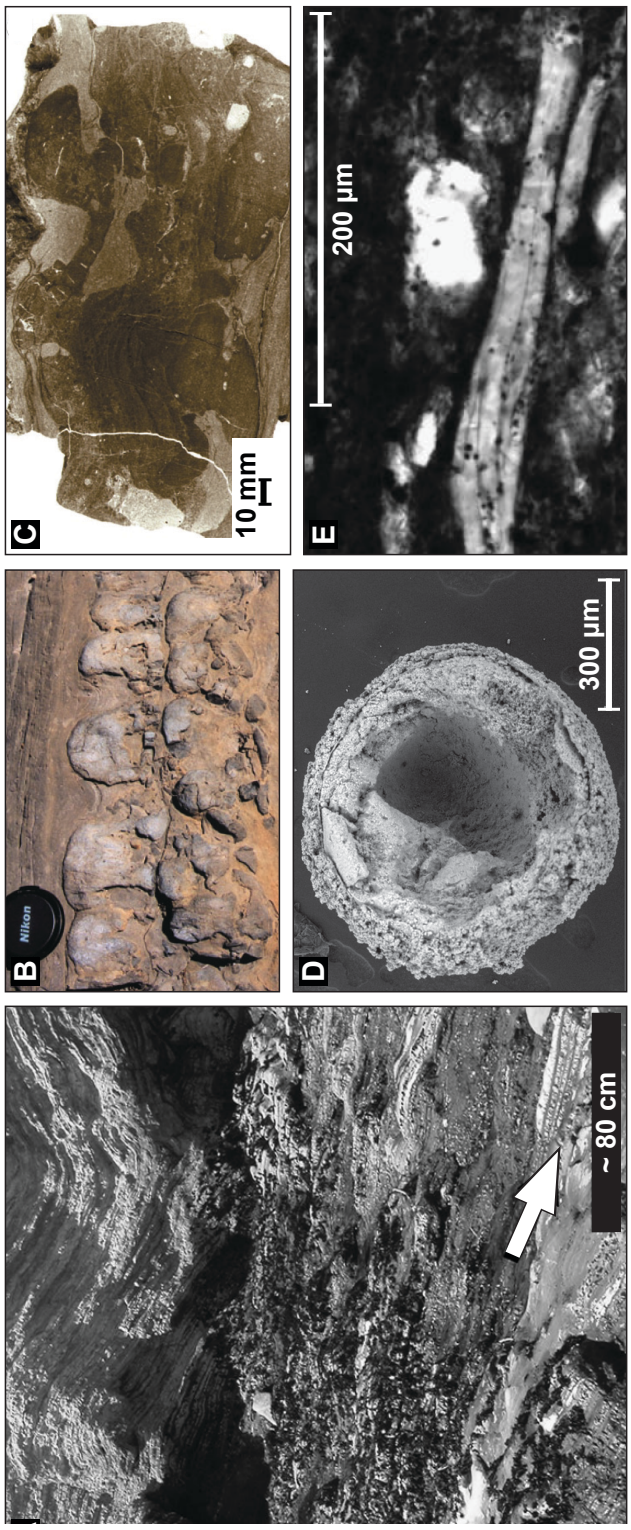

(**A**) Phosphorites (arrow) overlain by diatomites from the Miocene Monterey Formation at Shell Beach, California, preserve filaments in E. (**B**) Phosphatic microbialite in condensed horizon developed in OC-rich sandy mudstone horizon. Winnowed phosphate nodules are incorporated in the microbialite. (**C**) Intergrowth of columnar and flat-laminated phosphatic structures developed as a result of microbial mat growth and sediment phosphatization in OC-rich sandy mudstone. Vertical section, polished surface after staining to obtain color contrast between phosphatic and nonphosphatic sediment. (**D**) SEM of ~600 Ma Doushantuo microfossil showing layering reminiscent of cell membrane. (**E**) Bundle of large phosphatized filaments resembles filamentous sulfide-oxidizing bacteria . Credits: (A) & (E) from (Bailey et al., 2009). (B) & (C) from (Krajewski, 2011).

References cited

Achbergerová, L., and Nahálka, J. (2011). Polyphosphate – an ancient energy source and active metabolic regulator. Microbial Cell Factories 10:63.

Arning, E.T., Birgel, D., Brunner, B., and Peckmann, J. (2009). Bacterial formation of phosphatic laminites off Peru. Geobiology 7**,** 295-307.

Arning, E.T., Birgel, D., Schulz-Vogt, H.N., Holmkvist, L., Jørgensen, B.B., Larsson, A., and Peckmann, J. (2008). Lipid biomarker patterns of phosphogenic sediments from upwelling regions. Geomicrobiology Journal 25**,** 69-82.

Bailey, J.V., Joye, S.B., Kalanetra, K.M., Flood, B.E., and Corsetti, F.A. (2007). Evidence of giant sulphur bacteria in Neoproterozoic phosphorites. Nature 445**,** 198-201.

Bailey, J.V., Orphan, V.J., Joye, S.B., and Corsetti, F.A. (2009). Chemotrophic microbial mats and their potential for preservation in the rock record. Astrobiology 9**,** 843-859.

Banerjee, D.M. (1971). Precambrian stromatolitic phosphorites of Udaipur, Rajasthan, India. Geological Society of America Bulletin 82**,** 2319-2329.

Baturin, G., Merkolova, K., and Chalov, P. (1972). Radiometric evidence of recent formation of phosphatic nodules in marine shelf sediments. Marine Geology 13**,** 37-41.

Baturin, G.N., Dubinchuk, V.T., and Zhegallo, E.A. (2000). Bacteriomorphous formations in phosphorites of the Namibia Shelf. Okeanologiya (Moscow) 40**,** 779-784.

Benitez-Nelson, C.R. (2000). The biogeochemical cycling of phosphorus in marine systems. Earth Science Reviews 51**,** 109-135.

Benzerara, K., Yoon, T.-H., Tyliszczak, T., Constantz, B., Spormann, A.M., and Brown, G.E.J. (2004). Scanning transmission X-ray microscopy study of microbial calcification. Geobiology 2**,** 249-259.

Brock, J., and Schulz-Vogt, H.N. (2011). Sulfide induces phosphate release from polyphosphate in cultures of a marine Beggiatoa strain. ISME Journal 5**,** 497-506.

Burnett, W.C., Veeh, H.H., and Soutar, A. (1980). "U-series, oceanographic and sedimentary evidence in support of recent formation of phosphate modules off Peru," in Marine Phosphorites. (Soc. Econ. Paleontologists Mineralogists), 61-71.

Canfield, D.E., Poulton, S.W., and Narbonne, G.M. (2007). Late Neoproterozoic deep-ocean oxygenation and the rise of animal life. Science 315**,** 92–95.

Cayeux, L. (1936). Existence de nombreuses bactéries dans les phosphates sédimentaires de tout âge. Cr. Acad. Sci. 23**,** 1198–1200.

Cook, P.J. (1970). Repeated diagenetic calcification, phosphatization, and silicification in the Phosphoria Formation. Geological Society of America Bulletin 81**,** 2107-2116.

Cook, P.J. (1976). "Sedimentary phosphate deposits," in Handbookof Strata-Bound and Stratiform Ore Deposits, ed. K.H. Wolf. (New York: Elsevier), 505-535.

Cook, P.J., and McElhinny, M.W. (1979). A reevaluation of the spatial and temporal distribution of sedimentary phosphate deposits in the light of plate tectonics. Economic geology 74**,** 315–330.

Cook, P.J., and Shergold, J. (1984). Phosphorus, phosphorites and skeletal evolution at the Precambrian-Cambrian boundary. Nature 308**,** 231-236.

Cook, P.J., and Shergold, J.H. (eds.) (1986). Phosphate deposits of the world: Proterozoic and Cambrian phosphorites. Cambridge: Cambridge University Press.

Cook, P.J., Shergold, J.H., Burnett, W.C., and Riggs, S.R. (1990). "Phosphorite Research: a Historical Overview," in Geological Society Special Publication No. 52 - Phosphorite Research and

Development, eds. A.J.G. Notholt & I. Jarvis. (London: Geological Society), 1-22.

Crocetti, G.R., Hugenholtz, P., Bond, P.L., Schuler, A., Keller, J., Jenkins, D., and Blackall, L.L. (2000). Identification of polyphosphate-accumulating organisms and design of 16S rRNA-directed probes for their detection and quantitation. Applied and Environmental Microbiology 66, 1175-1182.

Crosby, S.A., Millward, G.E., Butler, E.I., Turner, D.R., and Whitfield, M. (1984). Kinetics of phosphate adsorption by iron oxyhydroxides in aqueous systems. Estuarine, Coastal and Shelf Science 19**,** 257-270.

Cunningham, J.A., Thomas, C-W., Bengtson, S., Marone, F., Stampanoni, M., Turner, F.R., Bailey, J.V., Raff, R.A., Raff, E.C., and Donoghue, P.C.J. (2011). Experimental taphonomy of giant sulphur bacteria: implications for the interpretation of the embryo-like Ediacaran Doushantuo fossils. Proceedings of the Royal Society, London, Series B: Biological Science.

Dornbos, S.Q. (2010). "Phosphatization through the Phanerozoic," in Taphonomy, Second Edition: Process and Bias Through Time. Topics in Geobiology, eds. P.A. Allison & D.J. Bottjer. (Springer), 435-456.

Emigh, G.D. (1958). Petrography, mineralogy and origin of phosphate pellets in the Phosphoria Formation. Bureau of Mines and Geology.

Ferris, F.G. (1989). "Metallic ion interactions with the outer membrane of gram-negative bacteria," in Metal Ions and Bacteria, eds. T.J. Beveridge & R.J. Doyle. (New York: Wiley), 295-323.

Filippelli, G.M. (2011). Phosphate rock formation and marine phosphorus geochemistry: The deep time perspective. Chemosphere 84**,** 759-766.

Föllmi, K.B. (1996). The phosphorous cycle, phosphogenesis and marine phophate-rich deposits. Earth Science Reviews 40**,** 55-124.

Garrison, R.E., and Kastner, M. (1990). Phosphatic sediments and rocks recovered from the Peru margin during ODP leg 112. Proc. Ocean Drill. Program: Sci. Results 112**,** 111-134.

Garrison, R.E., Kastner, M., and Reimers, C.E. (1990). "Miocene phosphogenesis in California," in Phosphate Deposits of the World. Neogene to Modern Phosphorites, eds. W.C. Burnett & S.R. Riggs. (Cambridge University Press), 285-299.

Glenn, C.R., Föllmi, K.B., Riggs, S.R., Baturin, G.N., Grimm, K.A., Trappe, J., Abed, A.M., Galli-Oliver, C., Garrison, R.E., Ilyan, A., Jehl, C., Rohrlich, V., Sadaqah, R.M., Schidlowski, M., Sheldon, R.E., and Siegmund, H. (1994). Phosphorus and phosphorites: sedimentology and environments of formation. Eclogae geologicae Helvetiae 87**,** 747-788.

Goldhammer, T., Brüchert, V., Ferdelman, T.G., and Zabel, M. (2010). Microbial sequestration of phosphorus in anoxic upwelling sediments. Nature Geoscience 3**,** 557-561.

Gunnars, A., Blomqvist, S., and Martinsson, C. (2004). Inorganic formation of apatite in brackish seawater from the Baltic Sea: an experimental approach. Marine Chemistry 91**,** 15-26.

Hirschler A., Lucas J. and Hubert J-C. (1990). Apatite genesis: A biologically induced or biologically controlled mineral formation process? Geomicrobio J 7, 47-57.

Huldtgren, T., Cunningham, J.A., Yin, C., Stampanoni, M., Marone, F., Donoghue, P.C.J., and Bengtson, S. (2011). Fossilized nuclei and germination structures identify Ediacaran "animal embryos" as encysting protists. Science 334**,** 1696-1699.

Jarvis, I., Burnett, W.C., Nathan, J., Almbaydin, F.S.M., Attia, A.K.M., Castro, L.N., Flicoteau, R., Hilmy, M.E., Husein, V., Quitwanah, A.A., Serjani, A.A., and Zanin, Y. (1994). Phosphorite geochemistry: state of the art and environmental concerns. Eclogae Geologica Helvetiae**,** 643–700.

Jørgensen, B.B. (1977). Distribution of colorless sulfur bacteria (Beggiatoa-spp) in a coastal marine sediment. Marine Biology 41**,** 19-28.

Jørgensen, B.B. (1982). Mineralization of organic matter in the seabed – the role of sulfate reduction. Nature 296**,** 643-645.

Jørgensen, B.B., and Gallardo, V.A. (1999). Thioploca spp.: Filamentous sulfur bacteria with nitrate vacuoles. FEMS Microbiology Ecology 28**,** 301-313.

Krajewski, K.P. (2011). "Phosphatic microbialites in the Triassic phosphogenic facies of Svalbard," in Stromatolites: Interaction of Microbes with Sediments, Cellular Origin, Life in Extreme Habitats and Astrobiology, eds. V.C. Tewari and J. Seckbach (New York: Springer),187–222.

Krajewski, K.P., Leśniak, P.M., Łącka, B., and Zawidzki, P. (2000). Origin of phosphatic stromatolites in the Upper Cretaceous condensed sequence of the Polish Jura Chain. Sedimentary Geology 136**,** 89-112.

Krajewski, K.P., Van Cappellen, P., Trichet, J., Kuhn, O., Lucas, J., Martin-Algarra, A., Prévot, L., Tewari, V.C., Gaspar, L., Knight, R.I., and Lamboy, M. (1994). Biological processes and apatite formation in sedimentary environments. Eclogae Geol. Helv. 87**,** 701-745.

Krom, M.D., and Berner, R.A. (1980). Adsorption of phosphate in anoxic marine sediments. Limnology and Oceanography 25**,** 797-806.

Lamboy, M. (1990). Microstructures of a phosphatic crust from the Peruvian continental margin: Phosphatized bacteria and associated phenomena. Oceanol. Acta 13**,** 439-451.

Lavik, G., T. Stührmann, V. Brüchert, A. Van Der Plas, V. Mohrholz, P. Lam, M. Mußmann, B.M. Fuchs, R. Amann, U. Lass, and M.M.M. Kuypers (2009). Detoxification of sulphidic African shelf waters by blooming chemolithotrophs. Nature 457**,** 581-584.

Li, C., Love, G.D., Lyons, T.W., Fike, D.A., Sessions, A.L., and Chu, X. (2010). A stratified redox model for the Ediacaran ocean. Science 328**,** 80-83.

Lucas J. and Prévot L. (1985). The synthesis of apatite by bacterial activity: Mechanism. Sci Géol Mém 77, 83-92.

McFadden, K.A., Huang, J., Chu, X., Jiang, G., Kaufman, A.J., Zhou, C., Yuan, X., and Xiao, S. (2008). Pulsed oxidation and biological evolution in the Ediacaran Doushantuo Formation. Proceedings of the National Academy of Sciences of the United States 105**,** 3197-3202.

Mino, T., Tsuzuki, Y., and Matsuo, T. (1987). "Effect of phosphorus accumulation on acetate metabolism in the biological phosphorus removal process," in Adv. Wat. Pollut. Cont. Biological Phosphate Removal from Wastewaters (Pergamon Press), 27-38.

Murray, J., and Renard, A.F. (1891). Deep-sea deposits. Reports on the scientific results of the H.M.S. Challenger 1873-76. London: H.M.S.O.

Nancollas, G.H., Amjad, Z., and Koutsoukos, P. (1979). "Calcium phosphates – Speciation, solubility, and kinetic considerations," in ACS Symposium Series, ed. E. Jenne. (Washington, D. C.: American Chemical Society), 475-497.

Nathan, Y. (1984). "The mineralogy and geochemistry of phosphorites," in Phosphate Minerals, eds. J.O. Nriagu & P.B. More. (Berlin: Springer), 275-291.

Notholt, A.J.G., and Sheldon, R.P. (1986). "Proterozoic and Cambrian phosphorites-regional review: World resources," in Phosphate deposits of the world., ed. P.J. Cook, Shergold, J.H. (Cambridge University Press), 386.

O'Brian, G.W., and Veeh, H.H. (1980). Holocene phosphorite on the East Australian margin. Nature 238**,** 690-692.

Ohtake, H., J., K., Kuroda, A., and T, I. (1998). Regulation of bacterial phosphate taxis and polyphosphate accumulation in response to phosphate starvation stress. Journal of Bioscience 23**,** 491-499.

Omelon, S.J., and Grynpas, M.D. (2008). Relationships between polyphosphate chemistry, biochemistry and apatite biomineralization. Chemical Reviews 108**,** 4694-4715.

Papineau, D. (2010). Global biogeochemical changes at both ends of the Proterozoic: Insights from phosphorites. Astrobiology 10**,** 165-181.

Parker, R.J., and Andseisser, W.G. (1972). Petrology and origin of some phosphorites from the South African continental margin. Journal of Sedimentary Petrology 42**,** 434-440.

Penn, M.R., Auer, M.T., Doerr, S.M., Driscoll, C.T., Brooks, C.M., and Effler, S.W. (2000). Seasonality in phosphorus release rates from the sediments of a hypereutrophic lake under a matrix of pH and redox conditions. Can. J. Fish. Aquat. Sci. 57**,** 1033-1041.

Planavsky, N.J., Rouxel, O.J., Bekker, A., Lalonde, S.V., Konhauser, K.O., Reinhard, C.T., and Lyons, T.W. (2010). The evolution of the marine phosphate reservoir. Nature 467**,** 1088-1090.

Pufahl, P.K., Grimm, K.A., Abed, A.M., and Sadaqah, R.M.Y. (2003). Upper Cretaceous (Campanian) phosphorites in Jordan: Implications for the formation of a south Tethyan phosphorite giant. Sedimentary Geology 161**,** 175-205.

Rakovan, J. (2002). "Growth and Surface Properties of Apatite," in Reviews in mineralogy & geochemistry, vol. 48. Phosphates - Geochemical, geobiological, and materials importance, eds. M. Kohn, J. Rakovan & J. Hughes. (Washington, D. C.: Mineralogical Society of America), 51-86.

Reimers, C., Kastner, M., and Garrison, R.E. (1990). "The role of bacterial mats in phosphate mineralization with particular reference to the Monterey Formation," in Phosphate deposits of the world, vol. 3. Neogene to modern phosphorites., eds. W.C. Burnett & S.R. Riggs. (Cambridge: Cambridge University Press).

Riggs, S.R. (1979). Petrology of the Tertiary phosphorite system of Florida. Economic Geology 74**,** 195–220.

Riggs, S.R., and Sheldon, R.P. (1990). "Paleoceanographic and paleoclimatic controls of the temporal and geographic distribution of Upper Cenozoic continental margin sediments," in Phosphate deposits of the world, vol 3. Neogene to modern phosphorites, eds. W.C. Burnett & S.R. Riggs. Cambridge University Press), 53-61.

Robertson, L.A., and Kuenen, J.G. (2006). "The colorless sulfur bacteria," in The Prokaryotes., eds. M. Dworkin, S. Falkow, E. Rosenberg, K.-H. Schleifer & E. Stackebrandt. (New York: Springer), 985-1011.

Ruttenberg, K.C., and Berner, R.A. (1993). Authigenic apatite formation and burial in sediments from non-upwelling continental margin environments. Geochimica et Cosmochimica Acta 57**,** 991-1007.

Salman, V., Amann, R., Girnth, A.-C., Polerecky, L., Bailey, J.V., Høgslund, S., Jessen, G., Pantoja, S., and Schulz-Vogt, H.N. (2011). A single-cell sequencing approach to the classification of large, vacuolated sulfur bacteria. Systematic and Applied Microbiology 34, 243–259.

Schulz, H.N., and Schulz, H.D. (2005). Large sulfur bacteria and the formation of phosphorite. Science 307**,** 416-418.

Schulz, H.N., Strotmann, B., Gallardo, V.A., and Jørgensen, B.B. (2000). Population study of the filamentous sulfur bacteria Thioploca spp. off the Bay of Concepcion, Chile. Marine Ecology Progress Series 200**,** 117-126.

Sheldon, R.P. (1981). Ancient Marine Phosphorites. Annual Review of Earth and Planetary Sciences 9**,** 251-284.

Soudry, D. (2000). "Microbial phosphate sediment," in Microbial sediments, eds. R.E. Riding & S.M. Awramik (Springer), 127-136.

Soudry, D., and Champetier, Y. (1983). Microbial processes in the Negev phosphorites (southern Israel).

Sedimentology 30**,** 411-423.

Sterner, R.W., and Elser, J.J. (2002). Ecological stoichiometry: The biology of elements from molecules to the biosphere. (Princeton: Princeton Univ. Press.)

Suess, E. (1981). Phosphate regeneration from sediments of the Peru continental margin by dissolution of fish debris. Geochimica et Cosmochimica Acta 45**,** 577-588.

Swirydczuk, K., Wilkinson, B.H., and Smith, G.R. (1981). Synsedimentary lacustrine phosphorites from the Pliocene Glenns Ferry Formation of southwestern Idaho. Journal of Sedimentary Petrology 51**,** 1205-1214.

Van Cappellen, P., and Berner, R.A. (1988). A mathematical model for the early diagenesis of phosphorus and fluorine in marine sediments: Apatite precipitation. American Journal of Science 288**,** 289-333.

Veeh, H.H., Burnett, W.C., and Soutar, A. (1973). Contemporary phosphorites on the continental margin of Peru. Science 181**,** 844-845.

Williams, L.A. (1984). Subtidal stromatolites in Monterey Formation and other organic-rich rocks as suggested contributors to petroleum formation. American Association of Petroleum Geologists Bulletin 68**,** 1879-1893.

Williams, L.A., and Reimers, C. (1983). Role of bacterial mats in oxygen-deficient marine basins and coastal upwelling regimes: Preliminary report. Geology 11**,** 267-269.

Xiao, S., Zhang, Y., and Knoll, A.H. (1998). Three-dimensional preservation of algae and animal embryos in a Neoproterozoic phosphorite. Nature 391**,** 553-558.

Yin, L., Zhu, M., Knoll, A.H., Yuan, X., Zhang, J., and Hue, J. (2007). Doushantuo embryos preserved inside diapause egg cysts. Nature 446**,** 661-663

— DISCUSSION —

History of and current state of research re: microbes and apatite

Converging lines of evidence point to the likelihood that microbes may be directly or indirectly involved in the precipitation of sedimentary apatite. The first suggestion of this link was made nearly a century ago, by N. R. Kassin in his 1925 discussion of phosphorite formation (p31) (Baturin, 1982 and Kassin reference therein) but despite years of subsequent research, the mechanism of this connection has yet to be fully elucidated. Nonetheless, disparate approaches to a variety of questions have contributed to our understanding of the relationship between microbes and apatites.

In the 1960s, the dentist Dr. John Ennever noted that the bacterium *Bacterionema matruchotii* (reclassified in 1982 as *Corynebacterium matruchotii*) (Collins, 1982) precipitated apatite both intra- and extracellularly, and sought (not altogether successfully) to stimulate research into bacterial apatite formation (Ennever and Creamer, 1967; Ennever et al., 1974; Ehrlich, 1999).

By the 1960s, the use of so-called "activated sludge" [a kind of "probiotic" treatment that introduces live microbial communities into a Waste Water Treatment System (WWTS)] was in practice. The 'activating' microbial communities were recognized as influencing the efficiency of P removal primarily by microbial enzymatic breakdown of complex phosphate solids to release constituent phosphate ions which were then chemically precipitated and removed with the flocculated biomass. In their 1969 paper, Vacker et al. noted heightened (nearly 90% removal vs. the expected ≤ 28%) P removal from activated sludge at the San Antonio treatment plant in 1967 and recognized that phosphate added to sludge resulted in increased microbial uptake of excess phosphate in conjunction with aerobic conditions (Vacker et al., 1967). They considered whether this was due to biochemical processes to be speculative. Today it is recognized that a number of microbes are Polyphosphate Accumulating Organisms (PAOs) that take up 'luxury' phosphate (phosphate in excess of that believed to be required for, at least currently active metabolic processes) but as neither the biochemical mechanism nor the identity of the microbial communities involved in WWTS are fully understood, treatment systems are still subject to collapse, and robust research is ongoing.

In the mid 1980s, Liliane Prévot and Jacques Lucas performed experiments on microbially-induced apatite replacement after calcium carbonate, concluding that microbial phosphatases cleaved large P-bearing molecules (RNA), releasing phosphoric acid that dissolved calcium carbonate provided by foraminifera and released calcium ions to precipitate with the phosphate.

Further experimentation by Lucas & Prévot, utilizing RNA + aragonite + sodium fluoride (for the purpose of obtaining the more ideal crystalline form of apatite) also yielded calcium phosphate minerals, but only under non-sterile conditions, leading them to conclude that microbes were involved in the mineral precipitation (Hirschler et al., 1990).

Research into the rock record also suggested a relationship between microbes and phosphate rock formations. In 1983, David Soudry and Yves Champetier presented evidence of structures in the rock record suggestive of microbial involvement in formation of Cretaceous/Eocene phosphorites and speculated that microbes may contribute to phosphorite formation by binding 'phosphate particles' [sic] (Soudry and Champetier, 1983). Loretta Ann Williams & Claire Reimer also hypothesized a relationship between sulfur-oxidizing microbes and phosphate rock formation (Williams and Reimers, 1983). Yet in their 1983 analysis of apatite formation in Mexican continental margins, Jahnke et al. summarize factors leading to phosphorite formation as suggested in the literature to date, none of which refer to microbial activity (Jahnke et al., 1983).

In a 1993 paper, Nathan et al. note that the PAOs *Pseudomonas* & *Acinetobacter*, already implicated in wastewater P-removal systems, are present in areas of coastal upwelling and conclude that they are involved in the concentration of phosphate and subsequent formation of phosphorites, albeit in an indirect and passive role by increasing the amount of P-containing organic matter, providing nucleation sites on cell surfaces, changing pH conditions, and acting as 'mechanical traps' in microbial mats (Nathan et al., 1993).

In their 1994 work *Biological processes and apatite formation in sedimentary environments,* Krzysztof Krajewski et al. clarified a distinction between apatite precipitation and phosphorite formation, and recognized the potential of microbial involvement as "transitory fixation and release of phosphate by microbial communities [which] may be responsible, in part, for the elevated concentrations of dissolved pore phosphate observed in close proximity to the water-sediment interface at sites of present-day phosphorite formation." They go on to state that because SOxB thrive at the H_2S/O_2 interface, Eh-pH changes at the interface may lead to confined pulses of dissolved phosphate and induce conditions required for the precipitation of calcium phosphate solids (Krajewski et al., 1994).

Exploring the feasibility of a microbial involvement in phosphate rock formation, Jorg Brock & Heide N. Schulz-Vogt found laboratory evidence of the release of phosphate by the SOxB Beggiatoa upon (anoxic) exposure to sulfide (Brock and Schulz-Vogt, 2011), and Tobias Goldhammer et al. found laboratory evidence of P cycling through microbial biomass into precipitated apatite (Goldhammer et al., 2010a). From the rock record, evidence supporting the

finding of SOxB in fossil phosphate rock has been presented by Bailey et al. (Bailey et al., 2013). Research continues into the relationship between microbes and phosphate rock deposits.

The geobiological phosphorus cycle

As Gunter Faure notes in his text on geochemistry, "Every element is moved from one reservoir to the next by geological, geochemical, or biological processes" (Faure, 1991). And thus it is with P, which by virtue of all of these processes, cycles through a variety of molecules and reservoirs. The global P cycle incorporates many flows and eddies that operate at a wide range of timeframes, from the geologically slow to the virtually instantaneous speed of biochemical reactions.

The primary origin of the cycle lies within Earth's mantle. Although it is unclear exactly how much phosphorus is entrained in the mantle, estimates – based on analysis of ultramafic samples, stony meteorites, and calculations based on requirements that must be met to produce basaltic magmas – range from trace (<0.1%) to up to 0.34% phosphorus [p43-45] (Faure, 1991). In this initial aspect of the cycle, phosphorus-bearing magma rises within the mantle, solidifies, and eventually undergoes uplift and erosion. Over the course of Earth's history, this magma-borne aspect of the P cycle repeats as crustal material is subducted into the mantle, to eventually return again to Earth's surface and weathered. The time required for this aspect of the cycle is likely to be in the range of hundreds of millions of years, and recycling through the mantle is generally disregarded in discussion of the global P cycle. For discussion of mantle development and cooling, see (Zahnle et al., 2007).

In contrast to this geologically slow cycle, once the P-bearing material has been brought to Earth's surface, P enters a much more dynamic cycle, as erosion and subsequent transport of phosphorus initiates the bio-available aspect of the P cycle and the cycling of phosphorus can be said to effectively begin, as P-bearing particulates and inorganic phosphate ions are released from the rock matrix by weathering and enter the global subaerial or subaqueous P cycle.

Subaerial and near-surface mechanical weathering reduces rock to soil particulates that can remain locked in mineral matrices within soil, be swept up by the wind or transported by water, most eventually reaching lakes or oceans. These particulates may eventually also undergo chemical weathering, releasing soluble inorganic phosphate ions that may be adsorbed onto iron oxides in soil clays or assimilated by plant roots to enter the biological arm of the cycle. In the terrestrial biosphere, P may cycle through many macroscopic organisms and be further recycled

by scavengers and degraders as microbes fungi and various invertebrates assimilate solubilized P extracted from organic waste material (Li et al., 2006).

Within the biosphere P enters into many different organic molecules, and the number of compounds in which P is found greatly expands to include biologically-formed complex organic and inorganic molecules. Eventually, like particulate P, much of this material finds it way to the ocean, some unknown amount by groundwater seepage, but mainly by overland runoff and fluvial transport, and increasingly through engineered diversionary streams – primarily wastewater and storm water systems. A minor amount reaches the ocean on the wind, some carried far away from land to fall on oligotrophic oceanic regions.

Upon entering the ocean the bioavailable fraction is assimilated virtually immediately in the upper photic zone by organisms making a living on light and carbon dioxide as they proliferate in response to the influx of this essential, and often limiting, element. As these organisms die they fall through the water column as marine snow and their biomass is degraded by heterotrophs, thus recycling the P through the marine biosphere.

Some of the P that enters the ocean is not readily bioreactive. This recalcitrant fraction is largely bound in minerals or adsorbed onto other particles. Where delivered fluvially, these particulates generally become trapped in estuaries and upper shelf environments, where they settle in sediment. Further from land, wind-carried particulates are delivered to the ocean and sink to the seabed. Under prolific conditions above the continental shelves, the raining of organic matter enhances (aerobic) heterotrophy, and results in Oxygen Minimum Zones (OMZ) at depth.

Phosphorus cycling at the sea floor is a complex and likely iterative process not well characterized, but eventually recalcitrant P-containing sediment is buried and lithified. Once P has been removed from the biosphere and lithified, the burial of P in sedimentary rock is believed to be a stringent limitation on its bioavailability.

This then is an overview of the global P cycle: Uplift, weathering and erosion, aqueous & terrestrial cycling, resulting in recalcitrant and bioavailable fractions that eventually return to the ocean floor to become integrated into sediment and undergo diagenesis/relithification – the whole cycle repeating as the ocean floor undergoes uplift and exposure, or subduction and degassing. Indeed, the global P cycle is ultimately controlled by tectonic activity, with terrestrial/marine sub-cycles providing transfer points from the geosphere into the biosphere.

The place of P research in global and biological sciences

The biomass of all known life on Earth comprises a number of elements. The elements C, H, O, N, P & S make up the bulk of biomass and thus are most in demand,* and shortages of bio-available pools of these elements present the most common elemental bottlenecks in the proliferation of life. Among these elements, carbon comprises the primary building block of biomass and is ubiquitous and generally readily available in both atmospheric and aquatic environments as CO_2 (as well as degradable biomass); hydrogen is the most abundant element in the universe and the dominant electron carrier/supplier; oxygen is available as gaseous O_2 ; nitrogen is plentiful as gaseous N_2 ; and sulfur is continually released via magmatic/volcanic processes as sulfides or sulfur-oxides.

Of the bionecessary elements, P and N (along with iron) are the common limiting nutrients that may regulate the carbon cycle by controlling the extent to which life can proliferate. Nitrogen because, though plentiful, it is not assimilated by many organisms, and phosphorus because phosphate is initially released (through weathering) only into the hydrosphere, as it does not have a significant gaseous phase. In its aqueous phase in the hydrosphere, phosphate is readily scavenged by organisms that are in competition for it.

Hence, P exerts a strong influence on Earth's biosphere at large, providing a limiting control on global cycles of bio-necessary elements. The canonical Redfield C:N:P ratio (106:16:1) illustrates how strongly P availability can affect C fixation.

Much attention has been given to the carbon cycle and the influence of anthropogenic forcings on the fluxes and pools of carbon, and their subsequent impacts (fossil fuel utilization, greenhouse gases, global heat budget, climate change …) (Brunner and Rechberger, 2002). But less attention has been given to the availability and perturbations of the P cycle, though this is changing.

The anthropogenic use of phosphate rock, primarily as fertilizer, has resulted in the specter of a forthcoming depletion of this resource. Estimates as to when this will happen vary, but one estimate considers peak production likely to occur in the decade 2030-2040 as a result of a growing human population consuming more meat & dairy diets (Cordell et al., 2009). As the

---

* *There are many so-called 'trace' elements also required by organisms. These are not included in the familiar 'CHNOPS' list as they generally comprise less than 1% of an organism's (or cell's) biomass.*

human population continues to climb, along with the number of livestock fed P-based fertilized grains, the challenge of food security will become significant.

A clearer understanding of the geologic history of the phosphate rock we mine today, therefore, can be expected to inform our utilization of this commodity. In light of the established link of P between the geosphere and the biosphere, it may also provide insight into a number of questions of early Earth's development and the development of life on Earth.

Transition to next section: Microbial paleontology

The field of microbial paleontology, or micropaleontology, is based in the recognition that fossil microbes may be preserved in the rock record. Its roots lie in late 19th century discoveries of microbial kerogenous* remains in sediments. Advances in technology have enabled us to characterize not only kerogen maturation e.g. (Schopf et al., 2005), but also isotopic and geochemical evidence of microbial activity in the rock record, as well as subtle chemical and crystallographic characteristics of permineralized and microbially altered material.

Despite these tools, the search for signs of microfossil evidence of microbial life, especially in deep time, is challenging, and often results in inconclusive interpretations. Metamorphic alteration challenges the potential for preservation, resulting in cryptic evidence prone to mis-interpretation. Hence, the field of micropaleontology is almost inherently prone to controversy, as the objects of study are often fraught with ambiguity. We need to know where to look, how to look and how to handle rock samples in order to preserve evidence. Early discoveries were hotly debated and interpretations were not necessarily accepted on a dispassionate consideration of empirical evidence. It wasn't until Stanley Tyler's insistence on a pre-publication validation of his 1.9 Ga Gunflint chert microfossil find in 1953 initiated the practice of peer review in the field, that the field of microbial paleontology was established as a *bona fide* scientific endeavor (Barghoorn and Tyler, 1965).

---

* *Kerogen is "fossilized carbonaceous matter of established biological origin" (Schopf et al., 2005), too refractory to be readily degraded and hence persistent through geologic time. It is slowly altered as diagenetic and metamorphic influences drive non-carbon atoms off the carbon backbone, leaving increasingly ordered graphitic sheets of carbon rings (Pasteris and Wopenka, 1991). Kerogen is a strong indicator of life, but cannot be taken as definitive evidence of biogenicity, as non-biological carbonaceous material may also contain the polycyclic and double carbon bonds generally considered diagnostic of kerogen.*

Today, micropaleontological investigation of the ancient rock record continues to clarify the links between microbes, minerals and the atmosphere. Armed with a sense of the relationship between SOxB and calcium phosphate minerals, and taking the perspective of P as the starting point for research into questions of the relationship between geo- and biosphere, I began my research by examining stromatolitic phosphate rock from the 2 Ga Jhamarkotra phosphate rock formation. Two features of this formation in particular led me to anticipate signs of early organisms: the stromatolitic nature of the formation, and the high P content – particularly as the phosphatic minerals are restricted to the stromatolites. To investigate, I cut small blocks from a rock chip obtained by Jake Bailey from paleobotanist Mukund Sharma, and had thin sections made.

The results of this work have added data relevant to both Earth's and life's early evolution, and has been published in *Geology*. The paper is reproduced in the following section.

The short background in the concept of redox and its relevance to both the evolution of Earth and microbial/biological processes provided here are intended to set the background for this work. It will be seen that the two are tightly interwoven.

Chapter 3

—

Jhamarkotra Phosphatic Stromatolites

Introduction

"While our understanding of the ancient biosphere will never be complete, it is only through the confluence of our study of modern processes and the rock record that we will broaden our perspectives, improve our confidence in our interpretations, and appreciate the magnitude of our ignorance." (Bailey, 2008). To arrive at well-informed inferences from observations of putative microfossils, we must draw on a broad understanding of diverse fields, including taphonomic preservation processes, the environmental conditions under which the putative microorganisms lived, microbial chemolithotrophic strategies, and the conditions to which their remnants may have subsequently been subjected. In using this information *in toto* to develop a comprehensive interpretation we seek not only the existence and identity of ancient organisms, but also an understanding of mechanisms and processes that can connect the distant, whether in time or space, with the here and now.

Seeking evidence of microbial involvement in the formation of ancient phosphate rock, and building on the now-recognized relationship between currently-forming phosphorites and sulfide-oxidizing organisms (Schulz and Schulz, 2005; Goldhammer et al., 2010), we examined samples of a ~2 Ga stromatolitic formation, the Jhamarkotra Formation. Located roughly 25 km southeast of Udaipur, the capital of Rajasthan State, India, the Jhamarkotra formation is being mined for its unusually rich phosphate rock.

We obtained freshly exposed samples and cut three thin sections for analysis. Optical microscopic examination of two of them

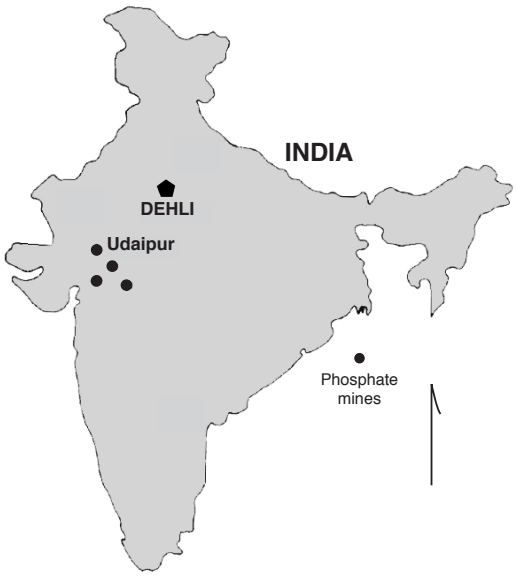

Figure 03 | **Locator map**
Jhamarkotra mine, Udaipur, India

revealed filamentous features that appeared biogenic, and we proceeded to analyze them for signs of biogenicity and affinity as follows:

1) Assess whether the filaments are biogenic
    - Determine whether kerogen is present
    - Analyze the mineralogy/chemistry of the filaments and the rock matrix
    - Describe the morphology of the filaments
    - Consider and assess likelihood of abiotic interpretations
2) Explore the possibility of assigning microbial affinity
    - Compare filament morphologies with those of known microbes
    - Search literature for information on depositional conditions
    - Consider data *in toto* to arrive at a likely affinity
3) Develop a reasonable environmental scenario
4) Consider implications

The next section is a reprint of the published results of this investigation, followed by a more in-depth discussion.

Fossil evidence of iron-oxidizing chemolithotrophy linked to phosphogenesis in the wake of the Great Oxidation Event

Chris H. Crosby[1], Jake V. Bailey[1], and Mukund Sharma[2]

[1] Department of Earth Sciences, University of Minnesota-Twin Cities, Minneapolis, MN 55455

[2] Birbal Sahni Institute of Palaeobotany, Lucknow 226007, India

Published in 'Geology' November 2014; v42:11, p. 1015-1018

 DOI: 10.1130/G35922

The oxygenation of Earth's atmosphere allowed for the diversification of metabolisms to include those that rely on oxygen and its derivatives. For example, chemolithotrophic oxidation of sulfide and iron both require oxygen or nitrate as terminal electron acceptors. A growing number of oxygen-utilizing chemolithotrophs are known to accumulate intracellular polyphosphate as an energy reserve that allows them to adapt to the fluctuating redox conditions in their distinctive-gradient habitats. Polyphosphate is also thought to play an important role in the formation of phosphatic mineral deposits. Here we present fossil evidence of iron-oxidizing bacteria preserved as filamentous iron oxides within phosphatic Paleoproterozoic stromatolites. The filaments include twisted stalks similar to those produced by modern iron-oxidizing bacteria that are known to metabolize polyphosphate and inhabit steep redox gradients. Fossil iron-oxidizing bacteria preserved within some of the oldest known phosphorites serve as indicators of O_2-Fe(II) gradients that may have supported microbially mediated phosphogenesis via polyphosphate metabolism and/or an active iron redox pump.

Introduction

The details of the oxygenation of Earth's atmosphere are still debated. It is generally believed that by ca. 2.2 Ga, Earth's atmosphere contained ≤10% of present levels of oxygen (i.e., Holland, 1999; Nisbet et al., 2007; Petsch, 2003), though recent work suggests that the oxygenation of Earth's atmosphere may have been under way as early as 3 Ga (Crowe et al., 2013), well before the "Great Oxidation Event" of ca. 2.3 Ga (Bekker et al., 2004).

Early marine systems were depleted in sulfur and enriched in reduced iron, as evidenced by the isotopic record of sedimentary sulfides (Farquhar et al., 2007; Canfield et al., 2000). With the onset of oxidative weathering, Earth's oceans transitioned from being sulfur poor and iron rich in the Archean to the sulfate-replete marine waters of the Phanerozoic. Recent geochemical findings suggest that ferruginous marine conditions may have remained extensive through the Mesoproterozoic and iron-rich waters may have underlain sulfidic waters well into Neoproterozoic times (Planavsky et al., 2011). The onset of oxidative weathering is also thought to have increased the supply of phosphorus to seawater (Papineau, 2010). How these transformations of major geochemical cycles influenced the coevolution of geological processes and microbial communities remains incompletely understood. Here we report on stromatolite-associated filamentous microfossils likely representing chemolithotrophic iron-oxidizing bacteria from ca. 1.7 Ga stromatolitic phosphorites from the Jhamarkotra Formation of the Aravalli Group of Rajasthan, India. Today, microaerophilic neutrophilic iron-oxidizing bacteria inhabit conditions with steep and fluctuating redox gradients. Redox gradients of these kinds provide a selective advantage to polyphosphate-accumulating organisms, the metabolism of which is linked to phosphogenesis in modern sediments (Goldhammer et al., 2010). Oxygenated waters overlying reducing settings also make possible the so-called "iron-redox pump" that is also linked to phosphogenesis in modern settings. The preservation of iron-oxidizing bacteria within some of the oldest known phosphorites may indicate that the conditions thought to be required for phosphogenesis in modern marine sediments were present by at least 1.7 Ga.

Geological setting

Recent dating of zircons by McKenzie et al. (2013) suggests a late Paleoproterozoic age (ca. 1.7 Ga) for the Jhamarkotra Formation, part of the Aravalli Group shales, sands, and carbonates that lie unconformably on the basement Banded Gneissic Complex (Choudhuri and Roy, 1986). The region has a complex tectonic history characterized by extensive folding but a low degree of metamorphism, with various geochemical indicators suggesting lower greenschist facies metamorphism (Papineau et al., 2009). At the sampling site, the Jhamarkotra Formation consists primarily of a dolomitic matrix that hosts densely packed, ~3-cm-diameter, meters-tall columnar stromatolites of unusually high phosphate content approaching ~36% P_2O_5. The stromatolites are believed to have developed in a low-energy, poorly oxygenated equatorial embayment (Roy and Paliwal, 1981; Roy, 2000).

Methods

Samples were collected from a phosphatic stromatolite column from within a bioherm recently exposed by mining in the Jhamarkotra area in Udaipur District, Rajasthan, India (24°28′21.5″N, 74°44′43.5″E). Thin sections, 30 µm thick, were imaged on an Olympus BX61 microscope with a Canon EOS Rebel T2i camera. Bulk mineralogy of the source rock was verified by powder X-ray diffraction (XRD) using a Rigaku Miniflex XRD, and analyzed via Jade7 analytical software. Spot mineralogy along a transect was analyzed on a Bruker D8 XRD Discover 2D running General Area Detector Diffraction System version 4.1.42.

Raman spectroscopy data was collected using a WiTec Alpha300R confocal Raman microscope with an Onmichrome argon ion laser at 514.5 nm excitation and ~8 mW output power, and processed using WiTecControl 1.38 software.

CrystalSleuth software (http://rruff.info/) (Downs, 2006) was used for Raman spectrum analysis, and Raman spectral maps were created by filtering spectra for wave numbers 348–502. Three-dimensional (3-D) rendering was performed in ImageJ software (version 1.47c) using Volume Viewer 2.01. Elemental data was collected using a JEOL JXA-8900 electron probe microanalyzer with an accelerating voltage of 15.0 kV.

Iron-rich microfossils in phosphatic stromatolites

The microfossils are hosted by a texturally nondescript apatite matrix that sits adjacent to a brown and orange phosphatic laminated portion of the rock (Fig. Jh.DR1). Powder XRD shows the bulk rock to be dolomite and fluorapatite and/or hydroxyapatite (Fig. Jh.DR6). The laminated portion includes minor siliciclastic material, but is otherwise composed of apatite. Microfossils exhibit two habits: swarms of subparallel filaments (Fig. Jh.1F), and masses of filaments in a rosette-like pattern (Fig. Jh.DR3). The filaments are ~5–6 µm in diameter, with inner lumina ~1–1.5 µm in diameter. The lumen observed by optical imaging is substantiated by 3-D renderings of confocal laser Raman data (Fig. Jh.2A). In some, the inner lumen presents as a twisted stalk (Fig. Jh.1C) similar to that produced by the freshwater iron-oxidizing bacteria *Gallionella ferruginea* and the marine *Mariprofundus ferrooxydans* (Figs. Jh.1D and Jh.1E) (Chan et al., 2011). Electron microprobe analysis reveals that the filaments lie within an apatite matrix and are composed primarily of an iron oxide (Fig. Jh.2A; Fig. Jh.DR2), which µXRD shows to be goethite (Fig. Jh.DR4). The filaments contain discontinuous kerogen, detected by confocal Raman spectroscopy (Fig. Jh.2C), providing support for a biogenic interpretation, as is further suggested by the sharp mineralogical distinctions between the filaments and the surrounding matrix and filament

morphologies that include networks, branching filaments, and twisted stalks characteristic of some iron-oxidizing bacteria, as shown in Figures Jh.1B– Jh.1E and Figure Jh.DR5 (Fru et al., 2013; Krepski et al., 2013). While some of the less-distinctive morphologies may represent a variety of microorganisms, the twisted-stalk morphology is thought to be diagnostic of chemolithotrophic iron-oxidizing bacteria such as *Gallionella* and *Mariprofundus* (Spring, 2006; Chan et al., 2009). The diameter of the lumen in these microfossils is consistent with that of *M. ferrooxydans* (~1 μm) (Krepski et al., 2013), though filament widths of extant iron-oxidizing bacteria and ancient microfossils thought to represent iron bacteria have been found to vary widely, reaching diameters up to 30 μm (Little et al., 2004).

Under microaerophilic conditions, neutrophilic iron-oxidizing chemolithotrophs oxidize soluble Fe(II) to Fe(III) which precipitates as a hydrous iron oxyhydroxide. Some iron-oxidizing bacteria precipitate the poorly crystalline or amorphous ferrihydrite on an extracellular stalk. Iron oxyhydroxide–coated stalks commonly catalyze further abiotic iron oxidation, which could have resulted in the accumulation of the iron oxides surrounding the twisted stalk–bearing lumen in these microfossils (an example of thick overgrowths in extant bacteria is shown in Figure Jh.1E and Figure Jh.DR5). Indeed, the lumina within the larger filaments may represent original stalks of filamentous iron-oxidizing organisms, with the bulk of the observed filamentous structure representing secondary precipitates that nucleated on the iron oxide–encrusted stalks (Chan et al., 2011). Bio-organic material in mats of iron-oxidizing bacteria is much less voluminous than the iron oxides they produce. This, along with diagenetic degradation, could account for the low amounts of kerogen preserved within the filaments (Emerson and Ghiorse, 1993; Hashimoto et al., 2007; Schieber and Glamoclija, 2007).

The presence of fossil iron-oxidizing bacteria within a marine stromatolite suggests that the iron-rich but oxygenated conditions of late Paleoproterozoic shallow environments supported communities of microaerophilic neutrophilic iron-oxidizing bacteria. This interpretation builds on the foundational work on other microfossils interpreted as iron-oxidizing bacteria recovered from Mesoproterozoic sediments (Barghoorn and Tyler, 1965; Cloud, 1965; Lee and Golubic, 1999; Strother and Tobin, 1987) and more recent work on iron isotope signatures and microfossils associated with Fe-rich stromatolites (Planavsky et al., 2009).

Phosphogenesis and chemolithotrophy: An ancient association?

The phosphorites of Rajasthan, along with similar phosphatic stromatolites of central India, record some of the oldest sedimentary phosphorite deposits (Cook et al., 1990; Papineau, 2010;

Lepland et al., 2013). The process(es) involved in localizing apatite within stromatolites, an enigmatic feature of Paleoproterozoic phosphorites from western and central India, are not well understood (McKenzie et al., 2013). The occurrence of iron-oxidizing bacteria within these phosphatic stromatolites, where phototrophs would likely have driven diurnal pO_2 fluxes, may provide clues to their origin.

In modern marine sediments, chemolithotrophic sulfide-oxidizing bacteria accumulate phosphate and store it as polyphosphate inclusions under oxic conditions (Schulz and Schulz, 2005). Upon exposure to anoxia and/or sulfide, these bacteria harness energy from the hydrolysis of polyphosphate and release orthophosphate into pore waters, supersaturating them with respect to francolite or other apatite-group precursors (Schulz and Schulz, 2005; Brock and Schulz-Vogt, 2011; Crosby and Bailey, 2012). Isotopic labeling experiments demonstrate that the phosphorus released from polyphosphate utilization by sulfide-oxidizing bacteria is rapidly incorporated into apatite in phosphogenic sediments in upwelling zones, suggesting that polyphosphate utilization by chemolithotrophs under fluctuating oxygen conditions is an important driver of apatite precipitation in many modern marine phosphogenic settings (Goldhammer et al., 2010). Fossilized filamentous sulfide-oxidizing bacteria are present in Neoproterozoic phosphorites, where they have been interpreted to record a potential association between the spread of ocean oxygenation and the unprecedented proliferation of the extensive phosphorites of the Neoproterozoic (Bailey et al., 2013), and evidence of possible polyphosphate-accumulating bacteria was recently reported from the 2 Ga phosphorites of the Zaonega Formation (Russia; Lepland et al., 2014). The iron-oxidizing bacterium *M. ferrooxydans* PV-1 is one of the only known marine organisms known to produce twisted iron-oxide stalks similar to those observed in this study. The genome of PV-1 includes the full suite of genes needed for accumulation and hydrolysis of polyphosphate (Singer et al., 2011). Polyphosphate accumulation has also been documented in other iron oxidizing bacteria such as *Leptothrix* (Emerson and Ghiorse, 1992). While the details of polyphosphate metabolism in iron-oxidizing bacteria have yet to be elucidated, Singer et al. (2011) proposed that energy derived from polyphosphate metabolism allows *M. ferrooxydans* cells to adapt to the rapid redox changes encountered in the steep-redox-gradient habitats occupied by iron-oxidizing bacteria. Geochemical indicators suggest steep redox gradients and fluctuating redox conditions in the lower Aravalli stromatolites (Papineau et al., 2013), consistent with the habitats of iron-oxidizing chemolithotrophs and polyphosphate-accumulating microorganisms in general. While the iron-oxidizing organisms represented by the microfossils described here may have contributed directly to the phosphogenesis via their ability

to store and hydrolyze polyphosphate inclusions, more generally they represent indicators of the types of redox gradients and/or fluctuating redox conditions that select for polyphosphate-metabolizing bacteria in modern phosphogenic settings, many of which may not have been preserved, as most of the mat material associated with the stromatolites here is not preserved as microfossils.

While polyphosphate metabolism is one of the primary mechanisms invoked to explain modern phosphogenesis, the other, commonly known as the iron-redox pump, also occurs in oxygenated waters overlying anoxic environments. Here, iron oxides adsorb phosphate under oxygenated conditions. Then, when these particles encounter the zone of iron reduction, the iron oxides dissolve, mobilizing adsorbed phosphate, concentrating it, and driving apatite precipitation (Heggie et al., 1990). Oxygen-rich micro-niches within the stromatolites may have provided a locally significant iron-redox pumping mechanism sufficient to account for these anomalously phosphate-rich stromatolites. However, if the iron-redox pump was responsible for the apatite precipitation in the Jhamarkotra Formation, it would need to have been operating in a very restricted manner on iron precipitates produced by the stromatolite-associated microbial mats in order for the phosphogenesis to be tightly confined to the stromatolite as it is here.

The presence of a fossilized microbe within an authigenic mineral deposit does not necessitate that those organisms were involved in the precipitation of those minerals, and the possibility exists that the Jhamarkotra phosphorites resulted from conditions partially or completely unrelated to iron-oxidizing bacteria. However, iron-oxidizing bacteria, or their fossilized remains, are intimately associated with various types of authigenic precipitates, from ancient ore deposits (Polgari et al., 2012) to modern cave rusticles (Florea et al., 2011), and their chemolithotrophic metabolisms are often used to provide specific explanations for the co-occurrence of the mineralized bacteria with specific authigenic minerals. Here we propose that the presence of fossil iron-oxidizing bacteria localized within some of Earth's oldest marine phosphorites suggests that the redox gradient conditions that make possible either, or both, of the primary mechanisms of phosphogenesis that are invoked to explain modern phosphogenesis were present in the era succeeding the initial oxidation of the surface environment.

Raman scan details

Raman 2D data collected by rastering across a 50x50 micron area data collected every 1/6 micron in x, y dimensions, every 1.6 micron in z. Integration time: 0.1s.

Acknowledgments

We thank Clara Chan and two anonymous reviewers for comments that helped improve this manuscript; Dan Jones for providing the images in Figure 1E and Figure DR5; and Bing Luo, Anette von der Handt, Linda Sauer, and Johnny Zhang for technical assistance. Sharma thanks the Director of the Birbal Sahni Institute of Palaeobotany for permission to collaborate with Bailey. Portions of this work were supported by U.S. National Science Foundation (NSF) grant EAR-1057119 and a University of Minnesota travel grant to Bailey. We also thank the participants and sponsors of the International Field Workshop on the Vindhyan Supergroup, including the Palaeontological Society of India. Raman analysis was carried out in the Characterization Facility at the University of Minnesota, which receives partial support from NSF through the MRSEC program. Electron microprobe analysis was carried out at the Electron Microprobe Laboratory, Department of Earth Sciences, University of Minnesota–Twin Cities.

List of Figures

List of Supplementary figures

• *Figure numbering consists of the dissertation figure number, followed, as applicable, by publication figure number.*

Figures

Figure 04 | Jh.01 | **Jhamarkotra rock and filament**

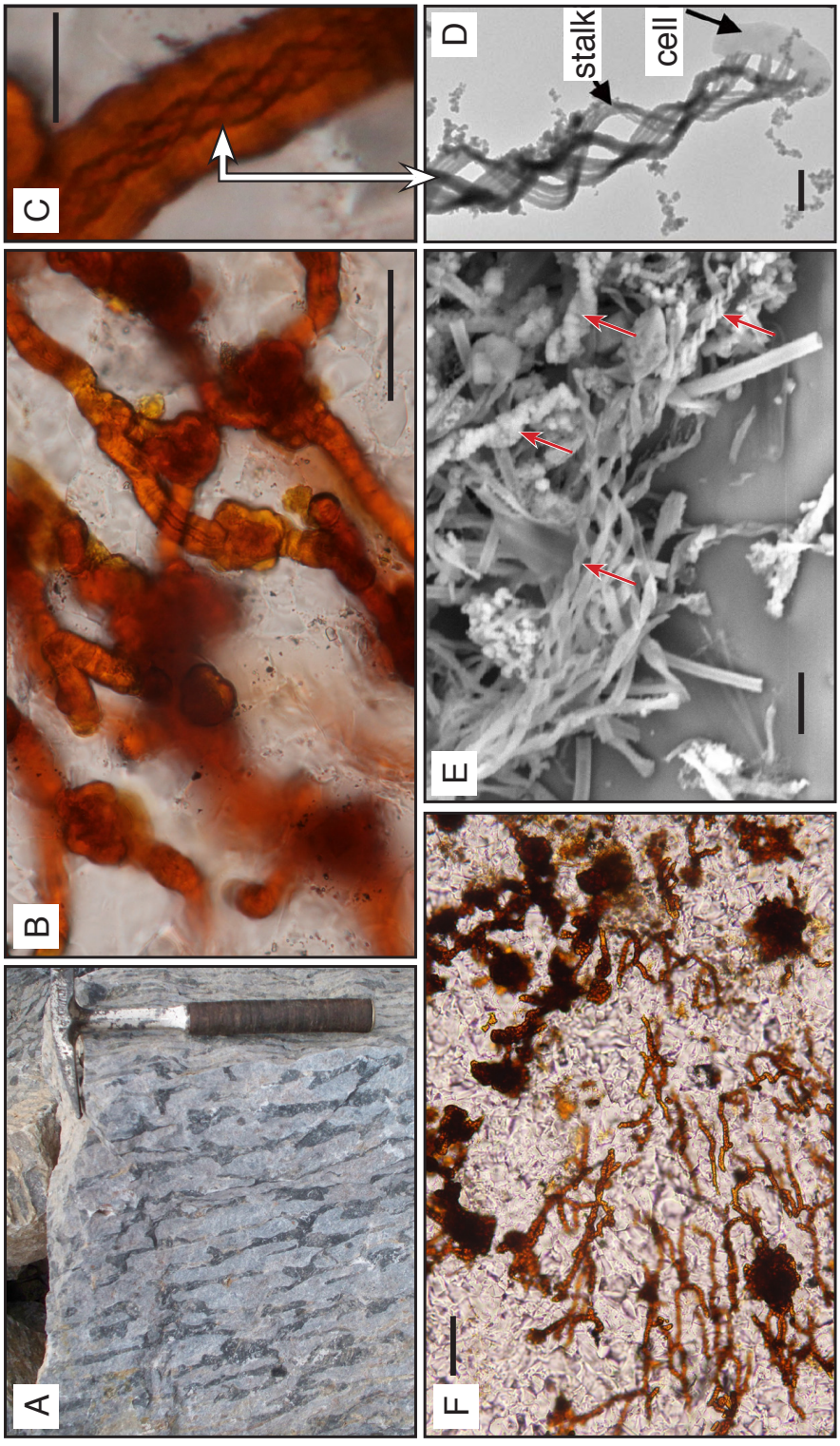

(**A**) Stromatolitic phosphate rock from the Jhamarkotra Formation (Rajasthan, India) sampling site. Microfossils are found within samples collected from the stromatolite columns. (**B**) Optical image of microfossil filaments, showing knobs, branching, and inner lumina. Scale bar is 20 µm. (**C**) Close-up of microfossil filament, showing twisted inner lumen and iron-oxide overgrowth. Scale bar is ~5 µm. Compare to D. (**D**) Scanning electron microscope (SEM) image of an extant filament-extruding iron-oxidizing bacterium. Scale bar is 500 nm. Image from Singer et al. (2011). (**E**) SEM image of extant iron bacteria sheaths and twisted stalks. Note the twisting Gallionella stalks, some with precipitate overgrowth. Arrows highlight variations in stalk diameters. Scale bar is 5 µm. Image courtesy of D. Jones (University of Minnesota, USA). (**F**) Filament swarm. Scale bar is 50 µm.

Figure 05 | Jh.02 | **Jhamarkotra filament Raman analysis**

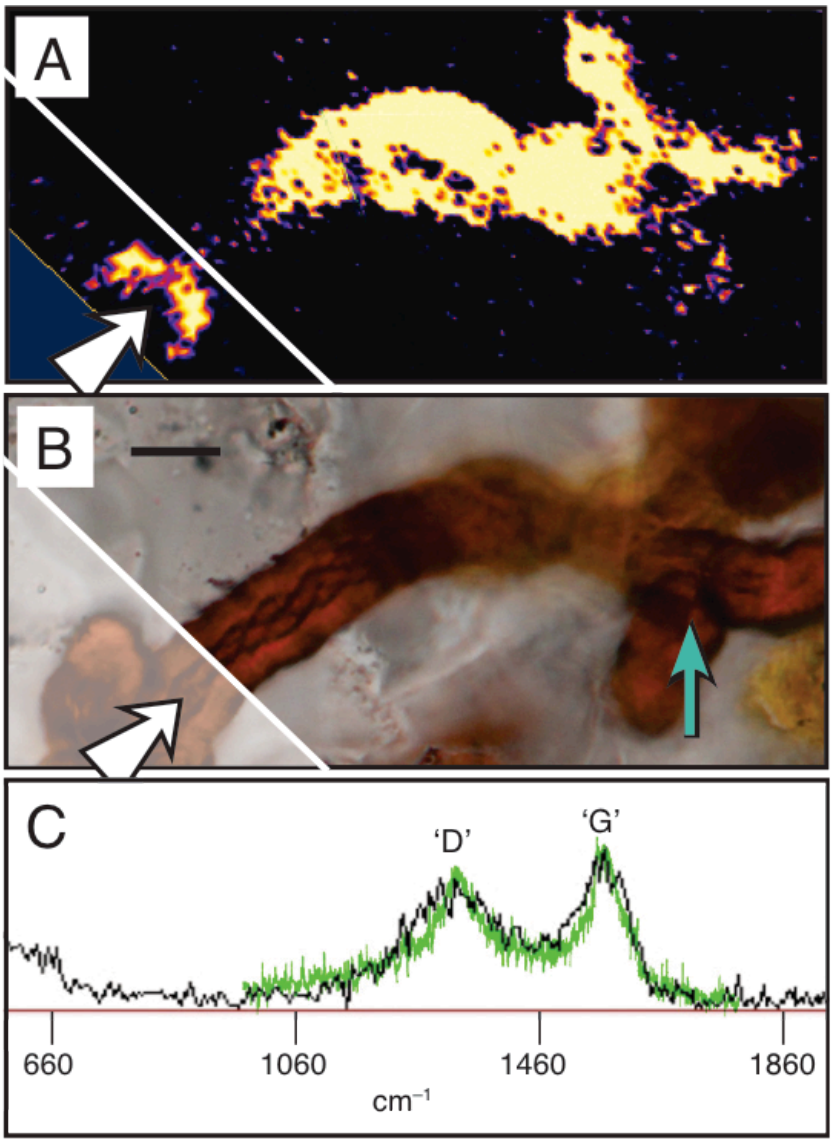

A) Three-dimensional rendering of Raman data, tilted to show two perpendicular planes. Arrow points into the lumen of a filament dipping beneath the surface before coming back up to intersect the surface. Yellow represents high Raman counts of iron-oxide (data filtered to highlight 348–502 cm^{-1} shift representative of metaloxides).(**B**) Transmitted microphotograph of same location as in A, focused on filament beneath surface. Scale bar: ~5 µm. Green arrow indicates location for spectrum in C. White lines in panels A and B delineate a cut through the thin section, perpendicular to the "top" plane. (**C**) Raman spectrum (black) taken from site of green arrow in panel B shows the diagnostic "D" and "G" bands characteristic of kerogen. Green reference spectrum obtained from kerogen that experienced greenschist facies metamorphic alteration (Jehlička and Beny, 1992).

Figure 06 | Jh.DR1 | **Jhamarkotra thin section**

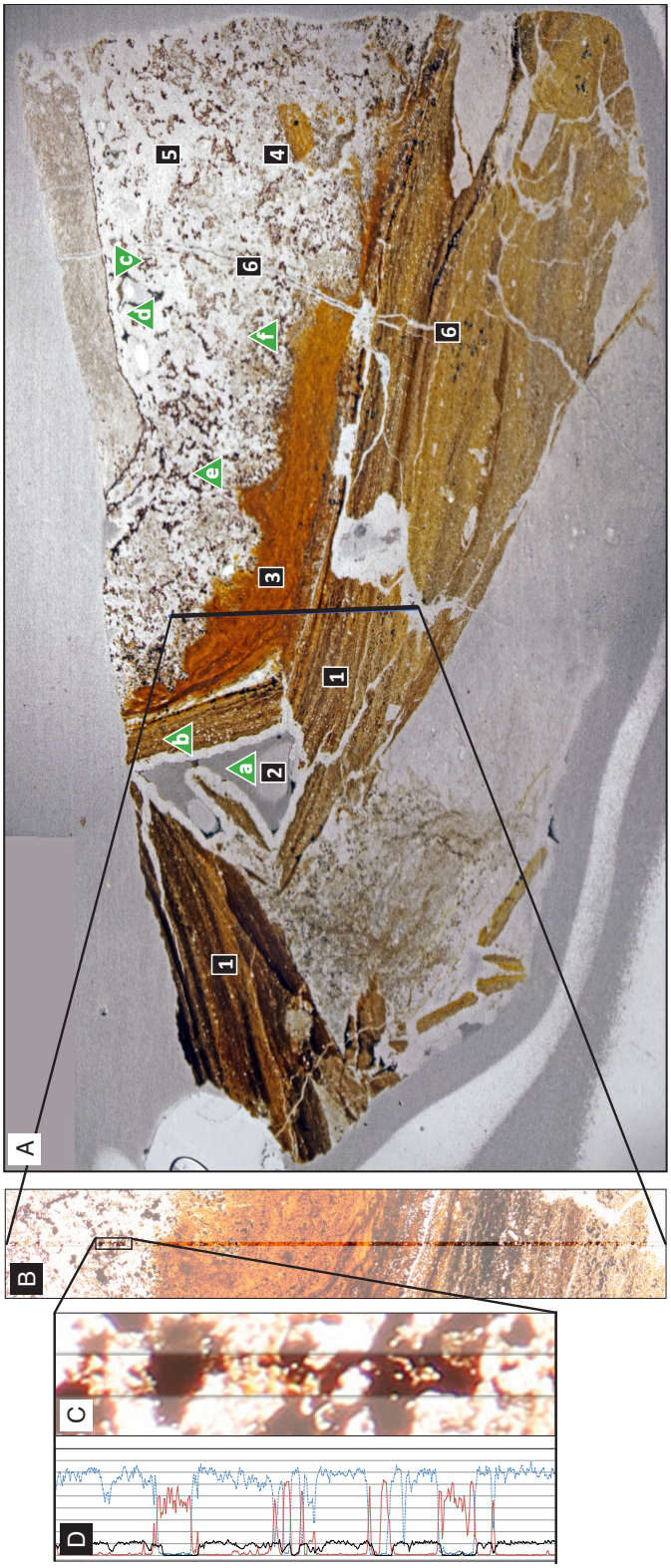

(**A**) Thin section of Jhamarkotra phosphate rock. The brown laminated apatite [1] sustained breakage that left cracks and an apatite-lined vug [2] and appears to have caused ductile deformation of the orange apatite layer [3] before that layer solidified and later sustained breakage – a piece of which [4] can be seen in the clear apatite area [5]. A conspicuous crack [6], lined in quartz, transects the brown, orange and clear apatite fractions. The microfossils are found in the clear apatite fraction. Triangles on thin section show location of spot analyses by electron microprobe. [a] = empty vug; [b] white vug lining and dark material bridging the vug lining = apatite; [c] small void = empty; [d] small void lining = quartz; [e, f] filaments = iron oxide in apatite. (**B**) Enlargement of electron microprobe analysis transect. (**C**) Enlargement of microfossil-containing portion of transect. (**D**) Microprobe elemental analysis showing that filaments are high in iron (red) and low in phosphorus (black) and calcium (blue, dotted line). Graph maximum count = 1800.

Figure 07 | Jh.DR2 | **Jhamarkotra EMPA analysis**

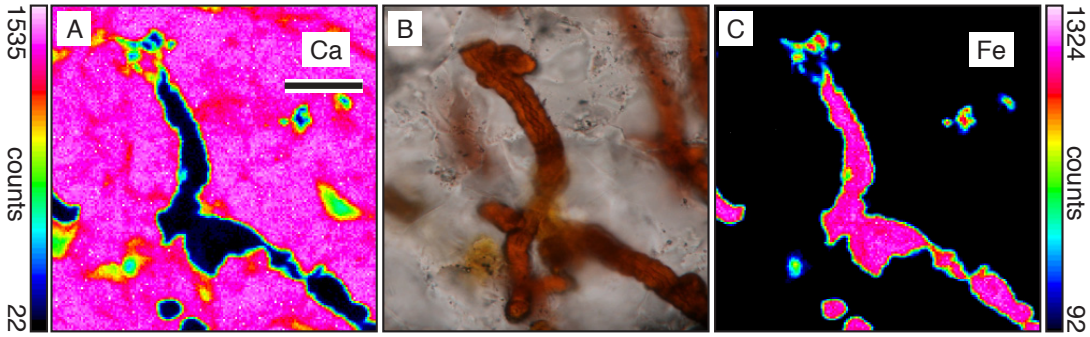

Electron microprobe analysis establishes that the filaments comprise iron oxides within an apatite matrix. (A) shows high calcium in the surrounding apatite [Ca5(PO4)3F,OH] matrix, (C) shows iron in the filaments. An optical photomicrograph of the same area is shown in (B). Note that the optical image is focused beneath the surface, while the microprobe maps portray surface data. Scale bar: 10 µm.

Figure 08 | Jh.DR3 | **Jhamarkotra filaments – rosette-like (dendritic) pattern**

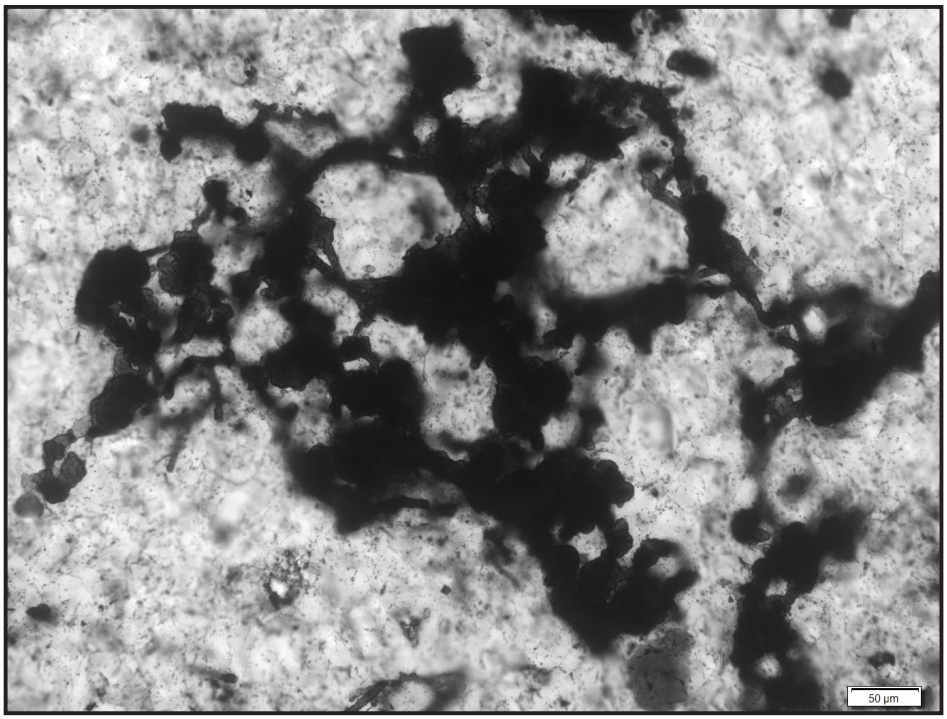

Microphotograph showing the 'rosette-like' habit exhibited by some of the microfossils. Scale bar: 50 microns.

Figure 09 | Jh.DR4 | **Jhamarkotra filaments – micro-XRD analysis**

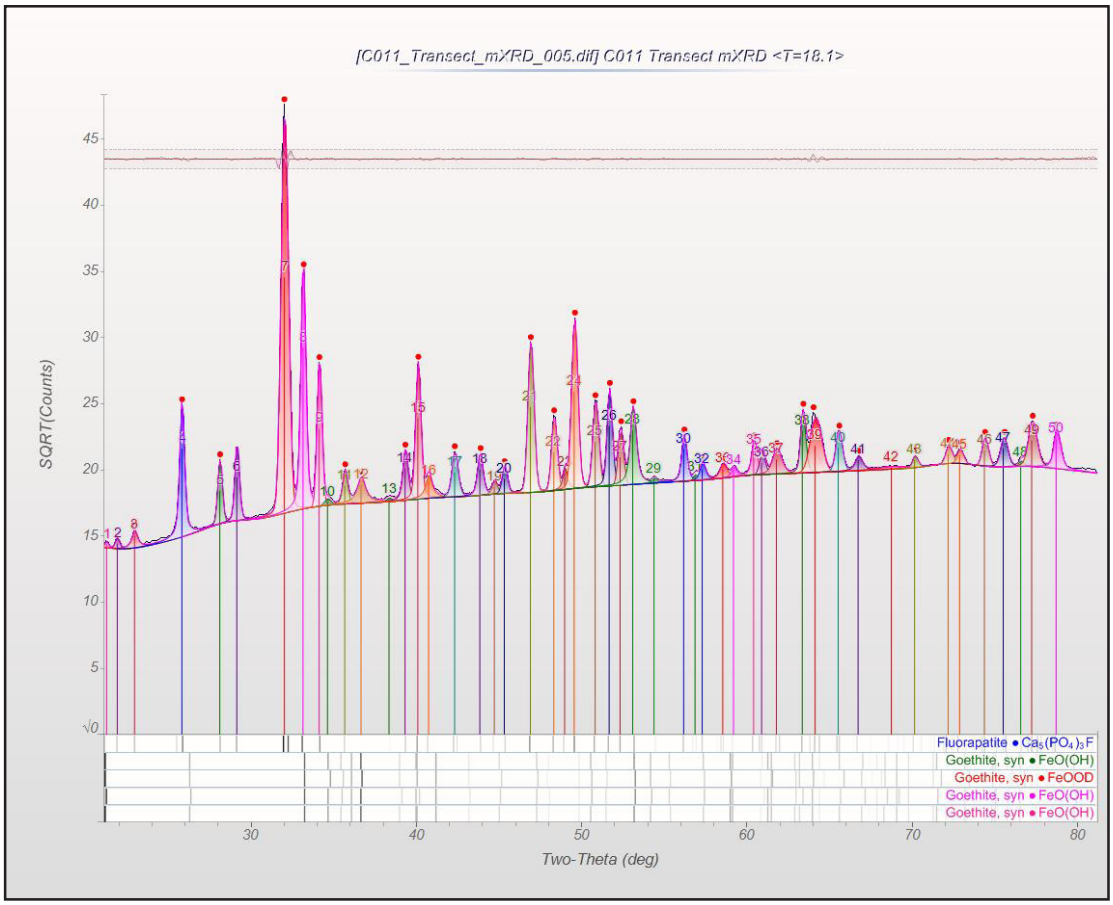

Micro-XRD spectrum obtained from site of a microfossil, showing fit of peaks to goethite standards.

Figure 10 | Jh.DR5 | **Jhamarkotra – extant FeOX**

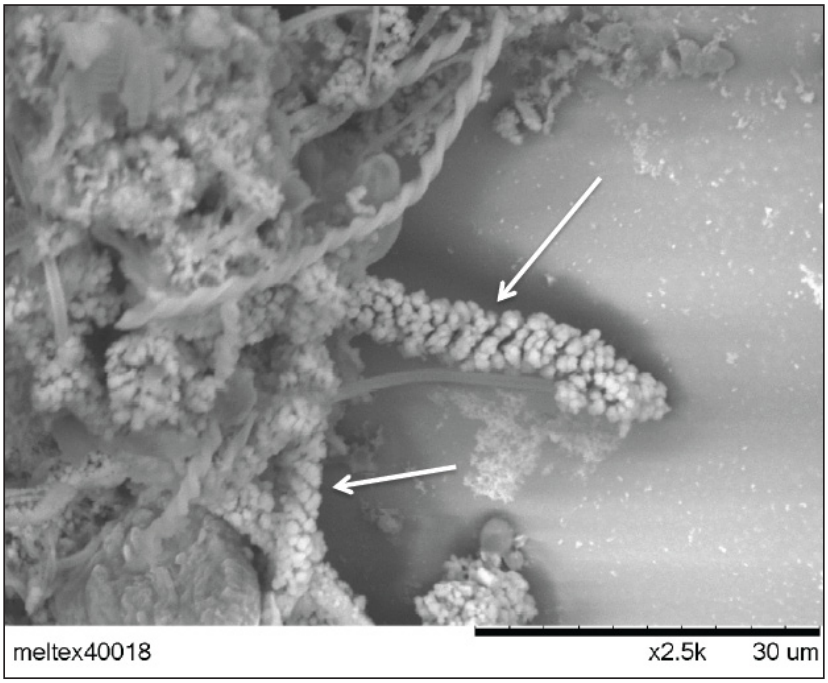

SEM image of iron-oxidizing filaments from the modern, arrows show twisting Gallionella stalks with precipitate overgrowth of diameters similar to those of our microfossils. Image courtesy of Dan Jones (unpublished.)

Figure 11 | Jh.DR6 | **Jhamarkotra – bulk XRD analysis**

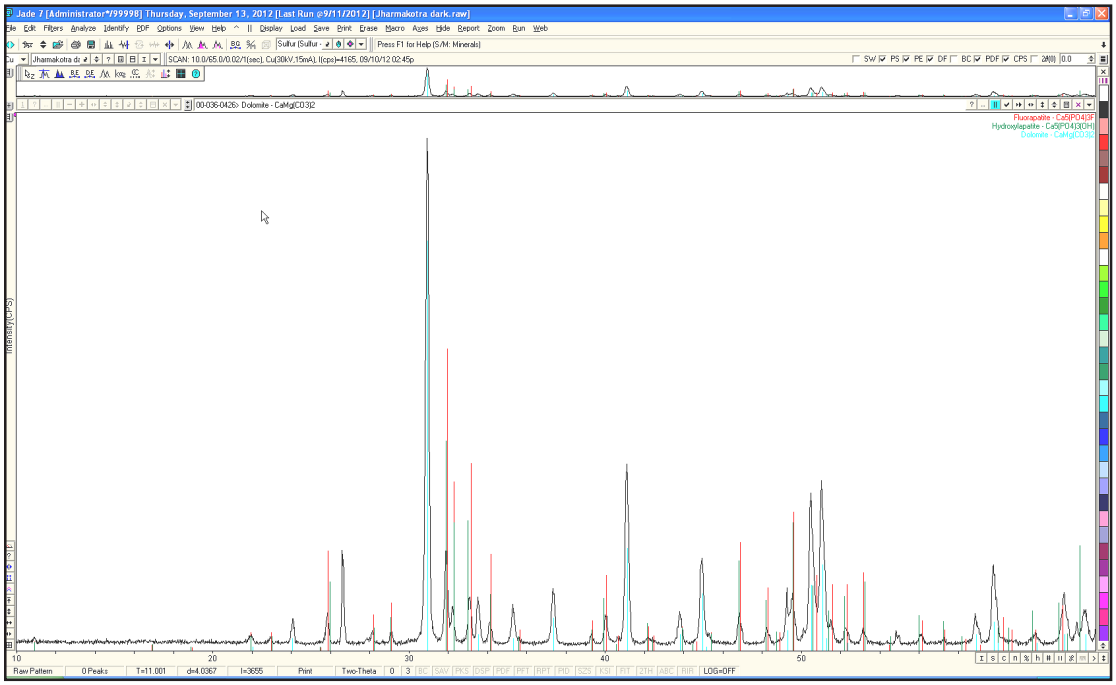

Bulk powder XRD spectrum showing FAP/HAP and matrix dolomite.

References cited

Bailey, J., Corsetti, F., Greene, S., Crosby, C., Liu, P., and Orphan, V., 2013, Filamentous sulfur bacteria preserved in modern and ancient phosphatic sediments: Implications for the role of oxygen and bacteria in phosphogenesis: *Geobiology*, v. 11, p. 397–405, doi:10.1111/gbi.12046.

Barghoorn, E.S., and Tyler, S.A., 1965, Microorganisms from the Gunflint Chert: *Science*, v. 147, p. 563–575, doi:10.1126/science.147.3658.563.

Bekker, A., Holland, H.D., Wang, P.-L., Rumble, D., III, Stein, H.J., Hannah, J.L., Coetzee, L.L., and Beukes, N.J., 2004, Dating the rise of atmospheric oxygen: *Nature*, v. 427, p. 117–120, doi: 10.1038 /nature02260.

Brock, J., and Schulz-Vogt, H.N., 2011, Sulfide induces phosphate release from polyphosphate in cultures of a marine Beggiatoa strain: The ISME Journal, v. 5, p. 497–506, doi:10.1038 /ismej .2010.135.

Canfield, D.E., Habicht, K.S., and Thamdrup, B., 2000, The Archean sulfur cycle and the early history of atmospheric oxygen: Science, v. 288, p. 658–661, doi:10.1126/science.288.5466.658.sag

Chan, C.S., Fakra, S.C., Edwards, D.C., Emerson, D., and Banfield, J.F., 2009, Iron oxyhydroxide mineralization on microbial extracellular polysaccharides: Geochimica et Cosmochimica Acta, v. 73, p. 3807–3818, doi:10.1016/j .gca .2009 .02.036.

Chan, C.S., Fakra, S.C., Emerson, D., Fleming, E.J., and Edwards, K.J., 2011, Lithotrophic iron oxidizing bacteria produce organic stalks to control mineral growth: Implications for biosignature formation: The ISME Journal, v. 5, p. 717–727, doi:10.1038/ismej.2010.173.

Choudhuri, R., and Roy, A.B., 1986, Proterozoic and Cambrian phosphorites—deposits: Jhamarkotra, Rajasthan, India, in Cook, P.J., and Shergold, J.H., eds., Phosphate Deposits of the World, Volume 1: Proterozoic and Cambrian Phosphorites: Cambridge, UK, Cambridge University Press, p. 202–219.

Cloud, P.E.J., 1965, Significance of the Gunflint (Precambrian) microflora: Science, v. 148, p. 27–35, doi:10.1126/science.148.3666.27.

Cook, P.J., Shergold, J.H., Burnett, W.C., and Riggs, S.R., 1990, Phosphorite research: A historical overview, in Notholt, A.J.G., and Jarvis, I., eds., Phosphorite Research and Development: Geological Society of London Special Publication 52, p. 1–22.

Crosby, C.H., and Bailey, J.V., 2012, The role of microbes in the formation of modern and ancient phosphatic mineral deposits: Frontiers in Microbiology, v. 3, p. 1–7.

Crowe, S.A., Døssing, L.N., Beukes, N.J., Bau, M., Kruger, S.J., Frei, R., and Canfield, D.E., 2013, Atmospheric oxygenation three billion years ago: Nature, v. 501, p. 535–538, doi:10.1038 /nature12426.

Downs, R.T., 2006, The RRUFF Project: An integrated study of the chemistry, crystallography, Raman and infrared spectroscopy of minerals, in Program and abstracts of the 19th General Meeting of the International Mineralogical Association, Kobe, Japan, p. 3–13.

Emerson, D., and Ghiorse, W.C., 1992, Isolation, cultural maintenance, and taxonomy of a sheath forming strain of Leptothrix discophora and characterization of manganese-oxidizing activity associated with the sheath: Applied and Environmental Microbiology, v. 58, p. 4001–4010.

Emerson, D., and Ghiorse, W.C., 1993, Ultrastructure and chemical composition of the sheath of Leptothrix discophora SP-6: Journal of Bacteriology, v. 175, p. 7808–7818.

Farquhar, J., Peters, M., Johnston, D.T., Strauss, H., Masterson, A., Wiechert, U., and Kaufman, A.J., 2007, Isotopic evidence for Mesoarchaean anoxia and changing atmospheric sulphur chemistry: Nature, v. 449, p. 706–709, doi: 10.1038/nature06202.

Florea, L., Noe-Stinson, C., Brewer, J., Fowler, R., Kearns, B.J., and Greco, A., 2011, Iron oxide and

calcite associated with Leptothrix sp. biofilms within an estavelle in the upper Floridan aquifer: International Journal of Speleology, v. 40, p. 205–219, doi:10.5038/1827-806X.40.2.12.

Fru, E.C., Ivarsson, M., Kilias, S.P., Bengtson, S., Belivanova, V., Marone, F., Fortin, D., Broman, C., and Stampanoni, M., 2013, Fossilized iron bacteria reveal a pathway to the biological origin of banded iron formation: Nature Communications, v. 4, 2050, doi:10.1038 /ncomms3050.

Goldhammer, T., Brüchert, V., Ferdelman, T.G., and Zabel, M., 2010, Microbial sequestration of phosphorus in anoxic upwelling sediments: Nature Geoscience, v. 3, p. 557–561, doi: 10.1038 /ngeo913.

Hashimoto, H., Yokoyama, S., Asaoka, H., Kusano, Y., Ikeda, Y., Seno, M., Takada, J., Fujii, T., Nakanishi, M., and Murakami, R., 2007, Characteristics of hollow microtubes consisting of amorphous iron oxide nanoparticles produced by iron oxidizing bacteria, Leptothrix ochracea: Journal of Magnetism and Magnetic Materials, v. 310, p. 2405–2407, doi:10.1016/j.jmmm.2006.10.793.

Heggie, D.T., Skyring, G.W., O'Brien, G.W., Reimers, C., Herczeg, A., Moriarty, D.J.W., Burnett, W.C., and Milnes, A.R., 1990, Organic carbon cycling and modern phosphorite formation on the East Australian continental margin: An overview, in Notholt, A.J.G. and Jarvis, I. eds., Phosphorite Research and Development: Geological Society of London Special Publication 52, p. 87–117.

Holland, H.D., 1999, When did the Earth's atmosphere become oxic? A reply: The Geochemical News, v. 100, p. 20–22.

Jehlička, J., and Beny, C., 1992, Application of Raman microspectrometry in the study of structural changes in Precambrian kerogens during regional metamorphism: Organic Geochemistry, v. 18, p. 211–213, doi:10.1016 /0146 -6380 (92) 90132-H.

Krepski, S.T., Emerson, D., Hredzak-Showalter, P.L., Luther, G.W., and Chan, C.S., 2013, Morphology of biogenic iron oxides records microbial physiology and environmental conditions: Toward interpreting iron microfossils: Geobiology, v. 11, p. 457–471, doi:10.1111 /gbi .12043.

Lee, S.-J., and Golubic, S., 1999, Microfossil populations in the context of synsedimentary micrite deposition and acicular carbonate precipitation: Mesoproterozoic Gaoyuzhuang Formation, China: Precambrian Research, v. 96, p. 183–208.

Lepland, A., Melezhik, V.A., Papineau, D., Romashkin, A.E., and Joosu, L., 2013, The earliest phosphorites—Radical change in the phosphorus cycle during the Palaeoproterozoic, in Melezhik, V., et al., eds., Reading the Archive of Earth's Oxygenation, Volume 3: Global Events and the Fennoscandian Arctic Russia—Drilling Early Earth Project: Berlin, Springer, p. 1275–1296.

Lepland, A., et al., 2014, Potential influence of sulphur bacteria on Paleoproterozoic phosphogenesis: Nature Geoscience, v. 7, p. 20–24, doi: 10.1038 /ngeo2005.

Little, C.T.S., Glynn, S.E.J., and Mills, R.A., 2004, Four-hundred-and-ninety-million-year record of bacteriogenic iron oxide precipitation at sea-floor hydrothermal vents: Geomicrobiology Journal, v. 21, p. 415–429, doi: 10.1080/01490450490485845.

McKenzie, N.R., Hughes, N.C., Myrow, P.M., Banerjee, D.M., Deb, M., and Planavsky, N.J., 2013, New age constraints for the Proterozoic Aravalli–Delhi successions of India and their implications: Precambrian Research, v. 238, p. 120–128, doi:10.1016/j .precamres .2013.10.006.

Nisbet, E.G., Grassineau, N.V., Howe, C.J., Abell, P.I., Regelous, M., and Nisbet, R.E.R., 2007, The age of Rubisco: The evolution of oxygenic photosynthesis: Geobiology, v. 5, p. 311–335, doi:10.1111/j.1472-4669.2007.00127.x.

Papineau, D., 2010, Global biogeochemical changes at both ends of the Proterozoic: Insights from phosphorites: Astrobiology, v. 10, p. 165–181, doi:10.1089/ast.2009.0360.

Papineau, D., Purohit, R., Goldberg, T., Pi, D., Shields, G.A., Bhu, H., Steele, A., and Fogel, M.L., 2009, High primary productivity and nitrogen cycling after the Paleoproterozoic phosphogenic event in the

Aravalli Supergroup, India: Precambrian Research, v. 171, p. 37–56, doi: 10.1016/j.precamres.2009.03.005.

Papineau, D., Purohit, R., Fogel, M.L., and Shields-Zhou, G.A., 2013, High phosphate availability as a possible cause for massive cyanobacterial production of oxygen in the Paleoproterozoic atmosphere: Earth and Planetary Science Letters, v. 362, p. 225–236, doi:10.1016/j .epsl .2012.11.050.

Petsch, S.T., 2003, The global oxygen cycle, in Schlesinger, W., et al., eds., Treatise on Geochemistry, Volume 8: Amsterdam, Elsevier, p. 515–555.

Planavsky, N., Rouxel, O., Bekker, A., Shapiro, R., Fralick, P., and Knudsen, A., 2009, Iron-oxidizing microbial ecosystems thrived in late Paleoproterozoic redox-stratified oceans: Earth and Planetary Science Letters, v. 286, p. 230–242, doi:10.1016/j.epsl.2009.06.033.

Planavsky, N., McGoldrick, P., Scott, C.T., Li, C., Reinhard, C.T., Kelly, A.E., Chu, X., Bekker, A., Love, G.D., and Lyons, T.W., 2011, Widespread iron-rich conditions in the mid-Proterozoic ocean: Nature, v. 477, p. 448–451, doi: 10.1038 /nature10327.

Polgari, M., Hein, J.R., Toth, L., Pal-Molnar, E., Vigh, T., Biro, L., and Fintor, K., 2012, Microbial action formed Jurassic Mn-carbonate ore deposit in only a few hundred years (Urkut, Hungary): Geology, v. 40, p. 903–906, doi: 10.1130 /G33304.1.

Roy, A., 2000, Geology of the Palaeoproterozoic Aravalli Supergroup of Rajasthan and northern Gujarat, in Deb, M., ed., Crustal Evolution and Metallogeny in the Northwestern Indian Shield: New Delhi, Alpha Science International, Ltd, p. 87–114.

Roy, A.B., and Paliwal, B.S., 1981, Evolution of lower Proterozoic epicontinental deposits: Stromatolite-bearing Aravalli rocks of Udaipur, Rajasthan, India: Precambrian Research, v. 14, p. 49–74, doi:10.1016/0301-9268(81)90035-8.

Schieber, J., and Glamoclija, M., 2007, Microbial mats built by iron bacteria: A modern example from southern Indiana, in Schieber, J., et al., eds., Atlas of Microbial Mat Features Preserved Within the Clastic Rock Record: Amsterdam, Elsevier, p. 233–244.

Schulz, H.D., and Schulz, H., 2005, Large sulfur bacteria and the formation of phosphorite: Science, v. 307, p. 416–418, doi:10.1126 /science .1103096.

Singer, E., et al., 2011, Mariprofundus ferrooxydans PV-1: The first genome of a marine Fe(II) oxidizing Zetaproteobacterium: PLoS ONE, v. 6, e25386, doi:10.1371/journal.pone.0025386.

Spring, S., 2006, The genera Leptothrix and Sphaerotilus, in Dworkin, M., et al., eds., The Prokaryotes: A Handbook on the Biology of Bacteria, Volume 5: New York, Springer, p. 758–777.

Strother, P.K., and Tobin, K., 1987, Observations on the genus Huroniospora Barghoorn: Implications for paleoecology of the Gunflint microbiota: Precambrian Research, v. 36, p. 323–333, doi:10.1016/0301-9268(87)90029-5.

The relevance of our interpretation is best discussed in the context of the early co-evolution of life and the Earth, in an interplay that profoundly affected the redox gradients of micro-niches and the geosphere at large.

Expanded description of provenance, age & depositional conditions

The Jhamarkotra stromatolites, located near Udaipur, Rajasthan, are part of the Proterozoic Aravalli Group, which lies unconformably on the basement Banded Gneissic Complex, and is composed primarily of shale, sand and carbonates. The Jhamarkotra Formation exhibits two distinct lithologies, interpreted as a near-shore belt hosting stromatolites (some of which are phosphatic, some carbonate) and a deep sea carbonate-free portion (Choudhuri and Roy, 1986). The boundary between the Banded Gneissic Complex and the overlying Aravalli sedimentation has been deformed by folding, but analysis of Aravalli basal volcanics indicate mixed sources, including tholeiitic basalts, rich in iron and relatively depleted in sodium. (Ahmad and Rajamani, 1991; Ahmad and Tarney, 1994).

The Indian subcontinent formed through the tectonic accretion of a number of smaller terranes, and has a complex tectonic history. Like the Aravalli generally, which exhibits an overall highly variable metamorphic grade (Papineau et al., 2009), the Udaipur area has undergone extensive folding, although analysis indicates that the Udaipur area has experienced a remarkably low degree of metamorphism (lower greenschist) despite evidence of much higher metamorphic grades nearby. (Roy and Paliwal, 1981; Roy, 2000; Papineau et al., 2009).

Dated at a minimum age of ~1921 ± 67 Ma by Pb-Pb isochron dating (Sarangi et al., 2006) and a maximum age of ~2440 Ma (Wiedenbeck and Goswami, 1994; Martin et al., 2013) (and references therein) the Jhamarkotra formation developed in a generally low-energy equatorial embayment sheltered between a continental landmass and offshore barrier shoals of an epi-continental sea, in a marine environment subject to tidal influences but largely isolated from the greater epeiric sea (Figure 12, next page) (Roy and Paliwal, 1981; Roy, 2000).

The Udaipur Epicontinental Sea is believed to have formed by ensialic rifting of continental crust (Roy, 2000) after global land masses collided in the formation of the Columbia super-continent (aka Nuna) during a “poorly defined” period 2.1~1.9 Ga (Zhao et al., 2002; Zhao et al.,

2004; Pradhan et al., 2012), though the timing of these events, and age of the underlying Banded Gneissic Complex (also known as the Mewar Gneissic Complex) (Roy, 2000), is still debated (Ahmad and Tarney, 1994; Buick et al., 2006; Azmi et al., 2008; Bengtson et al., 2009; de Wall et al., 2012).

The generally low-energy environment in which these phosphatic stromatolites developed received terrigenous clasts sporadically, possibly delivered by occasional storms sufficiently powerful to disrupt the stromatolites and dislodge terrestrial material (Chauhan, 1979), though extensive sedimentation apparently postdates stromatolite development (Roy and Paliwal, 1981).

The global location at the time of the stromatolite growth is still debated, with most interpretations placing it in a generally low-latitude location, based in part on paleomagnetic data (Pradhan et al., 2012) although other work, investigating the complex tectonic history of the Indian subcontinent, offers the possibility of a more northerly placement (Bhowmik et al., 2010). A low-latitude location would have been conducive to stromatolite development as well as intense karstic weathering of underlying carbonates that may have led to episodic breakage and collapse of stromatolites (Choudhuri and Roy, 1986; Zhao et al., 2002; Zhao et al., 2004).

Further detailed discussion and description of the geology of the area can be found elsewhere. (Roy and Paliwal, 1981; Choudhuri and Roy, 1986; Papineau et al., 2009).

A detailed stratigraphy of the Aravalli is shown in Figure 14.

Expanded description of the thin section & filaments

The thin section shown in Figure 06 contains distinct horizons, including the transparent apatite that hosts the microfossils, and brown strata that incorporate some sharply angular clay-containing clasts a few microns wide by up to ~75 µm long which may comprise weathering products from adjacent cliffs.

Thin sections and 3D imaging by X-ray computerized tomography (XRCT) (Figure 16) show that the rock contains numerous cracks and vugs, evidence of syngenetic breakage likely due either to disruptive storm energies or localized karstic collapse, rather than metamorphic

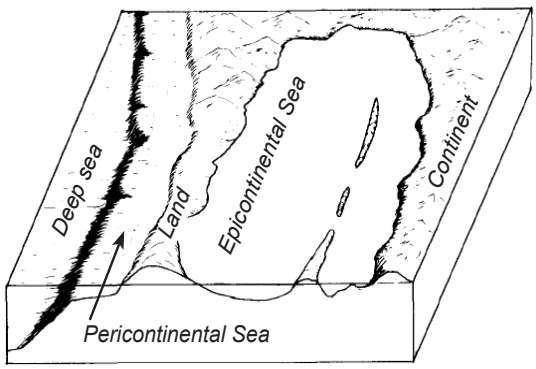

Figure 12
| **Conceptual model of epicontinental sea**
Showing distribution "Udaipur" basin. (Not to scale.) After Roy & Paliwal, 1981

pressures which would, instead, be expected to compress overall.

Based on cross-cutting relationships, our chrono-interpretation, detailed in Figure 06, suggests that the apatite-lined vug predates the quartz-lined vug, indicating a change in aqueous chemistry over time, and menisci and possible desiccation cracks may be evidence of periodic subaerial exposure as may be experienced in intertidal zones (Flugel, 2010).

A number of ruddy reddish filaments (figure 04) are found in the clear apatite horizon, and comprise two habits: swarms of sub-parallel filaments and masses of filaments in a roseate/ dendritic pattern (figure 18). The filaments suggest a twisted or bulbous morphology and are ~5-6 µm in diameter with an inner lumen of ~1-1.5 µm. The microfossils extend in filaments with variable branching distances of ~ 5 to >75 µm. Enlargements (dense, largely opaque red-pigmented sub-spherical features) visible at branching points and filament ends, range in size from ~15-30 µm. The analyzed filaments were found within one of these sub-parallel swarms.

The dendritic masses (figure 18) are dominated by enlargements among which filaments with a diameter of ~4-5 µm extend ~ 5-8 µm. Although these filaments also display branching, the dendritic masses are dominated by enlargements.

Raman analysis shows, and Electron MicroProbe Analysis (EMPA) corroborates, that the filaments are an iron oxide within an apatite matrix. Micro-XRay Diffraction (µXRD) analysis indicates that the iron oxide is goethite.

Unfortunately, we do not have data on the original orientation of the sample rock within the bioherm. However, the orientation of the sub-parallel filament swarms is notable, and may represent a response to tidal or fluvial flows, and/or may be evidence of some mode of substrate adhesion or holdfast. Alternatively, they may indicate chemotactic migration in response to oxygen produced by stromatolite-forming oxygenic photosynthetic organisms (or, if these organisms were photosynthetic, phototactic migration toward light.)

Similarly red-pigmented radial features also found in the clear apatite horizon may represent remnants of abiotic iron oxidation fronts, or possibly an ‘outward diffusion’ of precipitates originally nucleated on organic matter, as described by Knoll et al. (Knoll et al., 1988).

In addition to the filaments under discussion here, some few smaller yellowish features resembling filaments ~1-1.5 µm diameter are visible in the orange layer and await further investigation.

Goethite

Ferrihydrite is generally considered the first-forming of the metastable iron oxyhydroxides such as those that result from microbial iron oxidation by oxygen, though there is some evidence that goethite may sometimes be an initial phase (van der Zee et al., 2003). As an intermediate mineral after ferrihydrite, goethite (α-FeOOH) gradually transforms into the more stable iron oxide hematite through geological time and metamorphic processes (Goss, 1987).

Goethite is also found as a weathering product of hematite and considering the age of the sample, a finding of goethite was unexpected and we had to consider that the sample may have been exposed to post-depositional weathering, or that the filaments represented later, endolithic organisms. Concerned about how pristine the sample was, we confirmed with Dr. Mukund Sharma, the scientist who initially collected the sample and provided it to our lab, that it had been obtained from a newly accessed bioherm, opened by active mining.

The occurrence of goethite in the filaments may possibly be indicative of oxidation of ferrihydrites due to late oxygenation, as may have occurred over geological time if the filaments were not initially sufficiently buried to isolate them from later oxygenated waters. However, Schwertmann et al. (2004), sampling soils over a 12-year period, determined that the goethite-to-hematite ratio is set early on and state that "conditions favoring goethite disfavor hematite and vice versa [and] indicates that the conditions and the mechanisms of the two phases may be … contradictory." They note that as pH moves away from the ZPC of ferrihydrite* increasingly more goethite is formed rather than hematite, with the goethite-to-hematite ratio increasing the greater the deviation from circumneutral, whether toward acidic or basic conditions (Schwertmann et al., 2004). Ferrihydrite dissolution at either high or low pH raises the activity of aqueous Fe(II) to levels required for the neoformation of goethite, which is then resistant to alteration to hematite, an iron oxide that forms less by dissolution of precursor Fe-oxyhydroxides than by rearrangement of internal atoms (Schwertmann and Murad, 1983). Under the fluctuating oxygenic conditions assumed to be present in the stromatolites, pH can be expected to have fluctuated as phototrophic diurnal (daylight) carbon uptake drove both Eh and pH up.

It is also possible that original ferrihydrite filaments were converted to goethite over the long span of geologic time. Although it is likely that microbial EPS would have kept the stromatolite

---

* *ZPC: Point of Zero Charge, the pH value at which a mineral surface charge is null and mineral solubility is generally at a minimum. Ferrihydrite ZPC is pH ~7-8, under which conditions ferrihydrite is least soluble.*

hydrated, seasonal and meteorological effects on sea level may have resulted in periodic subaerial exposure that may have inhibited later conversion of ferrihydrite to goethite. As stated by Raiswell "Aggregation [of ferrihydrite molecules] caused by just one drying event produces a significant decrease in reactivity, which cannot be reversed by subsequent contact with, or storage in, water" (Raiswell, 2011) in which case, conversion may have been accomplished only by virtue of its deep, billion-year-plus age.

Extrapolating from analytical data indicating the presence of goethite in these filaments to an interpretation of the conditions under which they formed can be enhanced by use of Pourbaix (Eh-pH) diagrams, by which geochemists assess the likelihood of any given chemical species under a range of Eh and pH conditions, or alternatively, deduce Eh and pH conditions given a species. We note, however, that although the use of Pourbaix diagrams can be informative in developing an interpretation of the conditions under which a mineral may have precipitated, they cannot provide a definitive determination of the Eh and pH conditions under which different species formed. In fact, they can (and do) vary, sometimes significantly, depending on the dataset used, species concentrations (activities) at species boundaries, partial gas pressures of gaseous species, and temperature and pressure conditions. In addition, such diagrams assume chemical equilibrium, an assumption unlikely to be met in a dynamic situation. And lastly, in Eh-pH diagrams, the Eh and pH conditions under which any given species is shown to be present do not indicate that other species are not present under those conditions, but rather that the indicated species is the dominant one under those conditions (Essington, 2004).

Figure 17 shows differences in diagrams based on different datasets.

Kerogen

The presence of kerogen (large, complex and recalcitrant organics) in a putative microfossil is an oft-cited criteria of biogenicity, and we began our (non-visual) analysis of the filaments with a search for kerogen.

Kerogen alone, however, is not necessarily a definitive indication of biogenicity, as abiotic processes may also result in the Raman spectroscopic D ('disordered') and G ('graphitic') peaks characteristic of kerogen (Pasteris and Wopenka, 2003). Additionally, high grade metamorphism may alter kerogen toward a strongly dominant G peak and an increasingly diminished D peak, weakening an interpretation of biogenicity (Pasteris and Wopenka, 1991; Bourbin et al., 2013). Such a process of graphitization is irreversible, (Pasteris and Wopenka, 1991) and though the presence of a D peak in our kerogen analysis does not irrefutably establish that the kerogen is

biogenic, it does support our interpretation that the filaments are biogenic and did not undergo high grade metamorphism, lending credibility to the relevance of the kerogen findings.

The kerogen in these filaments, however, is cryptic at best. Initially, this raised concern about the reliability of a biogenic interpretation. However, our interpretation of the filaments as the oxidized residue of iron chemolithotrophy left behind by a motile respiring cell could easily account for sparse findings of kerogen within the filaments. Additionally, Bennett et al. (Bennett et al., 2014) have shown evidence that *Mariprofundus* PV1, an extant marine iron-oxidizer, does not readily entrain organic carbon in its stalks.

The presence of a central lumen is also cited as a criteria for filamentous microfossils, based on the premise that cell wall material will preferentially be preserved as recalcitrant kerogen (Javaux et al., 2003). Noting an apparent central lumen observed by optical imaging, we analyzed some of the filaments by Raman spectroscopy at several sequential depths (50 x 50 µm area, interrogated every 1/6 µm along the x and y axes and 1.6 µm in z, at 0.1 s integration time) for the purpose of 3-dimensional (3D) reconstruction of a sample of the filaments. ImageJ 3D rendering of Raman data substantiated the existence of a lumen, but the lumen in this case was within a metal-oxide sheath and not kerogen, as would be expected if the filaments represented cell wall material. Yet in our interpretation of the filaments as the oxidized residue of iron respiration, the occasional presence of aged kerogen internal to the filaments as determined by 3D analysis of Raman data (Figure 05) provides support of a biogenic interpretation and also attests to the syngeneity of the microfossil within the stromatolitic formation (instead of a later, endolithic interpretation, as discussed later.)

It is important to note that the interpretation of a kerogen Raman signal is not straightforward, and since kerogen is cited as an important indicator of biogenicity, its interpretation is a subject of ongoing discussion. Paleontologist J. William Schopf developed a 'Raman Index of Preservation (RIP)' for the interpretation of kerogen by variations in color and comparative D and G peak characteristics (Schopf et al., 2005), and research has shown that both the polishing and the orientation of microcrystalline kerogenous material may affect its Raman signal (Nakamizo et al., 1978; Wopenka and Pasteris, 1993).

The process of the alteration of carbonaceous material to kerogen is discussed by Wopenka & Pasteris (Wopenka and Pasteris, 1993).

The role of polyphosphates in adaptation to fluctuating redox conditions

Proterozoic phosphorites like those of the Jhamarkotra are unusual in being among the most P-rich known. The Jhamarkotra is also unusual in that this very high phosphorus content (~35% P_2O_5) is confined to the stromatolites, the surrounding matrix material being basically devoid of phosphate.

As already mentioned, the influence of microbes in phosphorite formation has long been speculated (Baturin, 1982), supported by experimental evidence of microbial uptake and release of phosphate in lake waters by unspecified 'sedimentary organisms' (Gachter et al., 1988) and later, the marine *Thiomargarita* (Schulz and Schulz, 2005).

A number of organisms, including the large sulfur oxidizing bacteria *Beggiatoa* and *Thiomargarita* ssp. are polyphosphate accumulating organisms (PAOs). Many of these organisms take advantage of fluctuating oxic-anoxic conditions by taking up so-called 'luxury' phosphate (phosphorus beyond that required for general metabolic use) under oxygenated conditions, store energy through polymerization of phosphate to form inclusions of polyphosphates (polyP) – and later access the stored polyphosphate bond energy under anaerobic conditions (Jørgensen, 2010) (Figure 19).

Intracellular polyphosphates are found across the tree of life, where they may serve any number of functions, including cellular osmoregulation, stress response and energy storage (Seufferheld et al., 2008; Lander et al., 2016) and recent research has shown that at least some extant marine iron oxidizers carry genes for the accumulation of polyphosphate (Singer et al., 2011a). In the Jhamarkotra phosphorites, with oxygen presumably supplied locally by oxygenic stromatolite-building phototrophs in otherwise ferric waters, iron oxidizers may have been able to adapt to fluctuating oxygenation conditions, utilizing energy gained from oxidation of Fe(II) to take up and polymerize phosphate under oxygenated conditions, and continuing metabolic processes under anaerobic conditions by accessing the energy released in the cleaving of phosphate ions from polyphosphate. In such a case, the concomitant phosphate expulsion into surrounding exopolysaccharides (EPS) under anaerobic conditions may have provided concentrations of phosphate sufficient for precipitation of apatite (Schulz and Schulz, 2005).

Possible alternative phosphate-concentrating mechanisms

An alternative mechanism of phosphate concentration is described as an Iron Redox Pump (IRP), in which, under aerobic and/or alkaline conditions, solid Fe(III)-oxides with abundant hydroxyl groups adhere phosphate ions (Figure 20). As the solid Fe(III)-oxides undergo

gravitational settling and encounter anoxic and/or acidic sediment conditions, they dissolve as the Fe(III) is reduced to Fe(II) and adsorbed phosphate ions are released into solution.

Where this occurs under confining conditions, such as in sediment pores or EPS, phosphate concentration may rise to a point of supersaturation with respect to calcium phosphate mineral precursors. This IRP mechanism may act as an abiotic process, though it may also be facilitated by microbial action (Roden et al., 2004). An IRP interpretation of stromatolite phosphate concentration is possible, but such an interpretation requires very steep redox gradients across the EPS surface.

A recent report also discusses another biological variation of the IRP, a 'Microbial Redox Pump' wherein microbial uptake of iron facilitates the dispersal of iron in the oceans (Li et al., 2014). The role of such a mechanism in the context of the evolving Proterozoic ocean, as ferric waters are undergoing a shift to becoming sulfidic, is unclear.

Whence the phosphate?

The initial source of phosphate (upwelling, terrigenous clastic, or volcanic) is unresolved (Roy and Paliwal, 1981; Choudhuri and Roy, 1986). The occurrence of the roughly coeval GOE, however, suggests that the source of at least some of the phosphate may be fluvial, by oxidative weathering of subaerial P-bearing rock within the nearshore watershed. Once a microbial community had been established, subsequent microbial degradation of organisms would likely also have contributed bioavailable P.

Primary P or replacement?

There is some evidence that some phosphatic stromatolites may involve primary phosphate precipitation (Sánchez-Navas and Martín-Algarra, 2001), although the currently prevailing interpretation of phosphatic stromatolites is that the apatite represents replacement of earlier-precipitated carbonate.

However, as already noted, the phosphatic nature of these Jhamarkotra stromatolites is unusual and, within the Indian subcontinent, a characteristic primarily restricted to the Jhamarkotra region, which can generally be divided into phosphatic and non-phosphatic domains, (Papineau et al., 2009). The presence of coeval phosphate-free carbonate stromatolites in nearby areas highlights the noticeable distinction between these phosphatic stromatolites and the more common nearby carbonate stromatolites. The Jhamarkotra stromatolites are also unusual in other regards: The intercolumnar dolomitic carbonates are, with the exception of rare clastic material

that may represent shards of broken stromatolites, virtually phosphate-free (Chauhan, 1979) and the slender and tall columnar Jhamarkotra stromatolite morphology is distinct from many of the nearby stromatolites, which tend to present as more laterally extensive algal mats.

It is unclear whether the apatite in the Jhamarkotra stromatolites was primary or replacement after carbonate. An interpretation of phosphate-accumulating organisms diurnally fluxing phosphate into EPS-confining stromatolitic pore waters under fluctuating redox regimes lends credence to the intriguing possibility that these stromatolites may represent primary apatite (or precursor calcium phosphate species) precipitation. Analytically, electron microprobe analysis of our specimen shows very low magnesium, which may also support an interpretation of primary apatite as described in Khan et al. (Khan et al., 2012). Alternatively, or additionally, the very high phosphate content of these stromatolites may involve a cyclic interplay, with apatite serving as a P source for organisms capable of solubilizing phosphate and thereby promoting microbial growth (Kan et al., 2013), perhaps providing a positive feedback mechanism to drive the very high P content of the stromatolites, ~35% P_2O_5, a value found almost exclusively among the early stromatolitic phosphorites of the Proterozoic such as this one.

Iron utilization

The sharp mineralogical distinction between the microfossils described here and the surrounding matrix suggests the involvement of microbes in iron lithotrophy, as is seen in extant iron-oxidizing bacteria such as *Gallionella* and *Leptothrix*, and implies conditions under which microbes are able to outcompete abiotic iron oxidation, positioned at the specific interface between anoxic waters hosting soluble Fe(II), and adjacent O_2-hosting waters, where both Fe(II) and O_2 are present and organisms can intercede before an inorganic redox reaction renders them less reactive.

In our interpretation, oxygen serves as a terminal electron acceptor for ancient iron-oxidizing organisms able to utilize phosphate for energy storage.

As early Earth is believed to have been largely devoid of reactive molecular oxygen, the earliest microbes probably subsisted by harnessing the energy inherent in redox gradients present at the interface of mineral solid phases and aqueous solutions and are therefore largely considered likely to have been metal oxidizers able to capitalize on the multiple oxidation states of metals. Today, iron oxidation is widespread across bacterial phylogenies (Edwards et al., 2004). Hence, iron oxidation as a microbial energy-attaining strategy is thought to have developed during the early rise of oxygen when the ability to take advantage of iron-rich and oxygen-poor conditions

of the early Earth would give it an advantage in a specific niche, positioned at the 'sweet spot' between oxic and ferrous waters, so early FeOX may have been well-positioned to adapt as needed to an increasingly oxygenated environment.

In addition to providing a source of electrons to iron-oxidizing microbes, iron is central to many metalloenzymes, another indication that biological utilization of iron is ancient as this characteristic, too, is shared across virtually all of biology. Because iron is a required (assimilatory) nutrient, today many aerobic (and facultative anaerobic) microbes release siderophores, iron chelating agents that provide an advantage over competitor organisms and/or abiotic iron oxidation (Neilands, 1995; Duckworth et al., 2009). Today, the degree of siderophore production is controlled by the concentration and speciation of ambient iron ions and iron-containing minerals – the less available iron, the more critical the need for siderophores (Hersman et al., 2000). In the context of the Jhamarkotra microfossils, however, the role of siderophores in iron-oxidizing microbes is speculative, as ferrous marine conditions are presumed. With aqueous iron plentiful and oxygen generally not present, abiotic competition for iron would be minimal. More likely, ancient microbes may have produced EPS with carboxyl groups that binds Fe(II) and enhances iron oxidation under circumneutral conditions (Chan et al., 2009; Ishihara et al., 2013).

Circumneutral iron oxidation

As noted by Emerson and Weiss: "The kinetics of Fe(II) oxidation are critically dependent upon pH, and oxygen concentration" (Emerson and Weiss, 2004) as shown in equation 5, below.

$$\frac{-d[\mathrm{Fe(II)}]}{dt} = k[\mathrm{Fe(II)}][\mathrm{OH^-}]^2\, p\mathrm{O_2} \qquad 5$$

The rate of abiotic oxidation of Fe(II) rises with increasing pH and/or increasing $p\ O_2$. Hence, abiotic iron oxidation imposes a requirement for "very low oxygen concentrations (≤1% ambient) and relatively low Fe(II) concentrations, preferably coupled to moderate or high flux of Fe(II)." (Emerson and Weiss, 2004).

Acknowledging that the waters in which these stromatolites formed are presumed to be ferrous, generally anoxic and probably acidic, it can be expected that at least initially, abiotic iron oxidation would be inhibited. Conditions within microbially-exuded EPS, however, may have been sufficiently viscous as to slow the diffusion rates of both oxygen and Fe(II), effectively

providing an expanded 'sweet zone' within which iron-oxidizing microbes may have access to both a plentiful yet controlled source of electrons from reduced iron, and terminal electron acceptors in oxygen provided by oxygenic photosynthetic and EPS-producing organisms.

Conclusion: Arriving at a microbial iron-oxidizing interpretation

Considering their age and provenance, these Jhamarkotra iron-oxidizing microfossils may represent early organisms able to thrive at the oxic/anoxic boundary by taking advantage of oxygenated micro-niches created by stromatolite-forming organisms in a world only locally oxygenated.

The occurrence of iron filaments precipitated on organic polysaccharides is a ubiquitous marker of iron-oxidizing microbes, and our interpretation of the Jhamarkotra microfossils incorporates this fact. (Chan et al., 2004; Chan et al., 2009).

The filamentous microfossils described here are composed of Fe-oxides within apatite rock, and can more generally be considered biomarkers than remnants of cellular material. The sharp mineralogical distinction between the filaments and the surrounding matrix suggests the involvement of microbes in iron redox chemistry, as is seen in extant iron-oxidizing bacteria such as *Gallionella* and *Leptothrix* (Spring, 2006; Konhauser, 2007). In tapping the redox potential of reduced iron, iron oxidizing organisms divert electrons to the microbial electron transport chain, and use the electron energy to drive cellular metabolic reactions. As a result, soluble Fe(II) is converted to Fe(III) which precipitates as a hydrous iron oxyhydroxide. The oxidized end product may take the form of a poorly crystalline or amorphous ferrihydrite sheath encircling cells, as by Leptothrix spp., or a stalk propelled away from the cell, as is formed by Gallionella spp. (e.g. Figure 26e) and *Mariprofundus* (Figure Jh.01f) (Emerson and Ghiorse, 1993; Hashimoto et al., 2007; Schieber and Glamoclija, 2007; Singer et al., 2011b).

After their initial precipitation, the surface properties of iron oxides promote additional mineralization, providing a possible explanation for the tendency of the filaments to appear bulbous and fluctuate in filament diameter. Indeed, the lumen observed within the filaments may represent the area between strands of organic material extruded as dual, roughly helical strands and upon which waste oxidized iron precipitated, as illustrated by the stalk of *Mariprofundus* (Figure 21a) (Chan et al., 2004; Singer et al., 2011b) which may also be the initial source of the cryptic kerogenous signal within these fossil features.

Oxygen's high electronegativity makes it a strong oxidant (second only to fluorine), giving organisms that utilize it as TEA the advantage of accessing high redox potentials. However,

oxygen metabolism also produces radicals that are toxic to organisms (Salgado et al., 2013). Over time, organisms have evolved to develop defenses against these, including enzymes such as superoxide dismutase and catalase. However, while oxygen levels were still relatively low it is unlikely that most organisms would have yet developed these defenses. Instead, the binding of oxygen into ferrihydrite sheaths via iron oxidation may have offered a possible defense against increased pO_2, and may offer another rationale for the apparent early emergence of iron oxidation as a metabolic strategy (Nealson, 1982).

— CONSIDERATION OF ALTERNATIVE INTERPRETATIONS —

Seeking to address the potential of confirmation bias in our interpretation, a number of other options were considered in the process of our analysis including the possibility that the filamentous features were abiotically produced, were endoliths not syngenetic with the host rock, or represented ancestral eukaryotes.

Following is a short discussion of these lines of thought.

Alternative interpretations: Abiotic artifacts

Of initial concern was whether the filaments were genuine biologically-produced microfossils. The possibility that these features were abiotic had to be considered and rejected to support a biogenic interpretation, particularly in light of the dearth of kerogen. Among possible abiotically produced features are Ambient Inclusion Trails (AITs), diffusion fronts and grain boundaries that might mimic filamentous microfossils.

AITs (Figure 22a) (Wacey et al., 2016) are tubular features formed as a result of a very small crystal being propelled through a rock (Buick, 1990; Wacey et al., 2016). These features may have diameters similar to those of the Jhamarkotra microfossils and may appear to exhibit apparent branching, superficially resembling the Jhamarkotra microfossils.

However, the distinguishing features of AITs – parallel striations along the length of the feature, and the common presence of the propelled crystal at the end of the feature – are consistently not observed in these Jhamarkotra microfossils, allowing us to reject this possibility.

Diffusion fronts and crystal boundaries can also sometimes be mistaken for filamentous microfossils. Close observation of our thin sections showed apparent cases of these (Figure

22b,c), allowing observation of features within the same thin section. In such comparisons, the microfossils exhibit a number of characteristics, including distinct margins, bulbous filamentous morphologies, true branching and an inner twisting lumen, that clearly distinguish them from these abiotically-produced artifacts.

A variety of other abiotically-produced filamentous features can also closely mimic those of the Jhamarkotra microfossils, including pseudomorphs produced by Hawley (figure 22d) (Hawley, 1926) and by Garcia-Ruiz et al. (figure 22e) (Garcia-Ruiz, 1994; Hyde et al., 2004). And Ivarsson et al. describe ferric filamentous features observed in ≤ 80 Ma seamount basalts which they interpret as abiogenic structures that form when hot lava extruded into sea water vaporizes some water that then rises in bubbles through the still pliant lava, forming micron-scale features that look very much like filamentous and septate microfossils: sequential knobs that result in apical growth resembling filamentous septate microbes in size and shape (figure 22f) (Ivarsson et al., 2008). Though these features resemble the Jhamarkotra microfossils, this explanation can be rejected for our microfossils, as it requires a depositional environment very different than that of our microfossils. There is no evidence of the viscous lava nor the high heat required to vaporize water having been present.

Similarly, the chemical conditions of laboratory experiments that have resulted in structures that appear to be biologically produced (Hyde et al., 2004; García-ruiz et al., 2009) are inconsistent with apparent reasonable *in situ* conditions of provenance.

Alternative interpretations: Fungal, eukaryotic

The branching morphology of the Jhamarkotra microfossils, resembling fungal hyphae, deceptively suggested a eukaryotic interpretation – an interpretation that would have extended the emergence of multicellular eukaryotes by nearly a billion years. The earliest resolved instance of a multicellular fossil eukaryote is the 1.2 Ga Bangiomorph (Butterfield, 2000).

The distinctive fungal-like morphology of the Jhamarkotra microfossils closely resembles the much later fossil fungi (~16-14 Ma) described by Ivarsson et al., including branching and enlargements that may represent remnants of algal holdfasts or fungal sporangia (Ivarsson et al., 2011). Identification of chitin residues within our microfossils would have bolstered a eukaryotic interpretation. However in a study of chitin recalcitrance, Flannery et al., found that only 0.5% of original chitin remained after 25 Ma. The advanced age of our specimen would have resulted in even more loss, making verification of chitin not possible (Flannery et al., 2001).

Instead, confirmation that the filaments comprise iron oxides strongly suggests that these are not remnants of eukaryotes, as no eukaryotes are known to produce twisted stalks rich in iron. This, and the fact that the age of the Jhamarkotra microfossils is decidedly inconsistent with what we know of the emergence of fungi convincingly denied an interpretation of these microfossils as ancestral eukaryotes.

The timing of the emergence of eukarya remains unresolved, and although some have entertained an interpretation of some >2.5 Ga microfossils as eukaryotes, this interpretation is based on single-celled organisms sporting elaborately ornamented cell walls (Javaux et al., 2003) as is thought to be common among single-celled eukaryotic acritarchs (Buick, 2010), and not filamentous microbes.

Although a branching morphology does suggest a fungal interpretation, a few prokaryotes also share this trait. Extant Actinobacteria are characterized by their true branching (Schaal et al., 2006), a trait not generally shared by other bacterial species, but sometimes also found in cyano-bacteria (Finsinger et al., 2008). In light of this, it is interesting to consider the possibility that these Jhamarkotra microfossils may represent ancestral cyanobacteria – oxygenic phototrophs able to utilize Fe(II) as electron donors.

Alternative interpretation: Endoliths?

The possibility that these microfossil may represent endoliths was also considered, as endolithy would almost certainly argue against syngeneity with the host rock and may require a reframing of our interpretation.

Endolithy (rock boring) is practiced by a range of organisms including fungi, bacteria, archaea and algae (McLoughlin et al., 2007) and this possibility would be particularly heightened in a fungal interpretation, as one of the characteristics of many fungi is the ability of fungal hyphae to invade nutrient sources and mineral substrates (Golubic et al., 2005). However, taking into account the analyses performed on these filamentous features and the presence of aged kerogen consistent with the age and metamorphic grade of the source rock within the body of the filaments is taken as evidence of syngeneity of the organisms within the host rock, arguing against recent contamination. In any event, borings of ancient microbes within a few millennia of host rock formation would not significantly alter the dating the microfossils at ~2 Ga, although it may call for a reconsideration of our interpretation.

Closing remarks

We have presented evidence of ≥ 2 Ga microfossils in a phosphate rock that we have interpreted as representing iron oxidizing bacteria. We propose that they represent early specimens of organisms that thrived at the oxic-anoxic boundary by taking advantage of oxygenated conditions created by putative oxygenic stromatolite-forming cyanobacteria in a world still largely not oxygenated, and may also represent an early adaptation of polyphosphate utilization for accommodating fluctuating redox regimes.

This interpretation required, first and foremost, convincing evidence of the biogenicity of the observed features. As mentioned, establishing the *bona fide* biogenicity of a putative microfossil is often very challenging. Many forces alter the morphology and chemistry of microfossils, making a determination of biogenicity difficult and often contested. Nonetheless, as noted by Knoll & Golubic, interpretations of ancient stromatolite-forming filamentous bacteria should be made based on "systematic, ecological and taphonomic investigations of living microorganisms found in analogous physical environments." (Knoll and Golubic, 1992).

Although we have little more than this reasonable consideration with which to work, it is important to remember that this presumes environments and organisms similar to those that can be found today.

Following the figures for this discussion section, the next chapter addresses some of the issues of establishing biogenicity.

Figure 13 | **Jhamarkotra : Geological map & cross section**

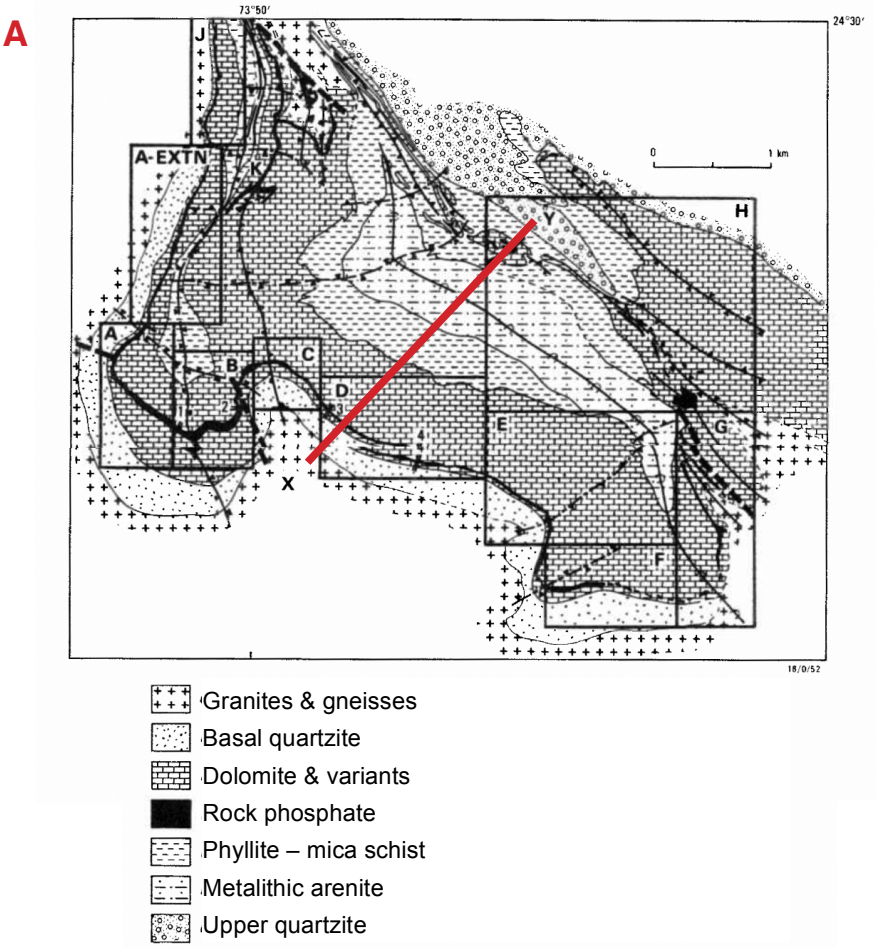

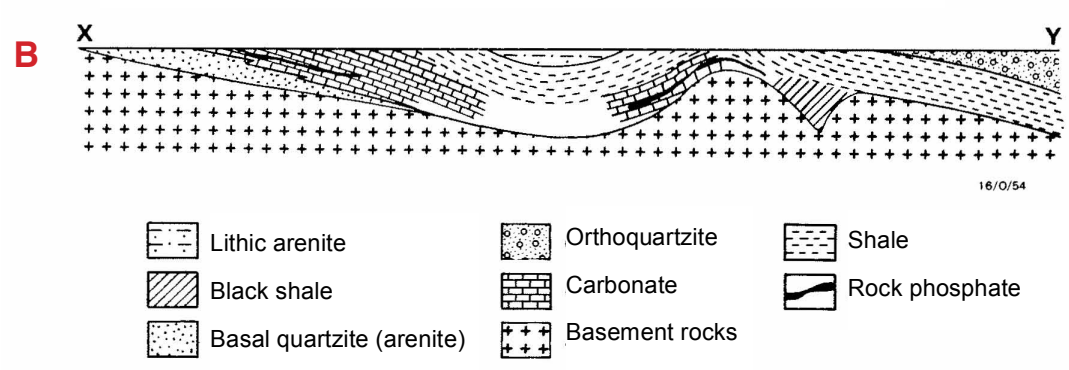

(**A**) Geological map of the Jhamarkotra rock phosphate deposit, based on Roy et al. 1980. The phosphate outcrop is based on the Indian Directorate of Mines & Geology, 1977. The X-Y line delineates the cross section shown in B. (**B**) Generalized section through the X-Y line, showing sedimentary facies and environment. Vertical scale exaggerated. From Choudhuri & Roy, 1986.

Figure 14 | **Jhamarkotra : Stratigraphy**

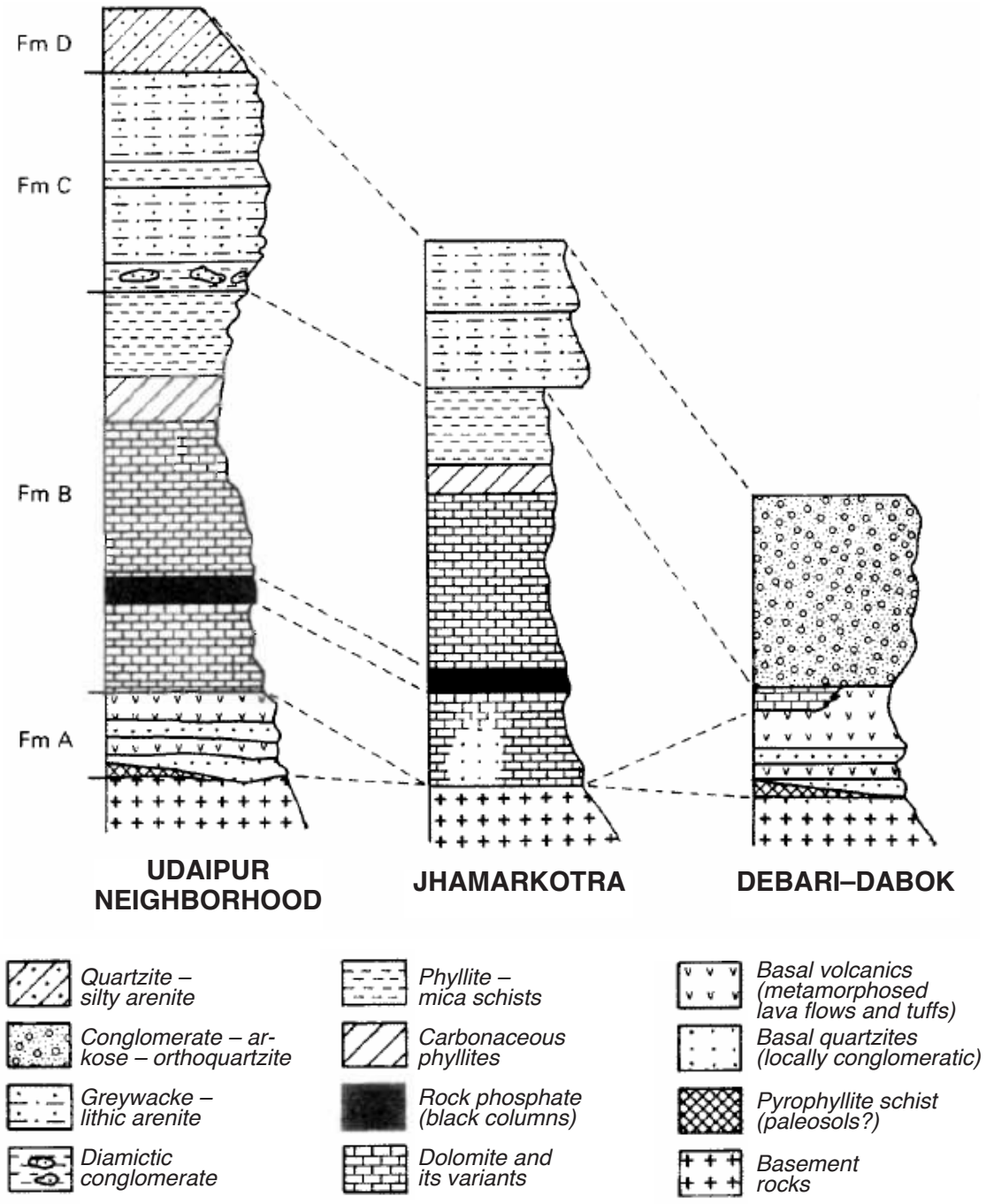

Schematic stratigraphic correlation of the rocks of Jhamarkotra, the nearby Udaipur neighborhood and Debari-Dabok areas. From Choudhuri & Roy, 1986.

Figure 15 | **Jhamarkotra : Mining site and stromatolite**

(**A**) Jhamarkotra phosphate rock exposed by active mining, and from which our sample was obtained. The vertical, darker grey areas comprise lithified stromatolites, within a lighter grey dolomitic matrix. Photo from Mukund Sharma.

(**B**) Open pit mining of the Jhamarkotra mine of Rajasthan, India. Source: Rajasthan State Mines & Minerals Limited, http://www.rsmm.cim/mining-phos.htm.

Figure 16 | **Jhamarkotra : Rock sample – hand specimen & XRCT images**

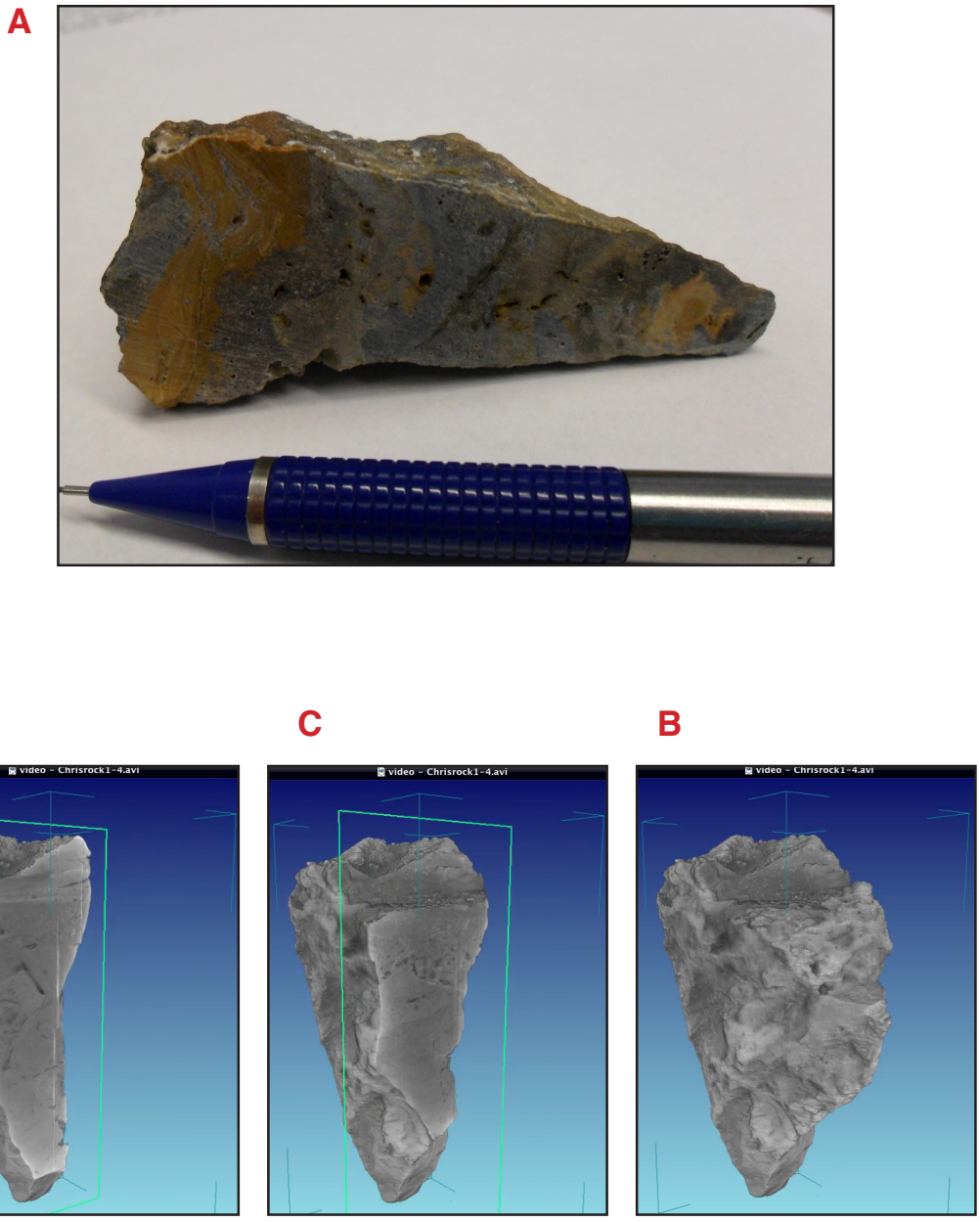

(**A**) What remains of the rock from which the thin sections were cut. Mechanical pencil shown for scale. (**B-D**) Right-to-left, sequentially deeper µCT views of the same, showing some of the voids in the interior of the rock.

Figure 17 | **Pourbaix** (Eh-pH) **diagram variations by datasets,** system gte-hem-fhd

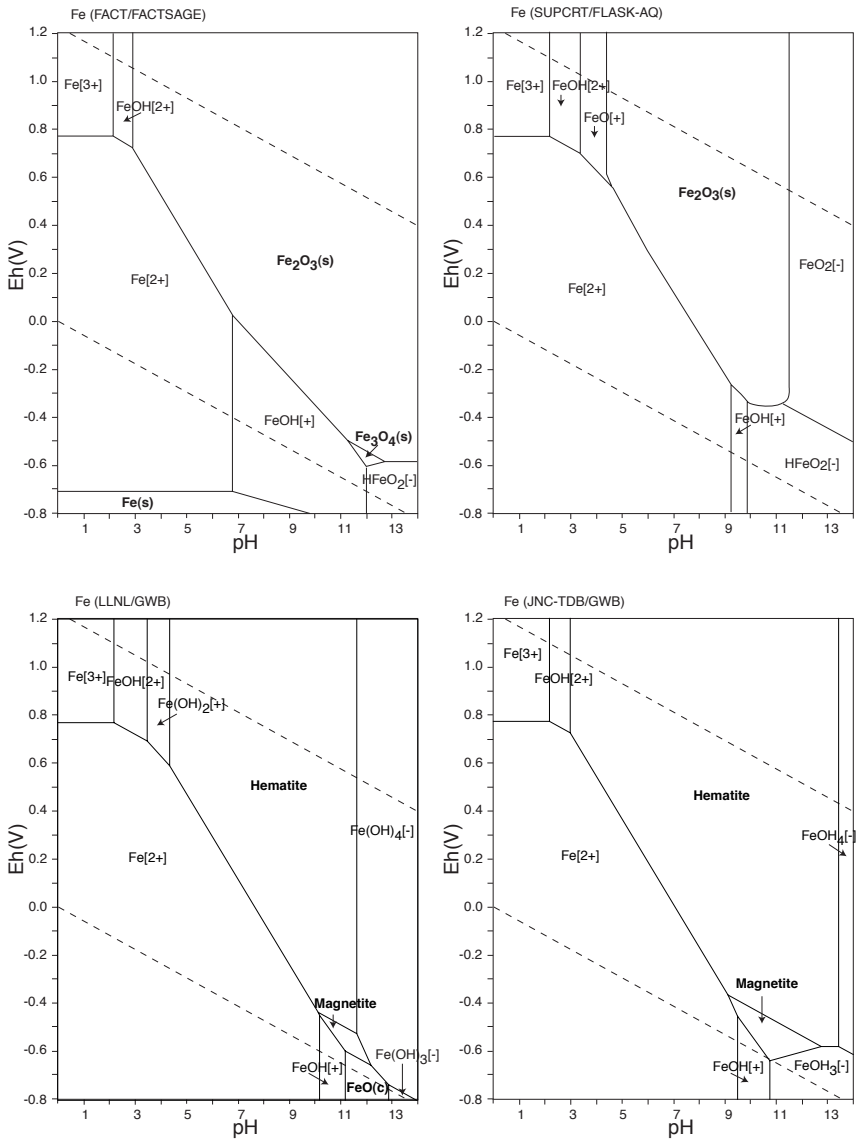

Four slightly different Eh-pH diagrams of the system Fe-O-H (total Fe = 10^{-10}, 298.15K, 10^5 Pa) using different databases for source information and illustrating how variations in database and/or conditions can affect the finer aspects of analytic results. Details can be found in "The Atlas of Eh-pH diagrams – Intercomparison of thermodynamic databases."

Figure 18 | **Jhamarkotra in context of Earth's oxygenation**

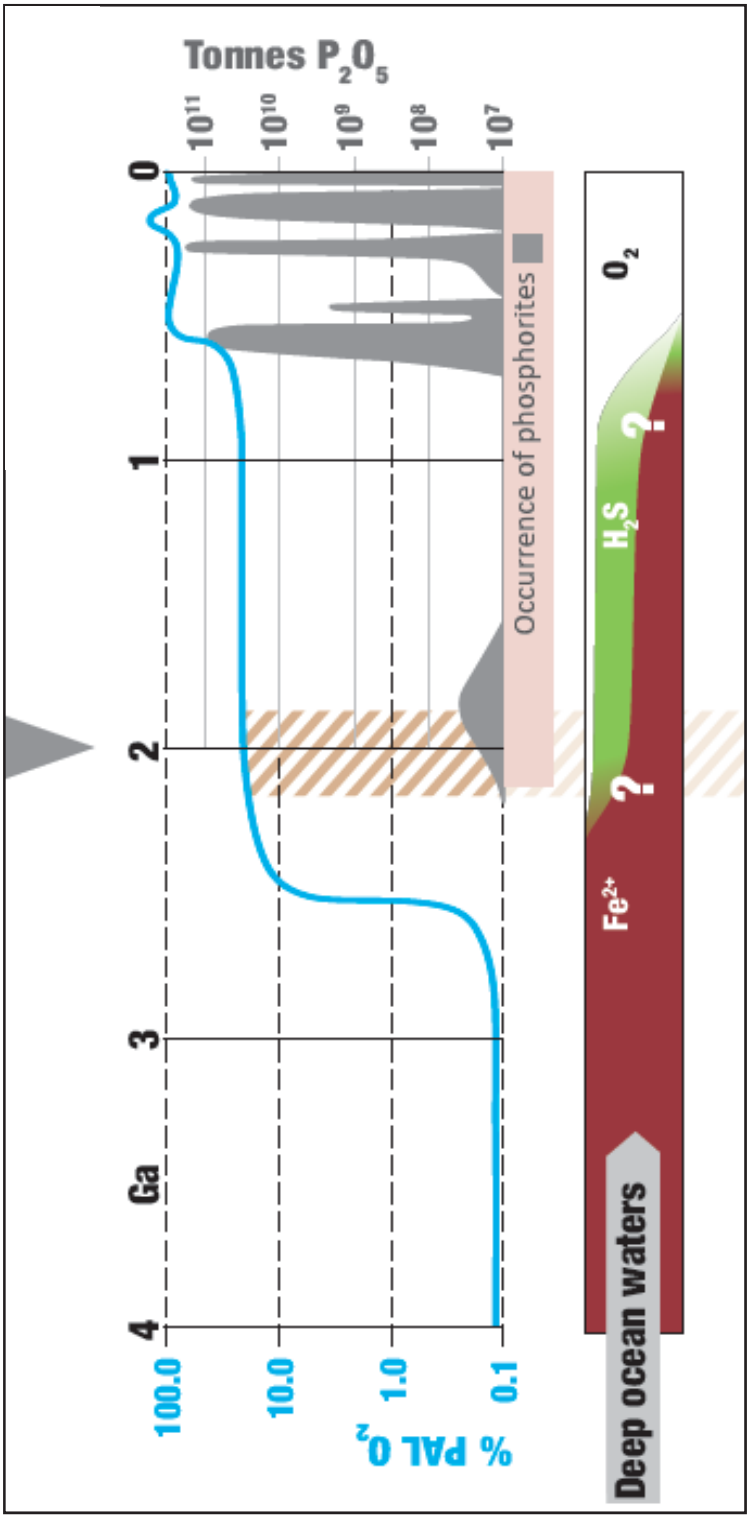

Placement of the Jhamarkotra microfossils in the context of atmospheric oxygenation, ocean water chemistry, and phosphorite formations over time. Nearshore waters, where oxygenic phototrophs contributed to growth of stromatolites are likely to have experienced steep Fe(II)–O2 redox gradients locally.

Figure 19 | **Polyphosphate utilization strategy** (diagram)

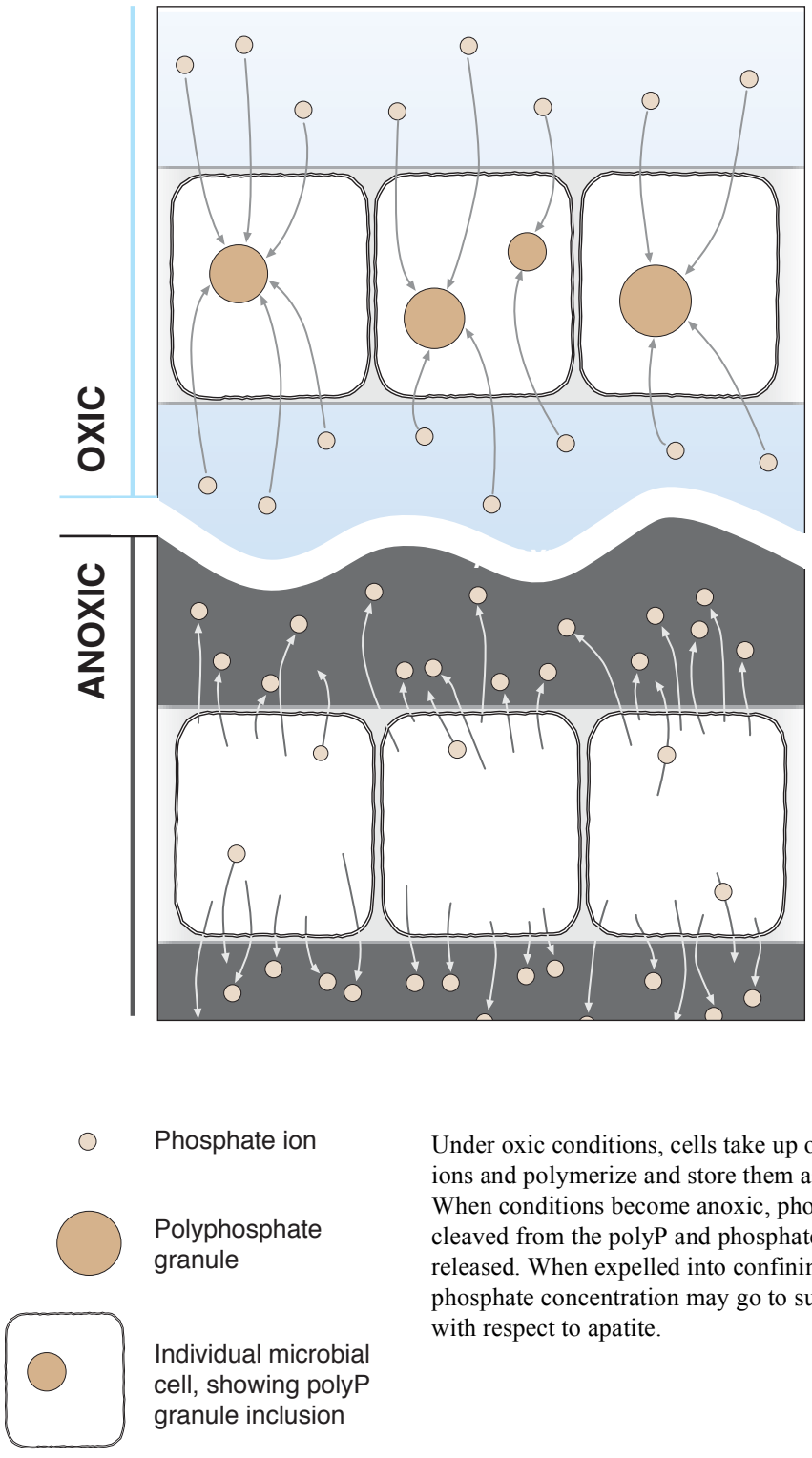

Under oxic conditions, cells take up orthophosphate ions and polymerize and store them as polyP granules. When conditions become anoxic, phosphate ions are cleaved from the polyP and phosphate ions are released. When expelled into confining spaces, phosphate concentration may go to supersaturation with respect to apatite.

Figure 20 | **Iron redox phosphate pump** (diagram)

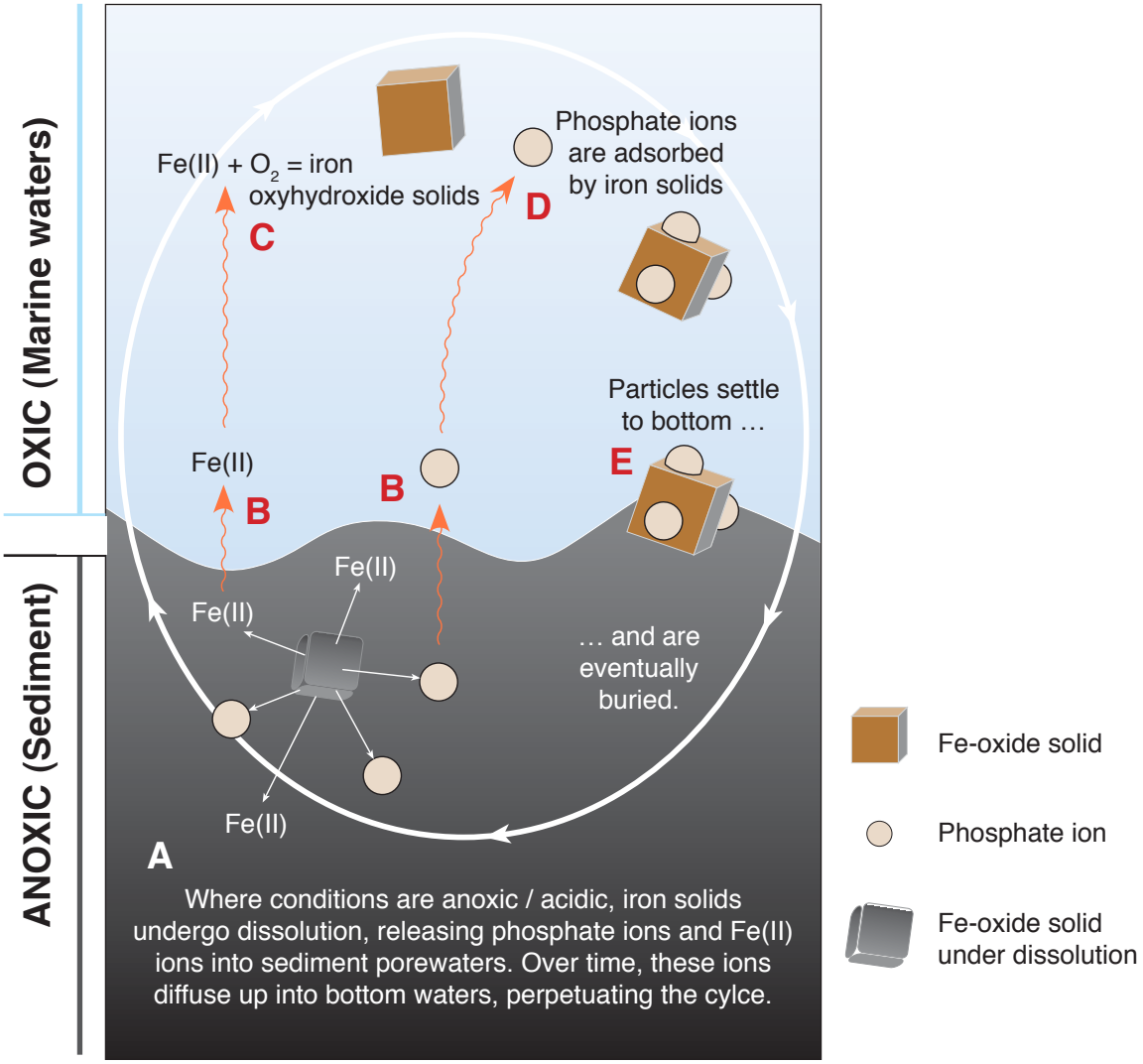

The iron redox pump acts as a cyclic shuttle of iron between sediment to bottom waters. Eh is drawn down in sediment where it is deprived of oxygen as a result of aerobic heterotrophy. Additionally, microbial activity may acidify pore waters as they maintain a proton gradient. The release of phosphate in proximity to sediment-borne microbes makes it available for microbial uptake.

(**A**) Under anoxic/acidic conditions iron-oxyhydroxides undergo dissolution,
(**B**) releasing phosphate ions and Fe(II) ions that eventually diffuse up into bottom waters.
(**C**) In oxygenated bottom waters, Fe(II) is subjected to oxygenation and converted to solid iron-oxyhydroxides.
(**D**) The iron-oxyhydroxides carry sufficient positive surface charge to attract negatively charged phosphate ions, leading to adsorption of phosphate to iron solids.
(**E**) Over time these particles settle as sediment, and are eventually buried in sediment.
(**A**) As they encounter anoxic, acidic conditions, the iron-oxyhydroxides dissolve, releasing the phosphate ions and the iron as Fe(II).

Figure 21 | **Helical iron-oxide sheath**

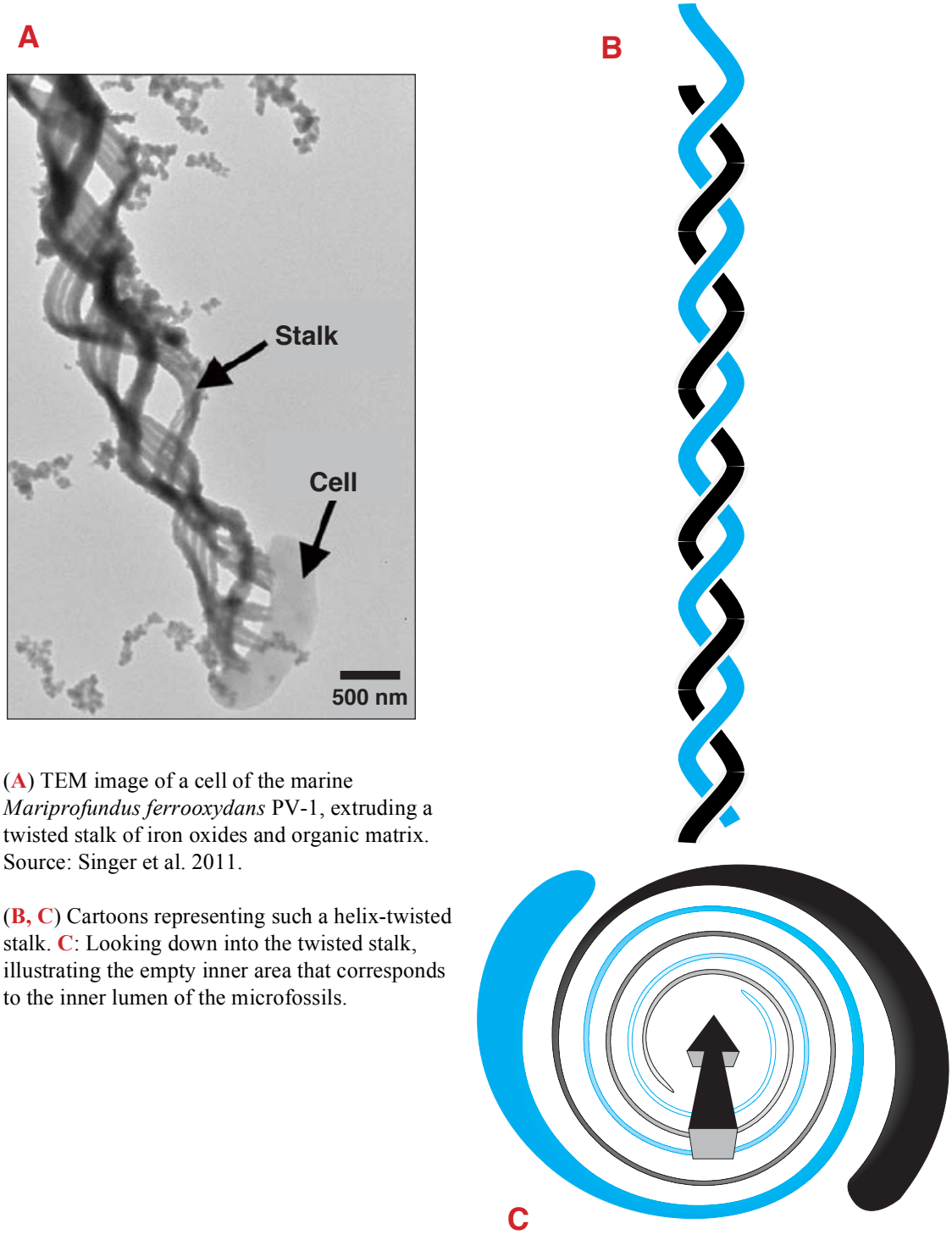

(**A**) TEM image of a cell of the marine *Mariprofundus ferrooxydans* PV-1, extruding a twisted stalk of iron oxides and organic matrix. Source: Singer et al. 2011.

(**B, C**) Cartoons representing such a helix-twisted stalk. **C**: Looking down into the twisted stalk, illustrating the empty inner area that corresponds to the inner lumen of the microfossils.

Figure 22 | **Jhamarkotra : Comparative features of similar morphologies**

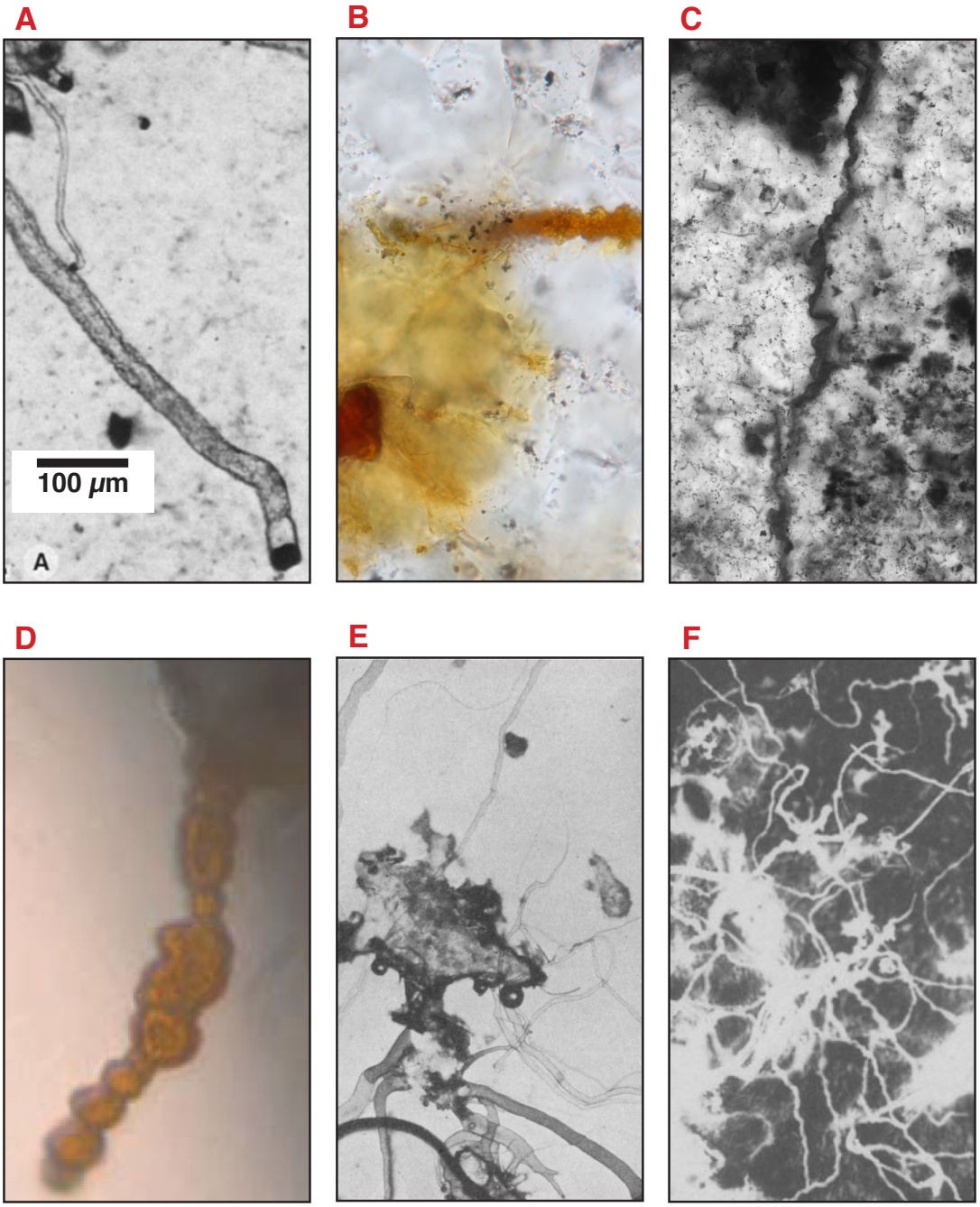

A–D: Naturally occurring features that can resemble filamentous microfossils. (**A**) Ambient Inclusion Trails (AITs), (**B**) Diffusion front, (**C**) Crystal boundaries, (**D**) Example of abiotically produced filaments formed as described in Perfit et al. 2013.
E–F: Artificially produced features resembling filamentous microfossils, as shown by (**E**) Hawley (Hawley, 1926) and (**F**) Garcia-Ruiz. (Garcia-Ruiz, 1993)

Chapter 4

—

Biogenicity and the challenge of pseudofossils

Introduction

Fossils provide evidence of the details of early life on Earth. Macroscopic fossils are usually fairly readily recognized as *bona fide* fossils, but as we probe deeper in time – into a world not yet inhabited by macroscopic eukaryotes – fossils become more difficult to detect, smaller in size and more cryptic, making a determination of biogenicity a necessary task before one can reliably interpret the presence and implication of a fossil organism. Hence, of foremost concern to the micropaleontologist is the establishment of a putative microfossil's biogenicity.[*]

Layers of difficulty make this a non-trivial pursuit. As indicated in the previous chapter, not every apparent microfossil is in fact a true fossil. The literature is replete with examples of misidentifications, and debates are common. Indeed, the open discussion of putative microfossils is a good example of how scientific discovery is an iterative, community process that builds on the cooperative interaction and informed insights of scientists. This is manifestly evident in the issue of establishing microfossil biogenicity. As we seek insights into the deep past and interpret clues presented by putative microfossils, the reliability of those clues rests on our accurate establishment of putative microfossils as *bona fide* microfossils – the accuracy of our assessment of biogenicity, the characteristic of having been produced or brought about by living organisms.

Working with the implications of this definition, we find ourselves peering down a bit of a rabbit hole. If biogenicity requires the agency of a living organism, don't we need to know what it is to be a living organism?[†]

This becomes increasingly significant as we move deeper into the past.

---

[*] *Appendix B, "Assessing microfossil biogenicity," discusses this issue and gives some of the commonly accepted criteria in assessing biogenicity.*

[†] *For a discussion of some of the characteristics of life, see Appendix A, "What is life?"*

The importance and challenge of determining biogenicity

The search for the origin of life

The timing and details of the emergence of life on Earth is one of the primary subjects of ongoing micropaleontological research. Although cellular life is believed to have emerged on Earth within its first billion years, the search for evidence of its earliest manifestations is challenged by the subduction and/or metamorphic alteration of microfossil-containing matter and the ambiguity of the morphological features of simple, early organisms.

When Charles Darwin published "On the Origin of Species" in 1859, detailing evidence of species evolution, he realized that if life had evolved from simple organisms to include all of the complex organisms we see today we should find evidence of the 'missing links' between the earliest life forms and the animals found in the Proterozoic ('Darwin's Dilemma.') At the time, we had no record of the precursors of the shelly invertebrates at the base of the Cambrian.[*]

The missing evidence has been slow in coming, but ever more discriminating technology is allowing us to make inroads and expand our understanding of the impact of microbial life on the early Earth.

At the turn of the 20th century it was still popularly believed [and indeed, still is among some (Newport, 2014)] that all life forms have always existed as they are today. Among scientists, some believe that life somehow originated as a spontaneous autotrophic algal-like organism, a primary producer at the base of what would develop into a food chain of heterotrophy and diversity, as suggested for instance by Günter Wächtershäuser's iron-sulfide theory of the origin of life (Wächtershäuser, 2006). Others believe that autotrophic life originated in alkaline hydrothermal vents, as put forth by Nick Lane and others (Sojo et al., 2016). Yet others, such as Alexander Oparin, suggested that the first living organisms were metabolically simple heterotrophs that did not have or require the pathways needed to fix carbon[†] but rather relied on inorganic processes to incorporate carbon into bio-accessible molecules (Schopf, 1999). Oparin's

---

[*] *Small Shelly Invertebrates: A variety of fossils exhibiting a wide variety of size and form, found to precede the Cambrian and taken as evidence of an earlier rise of animals than the once accepted Cambrian. Most of the shelly invertebrates have been found preserved by phosphate.*

[†] *The word 'fix' is a good example of how different fields use the same term to mean very different things. In the world of biochemistry, to fix carbon or nitrogen, for instance, is to incorporate it into biomass, moving it from the inorganic geosphere to the organic biosphere.*

view, along with the notion of J.B.S. Haldane, who theorized that early Earth had a reducing atmosphere* conducive to the abiotic production and preservation of reduced carbon molecules, became known as the "Oparin-Haldane Heterotroph Hypothesis" (Podolsky, 1996).

Current research into the processes and mechanisms involved in the origin of life include a number of approaches, including a 'top-down' orientation (the simplification of extant organisms by removal of genes, to arrive at a minimum required to support life) (Gibson et al., 2010), a 'bottom-up' orientation (the concatenation of synthesized genes to the point at which life can be supported) (Szostak et al., 2001), and ideas ranging from the involvement of an RNA world (Taylor, 2006), a pivotal role of viruses (Forterre, 2010), the role of apatite in the formation of early primitive cells (Kostetsky, 2005) and the role of various energy forms, such as shock waves, in the steps required in the origin of life (Suzuki et al., 2015).

Historically, the scientific search for an understanding of the evolution of life has been largely the domain of macroscopic paleontology. In contrast, the search for the signs of earliest life belongs to microbial paleontology (micropaleontology,) with candidate organisms often initially identified by morphological signatures suggestive of fossil organisms. The field of micropaleontology and the recognition of microfossils, which are generally too small to be seen by the naked eye, had to wait for the development of microscopy and techniques amenable to the search, such as the thin section technology developed in the 1840s by the geologist and microscopist Henry Sorby (Walsh and Da Mommio, 2013). Such advances in microscopy and other analytical techniques and methods – including the quickly advancing supercomputing capacity that enables use of genomic bioinformatics – have enabled us to extend the search for the origin and evolution of life from the realms of philosophy and theology, to a respected place in scientific exploration of early life, the validity of which is necessarily based on establishing the biogenicity of putative microfossils.

Establishing biogenicity

Morphologies that have been altered through millennia by the forces of metamorphism and geochemical alteration may be so altered that what we find today are often only cryptic clues assessed for likelihood of authentic biogenicity. In addition, microbial biomass is likely to have

---

* *A reducing atmosphere is one in which the preponderance of molecules can be classified as reduced, aka rich in electrons that may be susceptible to removal by atoms/molecules of higher electronegativity.* *See redox section, page 7.*

been degraded through biological scavenging, sometimes leaving at best only remnant molecules, such as kerogen, which is discussed on page 57.

Hence, interpretations of putative microfossils continue to be debated, for these reasons and because of the ambiguities and uncertainties inherent in extrapolating from the modern to the ancient,[*] as well as the continuing refinement of criteria for establishing *bona fide* biogenicity – rendering the work involved in establishing the biogenicity of ancient microfossils both challenging and challenged, and subject to ongoing refinement. The debate regarding the authenticity of the early filamentous ~3.465 Ga Apex Chert microfossils witnesses the difficulty in establishing consensus re: biogenicity (Schopf, 1993; Brasier et al., 2002; Schopf et al., 2002; Marshall et al., 2011), although each new discovery adds to the body of evidence of microbial preservation – even those that prove to be abiotic artifacts, as described in the following section and the "Alternative interpretations" beginning on page 64, as they serve to hone our ability to distinguish ancient microfossils from morphologically similar pseudofossils.

Morphology, the initial criteria

The question of morphological significance in determining biogenicity is confused not only by morphologies that can be explained by abiotic processes but also by *bona fide* morphologies that can challenge our notion of biologically-produced morphologies, such as the square halo-archaeon *Haloquadratum walsbyi* (Bolhuis et al., 2006; Burns et al., 2007).

In an attempt to help clarify the issue and standardize micropaleontological standards and methods, a number of criteria have been put forth for use in assessing biogenicity, some of which are listed in Appendix B. By the early 1980s, J. William Schopf was developing criteria for the

[*] *A note of caution in extrapolating from the present into the past: In addition to the already pointed out difficulties of establishing biogenicity, note that it may not necessarily be valid to extrapolate from the present into the past, as extant organisms have developed their traits in response to various evolutionary pressures through time that in retrospect we cannot know how to recreate – such as genetic drift due to bottlenecks and/or extinctions, for instance. Such occurrences would likely have forced life to preferentially follow a specific evolutionary path to the exclusion of other possible paths. In looking from the present into the past, our attention is directed down the one path that allowed life to persist, implicitly disregarding other paths that may have once been viable and may have left microfossil and/or geochemical signatures. Hence, although we have little else to work with, we are well advised to remain mindful that assessing biogenicity of putative fossil organisms by criteria based on extant organisms may encourage us to disregard potentially valid criteria that, by virtue of evolutionary pressures through time, were not selected for but at one time may nonetheless have been significant and influential.*

establishment of biogenicity of putative microfossils (Awramik et al., 1983) which have since been expanded, elaborated and revised by himself and others.

Non-morphological signatures of biogenicity

Ongoing scientific and technological progress continues to advance our ability to characterize and assess putative fossil material. For instance, we are increasingly able to characterize isotopic fractionation, a mass-dependent fractionation commonly effected by biological processes that favor the incorporation of an element's lighter isotopes over heavier ones. Analysis of isotopic fractionation is most accurately performed on low-mass elements, for which different numbers of neutrons can make a significant difference in mass, but we are becoming increasingly able to distinguish among isotopes of elements of greater mass and our ability to access biologically-induced isotopic fractionation data as another potential biomarker is becoming more refined and discriminatory. As is true of any potential biomarker, isotopic fractionation is only reliable as a biomarker to the extent that it cannot be produced abiotically and spatial fractionation is retained sufficiently to delineate the impact of biological fractionation.

Iron isotopes are an example in which isotope technology is becoming increasingly relevant to issues of biogenicity: Ivarsson et al. have explored the possibility of a definitive isotopic biosignature of iron-oxide microfossils, and found that, although isotopic variations seem to imply biogenicity they are not definitive, and like so many clues, must be used as one piece of evidence within a suite of arguments (Ivarsson et al., 2008; Krepski et al., 2013). Adding to its ambiguity, ocean iron isotopic signatures can differ as a function of their sources (Homoky et al., 2013), and the possibility of abiotic iron isotope fractionation, as described by Icopini et al. (Icopini et al., 2004) must also be considered.[*]

Exploration of microfossils has also extended to other biomarkers, including molecules uniquely produced by only specific organisms, such as methylhopanes which are today found to be produced only in cyanobacteria, so when they are found in the rock record they are taken as evidence of cyanobacteria (Summons et al., 1999; Summons et al., 2008).

---

[*] *Iron isotopic analysis of the Jhamarkotra microfossils would have been interesting, but we opted not to perform this analysis, as we had very limited microfossil volume in our two thin sections, making such an analysis very difficult, if not impossible, while also requiring obliteration of the thin section.*

Background : Doushantuo microfossils

In the quest to establish the timing of the emergence of animal life, one site is particularly informative. Some of the earliest animal microfossils found to date have been found in the phosphatic ~650–550 Ma Neoproterozoic Doushantuo formation of southeast China. Among the extensive and rich phosphorites that appear during the Neoproterozoic−Cambrian times (Cook and Shergold, 1984), this thick formation is significant for its dense fossil content with nearly continuous beds of well preserved phosphatized microfossils of a number of morphologies (spherical, collapsed, aggregates, internally divided) and surface textures (smooth, 'ornamented,' spiny) (Glenn et al., 1994).

These microfossils* are the object of extensive investigation and are proving to be a rich source of dialogue as various workers, applying advanced analytical techniques and noting morphological similarities of the microfossils to extant organisms, provide numerous and often contradictory interpretations, including: Acritarchs (possible cysts of unicellular eukaryotes), cyanobacteria, multicellular algae (sporulating green algae) (Kremer et al., 2012), microscopic metazoans exhibiting reductive cell division, nonmetazoan holozoans (Huldtgren et al., 2011; Huldtgren et al., 2012; Xiao et al., 2012), bilaterians (Chen et al., 2000) chlorophyta (Yao-song et al., 1995) and reductively dividing sulfur bacteria (Bailey et al., 2006).

Among these microfossils, the *Megasphaera ornata* exhibit an 'ornamented' surface texture resembling that of extant sea urchin embryos, leading some to interpret *Megasphaera ornata* as animal eggs and embryos, and bearing on our understanding of the timing and early evolution of animal life (Raff et al., 2006; Yin and Zhu, 2012).

Although by now the interpretation of many of the Doushantuo fossils as eukaryotes is well accepted, interpretations of some of the fossils as embryos is not without challenge. For one thing, the fossils exhibiting dividing cells are largely limited to 2 and 4-cell stages, whereas extant embryos divide many more times than this. Dornbos et al. speculate that the shortage of embryos with more than 4 cells is because the embryos become increasingly delicate as they continue to divide. They attribute the fine preservation of the 2 and 4-cell stage embryos to a P-rich yolk supplying enough P to reach supersaturation with respect to apatite before the embryos divide further and become so fragile that they succumb to degradation (Dornbos et al., 2005).

---

* *The size of Doushantuo microfossils approaches ~1 mm in diameter, so they are not technically 'microfossils' by size.*

On the other hand, support for the interpretation of Doushantuo embryos includes the fact that a number of different cell-division stages (primarily one-, two- and four-celled) all of roughly the same diameter have been found, as is the case in the reductive cell division cleavage evident in extant early-stage embryos.

Research question

Curious about the possibility that some of the morphological features of the Doushantuo microfossils may represent diagenetic or post-depositional abiotic over-precipitation, we sought to test the authenticity of the biogenic interpretations of some of the Doushantuo surface textures and morphologies by investigating whether they could be formed abiotically. To test this, I performed experiments in which phosphatic spheres were placed in a diffusing gelatin that separated solutions of the anions and cations of fluorapatite (a 'Double Diffusion' setup.) The gelatin slowed the diffusion of the ion fronts toward each other until they eventually met and induced fluorapatite precipitation on the surfaces of the spheres. These experiments did produce some of the distinct surface textures (over-print precipitation patterns) noted in the literature, as did follow up runs with quartz grains as the nucleating substrate.

More interestingly, in the course of the experiments we noticed small authigenic features forming in the gel matrix of our double diffusion setup. These small precipitates exhibited morphologies resembling blastula, and to enhance observation of the nucleation and growth of these features I modified the original setup in an attempt to better characterized them.

Approach method

Material was imaged by optical microscopy and ESEM. As the purpose of the initial investigation was to examine the texture of over-precipitation on a substrate object, we imaged the same objects by ESEM both before and after experimental runs.[*]

Chapter 5 provides a description of the setup and extraction methods.

The next section is a reprint of the results of this investigation, followed by a more in-depth discussion.

---

[*] *Despite the fact that imaging of a circumspherical object is limited to (less than) half the surface of any object in a single imaging session, we were nonetheless able to document the overall surface textures of the objects before and after the experimental run by adhering them to SEM stubs with a water soluble paste that allowed their removal and subsequent experimental use, after which the same objects were again imaged.*

Experimental precipitation of apatite pseudofossils resembling fossil animal embryos

Chris H. Crosby,* Jake V. Bailey*

* University of Minnesota–Twin Cities, Minneapolis, MN. 55455, USA.

*Correspondence to: crosb118@umn.edu, baileyj@umn.edu.

Published in 'Geobiology' October 2017; 2017;00:p. 1-8

 DOI: 10.1111/gbi.12264

Certain phosphatic grains preserved in the rock record are interpreted as microfossils representing a diversity of microorganisms from bacteria to fossil embryos. In addition to *bona fide* primary biological features, phosphatic microfossils and fossil embryos commonly exhibit features that result from abiotic precipitation or diagenetic alteration. Distinguishing between abiotic and primary biological features can be difficult, and some features thought to represent biological tissue could instead be artifacts that are unrelated to the original morphology of a preserved organism. Here, we present experimentally generated, abiotically produced mineral precipitates that morphologically resemble biologically produced features, some of which may be observed in the rock record or noted in extant organisms, including embryos. These findings extend the diversity of biomorphic features known to result from abiotic precipitation.

Introduction

Morphology is one of the primary criteria used to establish the biogenicity and taxonomic affinities of a potential microfossil (Schopf and Walter, 1983; Buick, 1990; Westall and Folk, 2003; Hofmann, 2004; Brasier et al., 2005; Sugitani et al., 2007). And yet morphology of single cells and cell aggregates can be conservative and indistinguishable among phylogenetically-diverse taxa. Moreover, abiotic features that appear to be biological can be misinterpreted as fossilized cells or biological features. The diagnostic capabilities of morphological characteristics to establish biogenicity or taxonomic affiliation are only as robust as the specificity of those features to life generally, or to specific clades in the case of the use of morphology for taxonomic

assignment. In the case of possible fossilized microbes, some Precambrian microfossils are widely thought to represent fossilized cells because they meet certain criteria (Buick, 1990), while other claims of biogenicity for certain features in Precambrian rocks and Mars meteorites are controversial (Brasier et al., 2015 ; Bradley et al., 1997).

Other microfossils are controversial not because there is debate about their biogenicity per se, but because there is debate about the taxonomic affinities of the structures. One example of such an assemblage of microfossils, known as the Weng'an Biota, comes from the Neoproterozoic Doushantuo Formation, deposited in southern China ca. 570-609 Mya. This assemblage of reworked phosphoclasts includes apparent cell clusters that have been variously interpreted as metazoan diapause-stage embryos, sulfide-oxidizing bacteria, and protists (Bailey, et al. , 2007; JCunningham et al., 2011; Huldtgren et al., 2011; Xiao, Zhang, & Knoll, 1998; L. Yin et al., 2007). Claims of animal affinities, including reductive cell division, Y-shaped cell junctions, and the enrobement of some specimens in textured enveloping precipitates, are not diagnostic characteristics of animal affinities (Cunningham et al., 2017) even if they do represent primary biological features. In addition, it is now known that some features initially interpreted as biological in origin, may instead result from non-biological processes, including those that result from diagenetic changes following initial authigenic mineral precipitation (Bengtson & Budd, 2004; Cunningham et al., 2012). It is also possible that some features interpreted as representing original biological characteristics instead record the complex morphologies that can result from the precipitation of calcium phosphate minerals within an organic matrix.

In igneous systems, pegmatitic euhedral apatite crystals exhibit a hexagonal prism habit. However, when precipitated and grown in polymeric gels, as may be found in microbial mat EPS, the repeating polymeric motifs of the gel alter precipitation morphology at a sub-micron scale by forcing kinks in the crystal growth direction, resulting in a changing morphology with growth: early stage prisms mature to take on a dumbbell, or bowtie, shape that eventually closes as a sphere. The closed sphere may encase a torus-shaped void, and is eventually clad in an outer coat of radially-oriented acicular apatite similar to that shown in Figure 1a. Potential mechanisms leading to these morphologies are described in (Busch et al., 1999; Kawska, Hochrein et al.,, 2008). We have observed similar morphologies in material precipitated in a double diffusion gradient setup in our lab.

In double-diffusion precipitation experiments, anion and cation solutions of a mineral of interest are initially separated by a gel through which counter-ions slowly diffuse toward each

other (e.g. Busch et al., 1999). The slowed diffusion prevents the instantaneous precipitation that would occur upon direct mixing of the ion solutions, slowing precipitation to a rate more closely resembling *in situ* sediment conditions and hence more conducive to crystal growth over time. The polymeric nature of the gel serves as a proxy for microbially produced extracellular polymeric substances (EPS) that are abundant in sediments that host microbial mats. Additionally, initial ion concentrations in excess of super-saturation provide a proxy for time by providing ions sufficient to allow growth that would require extended time to accumulate *in situ*.

Here we report on mineral precipitates produced in double-diffusion precipitation experiments that have a potential bearing on the interpretation of the Doushantuo Weng'an Biota and perhaps other phosphoclasts in the rock record.

Methods

These results were obtained in both of two double diffusion experimental setups.

Experimental Setup Type 1 : Figure S2a shows the experimental Type 1 setup. Gelatin (pH ~4) is drawn into sterile tubing by suction via syringe and allowed to set, whereupon cation (Ca^{2+}: 0.133M $CaCl_2 \bullet 2H_2O$) and anion [$(PO_4)^{3-}$: 0.08M $NaHPO_4$ and 0.027M F^-: $KF \bullet 2H_2O$] solutions (pH ~8) of the stoichiometry of calcium fluorapatite, $Ca_5(PO_4)_3F$, (5:3:1) are added to the tubing on either side of the gelatin. Tubing ends are loosely covered and the setup is photographed periodically during precipitation. Evidence that the ion fronts had begun to interact was visible within ~30 hours, as a white band of precipitates developed within the gel (Figure S2b).

Setup Type 1 – Sample harvesting : Harvesting of unconsolidated band material and individual precipitates was performed under a dissecting microscope to expose and isolate the portion of gel containing the precipitated material of interest. The tubing was cut adjacent to the precipitates, the gelatin plug was extruded from the tubing, and a small amount of gel containing the material of interest was removed and placed on double-sided carbon tape on a 17mm SEM stub. Once on the stub, gel was removed from the precipitate by repeatedly: 1) administering small volumes (~5-20 µL) of hot sterile water via pipette, 2) letting the hot water melt the gel, and 3) removing the melted gel and water by pipette.

Experimental Setup Type 2 : To observe experimental progression at the microscopic scale, we developed an alternate, Type 2 setup (Figure S2c). In this setup, gelatin (pH ~4) is added in a thin (~1 mm) layer sandwiched between two cover slips and allowed to set. The gel is located

between two ion solution wells connected to the gel by small channels to allow ion flow into the gel. Ion solutions (pH ~8) of the stoichiometry of calcium fluorapatite, $Ca_5(PO_4)_3F$, (5:3:1) are: cation (Ca^{2+}: 0.133M $CaCl_2 \cdot 2H_2O$) and anion [$(PO_4)^{3-}$: 0.08M $NaHPO_4$ and 0.027M F^- : $KF \cdot 2H_2O$]. For a more in-depth description of this setup, see (Crosby and Bailey, 2017). Though this setup differs from the Type 1 setup in size, shape, and assembly protocol, the same chemical parameters are used in both setups. Details of precipitation, including the differentiation of the initial diffuse band of precipitation into discrete bands (Figure S2c, S2d) and the nucleation and growth of authigenic spheroids (Figure S2b, S2d) is more easily distinguished in this Type 2 setup than the Type 1 setup, due to both the thinness of the gel and the opportunity to observe microscopically under a flat cover slip, undistorted by cylindrical tubing.

Setup Type 2 – Sample harvesting : Harvesting of unconsolidated band material and individual precipitates was performed under a dissecting scope. The setup was disassembled and portions of gel encasing precipitates were cut away with a scalpel. The removal of residual gel from precipitates was done in one of two ways: Small gel plugs holding visibly large precipitates were placed on stubs and rinsed with hot water, as described above. Gels with smaller or more numerous precipitates were placed in an 1.5ml tube of hot water, immersed in a hot water bath, shaken gently, held vertically in the hot water bath to allow precipitates to settle, and the supernatant was slowly removed by pipette. This was repeated at least 4 times, to assure removal of gel from precipitates. The final, rinsed precipitates, plus bottom rinse water, were removed from the epitube by pipette and placed on a carbon-taped stub. Once the water had evaporated, the precipitates on the stub were further rinsed with hot water as described above.

Imaging: Harvested precipitates were imaged on a Hitachi TM-1000 Tabletop Environmental Scanning Electron Microscope (ESEM) operated at 15.0 kV accelerating voltage, and analyzed by energy-dispersive X-ray spectroscopy (EDS) using Bruker Quantax 50 software to obtain elemental data. Samples were not carbon coated. For more precise elemental mapping, one of these samples was also analyzed on a FEM/SEM Jeol SM 6500F, at 15.0 kV accelerating voltage (Figure S4).

Elemental analysis: Where a few precipitates were broken in the harvesting step, a more complex interior could be seen. One of these samples, (Figure 3), was analyzed on a FEM/SEM Jeol SM 6500F for confirmation/clarification of the ESEM EDS results (Figure S4).

Visualization of internal features: A few spheroids fractured during harvest and rinsing, allowing direct observation of internal features. An attempt was made to characterize internal morphology by micro-scale computed tomography (micro-CT), but resolution was insufficient to provide additional detail beyond what could be observed by SEM. In those cases in which nucleation initiated on an internal surface of the setup apparatus, the precipitate grew as a hemisphere instead of a sphere. This allowed examination of inner morphology without requiring fracturing of the sphere (see Figures 3, S4).

Results

Within ~30 hours, evidence that the ion fronts had begun to interact was visible as a white band of precipitates developing near the phosphate/fluoride (P/F) channel (Figures S2b and S1(d)). Within one week, additional bands and spheroidal precipitates not associated with the banding were seen forming within the gel (Figure S2c,d). Numerous examples of morphotypes resembling microfossils, including some of those that are interpreted as animal embryos (Figure S3) were observed among our experimentally-produced precipitates (Figure 1a–e, f–j). In particular, some surface morphologies resemble microfossils interpreted as early-division-stage blastula.

The retained material was replete with examples such as those presented here. Figure S1 shows that ≥ 20% of precipitates exhibit morphologies more complex than early-stage prism / dumbbell / simple sphere morphologies, showing that these more complex morphologies are not particularly unusual. Examples include 'doublet' pseudofossil spheres (Figure 1a) resembling dividing cell microfossils (1a'), multi-lobed precipitates (1b, 1c) resembling microfossils at 4 or 8-cell stages of division (1b', 1c'), and aggregates of spheres (1d) resembling multi-sphere morula-like microfossils (1d'). Also observed are polygonal indentations and decussate configurations with Y-shaped triple junctions (1e,f) resembling blastomere suture junctions in extant embryos. In some specimens, we also observed raised polygons (1f) of geometries similar to those found in certain fossil embryos (1g').

Also observed are holes in the encasing precipitates leading from the surface inward to an internal sphere (Figure 1g), as well as some spherical precipitates with penetrating processes (1h), wrinkled surface textures (1i), and cerebral-like surfaces (1j) resembling features described in the literature as a possible outer membrane.

Resemblances aren't limited to external features (figures 2 and 3). Some pseudofossils resemble multi-layered gastrula (Figure 2a) or exhibit an internal sphere within an outer layer (1g,

2b), internal features radiating from a central void (2c), and apparent tubules, some opening to the exterior (3b,d). Figure 3 shows additional internal features exposed in a broken pseudofossil, exposing a radial outer coating that resembles a blastocoel-containing membrane, and internal spheroidal features that resemble blastomeres. Figure 3c details the radial development of one of the internal spheres (encircled in white.) ESEM/EDS analysis of the sample shown in Figure S3 reveals that the outer layer is a calcium-phosphate (Ca-P), as is the inner material, although the variation in P% indicates that the inner material may represent a Ca-P precursor phase.

In addition to features resembling embryos, features resembling bacterial/archaeal microfossils are also observed, such as bowl-shaped morphologies (Figure 4a) similar to collapsed cells (4a'), and complex multi-layered spheres (4b) resembling specimens with a reticulated flange (4b').

Larger, ~200-300 µm diameter authigenic precipitates, such as that shown in Figure 3, were observed toward both ends of the diffusion gel – toward the ion entry ports. The size of these large precipitates allowed individual harvesting, which facilitated EDS interpretation via SEM (Figure S4).

Because the precipitates comprise hundreds of thousands of small individual objects that formed and aggregated within a gel matrix (instead of singular solid precipitates) they tended to disaggregate in the process of gel removal, resulting in the loss of a significant number of individual aggregates and particles. Despite the care taken in sample rinsing, we could not avoid a visible loss in the water-gel removal step. This winnowing of the particles must be assumed to have skewed the size distribution of retained precipitates relative to total precipitates formed. As a result, any size distribution analysis would necessarily be flawed.

Discussion

The rock record contains various features that have been interpreted as embryos. Examples include the late Neoproterozoic microfossil-rich Doushantuo formation of S.E. China (Bengtson & Zhao, 1997; Chen et al., 2004; Xiao & Knoll, 2000), which are thought to be the oldest evidence of animal embryos. Phosphatized embryos are also known from the early Cambrian *Olivooides* of both northwest Canada (Pyle et al., 2006) and China (Yue and Bengtson, 1999), as well as the lower Cambrian of Siberia, the Middle Cambrian in Australia and the Lower Ordovician *Markuelia* in North America (Donoghue et al., 2006; Kouchinsky et al., 1999). Among these, the Doushantuo Formation arguably provides the richest and best-preserved fossil evidence of microfossils interpreted as animal embryos to date, hence we present images showing

morphological similarities of our pseudofossils to microfossils of the Doushantuo Formation. We do not claim that our precipitates necessarily represent analogues to Doushantuo embryos. We also note that these pseudofossils don't invalidate an interpretation of eukaryotic microfossils for which additional characteristic structures exist, and further analysis of many *bona fide* microfossils provides strong evidence in support of eukaryotic interpretations, such as the examples shown in figure 5. For instance, some microfossils examined by SEM and thin section observation show distinctive cleavage patterns within an apparent enveloping membrane consistent with extant animal embryos (Xiao and Knoll, 2000) and thin section evidence of cell differentiation and germ layers suggests that they may represent early stem-group animals (Chen et al. 2014). Synchrotron-radiation X-ray tomography of Lower Cambrian microfossils reveals details of interior structures such as *Markuelia* spines and a possible digestive tract (Donoghue, et al., 2006) and Chen et al. contributed Synchrotron X-ray Microtomography and propagation phase contrast-based imaging analysis of numerous Doushantuo microfossils as indicative of an apparent diverse metazoan community (Chen et al., 2009), though claims of metazoan affinities remain controversial (Cunningham et al., 2017).

However, some embryo-like microfossils either have not been examined internally, or upon such examination do not show definitive evidence of internal structures indicative of eukaryote affinities or other clade-diagnostic features (Bengtson et al., 2012). The morphologies of the experimental precipitates presented here add to the challenge of interpreting ambiguous putative microfossils such as these.

Although experimental, the conditions under which these morphologies are observed fulfill some of the generally-accepted criteria required to support an interpretation of a geological structure as a microfossil: They are not isolated features. They form in the presence of features of similar size and shape, and they resemble both phosphatized and extant embryos in morphology (Raff et al. 2006).

Size may, or may not, be one criterion by which abiotic pseudofossils, such as these, can be distinguished from primary biological structures. Many of the precipitates generated in our experiments are an order of magnitude smaller than the Doushantuo microfossils that are commonly interpreted as embryos. However, some of our precipitates are comparable in size to some large Doushantuo microfossils (e.g. Figure 3). Additionally, the sizes of globular Doushantuo microfossils themselves range from <100um in diameter to over 1000um in diameter (Chi, 2009, Figures 5 & 6; Muscente, et al. 2014, Figure 5b,h,i), and the size of the textures associated with them exhibit a broad size range that overlaps on the small end with the range of

abiotic precipitates observed in our experiments (Yin and Zhu, 2012, compare Figure 1a to 1e and Figure 1c to 1g.). Whether or not slower precipitation, or alternative chemical environments in natural systems, would produce features as large as the largest precipitates interpreted as embryos and embryo-ornamentation in the fossil record remains an open question,

The chemical environment that resulted in these precipitates is also a plausible simulant of modern microenvironments that host active phosphogenesis. Although marine waters are generally not supersaturated with respect to apatite, certain conditions lead to a dispersed "background" precipitation of apatite extending across continental margins generally (Ruttenberg and Berner, 1993). Beyond this minor background precipitation, however, P-rich phosphorites are forming through mechanisms that are not yet fully clarified. One mechanism is thought to involve the benthic degradation of polyphosphate-accumulating organisms and the resulting release of recalcitrant intracellular polyphosphate that may then provide a nucleation surface for Ca-P precursor species (Diaz et al., 2008). Microbial concentration of phosphate by polyphosphate-accumulating bacteria has been correlated with active phosphogenesis (Schulz and Schulz, 2005). Where this may occur under confining conditions or narrow pore water horizons, such as may be found in EPS-rich stromatolites or heavily-colonized sediments, supersaturated fluids may co-occur with nucleating surfaces such as EPS and/or a variety of plentiful potential organic and inorganic substrate particles and surfaces. Microbial EPS polymers are dominated by poly-saccharides, similar to our diffusion gel in having the repeating motif of monomers in a three-dimensional structure that forces altered crystallographic maturation.

Conclusion

These observations do not refute the interpretation of certain Doushantuo Formation microfossils as eukaryotes generally, or embryos specifically. Rather, it has been well established that some morphological features of phosphatic microfossils may result from non-biological precipitation that mimics potential biological features (Bengtson et al., 2012; Cunningham et al., 2012). Here, we extend the diversity of biomorphic features able to be produced abiotically – to include globular pseudofossils exhibiting polygonal external textures, internal channels, clusters resembling 2^n cell division progression, and suture lines resembling division planes between apparent close-packed spherical features.

Ultimately, these findings serve as a reminder that features considered diagnostic of *bona fide* biogenicity and/or clade-specificity may result from non-biological processes, and hence, that the criteria used in assessing microfossil biogenicity and phylogenetic-affinity remain subject to

ongoing refinement. The interpretation of putative microfossil origins from morphology must be done with an awareness that taphonomic and diagenetic factors will eventually influence fossil morphology over geologic time, and that non-biological mineral precipitates, whether they form early or late, can result in features that mimic biological forms. The accurate interpretation of a putative microfossil requires that we eliminate the possibility that a particular structure formed through abiotic means. We offer these examples as an extension of our understanding of the potential complexity of abiotic apatite precipitates.

Acknowledgments

Portions of this work were supported by National Science Foundation grant #EAR-1057119 to JVB, and by funding from the University of Minnesota–Twin Cities Graduate Program and Department of Earth Sciences to CHC. SEM imaging and initial EDS analysis were performed at LacCore, Department of Earth Sciences, University of Minnesota–Twin Cities, supported by National Science Foundation grant #NSF-IF-1462297. Additional EDS analysis was carried out in the Characterization Facility at the University of Minnesota, which receives partial support from National Science Foundation through the MRSEC program. The assistance of Beverly Flood, Elizabeth Ricci, Beverly Chiu, Erica Sheline, Peter Schroedl, Nick Seaton and manuscript reviewers and editors is gratefully acknowledged.

List of accompanying figures

List of supplementary figures

Figures

Figure 23 | 01 | **Surficial resemblances of pseudofossils to microfossil embryos**

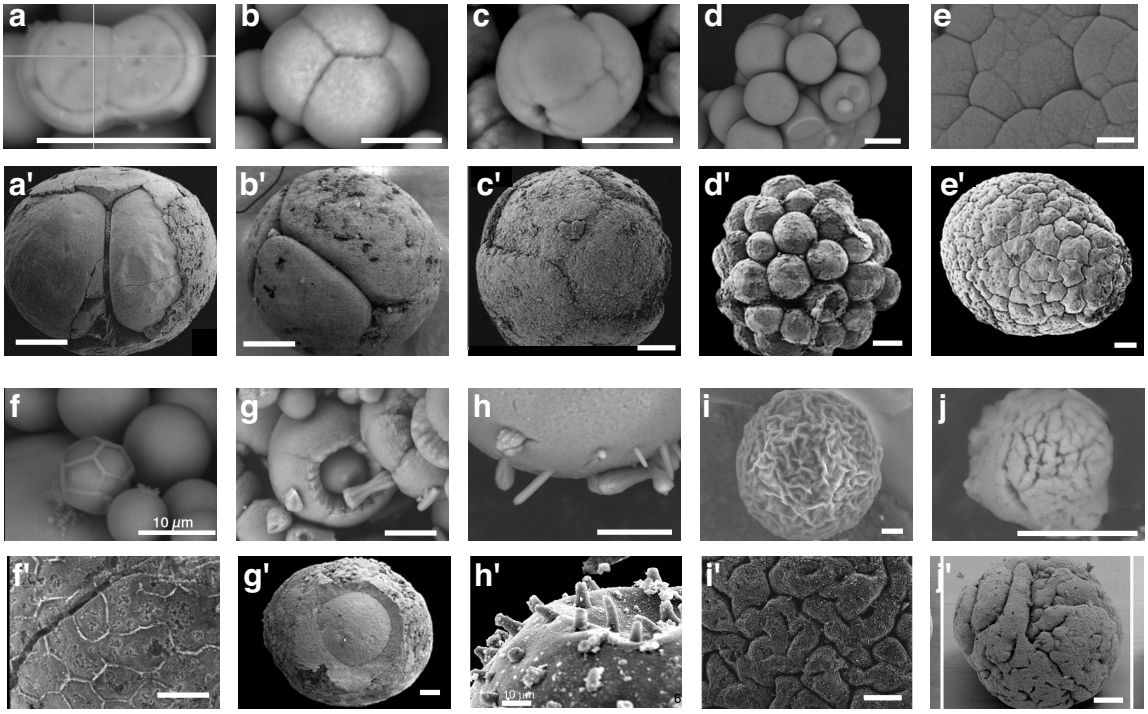

Multicell morphologies: (**A, B, C**) Pseudofossils resembling dividing cells at 2-, 4-, and 8-cell stages and showing Y-shaped triple junctions resembling embryo cleavage planes. (**D**) Mass of cells resembling morula (without enclosing membrane). Compare to microfossils *Parapandorina raphospissa*, **A′** (Xiao Zhang & Knoll, 1998); 4-cell stage *Megasphaera*, **B′** (Xiao, Knoll, Schiffauer, Zhou, & Yuan, 2012), 8-cell stage *Parapandorina raphospissa*, **C′** (Xiao & Knoll, 2000) and **D′** (Yin, Bengtson, & Yue, 2004) and *Tianzhushania ornata* **E′** (Yin et al., 2004).

Surface features: (**E**) Pseudofossils with polygonal indentations resembling blastomere junctions, and (**F**) some with raised polygonal features. (**G**) Holes leading from the surface inward to an internal sphere; (**H**) penetrating objects resembling microfossil processes; (**I, J**) wrinkled, cerebral-like surface textures. Compare to microfossil *Markuelia hunanensis*, **F′** (Dong, Donoghue, Cheng, & Liu, 2004); a "globular fossil with smooth envelope," **G′** (Yin et al., 2004); *Cavaspina acuminata*, **H′** (Xiao, Zhou, Liu, Wang, & Yuan, 2014); *Megasphaera ornata*, **I′** (Xiao & Knoll, 2000), and *Caveasphaera costata*, **J′** (Xiao et al., 2014). Scale bars: A–J: 10 μm; A′: 50 μm; B′: 200 μm; C′–G′, J′: 100 μm; H′: 10 μm; I′: 20 μm

Figure 24 | 02 | **Internal resemblances of pseudofossils to microfossil embryos**

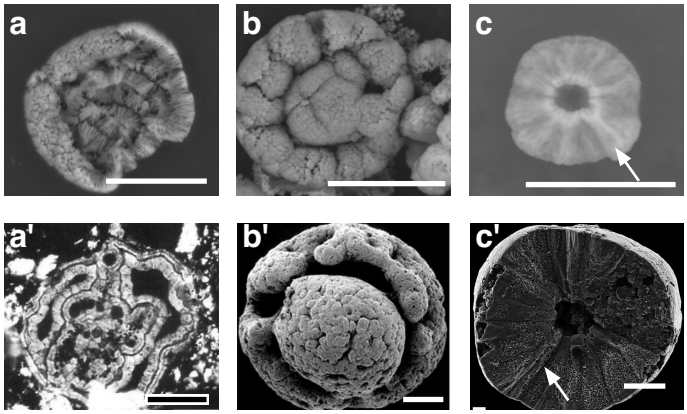

(**A**) Some pseudofossils resemble other structures interpreted as microfossils of metazoan origin. Compare to (**A′**) *Vernanimalcula* microfossil originally interpreted as an adult bilaterian (Chen et al., 2004); (**B**) pseudofossil showing internal sphere within an outer layer. Compare to *Caveasphaera* microfossil **B′** (Xiao & Knoll, 1999); (**C**) pseudofossil showing internal radial features. Compare to *Pseudooides* microfossil **C′** (Steiner, Zhu, Li, Qian, & Erdtmann, 2004). See text for comments on size comparison. Scale bars A–C: 10 µm; A′: 40 µm; B′: 50 µm; C′: 100 µm

Figure 25 | 03 | **Internal biomorphic features**

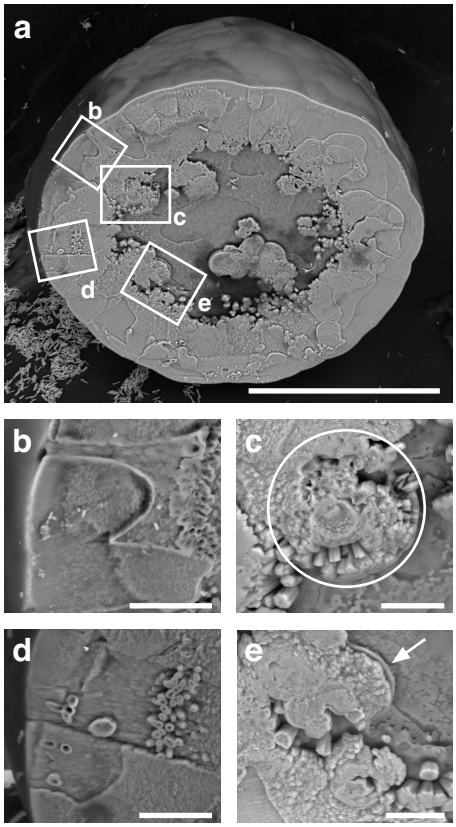

(**A**) Broken pseudofossil sphere exposing interior. Note numerous spheroid features; (**B**) channel from exterior to interior; (**C**) detail of radial growth in an internal spheroid; (**D**) detail of apparent penetrating tubules; (**E**) detail of internal sphere with possible outer membrane-like coating (white arrow). Scale bars A: 100 µm, B–E: 10 µm

Figure 26 | 04 | **Additional biomorphic features**

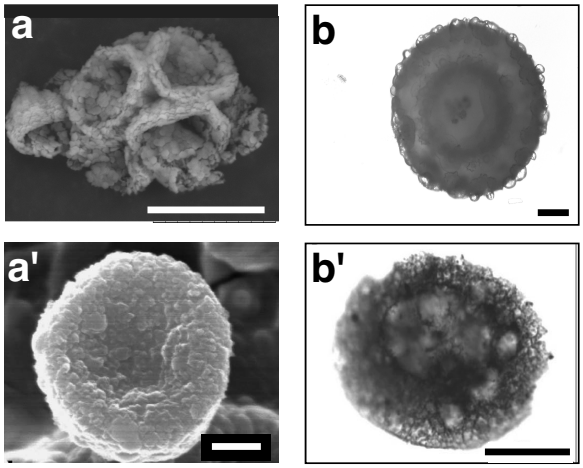

(**A**) Experimentally produced bowl-shaped precipitates, similar to collapsed cells, **A′** (Westall & Folk, 2003); (**B**) multisphere precipitate similar to ornamented sphere **B′** (Sugitani et al., 2015). Scale bars: A, B′: 10 µm; A′: 1 µm; B: 100 µm

Figure 27 | 05 | **Microfossil features not observed in our pseudofossils**

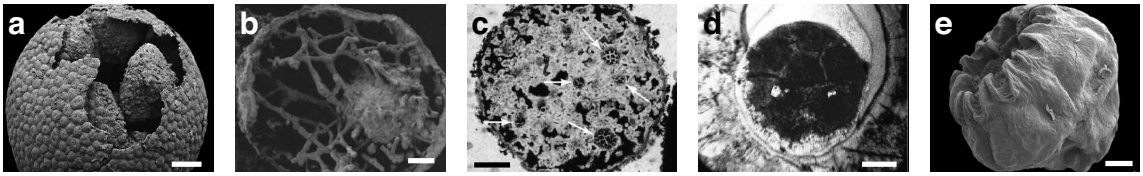

(**A**) Ornamented envelope, separate from, but encasing, apparent discontinuous blastomeres (Yin & Zhu, 2012); (**B**) internal filaments interpreted as organic (Xiao & Knoll, 1999); (**C**) matryoshkas (arrows) (Chen et al., 2014); (**D**) acanthomorphic acritarch (Yin et al., 2007); and (**E**) early Cambrian lobed embryo (Steiner, Qian, Li, Hagadorn, & Zhu, 2014). Scale bars: 100 µm

Supplementary figures

Figure 28 | S1 | **Progressive morphological development of Ca-P precipitates**

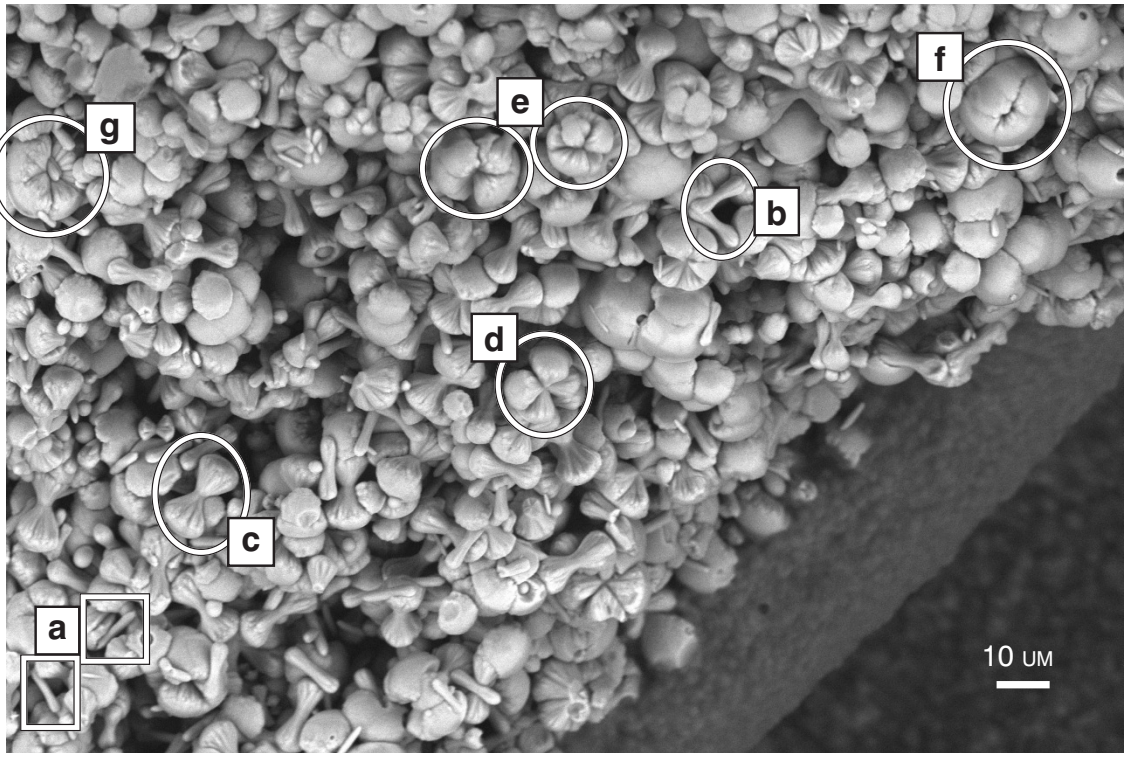

These harvested precipitates were concentrated on an SEM stub for analysis. Representative stages are circled. (**A**) small incipient prisms; (**B**) two (not connected) prisms, each beginning to expand at distal ends; (**C**) bowtie or dumbbell; (**D**) two intertwined dumbbells; (**E**) multi-lobed spheres; (**F**) closed multi-lobed spheroid, showing suture lines; (**G**) multi-dumbbell sphere, broken and showing a central internal sphere.

Figure 29 | S2 | **Experimental apparatus**

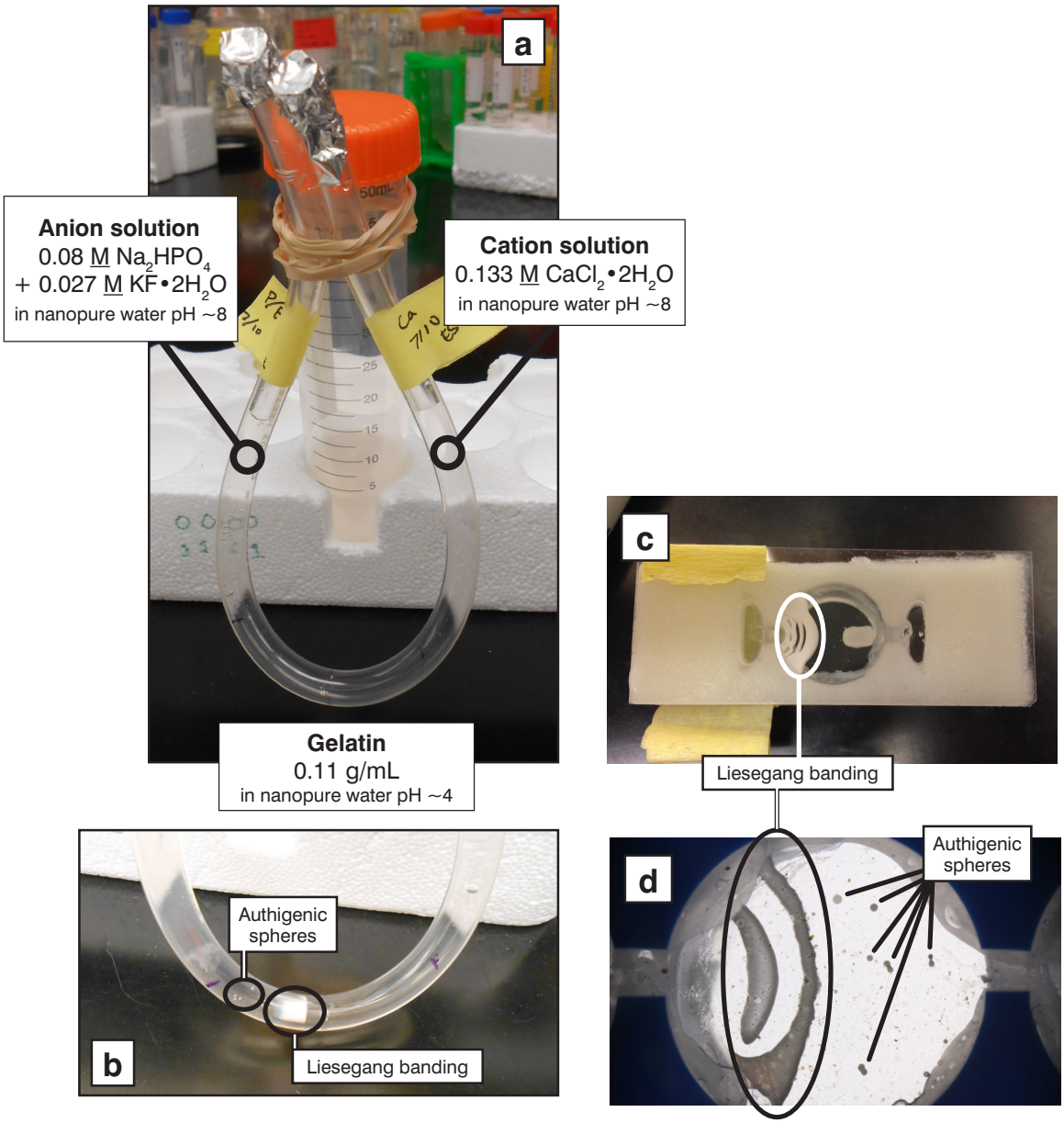

(A) type 1 setup, day 0. **(B)** type 1 setup at day 15, one day before harvest, showing Liesegang band and authigenic spheres to left. **(C)** type 2 setup (~60 x 20 mm, gel depth ~0.5 mm) showing center, gelatin-containing bore. White material outside of central bore obscures sight of the two distal ion-containing bores. **(D)** detail of the center bore of another type 2 setup, showing Liesegang bands, authigenic lone spheres and joined paired spheres ('doublets.') For details of type 2 setup, see Crosby & Bailey, 2017.

Crosby, C. H., & Bailey, J. V. (2017). Technical note: an economical apparatus for the observation and harvest of mineral precipitation experiments with light microscopy. Biogeosciences, 14(8), 2151–2154. http://doi.org/10.5194/bg-14-2151-2017

Figure 30 | S3 | **Stylized cartoon of stages of embryo development**

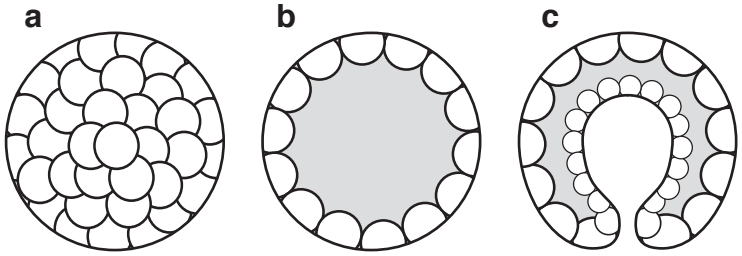

(A) Morula, representing multiple cells within an enclosing membrane; **(B)** blastula, showing cells surrounding an inner cavity; **(C)** gastrula, showing inpouching of the cells and forming an opening to the interior.

Figure 31 | S4 | **Elemental data**

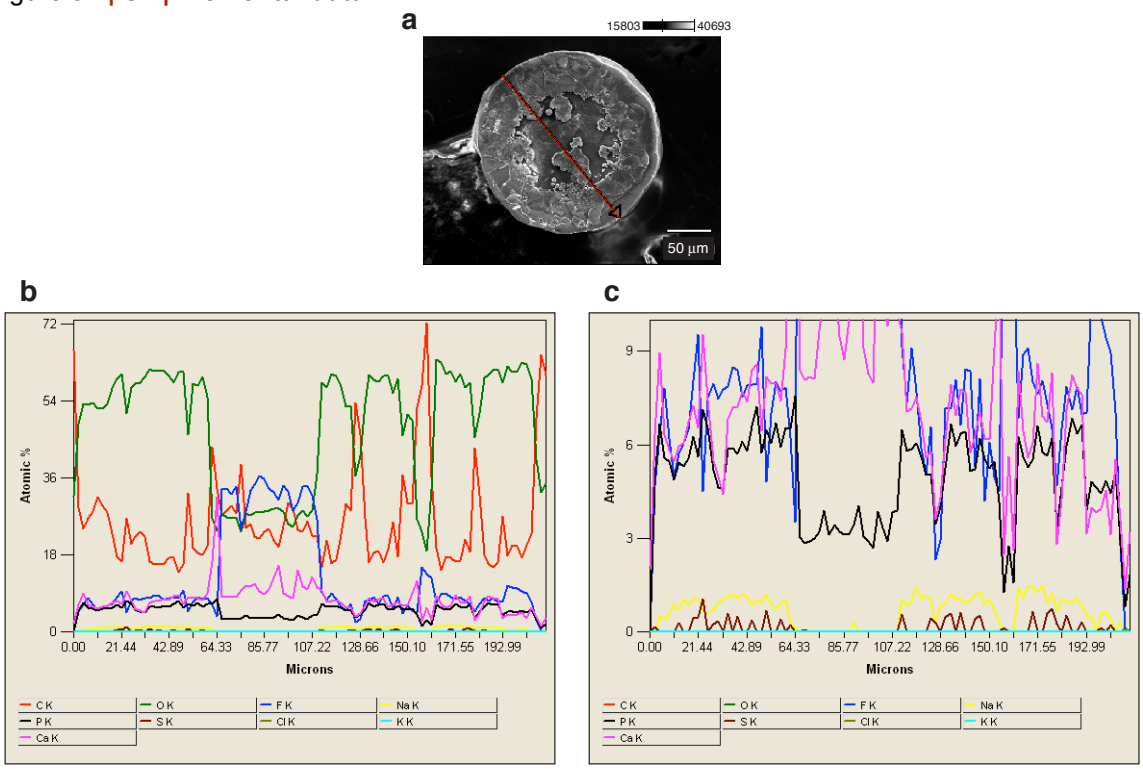

(A) Transect across broken blastula-like pseudofossil, showing EDS transect. **(B)** Elemental data. **(C)** Detail of Ca, P & F data. Data collected on Jeol JSM 6500F. Accelerating voltage: 15.0 kV, magnification: 350. As indicated in panels **B** and **C**, Ca:P ratios are inconclusive and variable, but tend toward a 1+:1 ratio, indicative of a fairly early calcium phosphate phase.

References cited

Bailey, J. V, Joye, S.B., Kalanetra, K.M., Flood, B.E., and Corsetti, F. a, 2007, Evidence of Giant Sulphur Bacteria in Neoproterozoic Phosphorites.: Nature, v. 445, no. 7124, p. 198–201, doi: 10.1038/nature05457.

Bengtson, S., and Budd, G., 2004, Comment on "Small bilaterian fossils from 40 to 55 million years befor the Cambrian": Science, v. 306, no. November, p. 1291.

Bengtson, S., Cunningham, J.A., Yin, C., and Donoghue, P.C.J., 2012, A merciful death for the "earliest bilaterian," Vernanimalcula: Evolution & Development, v. 14, no. 5, p. 421–427, doi: 10.1111/j.1525-142X.2012.00562.x.

Bengtson, S., and Zhao, Y., 1997, Fossilized Metazoan embryos from the earliest Cambrian: Science, v. 277, no. 12 September, p. 1645–1648, doi: 10.1126/science.277.5332.1645.

Bradley, J.P., Harvey, R.P., and McSween Jr., H.Y., 1997, No "nanofossils " in martian meteorite: Nature, v. 390, no. December, p. 454–456.

Brasier, M.D., Green, O.R., Lindsay, J.F., McLoughlin, N., Steele, A., and Stoakes, C., 2005, Critical testing of Earth's oldest putative fossil assemblage from the ~3.5 Ga Apex chert, Chinaman Creek, Western Australia: Precambrian Research, v. 140, p. 55–102, doi: 10.1016/j.precamres.2005.06.008.

Brasier, A.T., Rogerson, M.R., Mercedes-Martin, R., Vonhof, H.B., and Reijmer, J.J.G., 2015, A Test of the biogenicity criteria established for microfossils and stromatolites on Quaternary tufa and speleothem materials formed in the "Twilight Zone" at Caerwys, UK: Astrobiology, v. 15, no. 10, p. 883–900, doi: 10.1089/ast.2015.1293.

Buick, R., 1990, Microfossil recognition in Archean rocks: An appraisal of spheroids and filaments from a 3500 m.y. old chert-barite unit at North Pole, Western Australia: Palaios, v. 5, no. 5, p. 441–459.

Busch, S., Dolhaine, H., DuChesne, A., Heinz, S., Hochrein, O., Laeri, F., Podebrad, O., Vietze, U., Weiland, T., and Kniep, R., 1999, Biomimetic morphogenesis of fluorapatite-gelatin composites: Fractal growth, the question of intrinsic electric fields, core/shell assemblies, hollow spheres and reorganization of denatured collagen: European Journal of Inorganic Chemistry, v. 1999, no. 10, p. 1643–1653, doi: 143421948/99/101021643.

Chen, J.-Y., Bottjer, D.J., Davidson, E.H., Li, G., Gao, F., Cameron, R.A., Hadfield, M.G., Xian, D.-C., Tafforeau, P., Jia, Q.-J., Sugiyama, H., and Tang, R., 2009, Phase contrast synchrotron X-ray microtomography of Ediacaran (Doushantuo) metazoan microfossils: Phylogenetic diversity and evolutionary implications: Precambrian Research, v. 173, p. 191–200, doi: 10.1016/j.precamres.2009.04.004.

Chen, J., Bottjer, D.J., Oliveri, P., Dornbos, S.Q., Gao, F., Ruffins, S., Chi, H., Li, C.-W., and Davidson, E.H., 2004, Small bilaterian fossils from 40 to 55 million years before the Cambrian: Science, v. 305, p. 218–222.

Chen, L., Xiao, S., Pang, K., Zhou, C., and Yuan, X., 2014, Cell differentiation and germ-soma separation in Ediacaran animal embryo-like fossils: Nature, v. 516, no. 7530, p. 238–241, doi: 10.1038/nature13766.

Chi, H., 2009, The apatite crystal in fossil cells with fluorescence: Crystal Growth, v. 9, no. 2, p. 676–681, doi: 10.1021/cg7008539.

Crosby, C.H., and Bailey, J. V, 2017, Technical note: an economical apparatus for the observation and harvest of mineral precipitation experiments with light microscopy: Biogeosciences, v. 14, no. 8, p. 2151–2154, doi: 10.5194/bg-14-2151-2017.

Cunningham, J.A., Thomas, C.-W., Bengtson, S., Kearns, S.L., Xiao, S., Marone, F., Stampanoni, M., and Donoghue, P.C.J., 2012, Distinguishing geology from biology in the Ediacaran Doushantuo biota

relaxes constraints on the timing of the origin of bilaterians: Proceedings of the Royal Society B, v. 279, no. 1737, p. 2369–76, doi: 10.1098/rspb.2011.2280.

Cunningham, J.A., Thomas, C.-W., Bengtson, S., Marone, F., Stampanoni, M., Turner, F.R., Bailey, J. V, Raff, R.A., Raff, E.C., and Donoghue, P.C.J., 2011, Experimental taphonomy of giant sulphur bacteria: implications for the interpretation of the embryo-like Ediacaran Doushantuo fossils: Proceedings of the Royal Society B, v. 279, no. December, p. 1857–1864, doi: 10.1098/rspb.2011.2064.

Cunningham, J.A., Vargas, K., Yin, Z., Bengtson, S., and Donoghue, P.C.J., 2017, The Weng'an Biota (Doushantuo Formation): an Ediacaran window on soft-bodied and multicellular microorganisms: Journal of the Geological Society, v. 2016, no. 142, p. published online, doi: https://doi.org/10.1144/jgs2016-142.

Diaz, J., Ingall, E., Benitez-Nelson, C., Paterson, D., de Jonge, M.D., McNulty, I., and Brandes, J.A., 2008, Marine polyphosphate: A key player in geologic phosphorus sequestration: Science, v. 320, no. 2 May 2008, p. 652–655, doi: 10.1126/science.1151751.

Dong, X., Donoghue, P.C.J., Cheng, H., and Liu, J., 2004, Fossil embryos from the Middle and Late Cambrian period of Hunan, south China: Nature, v. 427, no. January, p. 237–240, doi: 10.1038/nature02221.1.

Donoghue, P.C.J., Bengtson, S., Dong, X., Gostling, N.J., Huldtgren, T., Cunningham, J.A., Yin, C., Yue, Z., Peng, F., and Stampanoni, M., 2006a, Synchrotron X-ray tomographic microscopy of fossil embryos: Nature, v. 442, no. August, p. 680–683, doi: 10.1038/nature04890.

Donoghue, P.C.J., Kouchinsky, Ã.A., Waloszek, D., Bengtson, S., Dong, X., Val'kov, A.K., Cunningham, J.A., and Repetski, J.E., 2006b, Fossilized embryos are widespread but the record is temporally and taxonomically biased: Evolution & Development, v. 8, no. 2, p. 232–238.

Hofmann, H.J., 2004, Archean Microfossils and Abiomorphs: Astrobiology, v. 4, no. 2, p. 135–136.

Huldtgren, T., Cunningham, J.A., Yin, C., Stampanoni, M., Marone, F., Donoghue, P.C.J., and Bengtson, S., 2011, Fossilized nuclei and germination structures identify Ediacaran "animal embryos" as encysting protists: Science, v. 334, no. 6063, p. 1696–1699.

Kawska, A., Hochrein, O., Brickmann, J., Kniep, R., and Zahn, D., 2008, The nucleation mechanism of fluorapatite-collagen composites: ion association and motif control by collagen proteins.: Angewandte Chemie (International ed. in English), v. 47, no. 27, p. 4982–5, doi: 10.1002/anie.200800908.

Kouchinsky, A., Bengtson, S., and Gershwin, L., 1999, Cnidarian-like embryos associated with the first shelly fossils in Siberia: Geology, v. 27, no. 7, p. 609–612.

Muscente, A.D., Hawkins, A.D., and Xiao, S., 2016, Fossil preservation through phosphatization and silicification in the Ediacaran Doushantuo Formation (South China): a comparative synthesis: Palaeogeography, Palaeoclimatology, Palaeoecology, v. 434, p. 46–62, doi: 10.1016/j.palaeo.2014.10.013.

Pyle, L.J., Narbonne, G.M., Nowlan, G.S., Xiao, S., and James, N.P., 2006, Early Cambrian Metazoan Eggs, Embryos, and Phosphatic Microfossils From Northwestern Canada: Journal of Paleontology, v. 80, no. 5, p. 811–825, doi: 10.1666/0022-3360(2006)80[811:ECMEEA]2.0.CO;2.

Raff, E.C., Villinski, J.T., Turner, F.R., Donoghue, P.C.J., and Raff, R.A., 2006, Experimental taphonomy shows the feasibility of fossil embryos: Proceedings of the National Academy of Sciences of the United States of America, v. 103, no. 15, p. 5846–51, doi: 10.1073/pnas.0601536103.

Ruttenberg, K.C., and Berner, R.A., 1993, Authigenic apatite formation and burial in sediments from non-upwelling, continental margin environments: Geochimica et Cosmochimica Acta, v. 57, no. 5, p. 991–1007, doi: 10.1016/0016-7037(93)90035-U.

Schopf, J.W., and Walter, M.R., 1983, Archean microfossils: New evidence of ancient microbes, *in* Schopf, J.W. ed., Earth's Earliest Biosphere, Princeton University Press, Princeton, p. 214–239.

Schulz, H.N., and Schulz, H.D., 2005, Large sulfur bacteria and the formation of phosphorite: Science (New York, N.Y.), v. 307, no. 5708, p. 416–418, doi: 10.1126/science.1103096.

Steiner, M., Qian, Y., Li, G., Hagadorn, J.W., and Zhu, M., 2014, The developmental cycles of early Cambrian Olivooidae fam. nov. (? Cycloneuralia) from the Yangtze Platform (China): Palaeogeography, Palaeoclimatology, Palaeoecology, v. 398, p. 97–124, doi: 10.1016/j.palaeo.2013.08.016.

Sugitani, K., Grey, K., Allwood, A., Nagaoka, T., Mimura, K., Minami, M., Marshall, C.P., Van Kranendonk, M.J., and Walter, M.R., 2007, Diverse microstructures from Archaean chert from the Mount Goldsworthy–Mount Grant area, Pilbara Craton, Western Australia: Microfossils, dubiofossils, or pseudofossils ? Precambrian Research, v. 158, p. 228–262, doi: 10.1016/j.precamres.2007.03.006.

Westall, F., and Folk, R.L., 2003, Exogenous carbonaceous microstructures in Early Archaean cherts and BIFs from the Isua Greenstone Belt: implications for the search for life in ancient rocks: Precambrian Research, v. 126, p. 313–330, doi: 10.1016/S0301-9268(03)00102-5.

Xiao, S., and Knoll, A.H., 1999, Fossil preservation in the Neoproterozoic Doushantuo phosphorite Lagerstatte, South China: Lethaia, v. 32, no. 219-240.

Xiao, S., and Knoll, A.H., 2000, Phosphatized animal embryos from the Neoproterozoic Doushantuo Formation at Weng'An, Guizhou, South China: Journal of Paleontology, v. 74, no. 5, p. 767–788, doi: 0022-3360/00/0074-767.

Xiao, S., Knoll, A.H., Schiffauer, J.D., Zhou, C., and Yuan, X., 2012, Comment on "Fossilized nuclei and germination structures identify Ediacaran "animal embryos" as encysting protists: Science, v. 335, doi: 10.1126/science.1218814.

Xiao, S., Zhang, Y., and Knoll, A.H., 1998, Three-dimensional preservation of algae and animal embryos in a Neoproterozoic phosphorite: Nature, v. 391, no. February, p. 553–558.

Xiao, S., Zhou, C., Liu, P., Wang, D., and Yuan, X., 2014, Phosphatized acanthomorphic acritarchs and related microfossils from the Ediacaran Doushantuo Formation at Weng'an (South China) and their implications for biostratigraphic correlation: Journal of Paleontology, v. 88, no. 1, p. 1–67, doi: 10.1666/12-157R.

Yin, C., Bengtson, S., and Yue, Z., 2004, Silicified and phosphatized Tianzhushania, spheroidal microfossils of possible animal origin from the Neoproterozoic of South China: Acta Palaeontologica Polonica, v. 49, no. 1, p. 1–12.

Yin, Z., and Zhu, M., 2012, New observations of the ornamented Doushantuo embryo fossils from the Ediacaran Weng'an Biota, South China: Bulletin of Geosciences, v. 87, no. 1, p. 1–11, doi: 10.3140/bull.geosci.1234.

Yin, L., Zhu, M., Knoll, A.H., Yuan, X., Zhang, J., and Hu, J., 2007, Doushantuo embryos preserved inside diapause egg cysts: Nature, v. 446, no. April, p. 661–663, doi: 10.1038/nature05682.

Yue, Z., and Bengtson, S., 1999, Embryonic and post-embryonic development of the Early Cambrian cnidarian Olivooides: Lethaia, v. 32, p. 181–195.

— DISCUSSION —

Replicating *in situ* conditions

Conditions under which precipitation such as those described here can be presumed to be found in microbially colonized sediments and/or growing stromatolitic fronts, where microbes and microbially-produced polysaccharides are prolific. (See 'Microbial EPS,' next page.)

As previously noted, the experimental apparatus we used was designed to replicate as well as possible *in situ* conditions, including a slowing of counter-ions as they approach and interact with each other as might be presumed in sediment or a polymeric matrix such as EPS, the use of high initial ion concentrations as a proxy for time, and a polysaccharide diffusion gel as a proxy for microbial EPS. Setup details will be found in the next chapter.

Role of P in taphonomy

Phosphatization as a mode of fossil preservation results in some of the finest retention of fossil soft tissue features. Phosphatization as a taphonomic process can proceed under conditions conducive to phosphogenesis, the formation of phosphate rock. Under these conditions, the preservation of soft tissue by phosphatization is thought to be mediated by the release of phosphate from decaying organics under pH conditions lowered by microbial metabolic activity (Briggs and Kear, 1993; Martin et al., 2005; Raff et al., 2006; Dornbos, 2011). Such conditions are most likely found in the thin band of sediment in which heterotrophic degradation and/or pH-induced decay of organics is favored, areas of low sedimentation where high rates of organic marine snow provide ample organics and microbes.

Although the finer details of the mechanism of phosphatization are not well understood, fossilization by phosphatization is believed to be biased toward recalcitrant material of small organisms already rich in P, a characteristic that may explain the dearth of larger phosphate-preserved organisms (Dornbos, 2011) as seems to be the case among the Doushantuo micro-fossils, among which late-stage multi-division embryos are yet to be found, as mentioned above. On the other hand, in systems with living phosphate-accumulating organisms, it may be induced by expulsion of phosphate in a manner like that illustrated in Figure 19. In either case, microbial EPS can be expected to influence phosphatization.

Microbial EPS – definition, nature and potential role

Most microbes in their natural habitat* are known to secrete various polymeric substances (EPS) some of which may remain in contact with the cell, some of which may be released into surrounding waters. Microbial biofilms comprise an assortment of cells effectively 'embedded' within such a polymeric matrix.

The acronym 'EPS' may be used for: Extracellular PolySaccharides, ExoPolySaccharides, ExoPolymerS, and Extracellular Polymeric Substances.

Various definitions of EPS have been put forward, including:

" '...substances of biological origin that participate in the formation of microbial aggregates' (Geesey 1982) and 'organic polymers of microbial origin which in biofilm systems are frequently responsible for binding cells and other particulate materials together (cohesion) and to the substratum (adhesion)' (Characklis and Wilderer 1989)." (Wingender et al., 1999b).

Although the nature of microbial EPS varies broadly among and within microbial species, EPS primarily comprise polymers of saccharides and can broadly be defined as "Extracellular Polymeric Substances" with the caveat that variations of EPS may contain significant fractions of proteins, nucleic acids, lipids, and other microbially-produced or environmentally-sourced molecules that have been entrained in the EPS matrix. Statements that imply that the EPS of a given prokaryote strain can be definitively determined are misleading, as the production of EPS is not only variable by species, but also controlled in large part by environmental conditions, the growth stage of the organism excreting it and the 'aging' of the EPS, which affects the nature and amount of exogenous material incorporated into it over time (Flemming et al., 2007).

The three-dimensionality of EPS is due to the fact that *in situ*, EPS is a highly hydrated complex, only a small fraction of which is the polymeric substance – the remainder, often up to 90 ~ 95% by volume, being water. The water facilitates retention of the EPS's 3D structure, and upon drying, this structure is lost, although it may be restored upon rehydration.

The propensity of EPS to contain non-saccharide molecules may be attributed to either 'intentional' or circumstantial integration, and this, particularly intentional integration, remains open to scientific investigation. The 'intentional' formation and excretion of EPS, as directed by

---

* *Under culture, microbes often lose their tendency to secrete EPS. It is believed that this may be due to the ideal conditions under which laboratory cultures are grown, making the defensive functions of EPS no longer necessary, and/or the fact that most laboratory cultures are monocultures, making inter-species communication unnecessary.*

metabolic processes, may be in response to environmental conditions, growth stage, or cell health, while circumstantial integration may be due to entrainment of microbially released molecules, including proteins, siderophores, contents of lysed cells, etc.

The manufacture of EPS exerts such a high cost in both energy and carbon resources that the EPS most certainly must serve important functions for the organism. These can be generally divided into: 1) functions relevant to interaction with the surroundings, and 2) nutritional functions. Some commonly accepted functions of EPS are listed on the next page in Table 01.

Of particular interest in relation to the Jhamarkotra microfossils of chapter three is the likely role of polymeric sheath material excreted by iron oxidizing microbes, as described by Chan et al. (Chan et al., 2004), who provide experimental evidence that not only does the microbially produced and excreted polymeric sheath provide ready nucleation sites for iron oxidation, its close proximity to the microbial cell also serves to contribute to the lowering of nearby pH conditions, as shown in the following equation:

Oxidation of a single Fe(II) ion, producing 2 protons and driving down local pH:

$$Fe(II) + 2H_2O \longrightarrow Fe(OH) + 2\ H^+ \qquad 6$$

As a result, the efficiency of energy capture by iron oxidizing microbes is improved through the subsequent steepening of the pH gradient across the cell membrane, an effect that may be heightened by the ability of EPS to significantly slow the diffusion of ions.

Potential mechanisms of EPS in mineral precipitation

Extracellular precipitation within EPS may represent simply an electrostatic attraction and concentration of ions to the point of saturation and precipitation, or it may represent a lowering of crystallization energy required to initiate precipitation via a polymeric matrix.

If pulsed expulsion of phosphate drives the ionic concentration above saturation with respect to apatite, the rate of expulsion relative to nucleation may result in distinct crystal sizes. Crystal size in turn affects other characteristics, such as surface charge and solubility (Waychunas and Zhang, 2008), possibly magnifying the effect of pulsed phosphate concentrations.

Expanding experiments to include living organisms and the spatial relationships between organism and precipitate may provide insight into the mechanisms of apatite biomineralization. For instance, intracellular precipitation (Streckfuss et al., 1974; Benzerara et al., 2004) may indicate sequestration and binding of ions for the purpose of maintaining appropriate intracellular

osmolarity. On the other hand, internally precipitated apatite in only dead or dying cells may suggest a deleterious impact on microbes (Ennever et al., 1974).

Table 01 | **Some of the functions of EPS**

Function	Relevance
Adhesion to & release from surfaces	Colonization and accumulation of bacteria on nutrient-rich surfaces under oligotrophic conditions; subsequent release from surfaces
Aggregation of bacterial cells, formation of biofilms	Bridging of cells and trapped environmental inorganic particles, immobilization of mixed colonies, development of high cell densities, acts as a medium for communication processes
Cell-cell recognition	Enhancement of cell-cell communications
Biofilm structures	Mechanical stability of biofilms, determination of EPS structure (capsule, slime, sheath)
Protective barrier	Resistance to attack by predators, antibiotics and DNAses, protection of cyanobacterial nitrogenase from harmful effects of oxygen
Retention of water	Prevention of dessication under water-deficient conditions
Sorption of inorganic ions	Accumulation of toxic metal ions (detoxification), promotion of polysaccharide gel formation, mineral formation
Enzymatic activity	Digestion of exogenous macromolecules for nutrient acquisition, release of biofilm cells by degradation of structural EPS of the biofilm
Interaction of polysaccharides with enzymes	Accumulation/retention and stabilization of secreted enzymes
Nutritional reserves	Storage of excess carbon for lean times
Sorption of exogenous organic compounds	Scavenging and accumulation of nutrients from the environment, sorption of xenobiotics (detoxification)
Establishment of microniches	Formation of protective enclave

Adapted from Wingender et al., Wolfaardt et al., and Decho (Decho, 1990; Wingender et al., 1999a; Wolfaardt et al., 1999).

Conclusion

This chapter has presented experimental results of abiotic precipitation of calcium-phosphate minerals in the context of a dissolvable diffusing polymeric gel serving as a proxy for EPS. The results of this work have implications for the establishment of *bona fide* biogenicity of putative microfossils, as well as the impact of microbes on precipitation of calcium-phosphate minerals as facilitated and influenced by microbial EPS. A reasonable extension of this work would seek to tease out the role of different EPS polymeric matrices in the precipitation of calcium-phosphate minerals, specifically addressing morphological distinctions in mineralization as determined by the characteristics of polymer geometry and chemistry.

Since evidence suggests that microbes may play a part in phosphogenesis, and virtually all known microbes (in their natural habitat) are believed to produce some form of EPS, the role of microbial EPS in phosphogenesis is strongly implicated. Retention by EPS of pulsed phosphate concentrations may not only provide nucleation surfaces for calcium-phosphate mineralization, but also provide a matrix that slows ion diffusion sufficiently to allow mineral crystal growth to proceed. How the geometric and chemical nature of that matrix may in turn affect calcium-phosphate precipitation and growth is still being explored. Alternative gels, less amenable to dissolution in harvesting than the water-soluble gelatin used in our experiments, will present new and appreciable challenges in the harvesting step, although some, such as *bona fide* EPS rich in proteins, may be degraded by enzymes such as trypsins and various amylases.

While it will be left to future work to explore the details of comparative precipitation and morphologies of calcium-phosphate minerals in different polymers, we have developed a physical setup and assembly protocol amenable to such further research. The next chapter provides the details of this setup.

Chapter 5

—

Apparatus for microscopic observation of mineral precipitation over time

Introduction : the need for a customized setup

The results shown in the previous chapter required a customized setup that allowed both microscopic monitoring during experiment runs and the undistorted harvesting of precipitates. The next section describes the apparatus and protocol developed for this purpose and followed by a more in-depth discussion.

Technical note: An economical apparatus for the observation and harvesting of mineral precipitation experiments with light microscopy

Chris H. Crosby[1], Jake V. Bailey[1]

[1]Department of Earth Sciences, University of Minnesota–Twin Cities, Minneapolis, 55455, USA

Published in 'Biogeosciences' 27 April 2017 doi: 10.5194/bg-14-2151-2017

We describe a small-scale, reusable, and low-cost double-diffusion setup that allows microscopic observation over time for use in mineral precipitation experiments that use organic polymers as a matrix. The setup uniquely accommodates changes in solution chemistry during the course of an experiment and facilitates easy harvesting of the precipitates for subsequent analysis.

Introduction

Investigations into the influence of organic materials and microbes on authigenic mineral precipitation has transformed our understanding of geosphere–biosphere interactions and improved our understanding of taphonomic processes that allow for the preservation of biological remains. The ability to observe nucleation, precipitation, and growth over time can provide insight into these processes. However, observation and imaging over the course of an experiment, as well as post-experimental analysis, place strict requirements on the experimental setup, including the following:

1) The setup must provide an approaching flux of counter-ions while simultaneously and sufficiently slowing diffusion to avoid the instantaneous precipitation that would inhibit further crystal growth.
2) To enable microscopic observation over time, the setup must fit a microscope stage during the course of an experiment. The diffusion gel material within which precipitation proceeds must be transparent to the imaging wavelength, and for undistorted optical imaging the region/material of interest should be housed within a planar (not tubular) transparent housing.
3) For post-experimental analysis of precipitates, the setup must allow harvesting of the materials of interest, which may be both precipitates and various nucleation substrates of interest.
4) The setup should be amenable to a variety of ambient conditions such as temperature, redox conditions and chemistry. Additionally, the ability to change experimental conditions mid-experiment should allow exploration of increasingly refined and focused questions.

Here, we describe a reusable, small-scale, and low-cost double-diffusion (DD) apparatus that satisfies these requirements and requires only small diffusion gel volumes – a significant advantage when the gel material is expensive or consists of low-volume microbially produced polymeric substances. The apparatus allows detailed observation of progressive precipitation in situ, an example of which can be seen in Fig. S2 of the Supplement.

Background

A variety of physical setups have been used for decades by chemists investigating mineral precipitation kinetics and are generally one of three types: The single diffusion (SD) method, in which an ion-containing gel is overlain with a solution of counter-ions that diffuse into the gel; the double diffusion (DD) method, in which solutions of constituent ions are separated by a

diffusion gel and into which the ions pass and ultimately meet (Becker et al., 2003); and the constant composition (CC) method (Morse, 1974; Tomson and Nancollas, 1978). As the name indicates, the CC method holds the ionic strength of constituent ions constant and allows sensitive observation of the impact of factors other than ionic strength. However, for exploring systems relevant to essentially confined environmental systems – such as sediment pores or spaces constrained within polymeric matrices such as those found under stromatolitic growth conditions – a diffusion setup is arguably more likely to reflect dynamic *in situ* conditions, where precipitation leads to falling ion concentrations over time. Hence, diffusion setups are suitable for, and have been used in, studies of biologically mediated precipitation (Hunter et al., 1985; Emerson et al., 1994; Becker et al., 2003).

The DD setup described herein is the result of many iterations and refinements of a setup similar to that described by Kniep et al. (Kniep and Busch, 1996; Busch et al., 1999). It resembles that of Emerson et al., (Emerson et al., 1994) designed to observe the responses of motile microbes to distinct gradients, but it differs in that this apparatus immobilizes biological material as counter-ions meet across the immobilized biological material.

In this system, the gel functions to both: 1) slow precipitation by retarding ion diffusion rates, and 2) serve as a proxy for microbially-produced polymeric substances, such as EPS (microbial extracellular polymeric substances), a matrix that is ubiquitous in microbial mats and biofilms. Considering the diffusion gel as the primary organic matrix, this setup will also accommodate secondary organics such as distinct EPS strands or pellets of microbial culture, which can be immobilized by slight heat fixation-adherence to the bottom cover slip before addition of the diffusion gel. Staining of secondary organics may also be accommodated. The setup is small and easily handled and fits unobtrusively in a laboratory refrigerator for low-temperature experiments. However, extra care will need to be taken when imaging low-temperature experiments, as the gel may be heated by the light source. In this case, preliminary tests with the microscope are strongly advised to determine the degree to which this may occur and methods for ameliorating it (such as blowing cooled air between the light source and apparatus.) Nominal monitoring of gel temperature might be possible by measuring the temperature of the two cover slips by remote sensing, such as may be obtained by an infrared digital laser thermometer.

Experiment goals will dictate protocol details. For instance, after adhering a marine culture, gentle rinsing may be required to remove NaCl precipitates or growth media if their presence would interfere with the goal of the experiment.

A variety of polymeric substances are available for use, including lab standard polymers such as gelatin and agar, or custom organic substrates such as lab-grown EPS. The characteristics of each polymer are unique, most significantly in the nature and location of their charge balances – a discussion of which can be found in Kniep et al. (Kniep and Simon, 2007) – and solubility (Whistler, 1973). The reader is referred to the book "Microbial Extracellular Polymeric Substances" (Wingender et al., 1999a) for discussion of EPS, and to Silverman & Boskey for a discussion of different polymers and the utility of DD setups in studying biomineralization (Silverman and Boskey, 2004). They also describe a constant-composition DD method comparing different proteins introduced into a gelatin matrix to illustrate their effects on calcium phosphate biomineralization.

The apparatus

Description

The active precipitation area of this setup is a thin diffusion gel, ~1 mm thick, sandwiched between a long coverslip and a square coverslip, into which ions are introduced from solution chambers via small channels leading into the gel (figure 29). Table 02 lists the required components. The setup block and adaptor can be easily made in-house. Detailed directions and solution concentrations suitable for reproducing our initial experiments can be found in the Supplement. The purchasable components of the setup are readily available.

Design considerations

The setup described here was designed with a cover slip bottom to allow use in an inverted microscope. Before constructing the setup, take into consideration the microscope that will be used and adjust dimensions as needed. For instance, an upright scope with objective lenses in a rotating turret may require a design with longer channels on either side of the center bore to avoid contact between the setup and the objective lenses.

If the precipitates are to be harvested from the diffusion gel for additional analysis, the solubility of the diffusion gel material should be taken into account. Gelatin is easily removed by repeated applications of hot water. Other gel materials are likely to require different treatments.

The success of this apparatus requires seals adequate to preclude leakage and evaporation and keep the ion solutions from bypassing the diffusion gel and mixing prematurely. A great deal of trial and error went into this protocol, the results of which are incorporated into the Supplement

step-by-step protocol. Please see the Supplement for details of the sealing method and precautions (Sect. S3.4 through S3.6) Assembly requires practice to achieve a full seal.

Experimental results – an example

Our interest in developing this apparatus and protocol stemmed from our exploration of the influence of organics on the precipitation of calcium phosphates (apatite and its precursor phases.) We designed the apparatus to replicate conditions that might be present under primarily confining conditions such as within the microbial EPS of growing stromatolites or sediment pore spaces.

Early iterations of the apparatus with 9.5 mm (3/8-inch) gel depths formed a thick opaque cloud of precipitates, precluding optical microscopic imaging of precipitate details. In the assembly being described, the thickness of the gel is determined by the spacer used in forming the adaptor-spacer, as shown in Fig. S1a, in which a square cover slip is used to create the spacer insert into which the diffusion gel is added. This thinner gel thickness allows details of the development and maturation of the precipitation cloud that had been hidden in the deeper gels to be revealed. A similar, initially diffuse precipitation cloud forms, but then develops into a much more pronounced band with distinct boundaries before dividing into a number of discrete bands (Liesegang bands) as shown in Fig. 1e. The phenomenon and dynamics of Liesegang banding remains an area of active research (Stern, 1954; Antal et al., 1999; Tripathi et al., 2015), and imaging and analysis of these separating Liesegang bands have shown differences in the size and morphology of the small constituent precipitates. [Preliminary data is presented in Appendix D.]

Conclusions

The features of this apparatus make it a versatile instrument for experiments in which microscopic observation of the precipitation process is desired. It is small and easily handled and fits unobtrusively in a refrigerator for low-temperature experiments. It requires only small amounts of diffusion gel and can accommodate secondary organics of interest. Experiments can be designed with any desired counter-ion solutions – the solution chemistry, pH and Eh of which can be changed mid-experiment by needle and syringe. When utilized in conjunction with time-lapse microscopy, this apparatus provides an efficient and economical opportunity to observe and document mineral precipitation throughout the process.

Acknowledgements

ESEM imaging and EDS analysis not described herein but utilized in the development of the setup and protocol was performed at the LacCore (National Lacustrine Core Facility), Department of Earth Sciences, University of Minnesota–Twin Cities (UMN). LacCore is funded by NSF and UMN. Portions of this work were funded by NSF grants #3002-1113-00019448 and #EAR-1057119 to JVB, and a UMN Graduate School Fellowship, Doctoral Dissertation Fellowship, and Department of Earth Sciences Fellowships to CHC. The assistance of Mark Griffith, Elizabeth Ricci, Beverly Chiu, Erica Sheline and Peter Schroedl is gratefully acknowledged.

List of accompanying table, figures & appendices

Table 02

Apparatus setup components

Component	Material	Dimensions *
Long coverslip	glass	24 x 60 mm
Square coverslip	glass	18 mm square
Setup block *	plastic or glass	~26 x ~62 mm (thickness: ~3/8 inch or as preferred)
Adaptor *	silicone epoxy	~26 x ~62 mm (thickness: standard glass slide)
Assembly material	sterile bandaging **	> 24 x 60 mm
Assembly material	clear tape	¾-inch
Assembly material	Vaseline/lanolin	

* Dimensions of the setup block and adaptor should be slightly narrower and shorter than the long coverslip.

** Half of a 2-3/8 x 2-3/4-inch 3M Nexcare™ Tegaderm™ bandage, or similar, works well where sterility is desired, but its adhesive surface is designed to allow the escape of moisture. Clear watertight tape will seal it from evaporative loss. The bandage/tape plies can be punctured by needle for exchange of solutions during experimentation and resealed.

Figures

Figure 32 | 1 | **Specifications and assembly of unit**

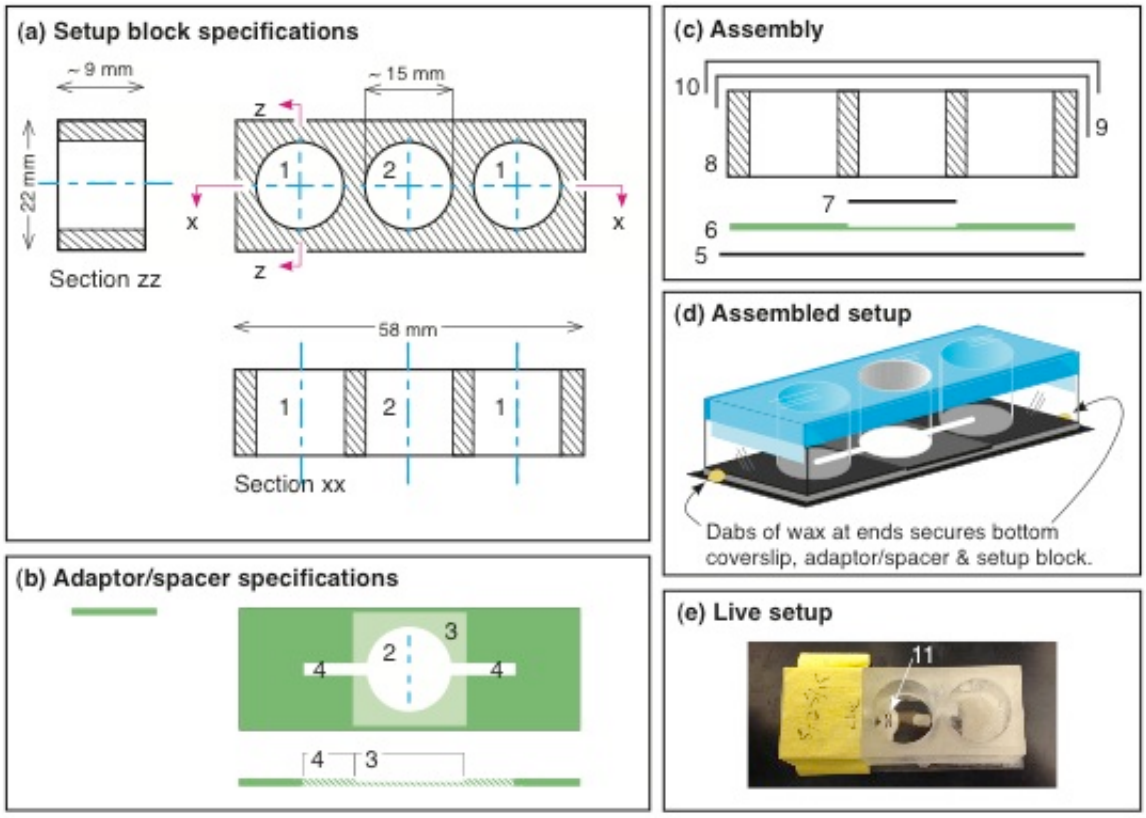

Legend

1: ion bore
2: gel bore
3: indent for square cover
4: ion channel
5: long cover slip
6: adaptor
7: square cover slip
8: setup block
9: sterile bandage material
10: clear tape
11: Liesegang bands

(**A**) Setup block diagram and specifications; (**B**) Adaptor diagram; (**C**) Exploded view showing assembly order; (**D**) Assembled setup, isometric view; (**E**) A version of a live setup, viewed from above and showing Liesegang banding.

Figure 33 | 2 | **Forming the adaptor**

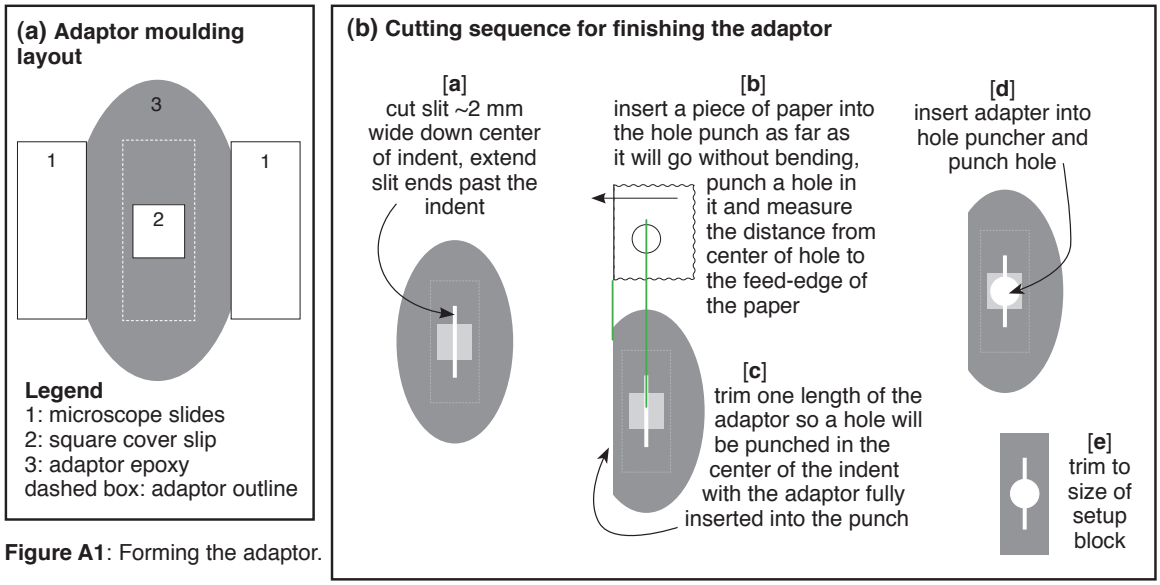

Figure A1: Forming the adaptor.

Supplemental information

Diffusion gel material and solution concentrations can be altered as required for different experiments, but the conditions under which this apparatus was developed, and those used to produce figure 1E, are as follows:

- ❑ gelatin: type A, 1 g/ml water, pH ~4
- ❑ cation solution: 0.133 M Ca^{2+} [$CaCl_2 \cdot 2H_2O$, pH ~8]
- ❑ anion solution: 0.08 M $(PO_4)^{3-}$ [$NaHPO_4$, pH ~8]
- ❑ anion solution: 0.027 M F^- [$KF \cdot 2H_2O$, pH ~8]

Nascent precipitation is observed within ~30 hours.

S1 Supplement A: Setup block & adaptor construction

Note: The width and length of the setup block and adaptor-spacer should be slightly smaller than the long coverslip. The dimensions shown in Fig. 1 assume a standard long coverslip size of 24 x 60 mm. The bore diameter should be ~3–4 mm less than a side of the square coverslip. The bore size shown in Fig. 1 assumes an 18 x 18 mm square coverslip. Revise the dimensions as required to accommodate differently sized cover slips.

S1.1 Setup block

Machine the setup block as indicated in Fig. 1a.

S1.2 Adaptor-spacer

S1.2.1 Material needed

- ❑ two clear, rigid flat surfaces ("sheets") such as 8 x 10 in. acrylic or glass sheets
- ❑ two microscope slides (of same thickness)
- ❑ one square coverslip
- ❑ silicone epoxy molding material (Castin'Craft® EasyMold silicone putty, or similar)
- ❑ cutting blade, such as an X-acto® blade or similar
- ❑ hole punch, ~16 mm or ~5/8-in.

S1.2.2 Molding procedure

- ❑ Position a square coverslip and two slides on one of the sheets as shown in Fig. S1a. The slides will serve as spacers to set the thickness of the adaptor-spacer and their positioning isn't critical, but they should be at least ~ 40 mm apart. The square coverslip will form an indent in the adaptor to accept a square coverslip in the assembled unit.
- ❑ Mix a small volume of silicone epoxy, per instructions.
- ❑ Form the epoxy into a cylinder and gently press it over the coverslip between the slides, avoiding air bubbles under the epoxy.
- ❑ Place the second sheet on the epoxy and press the epoxy into a sheet the thickness of the slides, again observing to avoid air bubbles between the sheets and the epoxy.
- ❑ Allow epoxy to set, per instructions.
- ❑ Remove the top sheet, pick up the molded epoxy and carefully remove the square coverslip.
- ❑ Put the epoxy, indentation side up, back on the sheet and cut out a slot, as shown in Fig. S1b(a).
- ❑ Insert a piece of paper into the hole punch as far as it will go without bending, and punch a hole in it Fig. S1b(b).
- ❑ Mark off the distance from the center of the hole to the feed-edge of the paper.
- ❑ Mark off the distance from the center of the hole to the feed edge of the paper.
- ❑ Using this distance, trim one length of the adaptor-spacer so that when it has been fully inserted into the punch a hole will be punched directly in the center of the indent as shown in Fig. S1b(c).
- ❑ Insert the adaptor-spacer into the hole punch, aligned side-to-side so that the hole will be punched in the center of the indentation Fig. S1b(d). (Practice positioning a sheet of paper in the hole punch before punching the adaptor.)
- ❑ Trim the adaptor to the size of the setup block Fig. S1b(e).
- ❑ Check the position of the hole and slot by holding it against a setup block.

S2 Supplement B: Preassembly preparation

S2.1 Preparing for experimental sterility

❑ To assure a controlled, sterile experiment, all objects and solutions in contact with the gel should be sterilized. Either autoclave them ahead of assembly, or sterilize them in 70% ethanol, as mentioned in § 3.2, below.

S2.2 Addition of secondary organics

❑ Secondary organic material (an organic substrate other than the gel material) can be immobilized before assembly of the setup. Place the material in the center of the long coverslip and immobilize/adhere it by allowing it to air dry or quickly passing it over a flame. Rinse as needed to remove media precipitates. Staining of organics may also be accommodated.

S2.3 Focusing aids (optional)

❑ Holding a square cover slip securely against a flat surface, carefully scribe a small 'L' extending from the middle of one side. Rinse off glass scrapings. The combined position and direction of the L will indicate which side is up – the scribed surface will be positioned against the gel and can be used to locate the 'top' surface of the gel layer under the microscope.

❑ Scribe another 'L' in the long cover slip parallel to the length, ~5-6 mm from the edge to indicate the 'bottom' outer surface of the gel layer. Rinse off glass scrapings. In the finished setup, these two scribe marks should overlap near the outer area of the gel, with the scribed surfaces both in contact with the gel surface.

S3 Supplement C: Assembling and activating the apparatus

Note: The steps listed here assume the use of gelatin as the primary organic polymer (the diffusion gel.) In developing this apparatus and protocol, gelatin was chosen as a diffusion gel because its gel is transparent and amenable to optical observation and imaging, and because it is soluble in hot water. It is intended that experimental details will represent conditions as desired by the experimenter, such as use of a different diffusion polymer. For work in which a different diffusion material is to be used, if extraction of precipitates is desired it will be important to consider both the solubility requirements of the diffusion material and the stability of precipitates and precursor molecules under whichever extraction method is required.

Ion solutions can be changed mid-experiment to alter solution chemistry, pH, Eh, etc. as desired. Addition to and/or removal and replacement of the initial ion solution(s) can be done under sterile conditions in a biological hood (see § S3.7, below.)

Some of these assembly steps are labelled "skill steps." Best results are attained with practice before attempting to assemble and activate a live setup. Components are joined by a layer of Vaseline™. If Vaseline doesn't stand up to your handling, thicken it by adding small amounts of paraffin and lanolin and melting them together. Paraffin will cause the mixture to set more solidly, but too much paraffin may cause it to set so quickly that you will have to work fast, and may make the material brittle and more prone to fracture during experiment handling. Alternatively, a dab of candle wax applied to each end of the assembly (Fig. 1d) can immobilize the setup block–adaptor–long cover slip assembly.

S3.1 Materials required for assembly [Assumes gelatin as primary polymer]

- ❑ setup components
- ❑ suction tool, such as a Model Pal™ Suction Handling Tool, or similar
- ❑ hot plate with magnetic stir capacity
- ❑ small stir bar
- ❑ 70% ethanol in a small container for sterilizing various parts and tools
- ❑ small beaker for mixing gelatin
- ❑ gelatin powder
- ❑ ≥ 10 mL nanopure or sterile water, for gelatin
- ❑ Vaseline®
- ❑ 2 of: 2 x 3-inch glass slide, or similar
- ❑ 3 of: 3 mL syringes with needles
- ❑ disposable pipette

❑ pointed tweezers

❑ sharp small blade

❑ fine metal probe

❑ cation solution

❑ anion solution

❑ small wax candle

❑ sterile water, for testing water-tightness

S3.2 Initial steps: mix gel

[Assumes gelatin as diffusion gel. Revise as needed for a different gel.]

❑ Before turning the hot plate on, clean its surface, sterilize it with 70% ethanol and allow it to dry.

❑ Place items that have not been autoclaved or sterilized (the stir bar, tweezers, probe tip, coverslips, two 2 x 3-inch slides, an adaptor-spacer & setup block, etc.) in a small container of 70% ethanol to sterilize them. Before using each of them in the following steps, remove them from the ethanol and allow them to dry.

❑ Turn hot plate to ~30C.

❑ Measure the nanopure water for the gel and heat it in the small beaker.

❑ Measure out the gel powder, add it to the heated water, add the small stir bar and mix.

❑ Dip the suction tool tip into the ethanol to sterilize it and use it to transfer the square coverslip, adaptor-spacer & setup block to the hot plate. Move the 2 x 3-inch slides to the bench top, and place the long coverslip on one of them.

❑ Wipe a thin even layer of Vaseline® onto bottom (flat) surface of the adaptor-spacer.

❑ Center the adaptor onto the long coverslip and press them together.

❑ Verify the seal by the appearance of the adapter material against the long coverslip. Air bubbles should look lighter or darker than well sealed areas and should be avoided where they could allow leakage.

❑ Check the mixing gel and slow the stir rod to release any air bubbles entrained in it.

S3.3 Add gel [skill step]

❑ Apply Vaseline along the edges of the recessed portion of the adaptor-spacer, avoiding the channels and the gel.

❑ [skill step] Pull ~1 mL of gel into one of the syringes, minimizing entrained air bubbles (pull the syringe plunger slowly, release the plunger and allow it to stop moving before removing the needle tip from the gel.)

❑ [skill step] Extrude a small volume of gel into the center bore to a slight convex meniscus.

❑ Immediately remove bubbles from the gel as needed, using the tweezers in a horizontal ‘cutting’ motion to pick up and remove bubbles.

S3.4 Add small cover slip

❑ Check that the Vaseline along the edges of the recessed portion hasn't been rubbed off.

❑ [skill step] Use the suction tool to pick up the square coverslip and press it over the gel and into the recessed portion of the adaptor-spacer. The gel should fill the volume beneath the square coverslip and a small volume of gel should push out the adaptor-spacer channels.

❑ Check that the square coverslip is sealed against the Vaseline® on the adaptor.

❑ [skill step] Verify that the channels are both clear of Vaseline®. If needed, use a fine probe to clear them of any Vaseline®. Gel intruding into the side bores is OK.

S3.5 Add setup block

❑ Apply a layer of Vaseline® onto the bottom of the setup block.

❑ [skill step] Place the setup block on the assembly. Apply downward pressure (only) as needed to get a complete seal (sideward pressure will cause the components to slip out of alignment.) See that seal is complete and neither cover slip has broken.

❑ To stabilize the long coverslip against the setup block during handling, place a small drop of candle wax on the setup block side of each end of the long coverslip where it meets the setup block (Fig. 1d).

❑ Gently remove any extraneous Vaseline® from the exterior and place the unit on a clean surface.

S3.6 Add ion solutions, seal side bores

❑ Pipette sterile water into one of the side bores, wait and watch that: 1) no water leaks out of the unit and 2) no water leaks into the other bore. This can happen if the seal between the long coverslip and the setup block is not water tight. If there is leakage, repair the seal or start over. Once confident that there is no leakage pour the water out and dry the unit.

❑ Repeat for other side.

❑ Add ion solutions to the side bores and label them.

❑ Wick off any water on the setup block exterior.

❑ Cut a section of sterile bandage material, leaving the backing paper on. If using 2-3/8 x 2-3/4-inch 3M Nexcare™ Tegaderm™, cut it lengthwise and set one of the halves aside.

❑ Remove the backing, stretch the bandage across the top of the three bores and press it onto the setup block to seal.

❑ Scotch Tape™ (or similar) across the length of the bandage to preclude evaporation through the bandage material.

❑ Use a small sharp blade to cut the tape+Tegaderm™ away from the center bore.

❑ Recheck all seals.

❑ The setup is now activated. Label the setup and place it on a paper towel or similar to detect leakages.

❑ Image as desired, handling carefully so as not to break the Vaseline® seals.

S3.7 Changing ion solutions mid-experiment

[optional – perform under sterile conditions, such as a biological hood**]**

❑ To keep the solution sterile, wipe a small amount of ethanol on the tape surface where it will be punctured.

❑ Using a sterilized blade, carefully cut a small slit in the sealing material over one of the solution wells.

❑ Use a sterile needle and syringe to remove the original solution.

❑ Use a different sterile needle and syringe to introduce a new solution.

❑ Reseal with Tegaderm™ or similar sterile material.

❑ Seal against evaporation with clear watertight tape as described in S3.6, above.

S4 Supplement D: Harvesting procedure

Note: Once the gel is exposed to air it will begin to harden, and chipping gel off coverslips may break them into slivers. The gel can be kept soft in cool water. When cutting portions of gel away from the coverslip, place the coverslip against a firm flat surface.

S4.1 Materials needed

❑ thin X-acto™ blade or similar

❑ dissecting microscope

❑ container for waste ion solutions

❑ small container of cool DI water

❑ small squeeze bottle of DI water

❑ beaker of hot DI water

❑ small (~5–25 µL) pipet and tips

❑ prepared SEM stubs or similar for follow-up analysis and/or imaging

S4.2 Procedure

❑ Open/remove the tape over the ion solutions and pour the solutions into a disposal container.

❑ Working over a catch tray, separate the long coverslip from the adaptor-spacer by gently sliding a thin X-acto™ blade between them and slowly applying a slight twisting pressure against the long coverslip. It

should bend a bit and allow the seal to break. Hold the unit so it reflects overhead light to see where the seal is broken – it will be lighter than the intact seal.

- ❑ Using the same procedure, remove the adaptor-spacer from the setup block. Only the square coverslip and gel plug should remain attached to adaptor-spacer. Leaving the gel plug attached to the cover slip will make it easier to handle. Place it on a firm even surface, such as the stage of a dissecting microscope.
- ❑ Cut away the portions of interest and place them on two-sided carbon tape on an SEM stub or similar.
- ❑ Rinse gel off the precipitates by repeatedly pipetting small amounts of hot sterile water onto the harvested precipitates, letting the gel melt, and then removing the melted gel + water. Repeat as needed to assure removal of gel from precipitates.
- ❑ For gels with smaller or more numerous precipitates: Place the gel plug in an epitube of hot water, immerse it in a hot water bath, shake it gently and hold it vertically in the hot water bath to allow precipitates to settle. Slowly remove supernatant by pipette. Repeat as needed to assure removal of gel from precipitates. Remove the final, rinsed precipitates + bottom rinse water from the epitube by pipette and place on a carbon-taped stub. Let the water evaporate and further rinse the precipitates on the stub as described above.

Supplemental figure

Figure 34 | S1 | **Photomicrographs of precipitated object**

Photomicrographs of a complex object that precipitated in the diffusion gel of the described apparatus. Image taken on an Olympus IX inverted microscope with DP73 camera. Left image is overview of the precipitated object (scale bar = 100 um). Internal details shown below (scale bar = 20 µm).

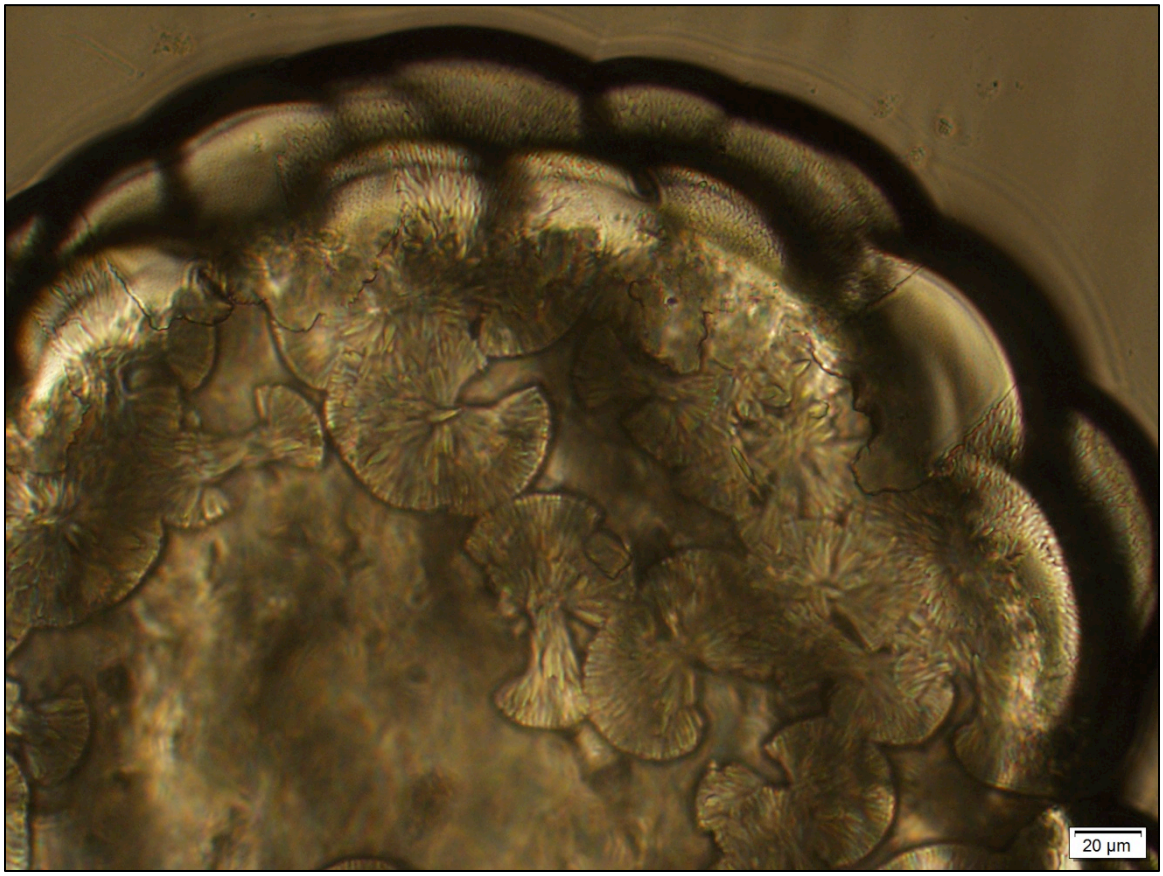

References cited

Antal, T., Droz, M., Magnin, J., and Rácz, Z., 1999, Formation of Liesegang patterns: A spinodal decomposition scenario: Physical Review Letters, v. 83, p. 2880–2883, doi: http://dx.doi.org/10.1103/PhysRevLett.83.2880.

Becker, A., Becker, W., Marxen, J.C., and Epple, M., 2003, In-vitro crystallization of calcium carbonate in the presence of biological additives – Comparison of the ammonium carbonate method with double-diffusion techniques: Journal for Inorganic and General Chemistryournal for Inorganic and General Chemistry, v. 629, p. 2305–2311, doi: 10.1002/zaac.200300229.

Busch, S., Dolhaine, H., DuChesne, A., Heinz, S., Hochrein, O., Laeri, F., Podebrad, O., Vietze, U., Weiland, T., and Kniep, R., 1999, Biomimetic morphogenesis of fluorapatite-gelatin composites: Fractal growth, the question of intrinsic electric fields, core/shell assemblies, hollow spheres and reorganization of denatured collagen: European Journal of Inorganic Chemistry, v. 1999, no. 10, p. 1643–1653, doi: 143421948/99/101021643.

Emerson, D., Worden, R.M., and Breznak, J.A., 1994, A diffusion gradient chamber for studying microbial behavior and separating microorganisms: Applied and Environmental Microbiology, v. 60, no. 4, p. 1269–1278, doi: 0099-2240/94.

Hunter, G.K., Allen, B.L., Grynpas, M.D., and Cheng, P.-T., 1985, Inhibition of hydroxyapatite formation in collagen gels by chondroitin sulphate: Biochemistry Journal, v. 228, p. 463–469.

Kniep, R., and Busch, S., 1996, Biomimetic growth and self-assembly of fluorapatite aggregates by diffusion into denatured collagen matrices: Angewandte Chemie (International edition in English), v. 108, no. 22, p. 2623–2626.

Kniep, R., and Simon, P., 2007, Fluorapatite-gelatine-nanocomposites: Self-organized morphogenesis, real structure and relations to natural hard materials: Topics in Current Chemistry, v. 270, no. July 2006, p. 73–125, doi: 10.1007/128.

Morse, J.W., 1974, Dissolution kinetics of calcium carbonate in sea water: III, a new method for the study of carbonate reaction kinetics: American Journal of Science, v. 274, no. 2, p. 97–107.

Silverman, L., and Boskey, A.L., 2004, Diffusion systems for evaluation of biomineralization: Calcified Tissue International, v. 75, no. 6, p. 494–501, doi: 10.1007/s00223-004-0019-y.

Stern, K.H., 1954, The Liesegang phenomenon: Chemical Reviews, p. 79–99.

Tomson, M.B., and Nancollas, G.H., 1978, Mineralization Kinetics: A constant composition approach: Science, v. 200, no. 4345, p. 1059–1060.

Tripathi, A., Srivastava, G. ji, Srivastava, S., and Das, I., 2015, Liesegang patterns, growth kinetics, inhibition and dissolution of calcium phosphate: A constituent of renal stone: Chemical Biology Letters, v. 2, no. 2, p. 30–40.

Whistler, R.L., 1973, Solubility of polysaccharides and their behavior in solution, *in* Isbell, H.S. ed., Carbohydrates in Solution, American Chemical Society, Washington, D. C., p. 242–255.

Wingender, J., Neu, T.R., and Flemming, H.-C. (Eds.), 1999, Microbial Extracellular Polymeric Substances – Characterization, Structure and Function: Springer-Verlag, Berlin.

— DISCUSSION —

Biomineralization

Biomineralization, the precipitation of minerals under the influence of biological agents, can be effected directly by (under the control of) organisms (biologically controlled mineralization), or indirectly, as a result of biologically induced changes in ambient conditions (biologically induced mineralization). One of the ways in which these are distinguished is by the utility or function of the resulting mineral material, with biologically induced mineralization providing little apparent metabolic function (other than possible protection against predation) and biologically controlled mineralization serving cellular functions (such as that provided by magnetosomes, support structures and enclosures, for instance) (Bazylinski and Frankel, 2003; Frankel and Bazylinski, 2003).

The influence of microbes on their surroundings, vis-á-vis the fact that they expel protons and can thereby raise nearby ambient pH, has been recognized since Peter Mitchell's elucidation of the chemiosmotic process in which the ejection of protons facilitates the phosphorylation of ADP to ATP (Mitchell, 1961; Mitchell, 1978).

Complex exoskeletal material of invertebrates, as well as vertebrate bones and teeth are clearly mineralized and formed to a pattern, under biological direction. Indeed, intentional precipitation of calcium-phosphate minerals in vertebrates, such as human bone and tooth formation and growth, are tightly controlled by biologically-produced factors, as generally human blood and saliva are supersaturated with respect to apatite, and yet we have not all turned to stone. However, various human calcium-phosphate pathologies, such as kidney stones and atherosclerosis, do occur and are the concern of a significant amount of medical research.

Murshed et al. have investigated some vertebrate proteins that promote mineralization – as well as others which prevent it – seeking to determine the biological controls on mineralization of extracellular matrices (Murshed et al., 2004). In the case of biologically-controlled mineralization, this generally proceeds within the framework of an organic matrix and requires that a space be created/set aside in which to form the mineral (Veis, 2003) or voids, as in the coccoliths (Young and Henriksen, 2003).

Hence, the significance of matrix geometry and charge is recognized in biologically mediated mineralization. It is reasonable to expect a similar impact by coincidental matrix materials such as microbial EPS.

Role of EPS, generally, and in phosphogenesis

With a discussion on the role of EPS in influencing the precipitation and/or morphology of calcium-phosphate minerals, this dissertation comes full circle. The role of microbes in the formation of phosphorites has long been suspected. The degree to which this can be closely attributed to active microbial metabolism, such as polyphosphate accumulation and expulsion or the production and presence of EPS, or more indirectly, as by induction of the conditions required to set an iron redox pump into play, continues to be explored. The arc of my research has moved toward exploring the potential role of polymeric matrices such as EPS on the precipitation of calcium-phosphate minerals. We are likely to find that in the natural world the truth comprises a complex interplay of factors.

Chapter 6

—

Conclusion

Overview

Our understanding of ancient Earth processes is necessarily hampered by the fact that we have no direct experience of early Earth. Yet we seek to understand the progression and processes that have resulted in both our habitable planet and the organisms that inhabit it, as well as the ways in which the biosphere and geosphere influence and impact each other. Armed with ever-increasing knowledge of chemical, mineralogical and biological processes and ongoing advances in technology, we venture into worlds removed from us by time, space and/or (human) habitability such as the ancient past, distant planets, and only recently accessible Earth environments like the seabed and the deep lithosphere. As we learn more about how life persists in these environments, we gain tools to help us understand the current state of the Earth in a broad geological, biological and environmental context. And as we become more knowledgeable in the ways in which geology and biology influence each other we become increasingly able to assess the likelihood of life in environments previously not thought to be capable of supporting life: other planets, as well as locations on Earth previously thought to be sterile of life.

Project recap

The projects described in this thesis represent different approaches to the general issue of microbe-mineral relationships in P-bearing rock.

Knowledge gained through this work contributes incremental advances in our understanding of microbial metabolic processes, taphonomic processes, and the co-evolution of Earth's geosphere and biosphere, and may be of interest to researchers in a variety of fields. Today, the mining of phosphate rock for use in fertilizers is resulting in the diminishing of mineable reserves, raising the possibility of an eventual 'phosphorus crisis.' Insight into the mechanisms of apatite precipitation may help us interpret the potential of such a crisis.

In the first project, I characterized microfossils of a ~2 Ga stromatolitic phosphate rock, in the wake of Earth's Great Oxidation Event (GOE.) Phosphorites of this age are relatively rare, as are phosphatic stromatolites themselves. The interpretation presented here offers a possible role of microbes in the formation of this unusual stromatolitic formation, and may suggest a 'missing

link' between these phosphatic stromatolites and an evolutionary adaptation of microbial life to the rise of oxygen.

The aim of the second project was to investigate the authenticity of putative textural and morphological biosignatures in sedimentary apatite. This investigation uncovered a new, not previously described phosphatic morphology resembling that of an embryo. This result joins a number of other abiotic morphologies that may be mistaken as having been produced biologically, and contributes to the ongoing discussion of criteria for the determination of microfossil biogenicity.*

This project also launched a search for the most advantageous apparatus and protocol by which to explore details of mineral nucleation and precipitation over time and in the context of a polymeric matrix, such as microbial EPS. This search became a long-term and iterative third project.

Each of these projects provide insight into some aspect of the mechanisms by which microbes and/or microbially-created polymeric macromolecules can induce and/or influence the precipitation of calcium-phosphate minerals. More broadly, the apparatus described in chapter 5 may be of use in a number of fields ranging across geology, paleontology and mineralogy, to medicine and civil/environmental engineering.

Why it matters

The cycling of phosphorus impacts the human world, as well as the natural. The necessity of feeding a growing population has hastened the use of phosphorus-based fertilizers for the purpose of increasing crop yields, resulting in a drawdown of phosphate-rich rock reserves and the subsequent spreading of it into a thin layer over agricultural land, diluting it to the point of irretrievability. At the same time, farmland runoff and the commercialization of P-based detergents have resulted in a diversion of P to the hydrosphere, where accelerated influx of P has often resulted in lake eutrophication and ocean 'dead zones,' altering natural biological rhythms and balances (Smil, 2000).†

Just as carbon is increasingly recognized as a vital element that cycles between the geosphere and the biosphere, so too is P. Like carbon, P is an element that is absolutely required by all living

---

* *See also Appendix B, "Assessing microfossil biogenicity."*
† *See also Appendix C, "A brief comment on anthropogenic impacts on the P cycle."*

organisms on Earth. And like carbon, flux rates in the global P cycle are undergoing unequivocal anthropomorphic alterations as increasingly more P is diverted from the geosphere to the biosphere.

Unlike carbon, P does not (appreciably) exist in the gaseous state, restricting its global cycle to the solid and aqueous phases. And although we extract energy from geologically-based (hydro)carbons to drive non-biological processes such as gasoline powered engines that release the most oxidized form of carbon (CO_2) to the atmosphere, phosphate chemical energy is largely restricted to the biomolecular level so that its anthropogenic deflection to the biosphere is basically reflected in increased global biomass.

The net impact of the anthropogenic use of (hydro)carbons is to preferentially transfer carbon from an arguably inert solid state pool to the gaseous atmospheric pool, where it influences the global heat budget. On a practical level, this impacts dynamic global weather patterns and ecological systems as organisms adapt to these changes through evolutionary and geographical shifts. Unlike carbon, anthropogenic influences on the global P cycle are ultimately reflected not in atmospheric load, but in the limits of biomass. Over time, the Earth system has undergone an inexorable transformation of matter from the geosphere to the biosphere, as matter is taken from the geosphere and incorporated into the biomass of living organisms. If we ever do deplete global P resources, we may have arrived at a point at which the macroscopic, plant and animal biosphere will have reached its expansion limit, and it may be left to microorganisms to reestablish a balance in the flux of P between the geosphere and the biosphere.

Since P is being mined at an increasing rate in the face of a growing global population, the need for a clear understanding of the phosphorus cycle and the state of P reserves seems obvious. Though projections vary as to when, we may indeed eventually experience a global phosphorus crisis. Insight into the mechanisms of apatite precipitation may enhance our understanding of the extent and rate of global phosphorus cycling, making us better able to interpret the trajectory of any imminent phosphorus drawdown. It may also enable us to better forestall such an eventuality. An understanding of the role of microbes and biological polymers in apatite precipitation may lead to better capture technologies to enhance the recycling of P instead of allowing it to stream into the ocean where it will ultimately be sequestered in an inaccessible mineral phase, arguably inaccessible for millions of years.

In addition, new knowledge advances our understanding of taphonomy, the evolution of Earth's geosphere and biosphere, and microbial metabolic processes at the microbe-mineral interface, including the non-periodic pulses of phosphate rock production.

In the meantime, science and technology continue to advance. Medical researchers are investigating the influence of biopolymers in P-related pathophysiology and bone, dental and cardiovascular medicine. Advances in genomics may one day lead to the engineering of a bacterial strain that can cheaply, efficiently and reliably extract phosphate from farm waste locally and convert it into a form that can be used as fertilizer at the same location. And recognizing the need for more access to phosphate resources, there are now active seabed mining projects involved in the harvesting of unconsolidated phosphate deposits, as off New Zealand and Namibia, though the environmental the impact of this remains to be seen (Grundlehner et al., 2012; Midgley, 2012).

– 30 –

Dissertation references

Achbergerova, L., and Nahalka, J., 2011, Polyphosphate - an ancient energy source and active metabolic regulator.: Microbial cell factories, v. 10, no. 1, p. 63, doi: 10.1186/1475-2859-10-63.

Ahmad, T., and Rajamani, V., 1991, Geochemistry and petrogenesis of the basal Aravalli volcanics near Nathdwara, Rajasthan, India: Precambrian Research, v. 49, p. 185–204.

Ahmad, T., and Tarney, J., 1994, Geochemistry and petrogenesis of late Archaean Aravalli volcanics, basement enclaves and granitoids, Rajasthan: Precambrian Research, v. 65, p. 1–23.

Antal, T., Droz, M., Magnin, J., and Rácz, Z., 1999, Formation of Liesegang patterns: A spinodal decomposition scenario: Physical Review Letters, v. 83, p. 2880–2883, doi: http://dx.doi.org/10.1103/PhysRevLett.83.2880.

Ashley, K., Cordell, D., and Mavinic, D., 2011, A brief history of phosphorus: from the philosopher's stone to nutrient recovery and reuse.: Chemosphere, v. 84, no. 6, p. 737–46, doi: 10.1016/j.chemosphere.2011.03.001.

Awramik, S.M., Schopf, J.W., and Walter, M.R., 1983, Filamentous fossil bacteria from the Archean of Western Australia: Precambrian Research, v. 20, p. 357–374.

Azmi, R.J., Joshi, D., Tiwari, B.N., Joshi, M.N., and Srivastava, S.S., 2008, A synoptic view on the current discordant geo- and biochronological ages of the Vindhyan Supergroup, central India: Himalayan Geology, v. 29, no. 2, p. 177–191.

Bailey, J.V., 2008, New perspectives on ancient microbes and microbialites: from isotopes to immunology: University of Southern California.

Bailey, J., Corsetti, F., Greene, S., Crosby, C., Liu, P., and Orphan, V., 2013, Filamentous sulfur bacteria preserved in modern and ancient phosphatic sediments: implications for the role of oxygen and bacteria in phosphogenesis: Geobiology, v. 11, no. 5, p. 397–405, doi: 10.1111/gbi.12046.

Bailey, J. V., Joye, S.B., Kalanetra, K.M., Flood, B.E., and Corsetti, F.A., 2006, Evidence of giant sulphur bacteria in Neoproterozoic phosphorites: Nature, v. 445, no. 7124, p. 1–4, doi: 10.1038/nature05457.

Bailey, J. V, Joye, S.B., Kalanetra, K.M., Flood, B.E., and Corsetti, F. a, 2007, Evidence of Giant Sulphur Bacteria in Neoproterozoic Phosphorites.: Nature, v. 445, no. 7124, p. 198–201, doi: 10.1038/nature05457.

Banfield, J.F., Welch, S.A., Zhang, H., Ebert, T.T., and Penn, R.L., 2000, Aggregation-based crystal growth and microstructure development in natural iron oxyhydroxide biomineralization products: Science, v. 289, p. 751–754, doi: 10.1126/science.289.5480.751.

Barghoorn, E.S., and Tyler, S.A., 1965, Microorganisms from the Gunflint Chert: Science, v. 147, no. 3658, p. 563–577.

Baturin, G.N., 1982, Developments in Sedimentology 33: Phosphorites on the Sea Floor: Elsevier Scientific Publishing Company, Amsterdam.

Bazylinski, D.A., and Frankel, R.B., 2003, Biologically controlled mineralization in Prokaryotes, *in* Dove, P.M., De Yoreo, J.J., and Weiner, S. eds., Reviews in Mineralogy & Geochemistry Volume 54 - Biomineralization, Mineralogical Society of America, Washington, D. C., p. 217–247.

Becker, A., Becker, W., Marxen, J.C., and Epple, M., 2003, In-vitro crystallization of calcium carbonate in the presence of biological additives – Comparison of the ammonium carbonate method with double-diffusion techniques: Journal for Inorganic and General Chemistryournal for Inorganic and General Chemistry, v. 629, p. 2305–2311, doi: 10.1002/zaac.200300229.

Bedau, M.A., 2003, Artificial life: organization, adaptation and complexity from the bottom up: Trends in Cognitive Science, v. 7, no. 11, p. 505–512, doi: 10.1016/j.tics.2003.09.012.

Bengtson, S., Belivanova, V., Rasmussen, B., and Whitehouse, M., 2009, The controversial "Cambrian" fossils of the Vindhyan are real but more than a billion years older.: Proceedings of the National Academy of Sciences of the United States of America, v. 106, no. 19, p. 7729–34, doi: 10.1073/pnas.0812460106.

Bengtson, S., and Budd, G., 2004, Comment on "Small bilaterian fossils from 40 to 55 million years befor the Cambrian": Science, v. 306, no. November, p. 1291.

Bengtson, S., Cunningham, J.A., Yin, C., and Donoghue, P.C.J., 2012, A merciful death for the "earliest bilaterian," Vernanimalcula: Evolution & Development, v. 14, no. 5, p. 421–427, doi: 10.1111/j.1525-142X.2012.00562.x.

Bengtson, S., and Zhao, Y., 1997, Fossilized Metazoan embryos from the earliest Cambrian: Science, v. 277, no. 12 September, p. 1645–1648, doi: 10.1126/science.277.5332.1645.

Benitez-Nelson, C.R., 2000, The biogeochemical cycling of phosphorus in marine systems: Earth-Science Reviews, v. 51, no. 1-4, p. 109–135, doi: 10.1016/S0012-8252(00)00018-0.

Benner, S.A., 2010, Defining life: Astrobiology, v. 10, no. 10, p. 1021–30, doi: 10.1089/ast.2010.0524.

Bennett, S.A., Toner, B.M., Barco, R., and Edwards, K.J., 2014, Carbon adsorption onto Fe oxyhydroxide stalks produced by a lithotrophic iron-oxidizing bacteria: Geobiology, v. 12, p. 146–156, doi: 10.1111/gbi.12074.

Benzerara, K., Menguy, N., Guyot, F., Dominici, C., and Gillet, P., 2003, Nanobacteria-like calcite single crystals at the surface of the Tataouine meteorite: PNAS, v. 100, no. 13, p. 7438–7442, doi: 10.1073_pnas.0832464100.

Benzerara, K., Menguy, N., Guyot, F., Skouri, F., DeLuca, G., Barakat, M., and Heulin, T., 2004, Biologically controlled precipitation of calcium phosphate by Ramlibacter tataouinensis: Earth and Planetary Science Letters, v. 228, p. 439 – 449, doi: 10.1016/j.epsl.2004.09.030.

Berner, R.A., 1965, Activity coefficients of bicarbonate , carbonate and calcium ions in sea water: Geochimica et Cosmochimica Acta, v. 29, p. 947–965.

Bhowmik, S.K., Bernhardt, H., and Dasgupta, S., 2010, Grenvillian age high-pressure upper amphibolite-granulite metamorphism in the Aravalli-Delhi Mobile Belt , Northwestern India : New evidence from monazite chemical age and its implication: Precambrian Research, v. 178, no. 1-4, p. 168–184, doi: 10.1016/j.precamres.2010.02.015.

Bolhuis, H., Palm, P., Wende, A., Falb, M., Rampp, M., Rodríguez-Valera, F., Pfeiffer, F., and Oesterhelt, D., 2006, The genome of the square archaeon Haloquadratum walsbyi: life at the limits of water activity: BMC Genomics, v. 7, no. 1, p. 169–181, doi: 10.1186/1471-2164-7-169.

Bourbin, M., Gourier, D., Derenne, S., Binet, L., Du, Y. Le, Westall, F., Kremer, B., and Gautret, P., 2013, Dating Carbonaceous Matter in Archean Cherts by Electron Paramagnetic Resonance: Astrobiology, v. 13, no. 2, doi: 10.1089/ast.2012.0855.

Bouwman, A.F., Beusen, A.H.W., and Billen, G., 2009, Human alteration of the global nitrogen and phosphorus soil balances for the period 1970–2050: Global Biogeochemical Cycles, v. 23, no. December, p. 1–16, doi: 10.1029/2009GB003576.

Brasier, M.D., Green, O.R., Jephcoat, A.P., Kleppe, A.K., Kranendonk, M.J. Van, Lindsay, J.F., Steele, A., and Grassineauk, N. V, 2002, Questioning the evidence for Earth ' s oldest fossils: Nature, v. 416, no. March.

Brasier, M.D., Green, O.R., Lindsay, J.F., McLoughlin, N., Steele, A., and Stoakes, C., 2005, Critical testing of Earth's oldest putative fossil assemblage from the ~3.5 Ga Apex chert, Chinaman Creek, Western Australia: Precambrian Research, v. 140, p. 55–102, doi: 10.1016/j.precamres.2005.06.008.

Briggs, D.E., and Kear, a J., 1993, Fossilization of soft tissue in the laboratory.: Science (New York,

N.Y.), v. 259, no. 5100, p. 1439–42, doi: 10.1126/science.259.5100.1439.

Brock, J., and Schulz-Vogt, H.N., 2011, Sulfide induces phosphate release from polyphosphate in cultures of a marine Beggiatoa strain: The ISME journal, v. 5, no. 3, p. 497–506, doi: 10.1038/ismej.2010.135.

Brunner, P.H., and Rechberger, H., 2002, Anthropogenic metabolism and environmental legacies, *in* Douglas, I. ed., Encyclopedia of Global Environmental Change, John Wiley & Sons, Chichester, p. 54–72.

Buick, R., 2010, Ancient acritarchs: Nature, v. 463, no. February, p. 885–886.

Buick, R., 1990, Microfossil recognition in Archean rocks: An appraisal of spheroids and filaments from a 3500 m.y. old chert-barite unit at North Pole, Western Australia: Palaios, v. 5, no. 5, p. 441–459.

Buick, I.S., Allen, C., Pandit, M., Rubatto, D., and Hermann, J., 2006, The Proterozoic magmatic and metamorphic history of the Banded Gneiss Complex, central Rajasthan, India: LA-ICP-MS U–Pb zircon constraints: Precambrian Research, v. 151, no. 1-2, p. 119–142, doi: 10.1016/j.precamres.2006.08.006.

Burns, D.G., Janssen, P.H., Itoh, T., Kamekura, M., Li, Z., Jensen, G., Rodríguez-Valera, F., Bolhuis, H., and Dyall-smith, M.L., 2007, Haloquadratum walsbyi gen. nov., sp. nov., the square haloarchaeon of Walsby, isolated from saltern crystallizers in Australia and Spain: International Journal of Systematic and Evolutionary Microbiology, v. 57, p. 387–392, doi: 10.1099/ijs.0.64690-0.

Busch, S., Dolhaine, H., DuChesne, A., Heinz, S., Hochrein, O., Laeri, F., Podebrad, O., Vietze, U., Weiland, T., and Kniep, R., 1999, Biomimetic morphogenesis of fluorapatite-gelatin composites: Fractal growth, the question of intrinsic electric fields, core/shell assemblies, hollow spheres and reorganization of denatured collagen: European Journal of Inorganic Chemistry, v. 1999, no. 10, p. 1643–1653, doi: 143421948/99/101021643.

Butterfield, N.J., 2000, Bangiomorpha pubescens n. gen., n. sp.: Implications for the evolution of sex, multicellularity, and the Mesoproterozoic/ Neoproterozoic radiation of eukaryotes: Paleobiology, v. 26, no. 3, p. 386–404.

Cady, S.L., Farmer, J.D., Grotzinger, J.P., Schopf, J.W., and Steele, A., 2003, Morphological biosignatures and the search for life on Mars: Astrobiology, v. 3, no. 2, p. 351–368.

Canfield, D.E., 2006, Gas with an ancient history: Nature, v. 440, no. March, p. 426–427.

Canfield, D.E., 2014, Oxygen – A Four Billion Year History: Princeton University Press, Princeton.

Canfield, D.E., Habicht, K.S., and Thamdrup, B., 2000, The Archean sulfur cycle and the early history of atmospheric oxygen: Science, v. 288, no. April, p. 658–661.

Chalmers, G.K., 1936, Sir Thomas Browne, True scientist: Osiris, v. 2, p. 28–79.

Chan, C.S., Fakra, S.C., Edwards, D.C., Emerson, D., and Banfield, J.F., 2009, Iron oxyhydroxide mineralization on microbial extracellular polysaccharides: Geochimica et Cosmochimica Acta, v. 73, no. 13, p. 3807–3818, doi: 10.1016/j.gca.2009.02.036.

Chan, C.S., De Stasio, G., Welch, S.A., Girasole, M., Frazer, B.H., Nesterova, M. V, Fakra, S., and Banfield, J.F., 2004, Microbial polysaccharides template assembly of nanocrystal fibers: Science, v. 303, no. 2004, p. 1656–1658, doi: 10.1126/science.1092098.

Chauhan, D.S., 1979, Phosphate-bearing stromatolites of the Precambrian Aravalli phosphorite deposits of the Udaipur region, their environmental significance and genesis of phosphorite: Precambrian Research, v. 8, p. 95–126.

Chen, J.-Y., Bottjer, D.J., Davidson, E.H., Li, G., Gao, F., Cameron, R.A., Hadfield, M.G., Xian, D.-C., Tafforeau, P., Jia, Q.-J., Sugiyama, H., and Tang, R., 2009, Phase contrast synchrotron X-ray microtomography of Ediacaran (Doushantuo) metazoan microfossils: Phylogenetic diversity and evolutionary implications: Precambrian Research, v. 173, p. 191–200, doi:

10.1016/j.precamres.2009.04.004.

Chen, J., Bottjer, D.J., Oliveri, P., Dornbos, S.Q., Gao, F., Ruffins, S., Chi, H., Li, C.-W., and Davidson, E.H., 2004, Small bilaterian fossils from 40 to 55 million years before the Cambrian: Science, v. 305, p. 218–222.

Chen, J.-Y., Oliveri, P., Li, C.-W., Zhou, G.-Q., Gao, F., Hagadorn, J.W., Peterson, K.J., and Davidson, E.H., 2000, Precambrian animal diversity: Putative phosphatized embryos from the Doushantuo formation of China: Proceedings of the National Academy of Sciences of the United States of America, v. 97, no. 9, p. 4457–62.

Chen, L., Xiao, S., Pang, K., Zhou, C., and Yuan, X., 2014, Cell differentiation and germ-soma separation in Ediacaran animal embryo-like fossils: Nature, v. 516, no. 7530, p. 238–241, doi: 10.1038/nature13766.

Chi, H., 2009, The apatite crystal in fossil cells with fluorescence: Crystal Growth, v. 9, no. 2, p. 676–681, doi: 10.1021/cg7008539.

Choudhuri, R., and Roy, A.B., 1986, Proterozoic and Cambrian phosphorites – deposits: Jhamarkotra, Rajasthan, India, *in* Cook, P.J. and Shergold, J.H. eds., Phosphate deposits of the world: Vol 1 - Proterozoic and Cambrian phosphorites, Cambridge University Press, Cambridge, p. 202–219.

Cloud, P., 1976, Beginnings of biospheric evolution and their biogeochemical consequences: Paleobiology, v. 2, no. 4, p. 351–387.

Cloud, P.E.J., and Abelson, P.H., 1961, Woodring Conference on Major Biological Innovations and the Geologic Record – National Academy of Sciences Conference: Proceedings of the National Academy of Sciences, v. 47, no. 11, p. 1705–1712.

Collins, M.D., 1982, Reclassification of Bacterionema matruchotii (Mendel) in the Genus Corynebacterium, as Corynebacterium matruchotii comb. nov.: Zentralblatt für Bakteriologie, Mikrobiologie, und Hygiene, v. 3, no. 3, p. 364–367.

Cook, P.J., and Shergold, J.H., 1984, Phosphorus, phosphorites and skeletal evolution at the Precambrian-Cambrian boundary: Nature, v. 308, p. 231–236.

Cordell, D., Drangert, J.-O., and White, S., 2009, The story of phosphorus: Global food security and food for thought: Global Environmental Change, v. 19, p. 292–305, doi: 10.1016/j.gloenvcha.2008.10.009.

Corliss, J.B., Dymond, J., Gordon, L.I., Edmond, J.M., von Herzen, R.P., Ballard, R.D., Green, K., Williams, D., Bainbridge, A., Crane, K., and van Andel, T.H., 1979, Submarine thermal springs on the Galápagos Rift: Science, v. 203, no. 4385, p. 1073–1083, doi: 10.1126/science.203.4385.1073.

Cosmidis, J., and Templeton, A.S., 2016, Self-assembly of biomorphic carbon/sulfur microstructures in sulfidic environments: Nature Communications, v. 7, p. 1–9, doi: 10.1038/ncomms12812.

Crosby, C.H., and Bailey, J. V, 2017, Technical note: an economical apparatus for the observation and harvest of mineral precipitation experiments with light microscopy: Biogeosciences, v. 14, no. 8, p. 2151–2154, doi: 10.5194/bg-14-2151-2017.

Crowe, S. a, Døssing, L.N., Beukes, N.J., Bau, M., Kruger, S.J., Frei, R., and Canfield, D.E., 2013, Atmospheric oxygenation three billion years ago: Nature, v. 501, no. 7468, p. 535–539, doi: 10.1038/nature12426.

Cunningham, J.A., Thomas, C.-W., Bengtson, S., Kearns, S.L., Xiao, S., Marone, F., Stampanoni, M., and Donoghue, P.C.J., 2012, Distinguishing geology from biology in the Ediacaran Doushantuo biota relaxes constraints on the timing of the origin of bilaterians: Proceedings of the Royal Society B, v. 279, no. 1737, p. 2369–76, doi: 10.1098/rspb.2011.2280.

Cunningham, J.A., Thomas, C.-W., Bengtson, S., Marone, F., Stampanoni, M., Turner, F.R., Bailey, J. V, Raff, R.A., Raff, E.C., and Donoghue, P.C.J., 2011, Experimental taphonomy of giant sulphur bacteria:

implications for the interpretation of the embryo-like Ediacaran Doushantuo fossils: Proceedings of the Royal Society B, v. 279, no. December, p. 1857–1864, doi: 10.1098/rspb.2011.2064.

Cunningham, J.A., Vargas, K., Yin, Z., Bengtson, S., and Donoghue, P.C.J., 2017, The Weng'an Biota (Doushantuo Formation): an Ediacaran window on soft-bodied and multicellular microorganisms: Journal of the Geological Society, v. 2016, no. 142, p. published online, doi: https://doi.org/10.1144/jgs2016-142.

Decho, A.W., 1990, Microbial exoploymer secretions in ocean environments: Their role(s) in food webs and marine processes: Oceanography and Marine Biology Annual Review, v. 28, p. 73–153.

Diaz, J., Ingall, E., Benitez-Nelson, C., Paterson, D., de Jonge, M.D., McNulty, I., and Brandes, J.A., 2008, Marine polyphosphate: A key player in geologic phosphorus sequestration: Science, v. 320, no. 2 May 2008, p. 652–655, doi: 10.1126/science.1151751.

Dold, B., 2014, Evolution of acid mine drainage formation in sulphidic mine tailings: Minerals, v. 4, p. 621–641, doi: 10.3390/min4030621.

Dong, X., Donoghue, P.C.J., Cheng, H., and Liu, J., 2004, Fossil embryos from the Middle and Late Cambrian period of Hunan, south China: Nature, v. 427, no. January, p. 237–240, doi: 10.1038/nature02221.1.

Donoghue, P.C.J., Bengtson, S., Dong, X., Gostling, N.J., Huldtgren, T., Cunningham, J.A., Yin, C., Yue, Z., Peng, F., and Stampanoni, M., 2006a, Synchrotron X-ray tomographic microscopy of fossil embryos: Nature, v. 442, no. August, p. 680–683, doi: 10.1038/nature04890.

Donoghue, P.C.J., Kouchinsky, Ã.A., Waloszek, D., Bengtson, S., Dong, X., Val'kov, A.K., Cunningham, J.A., and Repetski, J.E., 2006b, Fossilized embryos are widespread but the record is temporally and taxonomically biased: Evolution & Development, v. 8, no. 2, p. 232–238.

Dornbos, S.Q., 2011, Phosphatization through the Phanerozoic, *in* Allison, P.A. and Bottjer, D.J. eds., Taphonomy: Process and Bias Through Time, Topics in Geobiology 32, Springer Science+Business Media LLC, New York, p. 435–456.

Dornbos, S.Q., Bottjer, D.J., Chen, J.-Y., and Oliveri, P., 2005, Precambrian animal life: Taphonomy of phosphatized metazoan embryos from southwest China: Lethaia, v. 38, p. 101–109, doi: 10.1080/00241160510013187.

Dronamraju, K.R., 1999, Schrodinger and the origins of molecular biology: Genetics, v. 153, p. 1071–1076.

Duckworth, O.W., Holmström, S.J.M., Peña, J., and Sposito, G., 2009, Biogeochemistry of iron oxidation in a circumneutral freshwater habitat: Chemical Geology, v. 260, no. 3-4, p. 149–158, doi: 10.1016/j.chemgeo.2008.08.027.

Dunham-Cheatham, S., Rui, X., Bunker, B., Menguy, N., Hellmann, R., and Fein, J., 2011, The effects of non-metabolizing bacterial cells on the precipitation of U, Pb and Ca phosphates: Geochimica et Cosmochimica Acta, v. 75, p. 2828–2847, doi: 10.1016/j.gca.2011.02.030.

Dupraz, C., Reid, R.P., Braissant, O., Decho, A.W., Norman, R.S., and Visscher, P.T., 2009, Processes of carbonate precipitation in modern microbial mats: Earth Science Reviews, v. 96, no. 3, p. 141–162, doi: 10.1016/j.earscirev.2008.10.005.

Dworkin, M., 2012, Sergei Winogradsky: a founder of modern microbiology and the first microbial ecologist: FEMS Microbiology Reviews, v. 36, p. 364–379, doi: 10.1111/j.1574-6976.2011.00299.x.

Edwards, K.J., Bach, W., McCollom, T.M., and Rogers, D.R., 2004, Neutrophilic iron-oxidizing bacteria in the ocean: Their habitats, diversity, and roles in mineral deposition, rock alteration, and biomass production in the deep-sea: Geomicrobiology Journal, v. 21, p. 393–404, doi: 10.1080/01490450490485863.

Ehrlich, H.L., 1999, Microbes as Geologic Agents : Their Role in Mineral Formation Microbes as Geologic Agents : Their Role: Geomicrobiology Journal, v. 16, no. 2, p. 135–153.

Emerson, D., and Ghiorse, W.C., 1993, Ultrastructure and chemical composition of the sheath of Leptothrix discophora SP-6: Journal of Bacteriology, v. 175, no. 24, p. 7808–7818, doi: 0021-9193/93/247808.

Emerson, D., and Weiss, J. V, 2004, Bacterial iron oxidation in circumneutral freshwater habitats: Findings from the field and the laboratory: Geomicrobiology Journal, v. 21, p. 405–414, doi: 10.1080/01490450490485881.

Emerson, D., Worden, R.M., and Breznak, J.A., 1994, A diffusion gradient chamber for studying microbial behavior and separating microorganisms: Applied and Environmental Microbiology, v. 60, no. 4, p. 1269–1278, doi: 0099-2240/94.

Ennever, J., and Creamer, H., 1967, Guest Editorial: Microbiologic Calcification: Bone Mineral and Bacteria: Calcified Tissue Research, v. 1, p. 87–93.

Ennever, J., Vogel, J.J., and Streckfuss, J.L., 1974, Calcification by Escherichia coli: Journal of Bacteriology, v. 119, no. 3, p. 1061–1062.

Essington, M.E., 2004, Soil and Water Chemistry – An integrative approach: CRC Press, Boca Raton, Fla.

Falkowski, P.G., 2006, Tracing oxygen's imprint on Earth's metabolic evolution: Science, v. 311, p. 1724–1725, doi: 10.1126/science.1125937.

Farquhar, J., Bao, H., and Theimens, M., 2000, Atmospheric influence of Earth's earliest sulfur cycle: Science, v. 289, p. 756–758.

Faure, G., 1991, Principles and Applications of Geochemistry: Prentice Hall, Upper Saddle River, N.J.

Filippelli, G.M., 2008, The global phosphorus cycle: Past, present, and future: Elements, v. 4, p. 89–96, doi: 10.2113/GSELEMENTS.4.2.89.

Finsinger, K., Scholz, I., Serrano, A., Morales, S., Uribe-Lorio, L., Mora, M., Sittenfeld, A., Weckesser, J., and Hess, W.R., 2008, Characterization of true-branching cyanobacteria from geothermal sites and hot springs of Costa Rica: Environmental Microbiology, v. 10, no. 2, p. 460–73, doi: 10.1111/j.1462-2920.2007.01467.x.

Flannery, M.B., Stott, A.W., Briggs, D.E.G., and Evershed, R.P., 2001, Chitin in the fossil record: identification and quantification of d-glucosamine: Organic Geochemistry, v. 32, p. 745–754.

Flemming, H.-C., Neu, T.R., and Wozniak, D.J., 2007, The EPS Matrix: The "House of biofilm cells": Journal of Bacteriology, v. 189, no. 22, p. 7945–7947, doi: 10.1128/JB.00858-07.

Flugel, E., 2010, Microfacies of carbonate rocks – analysis, interpretation and application: Springer-Verlag, Berlin.

Forterre, P., 2010, Defining life: The virus viewpoint: Origins of Life and Evolution of the Biosphere, v. 40, p. 151–160, doi: 10.1007/s11084-010-9194-1.

Frankel, R.B., and Bazylinski, D.A., 2003, Biologically induced mineralization by bacteria, *in* Dove, P.M., De Yoreo, J.J., and Weiner, S. eds., Reviews in Mineralogy & Geochemistry Volume 54 - Biomineralization, Mineralogical Society of America, Washington, D. C., p. 96–114.

Gachter, R., Meyer, J.S., and Mares, A., 1988, Contribution of bacteria to release and fixation of phosphorus in lake sediments: Limnology and Oceanography, v. 33, no. 6, p. 1542–1558.

Garcia Ruiz, J.M., Carnerup, A., Christy, A.G., Welham, N.J., and Hyde, S.T., 2002, Morphology: An ambiguous indicator of biogenicity: Astrobiology, v. 2, no. 3, p. 353–369.

Garcia-Ruiz, J.M., 1994, Inorganic self-organization in Precambrian cherts: Origins of Life and Evolution of the Biosphere, v. 24, p. 451–467.

García-ruiz, J.M., Melero-García, E., and Hyde, S.T., 2009, Morphogenesis of self-assembled microcrystalline materials of barium carbonate and silica: Science, v. 323, no. 16 January, p. 362–365, doi: 10.1126/science.1165349.

Gest, H., and Blankenship, R.E., 2004, Time line of discoveries: anoxygenic bacterial photosynthesis: Photosynthesis Research, v. 80, p. 59–70.

Gibson, D.G., Glass, J.I., Lartigue, C., Noskov, V.N., Chuang, R., Algire, M.A., Benders, G.A., Montague, M.G., Ma, L., Moodie, M.M., Merryman, C., Vashee, S., Krishnakumar, R., Assad-Garcia, N., et al., 2010, Creation of a bacterial cell controlled by a chemically synthesized genome: Science, v. 329, no. July, p. 52–56, doi: 10.1126/science.1190719.

Glenn, C.R., Follmi, K.B., Riggs, S.R., Baturin, G.N., Grimm, K.A., Trappe, J., Abed, A.M., Galli-Olivier, C., Garrison, R.E., Ilyin, A. V., Jehl, C., Rohrlich, V., Sadaqah, R.M.Y., Schidlowski, M., et al., 1994, Phosphorus and Phosphorites: Sedimentology and Environments of Formation: Eclogae Geologicae Helvetiae, v. 87, no. 3, p. 747–788.

Goldhammer, T., Brüchert, V., Ferdelman, T.G., and Zabel, M., 2010, Microbial sequestration of phosphorus in anoxic upwelling sediments: Nature Geoscience, v. 3, no. 8, p. 557–561, doi: 10.1038/ngeo913.

Golubic, S., Radtke, G., and Campion-Alsumard, T. Le, 2005, Endolithic fungi in marine ecosystems: Trends in Microbiology, v. 13, no. 5, p. 229–235, doi: 10.1016/j.tim.2005.03.007.

Goss, C.J., 1987, The kinetics and reaction mechanism of the goethite to hematite transformation: Mineralogical Magazine, v. 51, no. September, p. 437–51.

De Gregorio, B., and Sharp, T.G., 2006, The structure and distribution of carbon in 3.5 Ga Apex chert: Implications for the biogenicity of Earth's oldest putative microfossils: American Mineralogist, v. 91, p. 784–789, doi: 10.2138/am.2006.2149.

Grundlehner, G., Castle, C., and Falconer, R.K.H., 2012, Document Preview – Offshore Technology Conference, *in* Offshore Technology Conference, Offshore Technology Conference, Houston, Texas.

Hashimoto, H., Yokoyama, S., Asaoka, H., Kusano, Y., Ikeda, Y., Seno, M., Takada, J., Fujii, T., Nakanishi, M., and Murakami, R., 2007, Characteristics of hollow microtubes consisting of amorphous iron oxide nanoparticles produced by iron oxidizing bacteria, Leptothrix ochracea: Journal of Magnetism and Magnetic Materials, v. 310, no. 2, p. 2405–2407, doi: 10.1016/j.jmmm.2006.10.793.

Hawley, J.E., 1926, An Evaluation of the evidence of life in the Archean: The Journal of Geology, v. 34, no. 5, p. 441–461.

Hazen, R.M., and Ferry, J.M., 2010, Mineral evolution: Mineralogy in the fourth dimension: Elements, v. 6, p. 9–12, doi: 10.2113/gselements.6.1.9.

Hersman, L.E., Huang, A., Maurice, P.A., and Forsythe, J.H., 2000, Siderophore production and iron reduction by Pseudomonas mendocina in response to iron deprivation: Geomicrobiology Journal, v. 17, p. 261–273, doi: 0149-0451/00.

Hirschler, A., Lucas, J., and Hubert, J.-C., 1990, Bacterial involvement in apatite genesis: FEMS Microbiology Ecology, v. 73, p. 211–220.

Hofmann, H.J., 2004, Archean Microfossils and Abiomorphs: Astrobiology, v. 4, no. 2, p. 135–136.

Hofmann, H.J., 1972, Precambrian remains in Canada: Fossils, dubiofossils, and pseudofossils: Proceedings of the 24th International Geological Congress, Section 1972, v. 1, p. 20–30.

Holland, H.D., 1999, When did the Earth's atmosphere become oxic ? A reply: The Geochemical News, v. #100, no. July, p. 20–22.

Homoky, W.B., John, S.G., Conway, T.M., and Mills, R.A., 2013, Distinct iron isotopic signatures and supply from marine sediment dissolution: Nature Communications, v. 4, p. 1–10, doi:

10.1038/ncomms3143.

Huldtgren, T., Cunningham, J.A., Yin, C., Stampanoni, M., Marone, F., Donoghue, P.C.J., and Bengtson, S., 2011, Fossilized nuclei and germination structures identify Ediacaran “animal embryos” as encysting protists: Science, v. 334, no. 6063, p. 1696–1699.

Huldtgren, T., Cunningham, J.A., Yin, C., Stampanoni, M., Marone, F., Donoghue, P.C.J., and Bengtson, S., 2012, Response to comment on “Fossilized nuclei and germination structures identify Ediacaran ‘animal embryos’ as encysting protists”: Science, v. 335, p. 1169–1170, doi: 10.1126/science.1219076.

Hunter, G.K., Allen, B.L., Grynpas, M.D., and Cheng, P.-T., 1985, Inhibition of hydroxyapatite formation in collagen gels by chondroitin sulphate: Biochemistry Journal, v. 228, p. 463–469.

Hyde, S.T., Carnerup, A.M., Larsson, A.-K., Christy, A.G., and García-Ruiz, J.M., 2004, Self-assembly of carbonate-silica colloids: between living and non-living form: Physica A, v. 339, p. 24–33, doi: 10.1016/j.physa.2004.03.045.

Icopini, G.A., Anbar, A.D., Ruebush, S.S., Tien, M., and Brantley, S.L., 2004, Iron isotope fractionation during microbial reduction of iron: The importance of adsorption: Geology, v. 32, p. 204–208, doi: 10.1130/G20184.1.

Ishihara, H., Suzuki, T., Hashimoto, H., Kunoh, H., and Takada, J., 2013, Initial parallel arrangement of extracellular fibrils holds a key for sheath frame construction by Leptothrix sp. Strain OUMS1: Minerals, v. 3, p. 73–81, doi: 10.3390/min3010073.

Ivarsson, M., Broman, C., Holmstrom, S.J.M., Ahlbom, M., Lindblom, S., and Holm, N.G., 2011, Putative fossilized fungi from the lithified volcaniclastic apron of Gran Canaria, Spain: Astrobiology, v. 11, no. 7, p. 633–650, doi: 10.1089/ast.2010.0593.

Ivarsson, M., Geho, S., and Holm, N.G., 2008, Micro-scale variations of iron isotopes in fossilized microorganisms: International Journal of Astrobiology, v. 7, no. 2, p. 93–106, doi: 10.1017/S1473550408004199.

Jahnke, R.A., Emerson, S.R., Roe, K.K., and Burnett, W.C., 1983, The present day formation of apatite in Mexican continental margin sediments: Geochimica et Cosmochimica Acta, v. 47, p. 259–266, doi: 0016-7037/83/020259-08503.00/0.

Jannasch, H.W., and Wirsen, C.O., 1979, Chemosynthetic primary production at East Pacific sea floor spreading centers: BioScience, v. 29, no. 10, p. 592–598.

Javaux, E.J., Knoll, A.H., and Walter, M., 2003, Recognizing and interpreting the fossils of early eukaryotes: Origins of Life and Evolution of the Biosphere, v. 33, p. 75–94.

Javaux, E.J., Knoll, A.H., and Walter, M.R., 2004, TEM evidence for eukaryotic diversity in mid-Proterozoic oceans: Geobiology2, p. 121–132.

Johnsson, M.S., and Nancollas, G.H., 1992, in Oral Biology & Medicine The Role of Brushite and Octacalcium Phosphate in Apatite Formation: , doi: 10.1177/10454411920030010601.

Jordan, T.H., and Grotzinger, J., 2008, The Essential Earth: W. H. Freeman and Company, New York.

Jørgensen, B.B., 2010, Big sulfur bacteria.: The ISME journal, v. 4, no. 9, p. 1083–4, doi: 10.1038/ismej.2010.106.

Jørgensen, B.B., and Boetius, A., 2007, Feast and famine--microbial life in the deep-sea bed.: Nature reviews. Microbiology, v. 5, no. 10, p. 770–81, doi: 10.1038/nrmicro1745.

Kan, J., Obraztsova, A., Wang, Y., Leather, J., Scheckel, K.G., Nealson, K.H., and Arias-thode, Y.M., 2013, Apatite and chitin mendments promote microbial activity and augment metal removal in marine sediments: Open Journal of metal, v. 3, p. 51–61, doi: 10.4236/ojmetal.2013.32A1007.

Van Kauwenbergh, S.J., 2010, World Phosphate Rock Reserves and Resources: International Fertilizer

Development Center, Muscle Shoals, Alabama.

Kawska, A., Hochrein, O., Brickmann, J., Kniep, R., and Zahn, D., 2008, The nucleation mechanism of fluorapatite-collagen composites: ion association and motif control by collagen proteins.: Angewandte Chemie (International ed. in English), v. 47, no. 27, p. 4982–5, doi: 10.1002/anie.200800908.

Khan, K.F., Khan, S.A., Dar, S.A., and Husain, Z., 2012, Geochemistry of phosphorite deposits around Hirapur- Mardeora area in Chhatarpur and Sagar Districts, Madhya Pradesh, India: Journal of Geology and Mining Research, v. 4, no. 3, p. 51–64, doi: 10.5897/JGMR11.044.

Kimberley, M.M., 2002, Iron formations: why the mystery persists, *in* Geological Society of America 2002 Denver Annual Meeting, Denver, CO.

Kluyver, A.J., and Donker, H.J., 1926, Die einheit in der biochemie (Unity in biochemistry): Chemie der zelle und gewebe, , no. 13, p. 134–190.

Kniep, R., and Busch, S., 1996, Biomimetic growth and self-assembly of fluorapatite aggregates by diffusion into denatured collagen matrices: Angewandte Chemie (International edition in English), v. 108, no. 22, p. 2623–2626.

Kniep, R., and Simon, P., 2007, Fluorapatite-gelatine-nanocomposites: Self-organized morphogenesis, real structure and relations to natural hard materials: Topics in Current Chemistry, v. 270, no. July 2006, p. 73–125, doi: 10.1007/128.

Knoll, A.H., and Golubic, S., 1992, Proterozoic and Living Cyanobacteria, *in* Schidlowski, M., Golubic, S., McKirdy Sr., D.M., and Trudinger, P.A. eds., Early Organic Evolution: Implications for mineral and energy resources, Springer-Verlag, Berlin, p. 450–462.

Knoll, a H., Strother, P.K., and Rossi, S., 1988, Distribution and diagenesis of microfossils from the lower Proterozoic Duck Creek Dolomite, Western Australia.: Precambrian research, v. 38, p. 257–79.

Knud-Hansen, C., 1994, Historical perspective of the phosphate detergent conflict: Conflict Resolution Consortium Working Paper 94-54,.

Konhauser, K.O., 2007, Introduction to Geomicrobiology: Blackwell Publishing, Malden, MA.

Kostetsky, E.Y., 2005, The possibility of the formation of protocells and their structural components on the basis of the apatite matrix and cocrystallizing minerals: Journal of Biological Physics, v. 31, p. 607–638, doi: 10.1007/s10867-005-2383-x.

Kouchinsky, A., Bengtson, S., and Gershwin, L., 1999, Cnidarian-like embryos associated with the first shelly fossils in Siberia: Geology, v. 27, no. 7, p. 609–612.

Krajewski, K.P., Van Cappellen, P., Trichet, J., Kuhn, O., Lucas, J., Martín-Algarra, A., Prévot, L., Tewari, V.C., Gaspar, L., Knight, R.I., and Lamboy, M., 1994, Biological processes and apatite formation in sedimentary environments: Eclogae geol. Helv., v. 87, no. 3, p. 701–745, doi: 0012-9402/94/030701-45.

Kremer, B., Bauer, M., Stark, R.W., Gast, N., Altermann, W., Gursky, H.-J., Heckl, W.M., and Kazmierczak, J., 2012, Laser-Raman and atomic force microscopy assessment of the chlorococcalean affinity of problematic microfossils: Journal of Raman Spectroscopy, v. 43, no. 1, p. 32–39, doi: 10.1002/jrs.2985.

Krepski, S.T., Emerson, D., Hredzak-Showalter, P.L., Luther, G.W., and Chan, C.S., 2013, Morphology of biogenic iron oxides records microbial physiology and environmental conditions: toward interpreting iron microfossils: Geobiology, v. 11, no. 5, p. 457–71, doi: 10.1111/gbi.12043.

Lander, N., Cordeiro, C., Huang, G., and Docampo, R., 2016, Inorganic polyphosphate (polyP) physiology – Polyphosphate and acidocalcisomes: Biochemical Society Transactions, v. 44, no. 1, p. 1–6, doi: 10.1042/BST20150193.

Lane, N., 2006, Batteries not included: Nature, v. 441, no. May, p. 274–277.

Li, H., Smith, S.E., Holloway, R.E., Zhu, Y., and Smith, F.A., 2006, Arbuscular Mycorrhizal Fungi Contribute to Phosphorus Uptake by Wheat Grown in a Phosphorus-fixing Soil Even in the Absence of Positive Growth Responses, *in* The New Phytologist, p. 536–543.

Li, M., Toner, B.M., Baker, B.J., Breier, J.A., Sheik, C.S., and Dick, G.J., 2014, Microbial iron uptake as a mechanism for dispersing iron from deep-sea hydrothermal vents: Nature Communications, v. 5, no. 3192, p. 1–8, doi: 10.1038/ncomms4192.

Lillie, R.S., and Johnston, E.N., 1919, Precipitation-structures simulating organic growth – A contribution to the physico-chemical amalysis of growth and heredity: Biological Bulletin, v. 36, no. 4, p. 225–260.

Lovelock, J.E., 1972, Gaia as seen through the atmosphere: Atmospheric Environment, v. 6, p. 579–580.

Marshall, C.P., Emry, J.R., and Marshall, A.O., 2011, Haematite pseudomicrofossils present in the 3.5-billion-year-old Apex Chert: Nature Geoscience, v. 4, p. 240–243, doi: 10.1038/ngeo1084.

Martin, D., Briggs, D.E.G., and Parkes, R.J., 2005, Decay and mineralization of invertebrate eggs: Palaios, v. 20, no. 6, p. 562–572, doi: 10.2110/palo.2004.p04-67.

Martin, A.P., Condon, D.J., Prave, A.R., and Lepland, A., 2013, A review of temporal constraints for the Palaeoproterozoic large, positive carbonate carbon isotope excursion (the Lomagundi–Jatuli Event): Earth Science Reviews, v. 127, p. 242–261, doi: 10.1016/j.earscirev.2013.10.006.

Martin, W., and Russell, M.J., 2003, On the origins of cells: a hypothesis for the evolutionary transitions from abiotic geochemistry to chemoautotrophic prokaryotes, and from prokaryotes to nucleated cells.: Philosophical transactions of the Royal Society of London. Series B, Biological sciences, v. 358, no. 1429, p. 59–83; discussion 83–5, doi: 10.1098/rstb.2002.1183.

McLoughlin, N., Brasier, M.D., Wacey, D., Green, O.R., and Perry, R.S., 2007, On biogenicity criteria for endolithic microborings on early Earth and beyond: Astrobiology, v. 7, no. 1, p. 10–26, doi: 10.1089/ast.2006.0122.

Midgley, J. (Enviro D., 2012, Namibian Marine Phosphate (PTY) Ltd – Appendix 1C – Sandpiper Project, Environmental Impact Assessment Final Report:.

Milorganite's History http://www.milorganite.com/Header-Links/About-Us/History.aspx,.

Misra, A.K., Acosta-Maeda, T.E., Sharma, S.K., McKay, C.P., Gasda, P.J., Taylor, G.J., Lucey, P.G., Flynn, L., Abedin, M.N., Clegg, S.M., and Wiens, R., 2016, "Standoff Biofinder" for fast, noncontact, nondestructive, large-area detection of biological materials for planetary exploration: Astrobiology, v. 16, no. 9, p. 715–729, doi: 10.1089/ast.2015.1400.

Mitchell, P., 1961, Coupling of phosphorylation to electron and hydrogen transfer by a chemi-osmotic type of mechanism: Nature, v. 191, no. 4784, p. 144–148.

Mitchell, P., 1978, David Keilin's respiratory chain concept and its chemiosmotic consequences (P Mitchell's Nobel lecture): Chemistry, p. 295–330.

Morse, J.W., 1974, Dissolution kinetics of calcium carbonate in sea water: III, a new method for the study of carbonate reaction kinetics: American Journal of Science, v. 274, no. 2, p. 97–107.

Murshed, M., Schinke, T., Mckee, M.D., and Karsenty, G., 2004, Extracellular matrix mineralization is regulated locally; different roles of two gla-containing proteins: Journal of Cell Biology, v. 165, no. 5, p. 625–630, doi: 10.1083/jcb.200402046.

Muscente, A.D., Hawkins, A.D., and Xiao, S., 2016, Fossil preservation through phosphatization and silicification in the Ediacaran Doushantuo Formation (South China): a comparative synthesis: Palaeogeography, Palaeoclimatology, Palaeoecology, v. 434, p. 46–62, doi: 10.1016/j.palaeo.2014.10.013.

Nakamizo, M., Honda, H., and Inagaki, M., 1978, Raman spectra of ground natural graphite: Carbon, v. 16, p. 281–283, doi: 0008-6223/78/0801-0281.

Nathan, Y., Bremner, J.M., Loewenthal, R.E., and Pedro, M., 1993, Role of bacteria in phosphorite genesis: Geomicrobiology Journal, v. 11, no. 2, p. 69–76.

Nealson, K.H., 1982, Microbiological oxidation and reduction of iron, *in* Holland, H.D. and Schidlowski, M. eds., Mineral Deposits and the Evolution of the Biosphere – Report of the Dahlem Workshop on Biospheric Evolution and Precambrian Metallogeny, Springer-Verlag, Berlin, p. 51–65.

Neilands, J.B., 1995, Siderophores: Structure and function of microbial iron transport compounds: The Journal of Biological Chemistry, v. 270, no. 45, p. 26723–26726.

Newman, D.K., and Banfield, J.F., 2002, Geomicrobiology: How molecular-scale interactions underpin biogeochemical systems: Science, v. 296, no. May, p. 1071–1077.

Newport, F., 2014, In U. S., 42 % Believe Creationist view of human origins: , p. 16–19.

Nickel, E.H., 1995, The definition of a mineral: The Canadian Mineralogist, v. 33, p. 689–690.

Nisbet, E.G., Grassineau, N. V., Howe, C.J., Abell, P.I., Regelous, M., and Nisbet, R.E.R., 2007, The age of Rubisco: the evolution of oxygenic photosynthesis: Geobiology, v. 5, no. 4, p. 311–335, doi: 10.1111/j.1472-4669.2007.00127.x.

Obersteiner, M., Peñuelas, J., Ciais, P., Velde, M. Van Der, and Janssens, I.A., 2013, The phosphorus trilemma: Nature Geoscience, v. 6, no. 11, p. 897–898, doi: 10.1038/ngeo1990.

Papineau, D., Purohit, R., Goldberg, T., Pi, D., Shields, G.A., Bhu, H., Steele, A., and Fogel, M.L., 2009, High primary productivity and nitrogen cycling after the Paleoproterozoic phosphogenic event in the Aravalli Supergroup, India: Precambrian Research, v. 171, p. 37–56, doi: 10.1016/j.precamres.2009.03.005.

Pasteris, J.D., and Wopenka, B., 2003, Necessary, but not sufficient: Raman identification of disordered carbon as a signature of ancient life: Astrobiology, v. 3, no. 4.

Pasteris, J.D., and Wopenka, B., 1991, Raman Spectra of Graphite as Indicators of Degree of Metamorphism: The Canadian Mineralogist, v. 29, no. 1, p. 1–9.

Paytan, A., and McLaughlin, K., 2007, The oceanic phosphorus cycle: Chemical Reviews, v. 107, no. 2, p. 563–576, doi: 10.1021/cr0503613.

Petsch, S.T., 2010, The global oxygen cycle, *in* Holland, H.D. and Turekian, K.K. eds., Isotope geochemistry: A derivative of the Treatise on Geochemistry, Academic Press, p. 515–555.

Podolsky, S., 1996, The Role of the virus in origin-of-life theorizing: Journal of the History of Biology, v. 29, no. 1, p. 79–126.

Pradhan, V.R., Meert, J.G., Pandit, M.K., Kamenov, G., and Ali, E., 2012, Paleomagnetic and geochronological studies of the mafic dyke swarms of Bundelkhand craton , central India : Implications for the tectonic evolution and paleogeographic reconstructions: Precambrian Research, v. 198-199, p. 51–76, doi: 10.1016/j.precamres.2011.11.011.

Pross, A., and Pascal, R., 2013, The origin of life: what we know, what we can know and what we will never know: Open Biology, v. 3, no. March.

Pyle, L.J., Narbonne, G.M., Nowlan, G.S., Xiao, S., and James, N.P., 2006, Early Cambrian Metazoan Eggs, Embryos, and Phosphatic Microfossils From Northwestern Canada: Journal of Paleontology, v. 80, no. 5, p. 811–825, doi: 10.1666/0022-3360(2006)80[811:ECMEEA]2.0.CO;2.

Raff, E.C., Villinski, J.T., Turner, F.R., Donoghue, P.C.J., and Raff, R.A., 2006, Experimental taphonomy shows the feasibility of fossil embryos: Proceedings of the National Academy of Sciences of the United States of America, v. 103, no. 15, p. 5846–51, doi: 10.1073/pnas.0601536103.

Rafols, I., Porter, A.L., and Leydesdorff, L., 2010, Science overlay maps: A new tool for research policy: Journal of the American Society for Information Science and Technology, v. 61, no. 9, p. 1871–1887,

doi: 10.1002/asi.21368.

Raiswell, R., 2011, Iron transport from the continents to the open ocean: The aging–rejuvenation cycle: Elements, v. 7, no. April, p. 101–106, doi: 10.2113/gselements.7.2.101.

Reijnders, L., 2014, Phosphorus resources, their depletion and conservation, a review: Resources, Conservation and Recycling, v. 93, p. 32–49, doi: 10.1016/j.resconrec.2014.09.006.

Roden, E.E., Sobolev, D., Glazer, B., and Luther III, G.W., 2004, Potential for microscale bacterial Fe redox cycling at the aerobic-anaerobic interface: Geomicrobiology Journal, v. 21, p. 379–391, doi: 10.1080/01490450490485872.

Roels, J., and Verstraete, W., 2001, Biological Formation of Volatile Phosphorus Compounds: Bioresource Technology, v. 79, p. 243–250.

Roy, A.B., 2000, Geology of the Palaeoproterozoic Aravalli Supergroup of Rajasthan and Northern Gujarat, *in* Deb, M. ed., Crustal evolution and metallogeny in the Northwestern Indian Shield, Alpha Science International, Ltd, p. 87–114.

Roy, A.B., and Paliwal, B.S., 1981, Evolution of Lower Proterozoic epicontinental deposits: Stromatolite-bearing Aravalli rocks of Udaipur, Rajasthan, India: Precambrian Research, v. 14, p. 49–74.

Ruttenberg, K.C., and Berner, R.A., 1993, Authigenic apatite formation and burial in sediments from non-upwelling, continental margin environments: Geochimica et Cosmochimica Acta, v. 57, no. 5, p. 991–1007, doi: 10.1016/0016-7037(93)90035-U.

Salgado, P., Melin, V., Contreras, D., Moreno, Y., and Mansilla, H.D., 2013, Fenton reaction driven by iron ligands: Journal of Chilean Chemical Society, v. 58, no. 4, p. 2096–2101.

Sánchez-Navas, A., and Martín-Algarra, A., 2001, Genesis of apatite in phosphate stromatolites: European Journal of Mineralogy, v. 13, p. 361–376, doi: 10.1127/0935-1221/.

Sarangi, S., Gopalan, K., Roy, A.B., Sreenivas, B., and Das Sharma, S., 2006, Pb-Pb Age of Carbonates of Jhamarkotra Formation: Constraints on the Age of Aravalli Supergroup, Rajasthan: Journal of the Geological Society of India, v. 67, p. 442–446.

Schaal, K.P., Yassin, A.F., and Stackebrandt, E., 2006, The Family Actinomycetaceae: The Genera Actinomyces, Actinobaculum, Arcanobacterium, Varibaculum, and Mobiluncus, *in* Dworkin, M., Falkow, S., Rosenberg, E., Schleifer, K.-H., and Stackebrandt, E. eds., The Prokaryotes - A Handbook on the Biology of Bacteria Vol 3: Archaea. Bacteria: Firmicutes, Actinomycetes, Springer Science+Business Media LLC, New York, p. 430–537.

Schidlowski, M., Hayes, J.M., and Kaplan, I.R., 1983, Isotopic inferences of ancient biochemistries: Carbon, Sulfur, Hydrogen, and nitrogen, *in* Schopf, W.J. ed., Earth's earliest biosphere, Princeton University Press, Princeton, p. 149–186.

Schieber, J., and Glamoclija, M., 2007, Microbial mats built by iron bacteria: a modern example from southern Indiana, *in* Schieber, J., Bose, P.K., Eriksson, P.G., Banerjee, S., Sarkar, S., Altermann, W., and Catuneau, O. eds., Atlas of microbial mat features preserved within the clastic rock record, Elsevier, Amsterdam, p. 233–244.

Schopf, J.W., 1976, Are the oldest "fossils", fossils? Origins Of Life, v. 7, p. 19–36.

Schopf, J.W., 1999, Cradle of Life – The Discovery of Earth's Earliest Fossils: Princeton University Press, Princeton.

Schopf, J.W., 1993, Microfossils of the Early Archean Apex Chert: New evidence of the of antiquity of life: Science, v. 260, no. 5108, p. 640–646.

Schopf, J.W., Kudryavtsev, A.B., Agresti, D.G., Czaja, A.D., and Wdowiak, T.J., 2005, Raman Imagery: A new approach to assess the geochemical maturity and biogenicity of permineralized Precambrian fossils: Astrobiology, v. 5, no. 3, p. 333–371.

Schopf, J.W., Kudryavtsev, A.B., Agresti, D.G., Wdowiak, T.J., and Czaja, A.D., 2002, Laser-Raman imagery of Earth's earliest fossils: Nature, v. 416, p. 73–76.

Schopf, J.W., and Packer, B.M., 1987, Early Archean (3.3-billion to 3.5-billion-year-old) microfossils from Warrawoona Group, Australia: Science, v. 237, no. 4810, p. 70–73.

Schopf, J.W., and Walter, M.R., 1983, Archean microfossils: New evidence of ancient microbes, *in* Schopf, J.W. ed., Earth's Earliest Biosphere, Princeton University Press, Princeton, p. 214–239.

Schrodinger, E., 1945, What is life? The Physical Aspect of the Living Cell: The Macmillan Company, New York.

Schulz, H.N., and Schulz, H.D., 2005, Large sulfur bacteria and the formation of phosphorite: Science (New York, N.Y.), v. 307, no. 5708, p. 416–418, doi: 10.1126/science.1103096.

Schwertmann, U., and Murad, E., 1983, Effect of pH on the formation of goethite and hematite from ferrihydrite: Clays and Clay Minerals, v. 31, no. 4, p. 277–284.

Schwertmann, U., Stanjek, H., and Becher, H.-H., 2004, Long-term in vitro transformation of 2-line ferrihydrite to goethite/hematite at 4, 10, 15 and 25C: Clay Minerals, v. 39, p. 433–438, doi: 10.1180/0009855043940145.

Seufferheld, M.J., Alvarez, H.M., and Farias, M.E., 2008, Role of polyphosphates in microbial adaptation to extreme environments.: Applied and environmental microbiology, v. 74, no. 19, p. 5867–74, doi: 10.1128/AEM.00501-08.

Sievert, S.M., and Vetriani, C., 2012, Chemoautotrophy at deep-sea vents: Past, present, and future: Oceanography, v. 25, no. 1, p. 218–233, doi: http://dx.doi.org/10.5670/oceanog.2012.21.

Silverman, L., and Boskey, A.L., 2004, Diffusion systems for evaluation of biomineralization: Calcified Tissue International, v. 75, no. 6, p. 494–501, doi: 10.1007/s00223-004-0019-y.

Singer, E., Emerson, D., Webb, E.A., Barco, R.A., Kuenen, J.G., Nelson, W.C., Chan, C.S., Comolli, L.R., Ferriera, S., Johnson, J., Heidelberg, J.F., and Edwards, K.J., 2011, Mariprofundus ferrooxydans PV-1 the first genome of a marine Fe(II) oxidizing Zetaproteobacterium: PloS one, v. 6, no. 9, p. e25386, doi: 10.1371/journal.pone.0025386.

Sleep, N.H., and Bird, D.K., 2008, Evolutionary ecology during the rise of dioxygen in the Earth's atmosphere: Philosophical Transactions of the Royal Society B: Biological Sciences, v. 363, no. May, p. 2651–2664, doi: 10.1098/rstb.2008.0018.

Smelser, N.J., and Baltes, P.B. (Eds.), 2001, History of Scientific Disciplines – Vol. 12, *in* International Encyclopedia of the Social & Behavioral Sciences, Elsevier Sciences, Ltd., Oxford, p. 13727–13731.

Smil, V., 2000, Phosphorus in the environment: Natural flows and human interferences: Annual Reviews of Energy and the Environment, v. 25, p. 53–88.

Smoukov, S.K., Lagzi, I., and Grzybowski, B.A., 2011, Independence of primary and secondary structures in periodic precipitation patterns: Journal of Physical Chemistry Letters, v. 2, p. 345–349, doi: 10.1021/jz101679t.

Snow, J., 1857, Cholera, and the Water Supply in the South Districts of London: British Medical Journal, p. 864–865.

Sojo, V., Herschy, B., Whicher, A., Camprubi, E., and Lane, N., 2016, The origin of life in alkaline hydrothermal vents: Astrobiology, v. 16, no. 2, p. 1–17, doi: 10.1089/ast.2015.1406.

Soudry, D., and Champetier, Y., 1983, Microbial processes in the Negev phosphorites (Southern Israel): Sedimentology, v. 30, p. 411–423, doi: 0037-0746/83/0600-0411.

Spring, S., 2006, The Genera Leptothrix and Sphaerotilus, *in* Dworkin, M., Falkow, S., Rosenberg, E., Schleifer, K.-H., and Stackebrandt, E. eds., Prokaryotes Vol. 6: Proteobacteria: Gamma Subclass,

Springer Science+Business Media LLC, New York, p. 758–777.

Steiner, M., Qian, Y., Li, G., Hagadorn, J.W., and Zhu, M., 2014, The developmental cycles of early Cambrian Olivooidae fam. nov. (? Cycloneuralia) from the Yangtze Platform (China): Palaeogeography, Palaeoclimatology, Palaeoecology, v. 398, p. 97–124, doi: 10.1016/j.palaeo.2013.08.016.

Steiner, M., Zhu, M., Li, G., Qian, Y., and Erdtmann, B.-D., 2004, New Early Cambrian bilaterian embryos and larvae from China: Geology, v. 32, p. 833–836, doi: 10.1130/G20567.1.

Stephan, A., 1999, Varieties of emergentism: Evolution and Cognition, v. 5, no. 1, p. 49–59.

Stern, K.H., 1954, The Liesegang phenomenon: Chemical Reviews, p. 79–99.

Sterner, R.W., and Elser, J.J., 2002, Ecological Stoichiometry: The Biology of Elements from Molecules to the Biosphere: Princeton University Press, Princeton.

Streckfuss, J.L., Smith, W.N., Brown, L.R., and Campbell, M.M., 1974, Calcification of selected strains of Streptococcus mutans and Streptococcus sanguis: Journal of Bacteriology, v. 120, no. 1, p. 502–506.

Sugitani, K., Grey, K., Allwood, A., Nagaoka, T., Mimura, K., Minami, M., Marshall, C.P., Van Kranendonk, M.J., and Walter, M.R., 2007, Diverse microstructures from Archaean chert from the Mount Goldsworthy–Mount Grant area, Pilbara Craton, Western Australia: Microfossils, dubiofossils, or pseudofossils ? Precambrian Research, v. 158, p. 228–262, doi: 10.1016/j.precamres.2007.03.006.

Summons, R.E., Albrecht, P., Mcdonald, G., and Moldowan, J.M., 2008, Molecular Biosignatures: Space Science Reviews, v. 135, p. 133–159, doi: 10.1007/s11214-007-9256-5.

Summons, R.E., Jahnke, L.L., Hope, J.M., and Logan, G.A., 1999, 2-Methylhopanoids as biomarkers for cyanobacterial oxygenic photosynthesis: Nature, v. 400, no. August, p. 554–557.

Suzuki, C., Furukawa, Y., Kobayashi, T., Sekine, T., Nakazawa, H., and Kakegawa, T., 2015, Shock wave synthesis of amino acids from solutions of ammonium formate and ammonium bicarbonate: Geochemistry, Geophysics, Geosystems, v. 16, p. 2382–2394, doi: 10.1002/2015GC005783.

Szostak, J.W., Bartel, D.P., and Luisi, P.L., 2001, Synthesizing life: Nature, v. 409, p. 387–390.

Tarbuck, E.J., and Lutgens, F.K., 2003, Earth Science: Pearson Prentice Hall, Upper Saddle River, N.J.

Taylor, W.R., 2006, Transcription and translation in an RNA world.: Philosophical transactions of the Royal Society of London. Series B, Biological sciences, v. 361, no. 1474, p. 1751–60, doi: 10.1098/rstb.2006.1910.

Tirard, S., Morange, M., and Lazcano, A., 2010, The definition of life: A brief history of an elusive scientific endeavor: Astrobiology, v. 10, no. 10, p. 1003–1009, doi: 10.1089/ast.2010.0535.

Tomescu, A.M.F., Klymiuk, A.A., Matsunaga, K.K.S., Bippus, A.C., and Shelton, G.W.K., 2016, Microbes and the fossil record: Selected topics in paleomicrobiology, *in* Hurst, C.J. ed., Their World: A Diversity of Microbial Environments, Advances in Environmental Microbiology Volume 1, Springer International Publishing, p. 69–169.

Tomson, M.B., and Nancollas, G.H., 1978, Mineralization Kinetics: A constant composition approach: Science, v. 200, no. 4345, p. 1059–1060.

Tripathi, A., Srivastava, G. ji, Srivastava, S., and Das, I., 2015, Liesegang patterns, growth kinetics, inhibition and dissolution of calcium phosphate: A constituent of renal stone: Chemical Biology Letters, v. 2, no. 2, p. 30–40.

Vacker, D., Connell, C.H., and Wells, W.N., 1967, Phosphate removal through minucipal wastewater treatment at San Antonio, Texas: Journal of the Water Pollution Control Federation, v. 39, no. 5, p. 750–771.

Veis, A., 2003, Mineralization in organic matrix frameworks, *in* Dove, P.M., De Yoreo, J.J., and Weiner, S.

eds., Reviews in Mineralogy & Geochemistry Volume 54 - Biomineralization, Mineralogical Society of America, Washington, D. C., p. 250–289.

Vernadsky, V.I., 1998, The Biosphere: Springer-Verlag, New York.

Visscher, P.T., and Sciences, M., 2000, Microscale observations of sulfate reduction : Correlation of microbial activity with lithified micritic laminae in modern marine stromatolites: v. 2, no. 10, p. 919–922.

Wacey, D., Saunders, M., Kong, C., and Kilburn, M.R., 2016, A new occurrence of ambient inclusion trails from the ~1900-million-year-old Gunflint Formation, Ontario: nanocharacterization and testing of potential formation mechanisms: Geobiology, p. 1–17, doi: 10.1111/gbi.12186.

Wächtershäuser, G., 2006, From volcanic origins of chemoautotrophic life to Bacteria, Archaea and Eukarya: Philosophical Transactions of the Royal Society B: Biological Sciences, v. 361, no. 1474, p. 1787–1808, doi: 10.1098/rstb.2006.1904.

de Wall, H., Pandit, M.K., and Chauhan, N.K., 2012, Paleosol occurrences along the Archean–Proterozoic contact in the Aravalli craton, NW India: Precambrian Research, v. 216-219, p. 120–131, doi: 10.1016/j.precamres.2012.06.017.

Walsh, K.L., and Da Mommio, A., 2013, History and precent developments in the visual presentation of optical microscopy, *in* Sixth International Symposium – Mineral Diversity Research and Preservation, Sofia, Bulgaria, p. 135.

Waychunas, G.A., and Zhang, H., 2008, Structure, chemistry, and properties of mineral nanoparticles: Elements, v. 4, no. 6, p. 381–387, doi: 10.2113/gselements.4.6.381.

Westall, F., 2008, Morphological biosignatures in early terrestrial and extraterrestrial materials: Space Science Reviews, v. 135, no. 95, p. 95–114, doi: 10.1007/s11214-008-9354-z.

Westall, F., and Folk, R.L., 2003, Exogenous carbonaceous microstructures in Early Archaean cherts and BIFs from the Isua Greenstone Belt: implications for the search for life in ancient rocks: Precambrian Research, v. 126, p. 313–330, doi: 10.1016/S0301-9268(03)00102-5.

Westheimer, F.H., 1987, Why nature chose phosphates: Science, v. 235, no. 4793, p. 1173–1178.

Whistler, R.L., 1973, Solubility of polysaccharides and their behavior in solution, *in* Isbell, H.S. ed., Carbohydrates in Solution, American Chemical Society, Washington, D. C., p. 242–255.

Wiedenbeck, M., and Goswami, J.N., 1994, High precision 207Pb/206Pb zircon geochronology using a small ion microprobe: Geochimica et Cosmochimica Acta, v. 58, no. 9, p. 2135–2141.

Williams, A.J., Alpers, C.N., Sumner, D.Y., and Campbell, K.M., 2016, Filamentous hydrous ferric oxide biosignatures in a pipeline carrying acid mine drainage at Iron Mountain Mine, California: Geomicrobiology Journal, v. 0451, no. June, p. 1–45, doi: 10.1080/01490451.2016.1155679.

Williams, L.A., and Reimers, C., 1983, Role of bacterial mats in oxygen-deficient marine basins and coastal upwelling regimes: Preliminary report: Geology, v. 11, p. 267–269.

Wingender, J., Neu, T.R., and Flemming, H.-C. (Eds.), 1999a, Microbial Extracellular Polymeric Substances – Characterization, Structure and Function: Springer-Verlag, Berlin.

Wingender, J., Neu, T.R., and Flemming, H.-C., 1999b, What are bacterial extracellular polymeric substances?, *in* Wingender, J., Neu, T.R., and Flemming, H.-C. eds., Microbial Extracellular Polymeric Substances: Characterization, Structure and Function, Springer-Verlag, Berlin, p. 1–19.

Withers, P.J.A., Elser, J.J., Hilton, J., Ohtake, H., Schipper, W.J., and van Dijk, K.C., 2015, Greening the global phosphorus cycle: how green chemistry can help achieve planetary P sustainability: Green Chemistry, v. 17, p. 2087–2099, doi: 10.1039/c4gc02445a.

Wolfaardt, G.M., Lawrence, J.R., and Korber, D.R., 1999, Function of EPS, *in* Wingender, J., Neu, T.R.,

and Flemming, H.-C. eds., Microbial Extracellular Polymeric Substances – Characterization, Sturcture and Function, Springer-Verlag, Berlin, p. 171–200.

Wopenka, B., and Pasteris, J.D., 1993, Structural characterization of kerogens to granulite-facies graphite: Applicability of Raman microprobe spectroscopy: American Mineralogist, v. 78, p. 533–557, doi: 0003-004X/93/0506-0533.

Xiao, S., and Knoll, A.H., 1999, Fossil preservation in the Neoproterozoic Doushantuo phosphorite Lagerstatte, South China: Lethaia, v. 32, no. 219-240.

Xiao, S., and Knoll, A.H., 2000, Phosphatized animal embryos from the Neoproterozoic Doushantuo Formation at Weng'An, Guizhou, South China: Journal of Paleontology, v. 74, no. 5, p. 767–788, doi: 0022-3360/00/0074-767.

Xiao, S., Knoll, A.H., Schiffauer, J.D., Zhou, C., and Yuan, X., 2012, Comment on "Fossilized nuclei and germination structures identify Ediacaran "animal embryos" as encysting protists: Science, v. 335, doi: 10.1126/science.1218814.

Xiao, S., Zhang, Y., and Knoll, A.H., 1998, Three-dimensional preservation of algae and animal embryos in a Neoproterozoic phosphorite: Nature, v. 391, no. February, p. 553–558.

Xiao, S., Zhou, C., Liu, P., Wang, D., and Yuan, X., 2014, Phosphatized acanthomorphic acritarchs and related microfossils from the Ediacaran Doushantuo Formation at Weng'an (South China) and their implications for biostratigraphic correlation: Journal of Paleontology, v. 88, no. 1, p. 1–67, doi: 10.1666/12-157R.

Yao-song, X., Tian-fu, T., Cong-liu, Y., and Chuan-ming, Z., 1995, Large spheroidal chlorophyta fossils from Doushantuo formation phosphoric sequence (Late Sinian), central Guizhou, South China: Acta Palaeontologica Sinica, v. 34, no. 6, p. 688–714.

Yin, C., Bengtson, S., and Yue, Z., 2004, Silicified and phosphatized Tianzhushania, spheroidal microfossils of possible animal origin from the Neoproterozoic of South China: Acta Palaeontologica Polonica, v. 49, no. 1, p. 1–12.

Yin, Z., and Zhu, M., 2012, New observations of the ornamented Doushantuo embryo fossils from the Ediacaran Weng'an Biota, South China: Bulletin of Geosciences, v. 87, no. 1, p. 1–11, doi: 10.3140/bull.geosci.1234.

Yin, L., Zhu, M., Knoll, A.H., Yuan, X., Zhang, J., and Hu, J., 2007, Doushantuo embryos preserved inside diapause egg cysts: Nature, v. 446, no. April, p. 661–663, doi: 10.1038/nature05682.

Young, J.R., and Henriksen, K., 2003, Biomineralization within vesicles: The calcite of coccoliths, *in* Dove, P.M., De Yoreo, J.J., and Weiner, S. eds., Reviews in Mineralogy & Geochemistry Volume 54 - Biomineralization, Mineralogical Society of America, Washington, D. C., p. 189–215.

Yue, Z., and Bengtson, S., 1999, Embryonic and post-embryonic development of the Early Cambrian cnidarian Olivooides: Lethaia, v. 32, p. 181–195.

Zahnle, K., Arndt, N., Cockell, C., Halliday, A., Nisbet, E., Selsis, F., and Sleep, N.H., 2007, Emergence of a Habitable Planet: Space Science Reviews, v. 129, p. 35–78, doi: 10.1007/s11214-007-9225-z.

van der Zee, C., Roberts, D.R., Rancourt, D.G., and Slomp, C.P., 2003, Nanogoethite is the dominant reactive oxyhydroxide phase in lake and marine sediments: Geology, v. 31, no. 11, p. 993–996, doi: 10.1130/G19924.1.

Zhao, G., Cawood, P.A., Wilde, S.A., and Sun, M., 2002, Review of global 2.1–1.8 Ga orogens: implications for a pre-Rodinia supercontinent: v. 59, p. 125–162.

Zhao, G., Sun, M., Wilde, S.A., and Li, S., 2004, A Paleo-Mesoproterozoic supercontinent: assembly, growth and breakup: Earth-Science Reviews, v. 67, p. 91–123, doi: 10.1016/j.earscirev.2004.02.003.

Appendices

Appendix A : What is life?

Determining whether a putative microfossil is indeed the remnant of a living organism implies an understanding of the definition of life. Attempts to define life range from myth- and theology-based explanations outside of the purview of the natural sciences, to fundamentally scientific, or physicochemical explanations, such as given by physicist Erwin Schrodinger in his treatise "What is life," in which he addressed the issues of heritability and the thermodynamics of living systems (Schrodinger, 1945; Dronamraju, 1999).

In no small part, the difficulty in defining life is intrinsic in its being a diachronic emergent property – that is, a property that "could not have been predicted in principle before [its] first instantiation." (Stephan, 1999) Such is the fundamental paradox of abiogenesis: the convergence of chemical processes that result in a spontaneous emergence of life out of inanimate material (Pross and Pascal, 2013).

Despite years of debate discussion and research, we still do not have consensus as to whether life can even *be* defined, as illustrated in the quotes below:

> *"Until the principles governing the process by which life on the Earth emerged can be uncovered, an understanding of life's essence ... will probably remain out of reach."* — *(Pross and Pascal, 2013)*

> *"Definitions of life must be open and must not be limited by our current state of knowledge. Perhaps what is required is more a framework than a precise definition. Answers to the question of what is life will be provided by different specialists working on different problems and from diverse perspectives, ranking from the origin of life on Earth, to synthetic biology, to the search for extraterrestrial life."* — *(Tirard et al., 2010)*

Nonetheless, we strive to grasp the scientific concept of life. Definitions range from detailed:

> *"A very simple definition of a living system might be: compartments separated from their surroundings that spontaneously multiply with energy gleaned through self-contained, thermodynamically favorable redox reactions."* — *(Martin and Russell, 2003)*

To deceptively simple statements such as the 'NASA definition' of life:

> *"... self-sustaining chemical systems capable of Darwinian evolution."*
> — *(Benner, 2010)*

In *Defining Life* (2010) Benner discusses how on the one hand, the NASA definition invalidates problematic issues in a variety of Star Trek and other sci-fi depictions of life, yet on the other hand is unsatisfyingly challenged by consideration of whether tool-using humankind has become 'supra-Darwinian,' (Benner, 2010). The issue arguably becomes more complex as we

witness the emergence and development of non-biological computers exhibiting artificial intelligence and the ability to learn and evolve in complexity (Bedau, 2003).

Despite these difficulties, most definitions converge on the following set of characteristics:

A living organism

- ❑ Has distinct physical boundaries (an 'inside' and an 'outside' such as a skin or, in the case of a single-celled organism, the cell wall)
- ❑ Has different internal structures which perform specific chemical processes
- ❑ Accesses, utilizes and transforms energy
- ❑ Builds body mass
- ❑ Responds to both internal and external environments to maintain a regulated internal state
- ❑ Generates progeny (reproduces)
- ❑ Maintains and vertically transmits a genetic code, which:
- ❑ Evolves through generations in response to selective pressure

Appendix B : Assessing microfossil biogenicity

Just how do we identify a microfossil?

Morphology is one of the first signals of a potential microfossil. And yet morphology can be so altered over time that many true microfossils probably go undetected. Conversely, many abiologically-produced features that appear to be biologically produced can be misinterpreted as microfossils. The work of establishing the *bona fide* biogenicity of a microfossil is no trivial task. How is it done?

Microfossils are generally defined as too small to be seen without magnification. So initially, observing thin sections (~30 μm thick slivers) of rock material under a microscope, our attention is drawn to features different from the encasing mineral/rock matrix. For instance we may notice an area of different color or refractive index, or a shape that appears biological. At this point, we seek an abiological explanation for the feature, using optical mineralogy. We also consider what we know of sedimentary/diagenetic processes, including some that are known to result in artifacts that may appear suspiciously biogenic.

A great deal of work has gone into the development and evaluation of biogenicity criteria, and published biogenicity criteria have varied according to the presumed complexity and/or geologic age of the putative microfossil and the refinement of analytical methods.

And if we're not sure?

As geologists, we are inclined to work within a framework guided by the principle of Uniformitarianism – that "the present is the key to the past." In some respects this is simply common sense – we know confidently only what we experience and/or can measure. Although this perspective provides a powerful analytical framework, scholars of Earth history and micropaleontology realize that this perspective is a starting point that begs to be challenged. Earth system chemistry and ecosystems have undergone profound changes over Earth's history, so that extrapolating from present to past may not be valid in terms of biological morphology, geology-biology interactions and ecosystems.

In addition to changes in Earth system dynamics, it is also possible that some authentic ancient biological features may have since been extinguished and so are not represented among extant organisms, which would make them difficult to recognize as biogenic. The succinctly made observation that "perhaps the biggest impediment to solving the iron-formation mystery is the assurance by some textbook authors that the problem already has been solved" (Kimberley, 2002) applies equally well to areas such as Earth history and micropaleontology.

Although often not reported in the literature, the challenge of establishing biogenicity can be illustrated by the examples of abiotic pseudofossils that have been published, including work as early as 1919, and continuing today (e.g. (Lillie and Johnston, 1919; Garcia Ruiz et al., 2002; Benzerara et al., 2003; Cosmidis and Templeton, 2016).

In 1972 H. J. Hofmann published a paper differentiating between a 'true' microfossil, a so-called dubiofossil, and a pseudofossil (Hofmann, 1972). Unfortunately, dubiofossil and pseudofossil findings are often not published, arbitrarily limiting the potential breadth of a broad 'comparative database' from which to develop criteria for interpreting biogenicity.

Changing & evolving approaches

Recently, Tomescu et al. (2016) have drawn a distinction between an early "Traditional Approach" that addresses issues of syngeneity and biogenicity, and a "Contextual Approach" that relies less on comparison with known structures and "instead of proving the biogenicity of

structures … strives to demonstrate that they cannot be abiogenic" by considering geologic, morphological, behavioral-taphonomic, and metabolic factors in assessing the likelihood of microfossil authenticity (Tomescu et al. 2016).

Biogenicity and the search for extraterrestrial life

More recently, our exploration of Mars has driven a renewed interest in biogenicity criteria, including recognition of biosignatures in Archean material thought to be analogous to early Martian material (Westall, 2008), and identification of the limitations of some commonly-accepted biogenicity criteria, as enumerated by Cady et al. (2003) (Cady et al., 2003).

Mars exploration has also resulting in the development of innovative methods for detecting biosignatures, such as the recently developed 'Standoff Biodetector' described as being "designed to locate a high-value fluorescent biological target with a noncontact, nondestructive approach" … that "is capable of detecting minute amounts of biological material, dead or alive." Although this approach may not be applicable to Earth fossils, it illustrates some of the ingenuity being applied to our search for the ability to distinguish biogenic material from abiogenic geological material (Misra et al., 2016).

Following is an assortment of different criteria that have been developed.

Differing criteria

Table 03

Biogenicity criteria – Archaea (Schopf, 1976)

Some of the earliest published criteria addressed the authenticity of Archaean microfossils. In 1976, J. William Schopf, recognizing the difficulty in establishing biogenicity of usually nondescript putative microfossils, wrote that he had developed:

> *"(a) set of simple statistical tests that could be used to differentiate between populations of unicellular microorganisms (both modern and fossil) and populations of unicell-like objects of known abiotic origin" for use in evaluating "Archean fossil-like microstructures."*
>
> *— (Schopf, 1976)*

Table 04

Biogenicity criteria – Archaea (Buick, 1990)

Roger Buick later refuted Schopf's statistical criteria, in light of the possibility of abiotically created features falling within these parameters (Buick, 1990). His approach to assessing putative Archaean microfossils was to apply a "hierarchy series of recognition criteria" which required that a putative microfossil:

- ❑ appear in thin section [rationale: microfossil by acid maceration/extraction was prone to introduce contaminants]
- ❑ occur in sedimentary rock [rationale: the possibility of preservation in igneous material is exceedingly unlikely]
- ❑ had undergone no more than low-grade metamorphism [rationale: higher grades would likely have altered organic components and compromised evidentiary data]
- ❑ consist of kerogen [reasoning based on the complex organic polymeric composition of extant microbes & most Proterozoic microfossils]
- ❑ be larger than the standardly accepted minimum size of independent, viable cells (~ 0.01 μm^3 or ~ 0.25 µm diameter)
- ❑ occur with others of similar morphology
- ❑ be hollow [reasoning based on evidence that Proterozoic microfossils retain only cell walls]
- ❑ exhibit cellular elaboration such as layered walls, internal bodies or ornate surfaces
- ❑ if filamentous:
  - — have septae separating cells with layered walls
  - — have variations in filament width and shape

In addition, he notes that adequate assessment of biogenicity must also rely on

- ❑ accurate local stratigraphic mapping
- ❑ thorough small-scale outcrop examination
- ❑ and multiple samplings

Table 05

Biogenicity criteria – Archaea (Schopf, 1993)

Around the same time, Schopf (1993) distilled criteria required to establish the authenticity of Archean microfossils to five key points:

- ❑ occur in rocks of known provenance
- ❑ occur in rocks of established Archean age
- ❑ be demonstrably indigenous
- ❑ be syngenetic with the primary deposition of the enclosing rock
- ❑ and be of assured biological origin

Table 06

Biogenicity criteria – Eukaryotes (Javaux et al., 2004)

Criteria for assessing later, eukaryotic microfossils add details thought to be unique to eukaryotes, including, as enumerated by Javaux et al. Although larger size was once considered indicative of eukaryotic fossils, Javaux et al., noting more recent discoveries of variances in the size of both prokaryotes and eukaryotes, refute that cell size can be considered a reliable means of distinguishing prokaryote from eukaryote fossils. (Javaux et al., 2004)

- ❑ wall structure & surface ornamentation
- ❑ processes that extend from vesicle walls
- ❑ encystment structures (openings through which cysts liberate their cellular contents)
- ❑ wall ultrastructure
- ❑ wall chemistry
- ❑ cell size no longer diagnostic

In summary, the table on the following page is an abridged adaptation of a table of biogenicity criteria from Sugitani et al. (2007). Some of the listed criteria are well accepted, others less so.

In the end, it tends to be true in both life and science that our expectations and openness to possibilities strongly influence what we see and how we interpret what we see.

Table 07

Compiled microfossil biogenicity criteria (Sugitani et al. 2007)

Sugitani et al. list the following 26 modified criteria for evaluating microfossils, based on works of (a) Schopf & Walter (1983), (b) Brasier et al. (2005), (c) Buick (1990), (d) Hofmann (1994), (e) Westall & Folk (2003), and (f) Hormann (2004). Asterisks indicate criteria that not all microfossils will meet.

Geological context

(1) occur in rock of known provenance (a, b)
(2) occur in rock of known age (a, b, c)
(3) occur in sedimentary or low-grade metasedimentary rock (a, b, c, d)
(4) occur in geologically plausible rock (b, d)
(5) make sense in geological context at a range of scales (outcrop to thin section) (b)

Indigenousness and syngeneity

(6) be indigenous to primary deposition of the enclosing rock (a, b)
(7) be syngenetic with primary enclosing rock phase (a, b)
(8) not be significantly different in color from kerogenous component of rock matrix (a, not b)
(9) not be endolithic (a, e)

Biological context

(10) occur in a geological context plausible for life (a, b, d)
(11) be abundant and present in a morphologically diverse biological community (a, b, d, f)
(12) fit within an established evolutionary context (b)
(13) * (ideally, but not necessarily) occur in colonies, communities and mats (d)
(14) * (rarely) exhibit orientation & distribution indicative of their role in forming biofabrics (3)
(15) * (rarely) exhibit cell envelopes, and be found in aggregates of cells, microborings or waste products within a restricted morphospace (b)
(16) show evidence of taphonomic degradation (f)

Morphological characteristics

(17) resemble extant or recent microbes (a, b, d)
(18) be larger than smallest extant free-living organism, >0.01 μm^3 (c)
(19) * be hollow, and exhibit ultrastructures (b, c, d)

Evidence of biological processes

(20) * not be uniform, but show variations such as in life cycle and degradation stages (a, b, d, f)

Biochemical context

(21) not only appear to be biological, but also pass analytical tests in support of biogenicity (a, b)
(22) * be carbonaceous (a, b, c, d)
(23) * show evidence of EPS (b, e)
(24) be dissimilar from coexisting but similar abiological bodies (a, b)
(25) chemical biomarkers should include carbon isotopes or specific organic compounds (b)

Other considerations

(26) null hypothesis (of an abiological origin) should be falsified (b)

Source: (Sugitani et al., 2007) based on (Schopf and Walter, 1983; Buick, 1990; Westall and Folk, 2003; Hofmann, 2004; Brasier et al., 2005)

Appendix C : A brief comment on anthropogenic impacts on the P cycle

The impact of anthropogenic CO2 release on the proliferation of life is a subject of intense research in these times of global climate change but the influence of P availability on the proliferation of biomass is also a significant issue facing mankind, as P reserves, mined for use primarily in agricultural fertilizers, are being depleted (Filippelli, 2008; Bouwman et al., 2009). Through much of human history, most terrestrial P was recycled with minimal diversion to the ocean, and human and animal waste, rich in P (as well as nitrogen) was returned locally to the land, to be again recycled through the biosphere. But today the P cycle has been profoundly altered by human activity, primarily through agricultural practices as well as the engineering of wastewater treatment systems. Human intervention is diverting P from its geological place in the 'natural' P cycle and accelerating its flux into the biosphere.

The beginning of significant human impact began over a century and a half ago, when the role of human and animal waste in causing disease began to be appreciated with Dr. John Snow's determination that water contaminated by a cesspool was the source of the 1848 cholera outbreak in London (Snow, 1857). In the 'sanitation revolution' that followed, urban land-based waste disposal was shifted to water-based sewage systems in a 'mandate to dispose rather than reuse,' dramatically increasing flux of 'waste' P to the oceans (Paytan and McLaughlin, 2007).

More recently, awareness of famines and the demands of an escalating global human population has led to improved agricultural and fertilizer technologies. The development of P-based fertilizers has resulted in the increased mining of phosphate reserves. Among the global phosphate reserves, the once plentiful bird and bat guano reserves have been depleted, leaving phosphate rock the only economically viable source of P.

In an attempt to ameliorate current and forestall further eutrophication, we are engineering intervention technologies such as wastewater recovery processes by which a significant portion of the P otherwise diverted to water bodies is recaptured. As early as 1926, the Milwaukee Metropolitan Sewerage District had developed a biosolid wastewater recovery system and used it to produce the commercialized dry fertilizer product Milorganite ("Milorganite's History"). Regulatory policy also addressed the inadvisable disposal of P, and the reduction in the use of phosphate-based laundry detergents which were banned in the United States in 1993 (as were dishwashing detergents in 2010) has slowed the efflux of phosphate to the hydrosphere (Knud-Hansen, 1994).

For a more detailed discussion of the anthropogenic alteration of the global P cycle, see Ashley et al. (2011) (Ashley et al., 2011) for a historical review, and Smil (2000) (Smil, 2000) for a discussion of other recent anthropogenic impacts.

Estimates for peak P production place the turning point at less than two decades in the future, after which production is predicted to fall, even as global population and agricultural needs increase (Van Kauwenbergh, 2010). Estimates for depletion range from ~80 to 900 years and considerable attention is being focused on how to ameliorate a potentially impending P crisis (Cordell et al., 2009; Obersteiner et al., 2013; Reijnders, 2014; Withers et al., 2015). Global P shortages can be expected to impact not only food resources, but also national/global security as the competition for this dwindling but necessary elemental resource escalates, with the most devastating impact likely to fall upon those with the fewest resources overall (Obersteiner et al., 2013).

Appendix D : Data – Liesegang banding

Liesegang banding is a phenomenon observed in both solid solution and aqueous-gelatinous solution that are not subjected to convective flow. As yet not fully understood, the most commonly cited mechanism is an "Ostwald-Liesegang supersaturation-nucleation-depletion cycle" mechanism, in which ion concentrations are locally depleted by the meeting of counter-ion fronts and the subsequent precipitation of mineral (or precursor) solids. This theory is largely based on Wilhelm Ostwald's 1897 Supersaturation theory, it is thought that once precipitation begins, ions are drawn toward the nascent particles as the crystals grow, drawing down ion concentration in proximity of the growing crystals (Stern, 1954; Smoukov et al., 2011).

Our refined precipitation apparatus afforded an enhanced view of Liesegang banding forming near the anion channel, where phosphate and fluoride entered the diffusion gel. Interested in the mineralogical distinctions between these bands, I harvested material from each of the bands, as seen in figure 35, and observed them by ESEM and analyzed them by EDS. I present here the preliminary data from this. Additional analysis and interpretation has yet to be performed.

List of following data

Table 08

Images log: 05.25.15 setup precipitates

(ESEM: June 21& 23, July 01, 05-07)

Sample #	Holder *	Description [bands numbered from 'outermost' (aka 'longest') to innermost]	image #s
L-band samples			
01.1 & 01.2	1a	Band 1, rim material (outermost layer)	200–227
02.1	1b	Band 1, minus rim material	228–232
01.3	1c	Band 1, distal end	233–239
03.	1d	Band 2, distal end	240–246
03.2	2a	Band 2, minus distal end	247–253
04.1	2b	Band 3	254–272
05.1	2d	Band 4 + faint band 5	
06.1	2c	Clear gel w/small spheres between bands five and the innermost part of L-band	001–088 273–358
07.1	3a	Last, innermost portion of L-band	377–396
06.1	3b	= "stub 4" Precips from Sample 01.1 & 01.2, after rinsing in epitube	089–199
Non L-band samples			
08.1	3c	'Cloud' precipitates	397–444
08.2	3d	'NON-cloud' precipitates	none

* stubs positioned in holder left-to-right, a-to-d (when cover hinges to open toward viewer)

* this is referred to as 'stub 4' in the lab book

Figure 35 | Liesegang banding

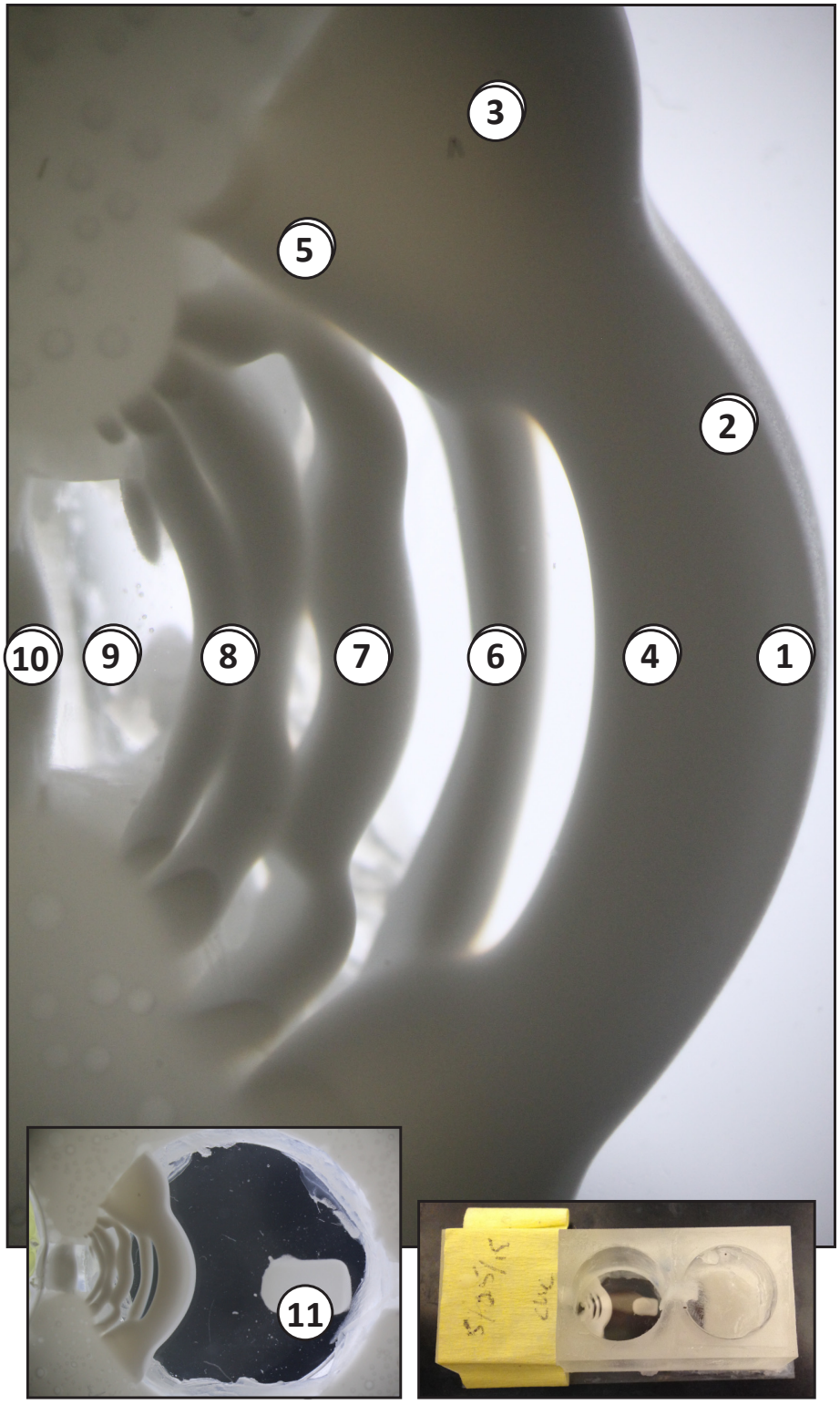

Close-up of Liesegang bands and the diffusion gel setup in which they formed, lower right. See Table 09, next page, for corresponding data.

.

Table 09

L-banding illustration key; calculated Ca:P ratios

samplesite	L-band stub	sst ID	image #s	Ca:P ratio avg
1.1 & 1.2	1a	1	200-227	2.987
1.1 & 1.2*	4	2	089-199	1.539
1.3	1c	3	233-239	1.840
2.1	1b	4	228-232	1.984
3.1	1d	5	240-246	3.380
3.2	2a	6	247-253	1.864
4.1	2b	7	254-272	2.215
5.1	2d	8	359-376	1.871
6.1	2c	9	001-088 273-358	1.812
7.1	3a	10	377-396	1.536
8.1	3c	11	397-444	1.935

• precips after rinsing

Table 10

Calcium Phosphate phases [and reference ratios]		Empirical formula		Molar Ca/P ratio
Dicalcium phosphate dihydrate	DCPD	$CaHPO_4 2H_2O$		1.00
Dicalcium phosphate	DCPA	$CaHPO_4$		1.00
Octacalcium phosphate	OCP	$Ca_6H_2(PO_4)_6 5H_2O$		1.33
beta-Tricalcium phosphate	TCP	$Ca_3(PO_4)_2$		1.50
Whitlockite	Mg-TCP	$Ca_{3-v}Mg_v(PO_4)_2$	$0 \le v \le 2$	3-v/2
Amorphous calcium phosphate	ACP	$Ca_9(PO_4)_6 \bullet H_2O$		1.50
Hydroxyapatite	HAP	$Ca_{10}(PO_4)_6(OH)_2$		1.67
Defect apatites		$Ca_{10-y}(HPO_4)_{6-y}(OH)_{2-y}$	$0 \le y \le 2$	10-y/6
Fluoroapatite	FAP	$Ca_{10}(PO_4)_6F_2$		1.67
Fluorohydroxyapatite	FHAP	$Ca_{10}(PO_4)_6F_z(OH)_{2-z}$	$0 \le z \le 2$	1.67

(Johnsson and Nancollas, 1992)

Table 11

Ca/P ratio data calculations – 05.25.15 setup

Sample	site: 2	3	4	5	6	7	8	9	10	11
1.684	0.552	1.566	1.698	3.380	1.864	1.866	1.510	1.478	1.33	1.704
4.290	0.883	2.114	2.269			2.297	1.925	1.478	1.469	1.72
	1.389					2.482	2.179	1.56	1.608	1.737
	1.636							1.688	1.735	1.751
	1.867							1.812		1.912
	2.033							1.883		1.937
	2.410							2.004		1.976
								2.166		1.993
								2.241		2.006
										2.035
										2.513
2.987	1.539	1.840	1.984	3.380	1.864	2.215	1.871	1.812	1.536	1.935
1.843	0.651	0.387	0.404	#DIV/0!	#DIV/0!	0.316	0.338	0.286	0.175	0.230
1.684	0.552	1.566	1.698	3.380	1.864	1.866	1.510	1.478	1.330	1.704
4.290	2.410	2.114	2.269	3.380	1.864	2.482	2.179	2.241	1.735	2.513

AVG.
ST DEV.
MIN.
MAX.

For raw data, see Tables 13 & 14

Site:	AVG.	ST DEV.	MIN.	MAX.
10	1.536	0.175	1.33	1.735
2	1.539	0.651	0.552	2.41
9	1.812	0.286	1.478	2.241
3	1.840	0.387	1.566	2.114
6	1.864	#DIV/0!	1.864	1.864
8	1.871	0.338	1.51	2.179
11	1.935	0.230	1.704	2.513
4	1.984	0.404	1.698	2.269
7	2.215	0.316	1.866	2.482
1	2.987	1.843	1.684	4.29
5	3.380	#DIV/0!	3.38	3.38

Table 12

Lab notes on morphologies, pg 1 of 2

Layer 1, rim material (01.1 & 01.2) 200–227 (n=28)
overall: Rinsing left distinct shapes with numerous knobs protruding from it.

Layer 1, minus rim material (02.1) 228–232 (n=5)
overall: Rinsing left distinct & rounded 'globs' of gel, with some knobs & surfaces covered in prisms.
• Stout prisms (~ 0.5 µm x 2 µm) beginning to widen, showing no apparent dissolution, but occasional cases of breakage
• Possible ≤ 100 nm small precipitates
all entrained in gel

Layer 1, distal end (01.3) 233–239 (n=7)
overall: Gel-entrained prisms grading into closing spheres
• Tangle of prisms (~ 0.2 µm x ≤ 1 µm) (at distal-most 'knob'?) giving way to:
• Well-developed dumbbells (no neck, ~3 µm long) & nearly-closed spheres generally ~ 6 µm diameter. These may represent material away from the distal ends (knobs) or maybe the 'interior' of the mass, under the prisms.

Layer 2, distal end (03.1) 240–246 (n=7)
overall: Rinsing left a distinct but rounded 'glob' of gel entraining small prisms, with a few spheres rinsed out of the glob.
• Tangle of prisms (~ 0.1 µm x 0.5 µm) in gel
• Some nearly-closed spheres (~8 µm)

Layer 2, minus distal end (03.2) 247–253 (n=7)
overall: Rinsing spread this into a thin layer on the stub, entraining variably-sized prisms, with a few prisms of unique features (see below) rinsed out of the mass.
• Tangle of variably sized prisms, ranging from ~ 0.3 µm to ~1 µm in length and generally neither expanding nor contracting at the ends, with:
• **X** Rinsed out prisms are ~ 2µm in length x ~0.30 µm wide in center and narrower at the ends. These are brighter (more electron dense) in the middle and along the edges, possibly due to dissolution?

Layer 3 (04.1) 254–272 (n=19)
overall: Rinsing left distinct shapes of gel, entraining prisms of a variety of sizes:
• Mass of widely variably sized prisms widely ranging in size, from ~0.3 x 0.15 µm to ~2 µm x 0.4 µm. Some masses are very tightly tangled. Mostly in the less tightly tangled masses, some of the larger prisms become narrower at the ends.
• Very tight tangles of prisms ~1 µm long.
• Very tight tangles of variably sized prisms widely ranging in size,

Layer 4 + faint layer 5 (05.1) 359–376 (n=18)
overall: Rinsing left curls of gel, with precipitates along the edges, primarily prisms, but also a portion of aggregated broken dumbbells. Mats and tangles appear to have been either rinsed out of the gel or exposed at the surface of gel.
• Some few prisms of the morphology **X**, above – may be an artefact of harvesting?
• A few areas populated with ~1.5 µm long very straight prisms
• Some ~5 to 6 µm long prisms beginning to flare at the ends
• Some ~5 to 6 µm long prisms narrowing slightly at the ends

Table 12
Lab notes on morphologies, pg 2 of 2

- Consolidated mats of the above 2 kinds of prisms
- Some ~8 to 9 µm long prisms flaring at the ends and breaking in the center
- Consolidated mats of the above 3 kinds of prisms
- Consolidated mats of variably sized prisms ranging from ~1 µm long to ~6 µm long, well mixed and tightly tangled
- Adjacent to a mat of prisms, morphology quickly grades into a collection dominated by broken dumbbells ~6 t0 8 µm diameter and showing signs of dissolution (?) sponge-like surface texture, and some dissolution down axis. Interspersed w/prisms.

Precips betw layer 5 & last layer (06.1) 001–088 & 273–358 (n=88 +

overall: The spheres in this fraction tend to be aggregates of inter-grown spheres, usually showing one of three surface textures: 'spiky,' 'spongy' and 'cortical.' Cases of 'ingrown prisms' are common. Occasional outer rims are visible, and appear to surround a layer of less density. Numerous cases of prisms growing into/out of spheres. A few small cubic precips (NaCl pr KCl) observed on some sphere surfaces and on the C-tape.

- A few loose prisms. Some are brighter in the center, a few are brighter at the ends. Some narrow toward the ends. A few mats of prisms ~6 µm long observed.

'Cloud' precipitates (08.1) 397–444 (n=47)

overall: Evidence of dissolution is widespread. This fraction includes at least a few of every observed morphology so far, as well as a newly observed one: Numerous 'birds nest' shapes. See #0411 for zoomed out overview. A few 'intact' prisms and dumbbells can be seen, but this fraction is dominated by intergrowing spheres of 'blastulae,' 'birds nests,' and 'exploded masses' morphologies, and half dumbbells with central axes strongly dissolved away. I see no examples of an outer hemispherical coating (but I observed only a small portion.)

- 'Birds next' morphology of what appears to be collapsed hollow spheres exhibiting a platy surface texture resembling the hexagonal surfaces that are in fact, distal ends of prisms. Varying sizes, but roughly ~3 to 10 µm outer diameter.
- Interspersed with these are instances of an 'exploded mass' morphology. These appear to be observed as though in X-section and show the internal radiating precipitates.
- Dumbbells show dissolution pitting and dissolving of central axes. Some examples show a 'septa' separating the distinct axes of dumbbells in multi-dumbbell units. A few good examples of preferential dissolution along radii of dumbbells.
- Some blastula, showing hexagonal surface texture, exhibit apparent dissolution (or zoning) in center of the hexagons (i.e. #0413)

'NON-cloud' precipitates (08.2) none

overall: no precipitates found. Perhaps the bubble rolled off the stub while it was drying in the chem hood?

Table 13

Ca:P ratio data – 05.25.15 setup harvested by L-band, pg 1 of 3

CODING LEGEND:	
Shape (applies to precipitates) :	*P=prism, D=dumbbell, S=sphere, B='blastula,' E='exploded' mass, C=cube, L=layer or rim, R=round, Z=zoom in, A= assortment of precips, wide FoV*
Condition (applies to precipitates) :	*D=dissolution pits, N=nearly closed, W=wrinkled,* Mx=multiple intergrown(x=#, +=uncountable,) *dP=slightly dipyramidal, dW=beginning to widen at distal ends, V=dividing prisms*
Number:	*(of shapes)*

EDS #	Image #	Atom % of element						Ca : P ratios [05.25 setup fractions]							
		Ca	P	F	C	O	Other misc.	Ca:P	% F	Sample site	sst ID #	Shape	Condition	Number	~ size (µm)
25	227	14.21	8.44	3.01	40.43	32.06	1.84	1.684	0.117	1.1 & 1.2	1	S	D	1	15
24	224	27.50	6.41	11.32	33.39	21.38	0.00	4.290	0.250	1.1 & 1.2	1	ZS	N		
23	219	2.97	0.00	0.00	57.54	14.26	25.23	#DIV/0!	0.000	1.2*	1	C	—	—	—
15	100	2.03	3.68	0.00	76.90	15.63	1.76	0.552	0.000	1.1 & 1.2	2	—	—	—	—
17	107	0.53	0.60	0.00	66.93	26.73	5.22	0.883	0.000	1.1 & 1.2	2	—	—	—	70
13	98	5.82	4.19	4.04	49.67	33.56	2.72	1.389	0.288	1.1 & 1.2	2	L			~1
19	121	13.40	8.19	2.85	40.78	34.78	0.00	1.636	0.117	1.1 & 1.2	2	S	D	M2	10
18	119	14.99	8.03	4.37	29.33	43.29	0.00	1.867	0.160	1.1 & 1.2	2	S	D, N	M2	8
14	99	5.55	2.73	0.00	68.76	22.96	0.00	2.033	0.000	1.1 & 1.2	2	—	—	—	—
21	190	8.99	3.73	0.00	62.86	15.54	8.88	2.410	0.000	1.1 & 1.2	2	L	—	—	~2
20	171	6.37	0.17	0.00	42.91	42.79	7.75	37.471	0.000	1.1 & 1.2	2	E	—	—	10+

Table 13

Ca:P ratio data – 05.25.15 setup harvested by L-band, pg 2 of 3

EDS #	Image #	Atom % of element						Ca : P ratios [05.25 setup fractions]							~ size (µm)
		Ca	P	F	C	O	Other misc.	Ca:P	% F	Sample site	sst ID #	Shape	Condition	Number	
16	104	1.17	0.00	0.00	73.20	25.13	0.50	#DIV/0!	0.000	1.1 & 1.2	2	—	—	—	—
22	199	0.00	0.00	0.00	82.04	11.74	6.22	#DIV/0!	#DIV/0!	1.1 & 1.2	2	—	—	—	—
28	239	6.81	4.35	0.00	60.00	28.84	0.00	1.566	0.000	1.3	3	AP	—	—	1
26	230	2.87	1.69	0.00	70.66	24.78	0.00	1.698	0.000	2.1	4	AP	—	—	—
27	231	13.59	5.99	4.18	44.91	30.81	0.51	2.269	0.176	2.1	4	ZP	—	—	1
30	245	17.27	8.17	3.21	35.88	35.01	0.45	2.114	0.112	3.1	5	D	—	1	5
29	241	9.43	2.79	1.19	60.77	25.82	0.00	3.380	0.089	3.1	5	AP	—	—	0.5
31	253	17.11	9.18	0.00	47.02	26.69	0.00	1.864	0.000	3.2	6	AP	—	—	
33	264	8.94	4.79	3.76	41.75	40.75	0.00	1.866	0.215	4.1	7	AP	—	—	
32	260	24.28	10.57	0.00	0.00	57.63	7.52	2.297	0.000	4.1	7	AP	—	—	2
34	270	9.43	3.80	0.00	68.89	16.19	1.69	2.482	0.000	4.1	7	AP	dP	—	0.5-1
44	376	21.55	14.27	0.00	32.07	32.12	0.00	1.510	0.000	5.1	8	APDS	—	—	3-5
42	368	20.25	10.52	0.00	37.84	31.39	0.00	1.925	0.000	5.1	8	AP	dP, dW	—	1-4
43	369	18.87	8.66	3.32	28.06	41.09	0.00	2.179	0.108	5.1	8	AP	dP, dW	—	3-5
37	276	29.48	19.95	0.00	37.03	13.54	0.00	1.478	0.000	6.1	9	P	dP	1	5
38	280	29.48	19.95	0.00	37.03	13.54	0.00	1.478	0.000	6.1	9	—	—	—	—
4	35	10.00	6.41	3.47	35.85	39.29	4.99	1.560	0.175	6.1	9	S	Dp	1	15
41	326	11.36	6.73	0.00	52.71	28.71	0.50	1.688	0.000	6.1	9	E	—	—	20
35	274	22.40	12.36	0.00	33.21	30.62	1.41	1.812	0.000	6.1	9	S	D/W	M+	10+
5	39	8.98	4.77	3.13	41.32	37.89	3.89	1.883	0.185	6.1	9	S	W	1	10
36	275	18.14	9.05	3.56	23.24	45.22	0.78	2.004	0.116	6.1	9	—	D	1	5
2	22	19.23	8.88	3.24	26.26	38.84	3.55	2.166	0.103	6.1	9	S	N, M2	2	15
8	53	19.72	8.80	0.00	33.47	36.15	1.87	2.241	0.000	6.1	9	S	D	M+	5-20
9	57	10.27	1.60	8.49	56.47	20.91	2.26	6.419	0.417	6.1	9	R		1	5
1	17	0.00	0.00	0.00	90.85	5.39	3.77	#DIV/0!	#DIV/0!	6.1	9	S	W	1	70
3	28	0.00	0.00	0.00	72.01	8.70	19.30	#DIV/0!	#DIV/0!	6.1	9	C	—	1	1
6	42	0.00	0.00	0.00	54.98	2.38	42.63	#DIV/0!	#DIV/0!	6.1	9	A	—	—	—
7	49	0.00	0.00	0.00	42.14	38.97	18.88	#DIV/0!	#DIV/0!	6.1	9	C	—	1	20

Table 13

Ca:P ratio data – 05.25.15 setup harvested by L-band, pg 3 of 3

		Atom % of element						Ca : P ratios [05.25 setup fractions]							
EDS #	Image #	Ca	P	F	C	O	Other misc.	Ca:P	% F	Sample site	sst ID #	Shape	Condition	Number	~ size (µm)
10	63	0.00	0.00	0.00	90.86	8.06	1.08	#DIV/0!	#DIV/0!	6.1	9	R		1	10
11	79	0.00	0.00	0.00	68.67	21.93	9.40	#DIV/0!	#DIV/0!	6.1	9	—	—	—	—
12	85	0.00	0.00	0.00	46.31	39.41	14.27	#DIV/0!	#DIV/0!	6.1	9	—	—	2	10
39	281	0.00	0.00	0.00	80.35	19.65	0.00	#DIV/0!	#DIV/0!	6.1	9				
40	286	0.00	0.00	0.00	73.65	18.26	8.09	#DIV/0!	#DIV/0!	6.1	9	—	—	—	—
45	381	22.09	16.61	0.00	31.15	30.15	0.00	1.330	0.000	7.1	10	A	D	M+	—
46	383	21.21	14.44	0.00	24.30	40.05	0.00	1.469	0.000	7.1	10	AP	dP, V	—	1-5
48	393	14.15	8.80	0.00	48.25	28.80	0.00	1.608	0.000	7.1	10	AS	N	—	1
47	387	25.90	14.93	0.00	15.97	43.20	0.00	1.735	0.000	7.1	10	APS	V, N	—	—
53	429	20.92	12.78	4.02	15.55	45.21	1.52	1.637	0.107	8.1	11	B	—	1	10
51	417	14.48	8.50	0.00	52.74	24.29	0.00	1.704	0.000	8.1	11	D?	?	1	8
52	428	35.05	20.38	0.00	0.00	41.15	3.43	1.720	0.000	8.1	11	S	layered	1	20
49	399	35.87	20.49	3.12	0.00	38.10	2.43	1.751	0.052	8.1	11	SB		1	12
57	441	31.88	16.67	0.00	32.16	19.26	0.00	1.912	0.000	8.1	11	S	—	1	15
56	436	24.76	12.78	0.00	28.30	34.16	0.00	1.937	0.000	8.1	11	?	?	1	15
55	435	15.75	7.97	3.00	39.35	33.94	0.00	1.976	0.112	8.1	11	S	hollow?	M4	8
58	442	17.52	8.79	1.70	43.05	27.17	1.78	1.993	0.061	8.1	11	L	—	—	—
59	443	17.79	8.87	2.86	35.45	35.04	0.00	2.006	0.097	8.1	11	L	—	—	—
54	432	25.74	12.65	3.56	13.19	43.18	1.69	2.035	0.085	8.1	11	S	N	1	10
50	404	33.97	13.52	0.00	20.99	31.52	0.00	2.513	0.000	8.1	11	D	D	1	10
60								#DIV/0!	#DIV/0!						

Table 14

Ca:P ratios – 05.25 setup L-bands – description / comments by sample pg 1 of 3

EDS #	Additional description / comments
25	
24	Closeup on image #224 - surface of ~400 nm spheres
23	Cubic precips - shows NaCl (under gel?)
15	Another spot as above
17	diatom
13	slightly botryoidal rim over Ca-P precips
19	interesting 'end' morphology exposed
18	
14	background gel behind #98, above - dominated by organics (gel)
21	See image 187 for context (similar to image 98) - maybe small precips trapped in gel?
20	shows Si, Ca, O - no P

Additional description / comments

Table 14

Ca:P ratios – 05.25 setup L-bands – description / comments by sample pg 2 of 3

EDS #	Additional description / comments
16	another as above
22	Tangle of gel - dominated by C & Al (from stub)
28	another location of mass of ~1µm long prisms in gel
26	overview of image #231 (mass of ~1µm long prisms in gel)
27	mass of ~1µm long prisms in gel
30	Broken dumbbell
29	Finer, smaller prisms
31	Mass of prisms ranging in size from 0.5 to ~2 µm in length
33	Tangle of prisms ranging in size from 0.5 to ~2 µm in length (denser, more variable)
32	Prisms pretty uniformly ~2 µm in length
34	Mass of spheres, some slightly dipyramidal
44	Assorted morphologies - prisms of various sizes, broken dumbbells & a few spheres
42	Tight tangle of prisms ranging in size, some expanding at ends, some contracting
43	Larger and more uniform than those in #368
37	Brighter prisms seem in image #274
38	Wrinkled gel, this spot EDS shows also Ca & P
4	Sphere w/cubic precips on surface = Ca-P w/a few NaCl adhering precips
41	meshlike' texture
35	Surface texture is pitted and separating into polygonal shapes
5	cortical surface texture
36	Amorphous shape of more electron-dense material over site of image #274
2	Adhering small ~100nm high-density precips on surface
8	multiple spheres of assorted sizes, intergrown & ranging from ~5 to ~20 µm
9	Round image but may not be a sphere - Shows Ca+Si w/some P+F
1	Sphere w/heavily wrinkled surface = gel over a sphere
3	8.54% K + 10.34% Cl (the C is the tape) = KCl
6	A shaving over various Ca-P precipitates : Shows Fe + Cr = a shaving from the stub?
7	Shows high Si, Al & K

Table 14

Ca:P ratios – 05.25 setup L-bands – description / comments by sample pg 3 of 3

EDS #	Additional description / comments
10	Round shape w/squiggle inside - dominated by Si
11	Mass of gel
12	'rice chex' diatom
39	Zoom out of #280 site
40	shows C & Al (from stub) - so these are probably blobs of gel
45	Sheet of conjoined spheres w/other precips, & dumbbells w/tight 'waist' & not 'curling'
46	Tight tangle of prisms, some bifurcating
48	Matt of spheres ~1µm
47	Matt of prisms w/a few nearly closed spheres
53	16-cell (?) blastula
51	Is this a dumbbell nearly fully dissolved? (note the dark central 'eyes')
52	Strange round item showing 'layers' from center out
49	
57	Multi-layered, or infolded layers - compare to coelom (Bengston+ 2012)
56	Is this a collapsed sphere?
55	These appear to be 'imploded' spheres
58	EDS of outer hexagonal 'surface' of #441
59	EDS of outer spiky 'surface' of #441
54	3-lobed- sphere (?)
50	Apparent portion of dumbbell half, with central portion dissolved

Figure 36 | Source images for Ca:P ratios, pg 1 of 5

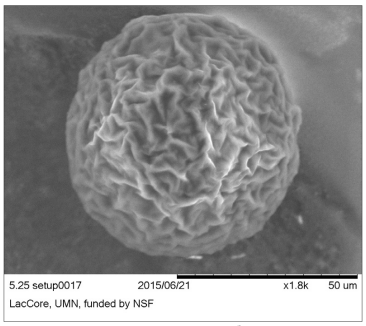

EDS 01 - image 17 - sample 6.1

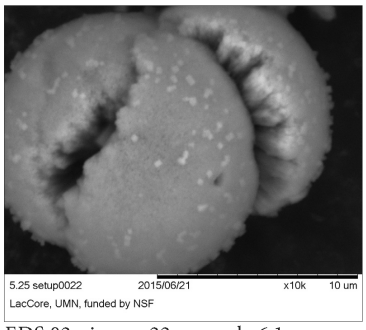

EDS 02 - image 22 - sample 6.1

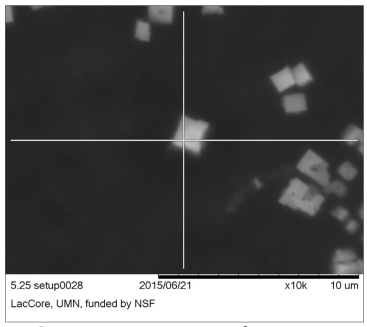

EDS 03 - image 28 - sample 6.1

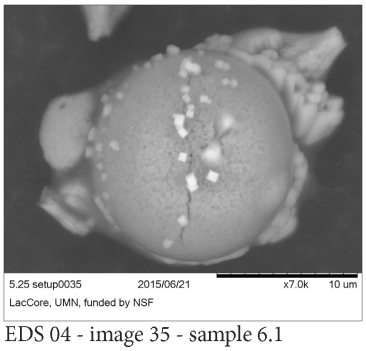

EDS 04 - image 35 - sample 6.1

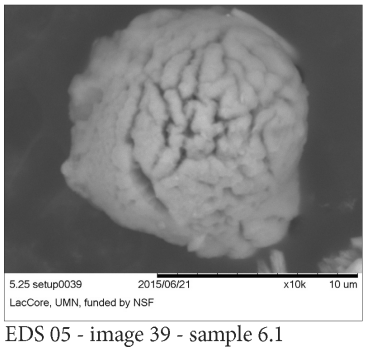

EDS 05 - image 39 - sample 6.1

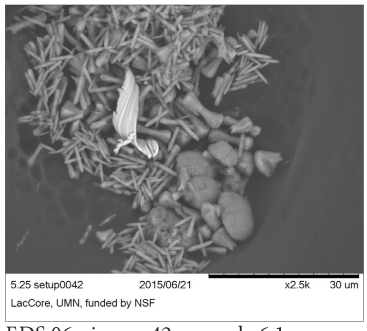

EDS 06 - image 42 - sample 6.1

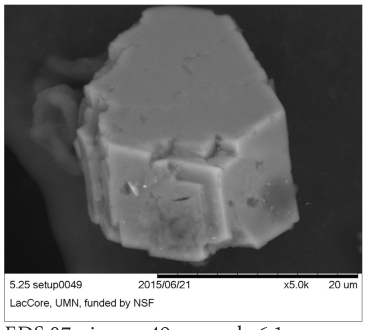

EDS 07 - image 49 - sample 6.1

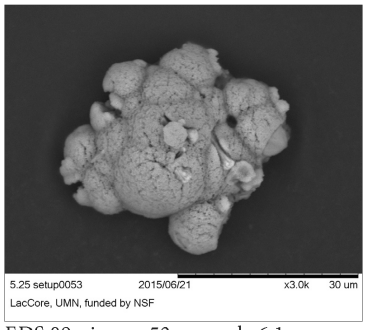

EDS 08 - image 53 - sample 6.1

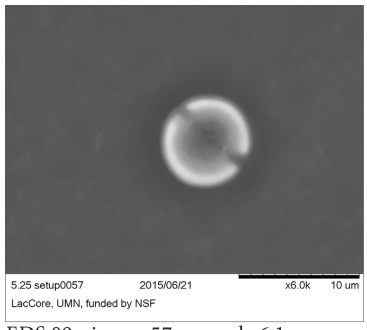

EDS 09 - image 57 - sample 6.1

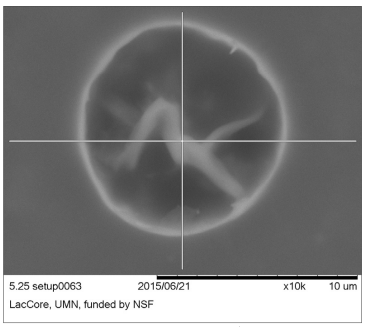

EDS 10 - image 63 - sample 6.1

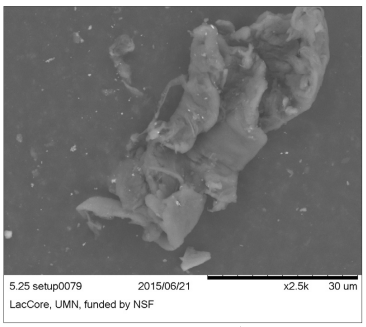

EDS 11- image 79 - sample 6.1

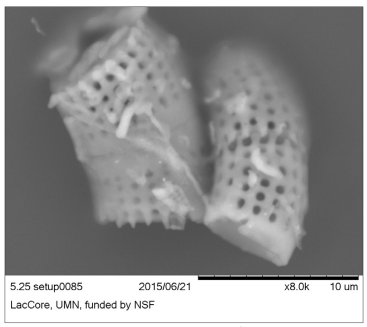

EDS 12 - image 85 - sample 6.1

Figure 36 | Source images for Ca:P ratios, pg 2 of 5

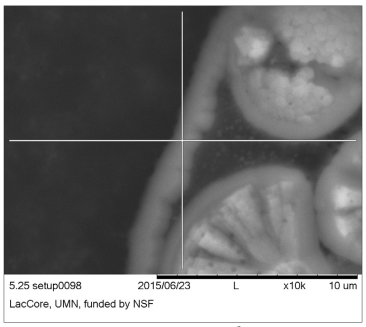

EDS 13 - image 98 - sample 6.1

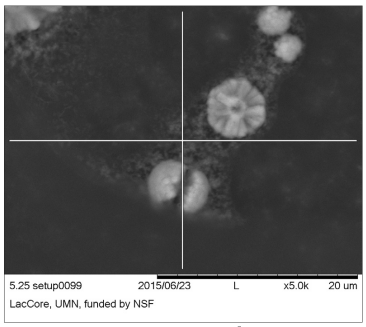

EDS 14 - image 99 - sample 6.1

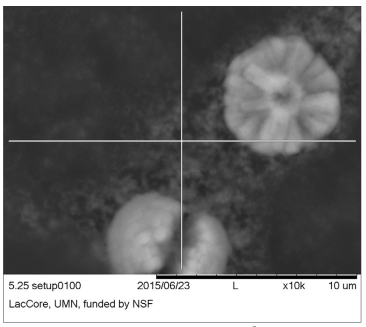

EDS 15 - image 100 - sample 6.1

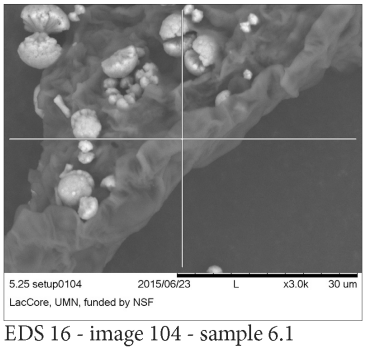

EDS 16 - image 104 - sample 6.1

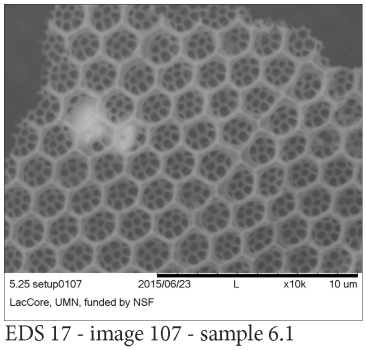

EDS 17 - image 107 - sample 6.1

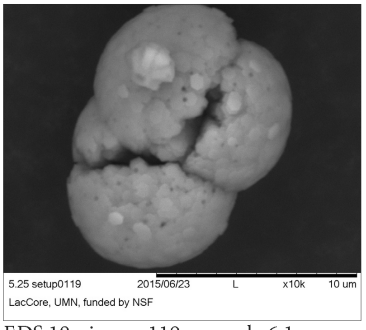

EDS 18 - image 119 - sample 6.1

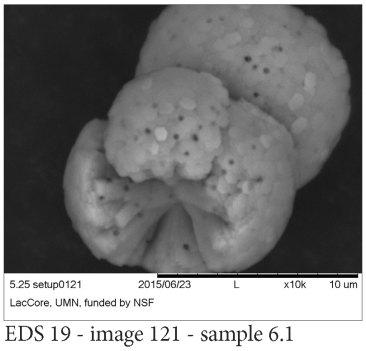

EDS 19 - image 121 - sample 6.1

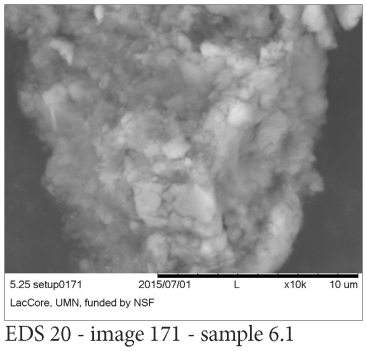

EDS 20 - image 171 - sample 6.1

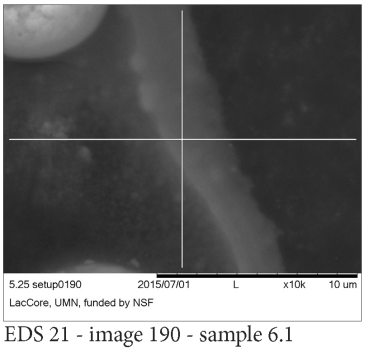

EDS 21 - image 190 - sample 6.1

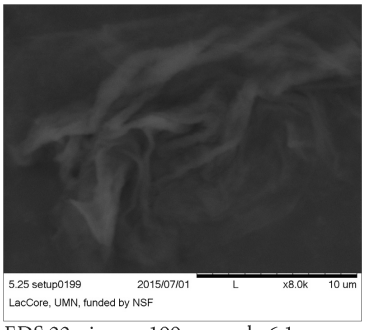

EDS 22 - image 199 - sample 6.1

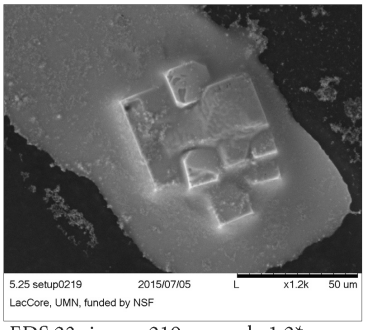

EDS 23- image 219 - sample 1.2*

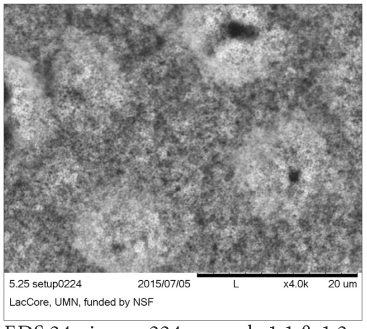

EDS 24 - image 224 - sample 1.1 & 1.2

Figure 36 | Source images for Ca:P ratios, pg 3 of 5

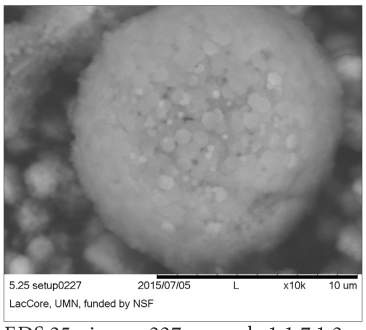

EDS 25 - image 227 - sample 1.1 7 1.2

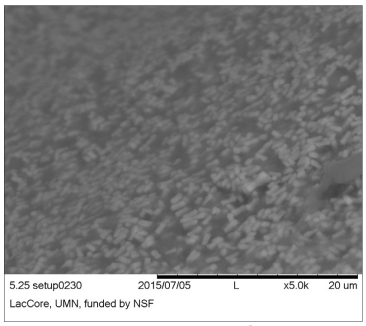

EDS 26 - image 230 - sample 2.1

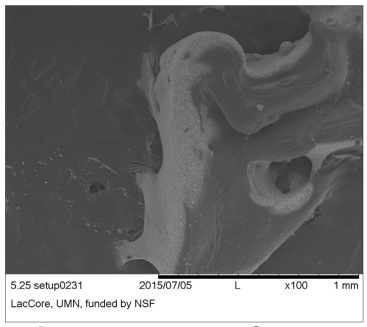

EDS 27 - image 231 - sample 2.1

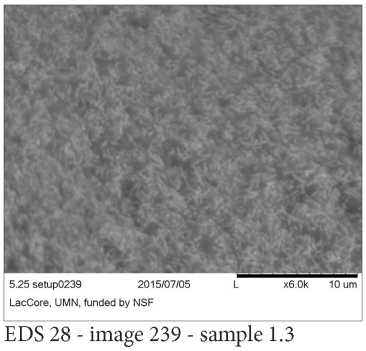

EDS 28 - image 239 - sample 1.3

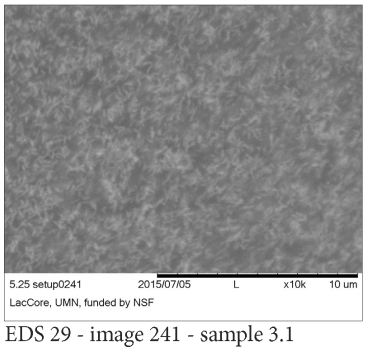

EDS 29 - image 241 - sample 3.1

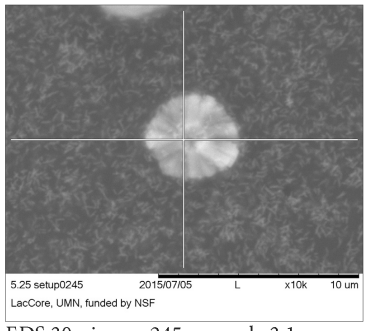

EDS 30 - image 245 - sample 3.1

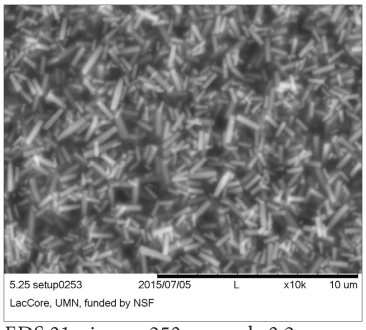

EDS 31 - image 253 - sample 3.2

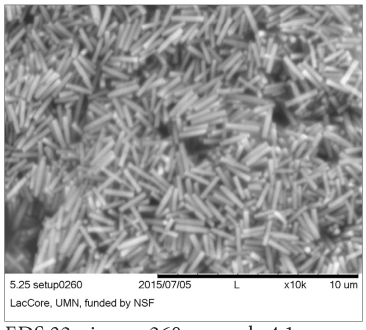

EDS 32 - image 260 - sample 4.1

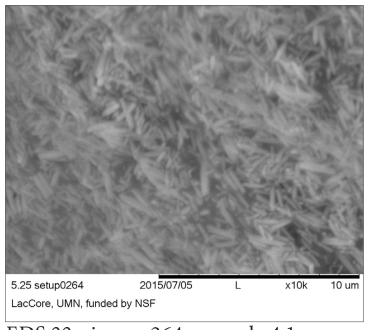

EDS 33 - image 264 - sample 4.1

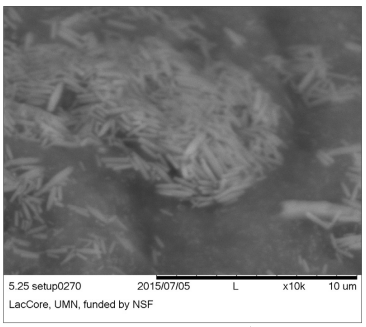

EDS 34 - image 270 - sample 4.1

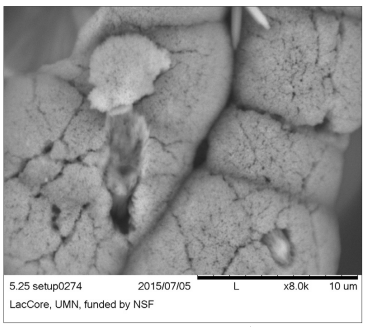

EDS 35- image 274 - sample 6.1

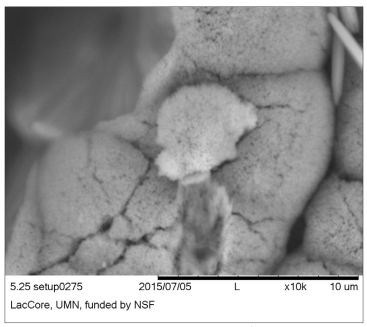

EDS 36 - image 275 - sample 6.1

Figure 36 | Source images for Ca:P ratios, pg 4 of 5

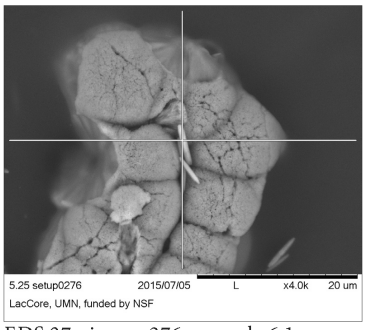

EDS 37 - image 276 - sample 6.1

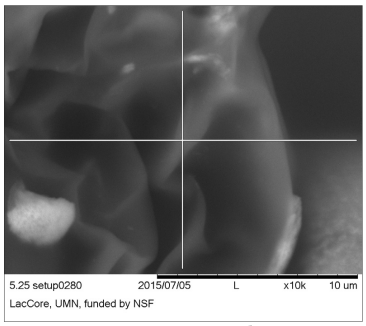

EDS 38 - image 280 - sample 6.1

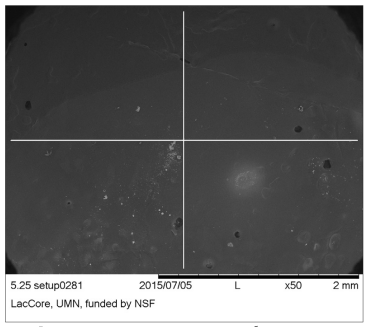

EDS 39 - image 281 - sample 6.1

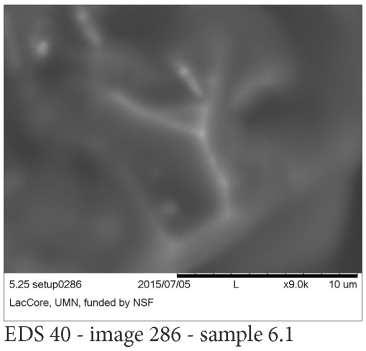

EDS 40 - image 286 - sample 6.1

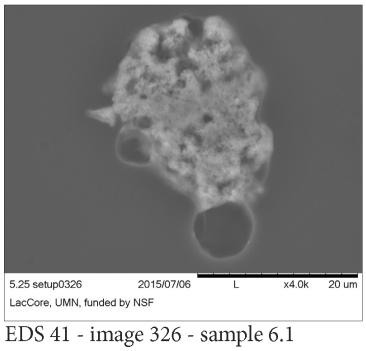

EDS 41 - image 326 - sample 6.1

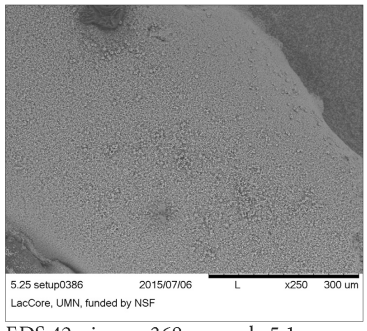

EDS 42 - image 368 - sample 5.1

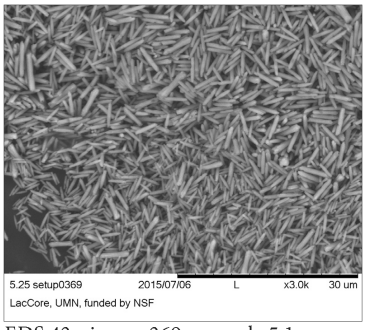

EDS 43 - image 369 - sample 5.1

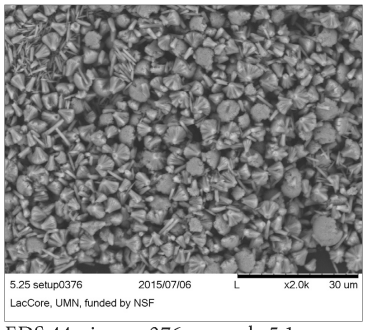

EDS 44 - image 376 - sample 5.1

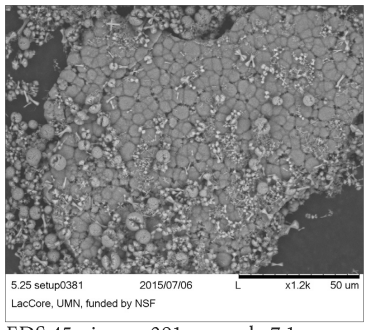

EDS 45 - image 381 - sample 7.1

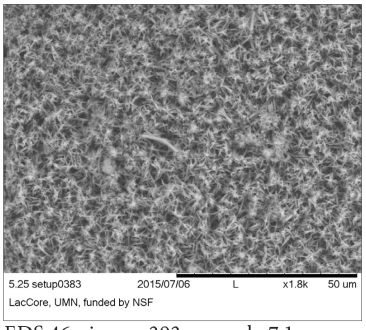

EDS 46 - image 383 - sample 7.1

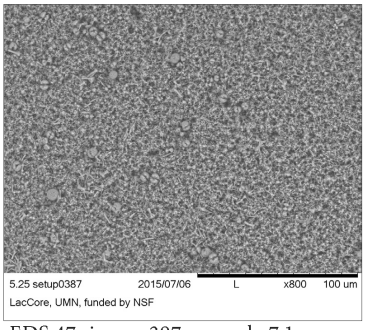

EDS 47- image 387 - sample 7.1

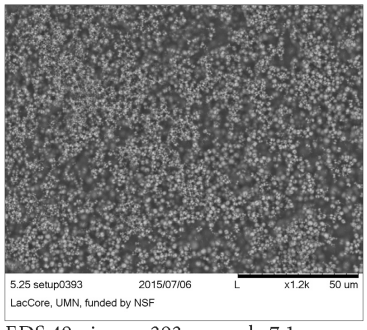

EDS 48 - image 393 - sample 7.1

Figure 36 | Source images for Ca:P ratios, pg 5 of 5

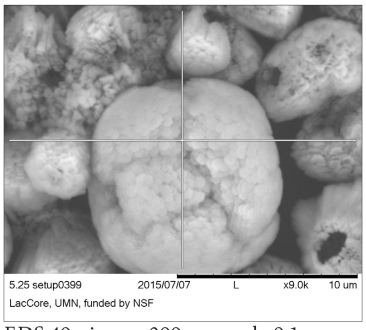

EDS 49 - image 399 - sample 8.1

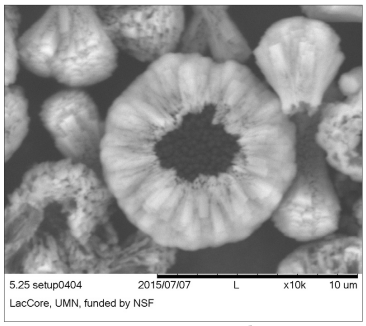

EDS 50 - image 404 - sample 8.1

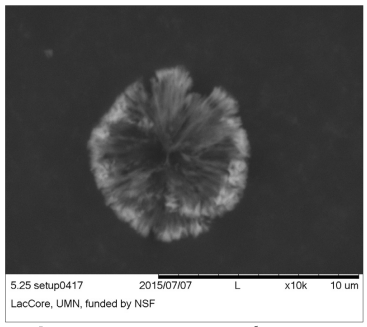

EDS 51 - image 417 - sample 8.1

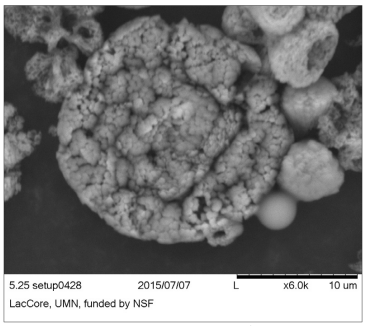

EDS 52 - image 428 - sample 8.1

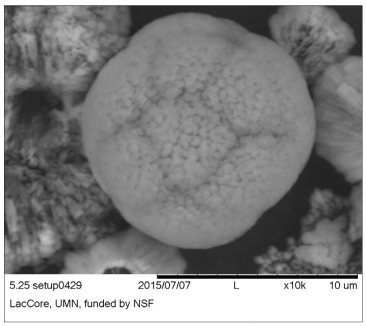

EDS 53 - image 429 - sample 8.1

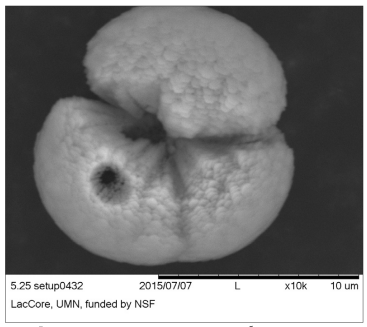

EDS 54 - image 432 - sample 8.1

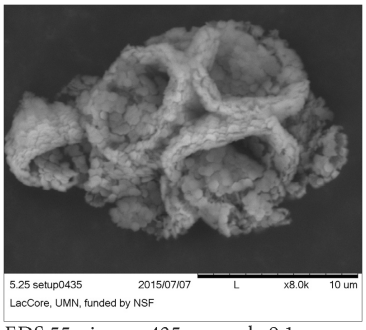

EDS 55 - image 435 - sample 8.1

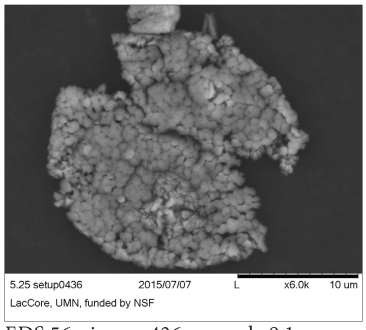

EDS 56 - image 436 - sample 8.1

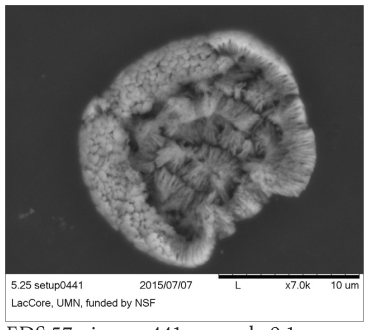

EDS 57 - image 441 - sample 8.1

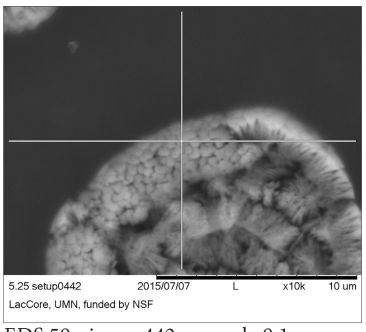

EDS 58 - image442 - sample 8.1

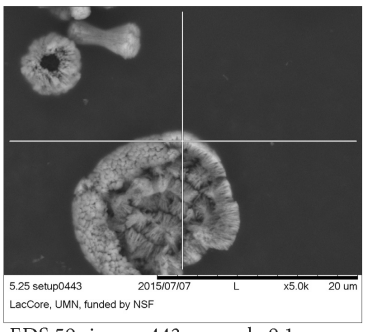

EDS 59- image 443 - sample 8.1

Appendix E : Morphotypes observed among diffusion gel precipitates

ESEM results show morphological progression from hexagonal prisms to 'dumbbells' to closed spheres, in a range of sizes. Below is a recap of some observations.

Table 15

Morphology	Size	(sample image #)
prisms	~500 nm	(uXRD8_130025)
	~1µm x ~200 nm	(L-band0001)
dumbbells	~1 µm lengths	(uXRD8_130023)
~90˚ crosses	~0.8 µm	(uXRD8_130025)
authigenic spheres	~400 nm	(Galaxy 0009)
	~20 µm	(Lband0011)
'spicules' into sphere		(L-band0005)
broken multi-unit showing segmentation:		(Lband0012)
'dividing' sphere pair		(Lband0015)
auth. sphere ~100 µm w/ ~10µm closing dumbbell overprint (?)		(Lband0016)
~70 µm spherical mass of prisms w/dumbbells		(Lband0017) (L-band0002)
acicular-surface		(L-band0025)
blastula	~10 µm	(Blast#1-0002)
multi-arm unit	~10 µm	(Blast#1-0007 &0008)
5-armed (?) unit	~8 µm	(Blast#1-0016)
side-view of cut		(Blast#1-0020 - 0023)
multiple stages	~10 µm	(Blast#1-0031)
intergrowing	~10 µm	(Blast#1-0042)
blastula, almost closed	~10 µm	(Blast#1-0075)